The search for biomarkers of facial eczema, following a sporidesmin challenge in dairy cows, using mass spectrometry and nuclear magnetic resonance of serum, urine, and milk

A thesis presented in partial fulfilment of the requirements for the degree of

Doctor of Philosophy in Sciences

at Massey University, Palmerston North, Manawatu, New Zealand

Zoe Maree Matthews

June 2015

Abstract

Facial eczema (FE) is a secondary photosensitisation disease of ruminants that is significant in terms of both its economic importance to New Zealand and its impact on animal welfare. The clinical photosensitivity signs, caused by the retention of phytoporphyrin, occur secondarily to hepatobiliary damage caused by the mycotoxin sporidesmin.

Currently it is difficult to diagnose subclinical animals and those in the early stages of the disease. The project was aimed at applying new analytical and statistical techniques, to attempt the early diagnosis of FE in dairy cows following the administration of a single oral dose (0.24 mg/kg) of sporidesmin. Well-established traditional techniques including production parameters, liver enzyme (GGT, GDH) activity measurements, as well as measurements of phytoporphyrin by fluorescence spectroscopy were made for comparison.

Serum, urine, and milk were analysed using ^{1}H Nuclear Magnetic Resonance (NMR), multivariate analysis (MVA), and time series statistics. Urine and milk did not prove useful for identification of sporidesmin intoxication. Serum metabolites differed between treated cows before and after administration of the toxin, and could distinguish samples belonging to the clinical group. The metabolites that were identified as being relevant to this classification were a mixture of glycoproteins, carboxylic acids, ketone bodies, amino-acids, glutamate, and glycerol, which were elevated for treated cattle, and acetate, choline, isoleucine, trimethylamine N-oxide, lipids, lipoproteins, cholesterol, and α-glucose, which showed decreased concentrations. Citrate was found to be at higher concentration in non-responders and subclinicals only.

When serum was analysed using ultra performance liquid chromatography electrospray ionisation mass spectrometry (UPLC/ESI-MS) and UPLC tandem MS (MS/MS), only samples from clinical cows could be discriminated. The molecular ions involved could be tentatively identified as a combination of taurine- and glycine-conjugated bile acids. These bile acids all became elevated.

This study confirmed that liver enzyme activities (GGT, GDH) and phytoporphyrin concentrations are not effective as markers of early stage sporidesmin damage. Additionally, the new techniques were unable to detect early stage FE. However, some markers of treated cows were identified. The research does provide a strong foundation for future applications of metabolomics analysis, with MVA and time series statistics, for early stage FE diagnosis.

Acknowledgments

The research presented in this thesis was a multidisciplinary project and could not have been completed without the help of an extensive list of people.

Firstly, I can't thank my supervisors Dr. Patrick Edwards, Dr. Peter Derrick, Mark Collett, Dr. Jonathan Marshall, and Dr. Ashton Partridge, enough. They took on a strong willed, (openly) opinionated, emotional person, and came out the other side smiling (I think). My supervisors changed many times throughout my PhD, which was difficult on me and those stepping in to help. I thank you all for stepping up to the plate, especially Pat for jumping in more than halfway through and providing me with amazing advice and encouragement. A special thanks to Mark, who has been on-board for the entire PhD. Not only did you rise early on many mornings to help with the cow sampling during the trial, but you also provided me with essential energy in the form of coffee, and continual support and guidance. I cannot begin to express my gratitude to you. "You can do it".

I need to thank Dr. Allan Sheppard for help with the original ideas for the trial; Neville Aymes for his advice on sporidesmin doses and administration, and providing the sporidesmin solution; and Dr. Ashton Partridge for his role in arranging financial support. This PhD was also partly supported by The University of Auckland and the Sinclair Cummings scholarship, and personal funding was provided by the MacDiarmid group and Massey University.

I would like to show gratitude to all the groups involved in the study: The Massey University Dairy No.4 staff where the experiment was carried out; the NZVP group, and in particular Tim Adam, for allowing me to infiltrate their laboratory weekly during the trial for serum analysis; Mike Hogan - post-mortem room technician – you are amazing; Veterinarian Dr. Jenny Weston for assessing and treating cows which became lame; the staff at Silver Fern Farms, particularly Neville Rolls, whom allowed access for liver sampling at the end of the trial; Andy Trow for acquiescing to a number of requests; the group at AgResearch who provided access to their laboratories and liquid chromatography and mass spectrometry equipment, as well as providing me with continual advice and support. In particular I would like to thank Dr. Scott Harrison, Dr. Karl Fraser, and Dr. Mingshu Cao; and finally, Massey University for extensive access to the 700 MHz NMR.

Many people have contributed to this project, whether it was during the animal trial, labelling tubes for samples, or just providing encouragement and advice and supplying me with a much needed wine or coffee (or 5). In particular I would like to thank my "science-geek" friends, particularly Aaron Gilmour for his amazing support and help throughout the years, and especially for getting up at 3 am

on cold and wet mornings to bring cows in for milking and to gather bodily fluids, and for listening to my complaints over umpteen coffees; Tessa – you really are just an amazing star, I don't think I could have made it this far without your phone calls and advice. Claire, I'm not sure why you thought it would be a good idea to offer your proofreading services, but I can't thank-you enough for this. You are amazing friends. Additionally, Dr. Wayne Campbell, Dr. Gaile Dombrowski, and Dr. Ariane Kahnt, for all their help and guidance.

Also my "non-science" friends who's continued support through some pretty hard times gave me the will and strength to get up every morning, I really cannot thank-you all enough: Zandra, Andy, Debbie, Sara, Brendan, Josh, Jodi, Tom, Ariane, Caroline, Amy, Stu, Belles, Sam, Sammy, Geoff, Karl, Kat, Tash, Nikki, Louise, Alison, Aleisha, Steph, Sarah and Jess.

Lastly, I want to thank my amazing family - mum, dad, Brion, and Fliss - and Ross, with all my heart, for always believing in me, no matter what; for asking about my work, and listening with interest even though they understood little of what was being said.

"A goal without a plan is just a dream"

PREFACE

The work presented here was multidisciplinary, and therefore required combined resources from educational and commercial institutes, and many different people.

Histological analysis, was conducted by Dr Mark Collett, at the Institute of Veterinary and Biomedical Sciences (IVABS), Massey University, Palmerston North, New Zealand.

The statistical models for GAM and time series analysis were developed by Dr. Jonathan Marshall, Institute of Fundamental Sciences (IFS), Massey University, Palmerston North.

UPLC/MS metabolite measurements of serum were carried out at AgResearch Grasslands, Palmerston North under the supervision of Scott Harrison and Karl Fraser. Data pre-processing was undertaken by Mingshu Cao, AgResearch, Palmerston North.

The UPLC/MS/MS data was obtained by Dr. Ariane Khant of Auckland University, New Zealand, at the Danish Technical University, Lyngby, Denmark.

NB:

Throughout this report, the use of the term sporidesmin denotes the sporidesmin A variant produced by *Pithomyces chartarum*.

The use of the term phytoporphyrin is used synonymously to phylloerythrin irrespective of its use in the relevant published article.

TABLE OF CONTENTS

LIST OF FIGURES

LIST OF TABLES

LIST OF ABBREVIATIONS

ACN	Acetonitrile
AGR	Albumin Globulin Ratio
AIC	Akaike information criterion
Alb	Albumin
ANIT	α-naphthylisothiocyanate
ANOVA	Analysis of variance
BA	Bile acid
BDL	Bile duct ligation
BHBA	β-hydroxybutyric acid
Bil	Bilirubin
BSP	Bromsulphthalein
CAT	Correlation-adjusted t-score
CI	Chemical ionisation
CID	Collision induced dissociation
CPMG	Carr, Purcell, Meiboom and Gill
Da	Daltons
DSS	4, 4 – dimethyl-4-silapentane-1-sulfonic acid
EI	Electron ionisation
ESI	Electrospray ionisation
ETP	Epidithiodioxopiperazine
FE	Facial eczema
GAM	Generalised additive model
GC	Gas chromatography
GDH	Glutamate dehydrogenase

GGT	Gamma-glutamyl transferase or γ-glutamyl transferase
Glo	Globulin
GPC	Glycerophosphocholine
GST	Glutathione S-transferase
H & E	Haematoxylin and Eosin
HDL	High density lipoproteins
HILIC	Hydrophilic interaction chromatography
HMDB	Human metabolome database
HPLC	High performance liquid chromatography
HSQC	Heteronuclear single quantum correlation
HSS	High strength silica
IFS	Institute of Fundamental Sciences
IVABS	Institute of Veterinary, Animal and Biomedical Sciences
JRES	J-Resolved spectroscopy
kHz	kilohertz
LC	Liquid chromatography
LDH	Lactate dehydrogenase
LDL	Low density lipoproteins
LIC	Livestock Improvement Corporation
MALDI	Matrix-assisted laser desorption/ionisation
Mgcv	Mixed GAM computational model
MHC	Major histocompatability complex
MPI	Ministry of Primary Industries
MS	Mass spectrometry
MS1	First mass spectrometer (in MS/MS series)
MS2	Second mass spectrometer (in MS/MS series)

MS/MS (MS^2)	Tandem mass spectrometry
MW	Molecular weight
MVA	Multivariate analysis
m/z	Mass to charge ratio
NAD+	Nicotinamide adenine dinucleotide oxidised form
NADH	Nicotinamide adenine dinucleotide reduced form
NMR (^1H)	Proton nuclear magnetic resonance
NOESY	Nuclear overhauser effect spectroscopy
NP	Normal-phase
NZ	New Zealand
NZIER	New Zealand Institute for Economic Research
NZVP	New Zealand Veterinary Pathology
OCT	Ornithine carbamoyl transferase
OPLS-DA	Orthogonal partial least squares-discriminant analysis
PAR	Pareto scaling
PCA	Principal components analysis
PCV	Packed cell volume
PLS-DA	Partial least squares-discriminant analysis
ppm	parts per million
RF	Radio frequency
ROS	Reactive oxygen species
RP	Reverse-phase
RT	Retention time
SDA	Shrinkage discriminant analysis
SCC	Somatic cell count
Spp	Species pluralis

SPS	Sire proving scheme
SW	Spectral width
TCA	Tricarboxylic acid cycle
TMAO	Trimethylamine N-oxide
TOCSY	2D ^{1}H - ^{1}H total spin correlation spectroscopy
TP	Total protein
TSP	3-(trimethylsilyl) propanoic acid
UPLC	Ultra performance liquid chromatography
UV	Univariate scaling
VIPcv	Variable importance in projection cross validation
VLDL	Very low density lipoproteins

Chapter 1

General Introduction

1.1 Facial eczema

Facial eczema (FE), sometimes referred to as pithomycotoxicosis or sporidesmin intoxication, is a hepatogenous photosensitisation disease of ruminant livestock. It is of major economic and animal welfare importance in New Zealand (NZ). It is caused by ingestion of the mycotoxin, sporidesmin A, held within spores of the saprophytic fungus *Pithomyces chartarum* which grows on pasture litter during late summer and autumn (Di Menna *et al.*, 2009). Damage caused by this mycotoxin to the hepatobiliary system, leads to the retention of phytoporphyrin, a breakdown product of chlorophyll, which reacts with light in peripheral tissues, causing the photosensitivity reaction, known as FE. Photosensitisation is a condition in which an animal becomes hyper-reactive to light of certain wavelengths because of the presence of a photodynamic agent in skin capillaries and/or cells. This substance may be from an ingested plant or drug, contact with certain plants or drugs, or congenital abnormalities in endogenous pigment metabolism. This accentuated response to light leads to a change in the integrity of non-pigmented (white) and/or exposed skin on the animal, such as the udder (Galitzer & Oehme, 1978; Radostits *et al.*, 2000). FE primarily affects cattle, sheep, goats, deer, and alpacas (Smith & Towers, 2002).

Facial eczema was first reported in New Zealand by Gilruth (1897) and although much work has been carried out since then, allowing the identification of the causative agent and an increased understanding of the pathogenesis of the disease, there is still much to be discovered. In addition, preventive methods have been devised and applied, but these have shortcomings; for example, prophylactic zinc administration can lead to toxicity and/or environmental pollution (Towers & Smith, 1978).

With the advent of new technologies for the analysis of biological material, there is potential for new discoveries. This thesis reports on the use of traditional metrics such as liver enzyme activities, as well as fluorescence analysis, nuclear magnetic resonance (NMR), ultra performance liquid chromatography (UPLC) coupled with Mass spectrometry (MS), and UPLC tandem MS (MS/MS) in the search for metabolites in serum, urine, and milk, that could potentially be used as diagnostic markers of early stage and/or subclinical FE in lactating dairy cows.

1.1.1 Nomenclature

Facial eczema is a secondary (hepatogenous) photosensitivity disease of ruminants. It was so named because the first identified affected animals, sheep, showed the development of photosensitivity as facial lesions. However, the name is a misnomer, as the lesions are not primarily localised to the

face, but can extend to any or all non-pigmented or exposed areas of skin, including the udder, vulva, escutcheon, ears, tongue and around the eyes. The term eczema is also misleading and ill-defined, and it has been suggested that photodermatitis may be a better choice (Di Menna *et al.*, 2009). Other terms, such as pithomycotoxicosis have also been proposed, but the use of 'facial eczema' has embedded itself firmly in farming vocabulary and scientific literature. It is well known in these fields what facial eczema represents, and therefore this term, and abbreviation, FE, will continue to be used throughout the present work.

1.1.2 Early work on facial eczema in New Zealand

Gilruth (1908) initially described only hoggets and two-tooth sheep as being affected. However in 1910, all classes of sheep were found to be suffering during an FE outbreak. Affected sheep exhibited signs of exudation and swelling around the ears and head. Over the following years it was observed that cattle were also affected by FE. Gilruth (1908) established that the disease was not infectious and years later Hopkirk (1936) recognised that the lesions were a photosensitive reaction to light associated with severe liver injury of unknown cause. He reported that the photosensitisation only occurred under particular weather conditions; where a dry period was followed by a downfall of rain, with fast growing pastures (Hopkirk, 1936). Additionally, it was found that soil and air temperatures were higher in years when outbreaks occurred (Cooper & Walker, 1940). It was observed, by means of post-mortem examinations, that animals with no liver damage and/or normal thickness bile ducts did not appear to have suffered photosensitivity of any kind (Perrin *et al.*, 1953).

The first 50 years of FE research focused primarily on supplementing knowledge on the pathology of the disease, the environmental conditions before and during outbreaks, and the search for a causative agent. It was thought that the latter was likely to be of plant origin, and early investigations included sampling of 'toxic' pastures. At that stage, research was somewhat unfocused, but primary research areas developed at the Department of Agriculture laboratories in Wellington, and stations at Ruakura (Waikato) and Manutuke (Gisborne), where FE outbreaks seemed to be prevalent (Di Menna *et al.*, 2009).

It was soon realised that the visible skin lesions were secondary to primary disease-causing lesions in the liver. This observation, correlated with high serum levels of bilirubin and phytoporphyrin (previously known as phylloerythrin), led Cunningham *et al.* (1942) to conclude that the photodynamic agent responsible for the photosensitisation was phytoporphyrin. This was confirmed by Clare (1944) who carried out analyses on serum and urine of natural cases during a

major outbreak in 1938, as well as more intensive studies during incidences in 1940 and 1941. Additional experiments demonstrated the photosensitising potency of phytoporphyrin, where a single intravenous injection of 0.6 mg/kg was sufficient to cause marked photosensitivity in sheep (Clare, 1944). Cunningham e*t al.* (1942) were the first to describe, in detail, the clinical, pathological and biochemical characteristics of FE in sheep.

1.1.2 Classification of photosensitivity

Clare (1952) produced a review of general photosensitisation of domestic animals. In 1955 he expanded on this, with the definition of three photosensitisation categories: primary (type I) photosensitivity, photosensitivity associated with aberrant pigment synthesis (type II, often known as congenital porphyria), and hepatogenous or secondary (type III) photosensitivity (Clare, 1952).

In primary (type I) photosensitivity, the photodynamic agent is usually a pigment, ingested or administered, which is absorbed unchanged from the gastrointestinal tract. Certain fluorescent dyes may also act as photodynamic agents when injected into the body. This photodynamic agent is not completely excreted or detoxified by the unimpaired liver and thereby accumulates in the body (Clare, 1952; Towers & Smith, 1978). The pigment or dye travels within the peripheral circulation to the skin (Kellerman *et al.*, 2005), where it reacts with light (Di Menna *et al.*, 2009; Towers & Smith, 1978). The known causes of primary photosensitivity include St John's wort (*Hypericum perforatum*), containing the compound hypericin, which causes poisoning in sheep (Bourke, 2003; Cunningham *et al.*, 1942) and calves (Araya & Ford, 1981), buckwheat (*Fagopyrum esculentum*) which contains fagopyrin (Clare, 1955; Di Menna *et al.*, 2009), and a range of plants containing furanocoumarins (Campbell *et al.*, 2010).

Type II photosensitivity is where a sensitizing agent is produced within the animal as a result of aberrant pigment synthesis or metabolism (Clare, 1952; Clare, 1955). Two examples of this are known to occur in cattle. The first is congenital bovine erythropoietic porphyria, otherwise known as 'pink tooth' (Tennant, 1998). This is where uroporphyrins and coproporphyrins accumulate in the body as a result of defects in the pathway of haem synthesis (Tennant, 1998). This photosensitivity is rare, but has been reported in a number of cattle in countries such as South Africa (Clare, 1955; Glenn *et al.*, 1964), and Australia (Seawright & Watt, 1972). The second example is bovine erythropoetic protoporphyria (EPP), which has been diagnosed in Limousin cattle in NZ. This is an uncommon genetic defect in Limousin and Blonde d'Aquitane cattle, characterised by severe photosensitisation (McAloon *et al.*, 2015; Pence & Liggett, 2002; Tennant, 1998).

The majority of photosensitivity diseases are hepatogenous (type III), where the photosensitivity develops secondarily to, and as a direct result of, liver damage, causing disturbances in hepatic function (Clare, 1952). Such liver damage may be caused by a plant poison or a mycotoxin. Hepatogenous photosensitisation is divided into two general groups: 1) that in which the parenchyma of the liver is affected, for example ngaio (*Myoporum laetum*) poisoning, and 2) that in which the biliary system is primarily affected, for example FE (Kellerman *et al.*, 2005). In both cases the liver damage results in the retention of phytoporphyrin, the photodynamic agent, which is a natural metabolite derived from the degradation of chlorophyll *a* by anaerobic microbial fermentation in the rumen of ruminant animals (Scheie *et al.*, 2002).

In addition to these three categories of photosensitisation, seemingly random cases of photosensitivity in grazing livestock are grouped under idiopathic (type IV) photosensitivity, with unknown cause (Clare, 1952). Such outbreaks are generally sporadic and a great source of frustration to farmers and veterinarians alike (Campbell *et al.*, 2010). Although it is likely that the large majority of these are of the primary photosensitivity type, since icterus is usually not observed, it is possible that some will belong to the hepatogenous group (Clare, 1952; Clare, 1955). Examples of idiopathic photosensitivities are trefoil dermatitis (clover disease) and spring eczema in weaned calves and adult cattle grazing NZ pastures during spring time (Campbell *et al.*, 2010; Collett *et al.*, 2008). Photosensitivity following grazing of *Brassica* spp. crops by cattle and sheep has previously been considered to be idiopathic (Clare, 1955; Morton & Campbell, 1997), however, recent studies have shown that photosensitisation in cattle grazing crops, such as turnip, rape and swede, is hepatogenous (type III) (Collett & Matthews, 2014).

1.1.3 Distribution and economic importance

Pithomyces chartarum has a world-wide distribution; however not all strains produce sporidesmin. This means that in many countries where *P. chartarum* is present, FE does not occur because the strains are non-toxic (Collin & Towers, 1995b; Fitzgerald *et al.*, 1998). However, FE has been reported as an outbreak disease in farm animals grazing improved pastures in a number of temperate climate zones of the world. Outbreaks in sheep have been reported in Australia and South Africa (White *et al.*, 1977), France (Bezille *et al.*, 1984), Portugal (Pinto *et al.*, 2005), United States of America (Hansen *et al.*, 1994) and Turkey (Ozmen *et al.*, 2008). While outbreaks in dairy cattle are less commonly reported, they have been observed in Argentina and Uruguay (Collin *et al.*, 1998b).

Facial eczema is seasonal, with the warm, humid conditions in late summer and autumn in NZ (February to May) being optimal for the rapid growth and sporulation of the fungus on improved pastures in the lower-lying areas of the North Island of NZ (Clare, 1955; Cullen *et al.*, 2006; Morris *et al.*, 1990) and some northern regions of the South Island (Collin *et al.*, 1998a). Sporulation requires humidity levels of more than 90 % and air temperatures of 10 - 30 ^{o}C, with 24 ^{o}C found to be optimal (Barr, 1998; Collin *et al.*, 1998b). It is because of these requisite conditions that FE is more prevalent in the North island (Di Menna *et al.*, 2009). During these months the combination of an increase in toxin production, higher levels of leaf litter on the pastures and intensive farming procedures lead to an increase in the quantity of toxin ingested by livestock. The pastures on which FE outbreaks occur commonly comprise predominantely perennial ryegrass (*Lolium perenne*) and white clover (*Trifolium repens*) (Clare, 1955). The prevalance of toxic pastures varies within a topographical region, and even between paddocks on a single farm. This, combined with weather variance and differences in susceptibility between animals and breeds, helps to account for the sporadic nature of the disease (Towers & Smith, 1978).

The fungus grows saprophytically on dead litter at the base of the grass sward, and spores are transported by wind and/or water to the surfaces of the pasture where they adhere (Kellerman *et al.*, 2005). Reported spore counts from pasture samples can vary from below 5,000 spores/g fresh grass to > 3,000,000 spores/g (Smith, 2000). Animals may be exposed to potentially toxic pastures for periods of weeks or months, which could mean that even levels of spores which would be considered to be insignificant may be cumulative, building-up damage to the liver, and subsequently producing what is essentially the same effect as a large dose of spores. Smith (2000) showed that the low daily dose rates, between 0.0042 and 0.0167 mg/kg bodyweight, administered over 6 days per week, for 8 weeks, more closely approximate the level of sporidesmin exposure likely in field outbreaks of FE. He saw similar effects on the bodyweight and organs of the dosed animals irrespective of whether they exhibited photosensitivity or not. This reinforces the potential animal welfare importance of FE; not only can the severe clinical signs lead to death, but also the subclinical effects over a period of time.

Facial eczema is the most important pasture-associated mycotoxicosis found in NZ (Collin & Towers, 1995a; Towers, 1986). In terms of economic impact, it is second only to nematode parasitism (Collin *et al.*, 1998b; Mortimer *et al.*, 1978b). The high prevalence in NZ is partially due to the highly efficient use of improved pastures (Mortimer *et al.*, 1978a), humid autumn weather, and the presence of the toxic isolate of *Pithomyces*; these factors in combination are not found in many other countries.

As FE is severely production-limiting it proves costly for NZ pastoral agriculture as well as having lasting detrimental impacts on animal welfare (Morris *et al.*, 2004). The disease has been calculated to cost the dairy industry between $6.8M and > $84.2M per annum (Morris *et al.*, 2007), and sheep farmers in excess of $63M per annum (Morris *et al.*, 2004). The dairy figures are based on a four year monitoring program of Manawatu and Taranaki regions and uses 2007 milk values. Using inflation rates from the 2007 first quarter to the 2015 first quarter, the present overall cost to the dairy industry can be estimated at $8M to > 99.6M. The sheep figures are based on data collected during the 1983-1988 seasons (Collin *et al.*, 1998a), and therefore can themselves only be used as an estimate of today's losses (est. $74.5M first quarter 2015). In addition, the cost to beef cattle, deer, and alpaca farmers has not been taken into account. Climatic changes, which have increased the length of the FE season and extended the spread across the country, also need to be considered. The wide range in these estimates reflects the importance of year to year climatic conditions on fungal spore counts and the consequent prevalence of facial eczema. Additionally, a DairyNZ report and SFF project report state that only 10 % of affected animals present clinical signs, indicating, for every clinical case, ten cows will have subclinical FE, which is much harder to identify (Morris, 2011; *New Zealand Dairy Statistics*, 2012-2013).

The dairy sector contributes significantly to the NZ economy as well as international economies. In NZ, the dairy farming and overall agricultural sector are the backbone of the national economy, and the source of livelihood for farmers globally (Schilling *et al.*, 2010). The Ministry for Primary Industries (MPI) reports that NZ accounts for around one third of global trade in dairy products, with exports to 151 countries in 2009 (MPI, 2010; Schilling *et al.*, 2010). In addition, NZ dairy production has risen 77 % over 20 years since 1989, with cow numbers increasing from three million in 1989 to more than six million in 2009 (Dillon, 2011).

The NZ Institute for Economic Research (NZIER) report to Fonterra and DairyNZ following the end of the 2010 season, states that the dairy sector directly added around $5 billion (~ 2.8 % of GDP) of value to the NZ economy (Schilling *et al.*, 2010). By way of comparison, this contribution accounts for over one-third of the GDP of the entire primary sector, which includes dairy and meat farming and processing, horticulture, fishing, forestry and mining. Furthermore, these figures exclude indirect and induced effects on the NZ economy, such as those accrued via supporting industries - through fertiliser, agricultural services, transport, or veterinary services (Schilling *et al.*, 2010).

There has been an assiduous drive to enhance dairy productivity at all levels of the sector, to continually meet the demands of expanding populations and the consumer driven increase in desire for good quality dairy products that follow more comprehensive animal welfare codes. The NZ dairy

industry has been a world leader in herd improvements, with the Livestock Improvement Corporation (LIC) and DairyNZ introducing processes for recording and tracking the performance of the national herd, through dairy core databases (Schilling *et al.*, 2010).

1.1.4 Sporidesmin

A study on samples of stored toxic pasture associated with natural outbreaks of FE illustrated that toxicity was retained (Clare *et al.*, 1959). Evans *et al.* (1957) showed that guinea pigs fed these stored samples developed liver damage. Also using guinea pigs, White (1958) produced an extract from these pastures using column chromatography. The extracted substance was non-toxic in itself, but appeared to be present when photosensitivity occurred, and for this reason was used to form the basis of the 'beaker test' to assess the presence of toxicity in pastures (White, 1958). The nature of this extract resembled products isolated from other fungi, which suggested that it was of fungal origin. This was the first indication of a link between FE and fungi in pastures (Russell, 1960). The extract was identified as sporidesmolide ($C_{33}H_{58}N_4O_8$), and this along with other analogues were classified as depsipeptides, emphasising their analogy to both depsides and peptides (Russell, 1960). A depside is considered to be a polyphenolic compound composed of two or more monocyclic aromatic units which are linked by an ester bond. Russell (1962) identified the structure of sporidesmolide I as well as other metabolic products of *P. chartarum*. The first isolation of the causative fungus occurred in 1958, when the fungus was initially identified as *Stemphylium*, then *Sporidesmium bakeri*, until finally its taxonomy was confirmed in 1960 as *P. chartarum* (Ellis, 1960). *P. chartarum* gave a positive beaker test and it was shown that clinical cases of FE could be produced by exposing lambs to *P. chartarum* extracts (Percival, 1959). The causative toxin was isolated from *P. chartarum* cultures and was named sporidesmin (Synge & White, 1959). Following this, its structure and conformation were determined (*Figure 1.1*), and procedures for the efficient extraction of sporidesmin from toxic pastures for use in future studies were refined.

1.1.4.1 Sporidesmin variants

P. chartarum produces seven structural variants of sporidesmin, of which sporidesmin A (*Figure 1.1*), the toxin causing hepatobiliary damage in FE, accounts for 80 - 90 % of the total sporidesmin produced by this fungus (Atherton *et al.*, 1974). The remainder are small amounts of sporidesmins B, C, D, E, F, G, H and J (Mortimer & Smith, 1983). Of these derivatives, only analogues B and E are known to be toxic to sheep. Due to their low level of production in *P. chartarum*, they have not been considered to be important in the hepatotoxicity found with FE (White *et al.*, 1977).

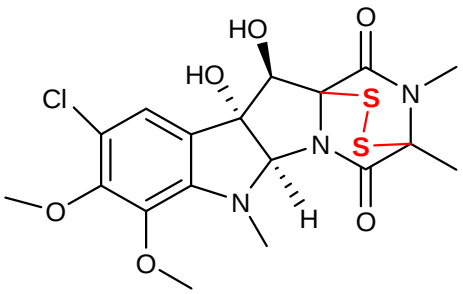

Figure 1.1 Sporidesmin A structure ($C_{18}H_{20}ClN_3O_6S_2$)**.** Showing the disulfide bridge (-S-S-) which bestows the molecule with the ability to produce reactive oxygen species in a cyclic manner.

1.1.4.2 Toxicity and mode of action

Facial eczema is a two step disease, with the first step involving ingestion and absorption of sporidesmin and subsequent tissue injury by this toxin to the hepatobiliary system. Step two is the retention and accumulation of phytoporphyrin in the blood due to a reduction in phytoporphyrin excretion in bile brought about by the damage to the biliary system.

Sporidesmin is an epidithiodioxopiperazine (ETP) mycotoxin. These compounds are characterised by the presence of a diketopiperazine ring with an internal disulfide bridge (*Figure 1.1*). It has been demonstrated that the cytopathogenic activity of sporidesmin that leads to hepatobiliary damage is due to the disulfide-bridged ring system of sporidesmin A (Jordan & Pedersen, 1986). Theories have been put forward to explain how the toxicologically active sulfurs may interact with the target tissues, including the interaction with the thiol groups of membrane proteins and cytoskeletal microfilaments (Jordan & Pedersen, 1986), and the production of reactive oxygen species (ROS) which are toxic to living cells (Munday, 1982). Jordan and Pederson (1986) reported that sporidesmin induces the detachment and vacuolation of cultured liver cells, and showed that these processes are preceded by disruption to the microfilaments of cells.

The disulfide bond in sporidesmin has been shown to be readily reduced to its dithiol analogue (Di Menna *et al.*, 2009). The dithiol undergoes auto-oxidation to regenerate sporidesmin (Munday, 1982), mediating the reduction of molecular oxygen to the superoxide anion (O_2^-) which is toxic to many biological systems (Halliwell & Gutteridge, 1999). This redox cycling between the thiol and disulfide means that a single molecule of sporidesmin can catalyse the production of multiple superoxide molecules. Inflammatory changes and necrosis to the hepatobiliary system, followed by peribiliary fibrosis and bile duct occlusion have been shown to be precipitated by sporidesmin free radical propagation (Barr, 1998; Munday, 1989). Enzymes that are activated during the process of liver damage include γ-glutamyl transferase (GGT) and glutamate dehydrogenase (GDH), which are

released with damage to the biliary epithelium and hepatocytes, respectively (Clark *et al.*, 1988). The release of these enzymes is considered to be due to an increase in the permeability of the cell membrane (Clark *et al.*, 1988), which may be brought about by a combination of damage by the superoxide molecules and the disruption of microfilaments in cells.

1.1.5 Phytoporphyrin toxicity and mode of action

Phytoporphyrin is a derivative of chlorophyll (Marchlewski, 1904). Fischer *et al.* (1931) validated this, showing the breakdown pathway of chlorophyll to phytoporphyrin, with the removal of the phytyl chain, the carbomethoxy group and the magnesium atom, leaving the isocyclic ring unbroken (*Figure 1.2*).

When the phytoporphyrin accumulates in the dermis and is exposed to visible light in the unprotected and/or non-pigmented areas of the skin it absorbs light between 422 and 424 nm and enters a higher energy state. When the molecule returns to its ground state, energy is emitted either in the form of fluorescence or passed onto other molecules with which they collide, thereby activating them (Clare, 1952). Collisions of these secondarily activated molecules creates free-radical chain reactions (Galitzer & Oehme, 1978). The singlet oxygen and other ROS produced through these redox reactions elicit oxidative changes to the unsaturated lipid components of cells in the skin and adjacent tissues leading to cell damage, leakage, and necrosis, and to the clinical signs of FE (Scheie et al., 2002).

Galitzer and Oehme (1978) state that the amino acids histidine, tryptophan, and tyrosine are oxidised by these chain reactions, thereby weakening cell structure. Porphyrins are thought to concentrate within lysosomes and destroy the integrity of the lysosomal membrane, which increases the permeability of the membranes and causes leakage of lytic enzymes into the cell (Galitzer & Oehme, 1978), which would act to increase the already toxic effects of ROS on the breakdown of cell integrity. The unsaturated lipid components of cell walls undergo alterations which result in the rupture of cells and the release of the hydrolytic enzymes and chemical mediators of inflammation into the surrounding tissues, leading to increased vascular permeability and the associated changes characteristic of photosensitisation. It has been shown by Scheie *et al.* (2002) that phytoporphyrin localizes in the Golgi apparatus and/or mitochondria, which may act to enhance its cytotoxic effect. A phytoporphyrin-excreting mechanism has been postulated by Johnson (1982), but no strong evidence has been reported.

Metabolic Degradation of Chlorophyll

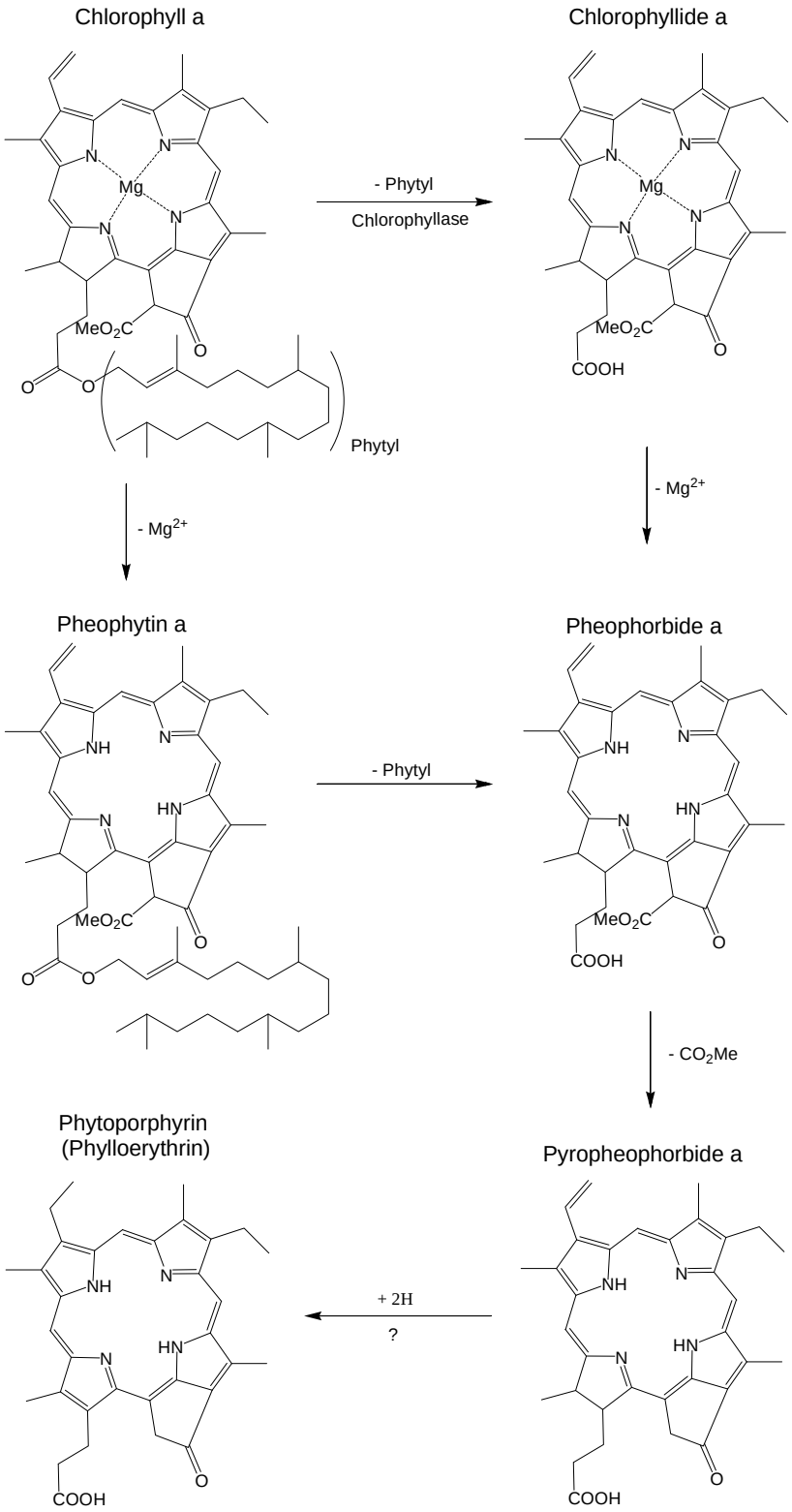

Figure 1.2 Degradation of chlorophyll *a* ***(****Campbell* et al*., 2010)*

1.1.6 Clinical signs of facial eczema

It has been shown that ruminants are the most susceptible species, including sheep, cattle, fallow deer, red deer, and goats (Radostits *et al.*, 2000; Scheie & Flåøyen, 2003; Smith & Embling, 1991); additional, cases of facial eczema have been reported in alpacas (Campbell *et al.*, 2010; Smith *et al.*, 1998). Fallow deer, sheep and alpacas are considered the most susceptible species (Smith *et al.*, 1997). All species are affected in a similar manner. Initial signs include transient diarrhoea, a drop in milk production, weight loss and, if animals become clinical, variable photosensitivity (Cullen *et al.*, 2006; Morris *et al.*, 2004; Morris *et al.*, 1991b; Towers, 1978). Photosensitised skin is characterised by a severe inflammatory reaction with marked oedema associated with an increase in capillary permeability (Galitzer & Oehme, 1978). When photosensitisation develops, animals become restless, show pruritus and general irritation, seek shade and shake their heads, ears and body (Galitzer & Oehme, 1978; Smith & O'Hara, 1978). Animals can become inappetant and lethargic. Affected tissues include the skin which is non-pigmented or exposed, such as around the eyes, face, ears, muzzle, teats, udder (*Figure 1.3*), vulva, and escutcheon, as well as the ventral tip of the tongue. Areas of the body that have light coloured hair are also affected, such as in Friesian cattle with white patches over their body. Jaundice can develop one or two days after the appearance of the first clinical signs and lesions in the urinary tract can also occur (Mortimer *et al.*, 1978a).

1.1.7 Clinical biochemistry of facial eczema

It has been demonstrated that increases in GGT activities are proportional to the severity of sporidesmin-induced liver damage (Towers & Stratton, 1978), with activities of GGT in serum rising 7 - 14 days after any sporidesmin challenge (Morris *et al.*, 2004). Serum GGT is a sensitive marker for bile duct damage and cholestasis, and although it is a specific marker for liver damage, it is not specific to FE (Morris *et al.*, 2004). It has a slower rate of increase in serum than the parenchymal enzymes, such as GDH, and its elevation remains sustained for longer and is therefore considered to be the most reliable indicator. However, elevations in liver enzymes can often be seen with minor liver dysfunction of any nature. A more reliable and specific indicator of FE itself would be useful for confident diagnosis of the disease and for continued work in improving advances in this area.

Figure 1.3 Cattle clinically affected by facial eczema in New Zealand

1.1.8 Pathology of facial eczema

Sporidesmin is readily absorbed from the intestine and transported to the liver by the portal venous blood where it concentrates in hepatocytes and is excreted largely in the bile (Towers, 1970). Sporidesmin causes inflammation and necrosis of medium and larger bile ducts and proliferation of granulation tissue, which results in cholestasis. Following damage to the bile ducts, substances which are normally removed in bile, gain entry to the circulatory system (Dodd, 1959).

Prior to the discovery of the causative agent, the pathology of field cases had been reasonably well described (Hopkirk, 1936). Dried toxic pastures fed to guinea pigs produced the same lesions as those seen in field cases of FE (Perrin, 1957; White, 1958). Following the discovery of sporidesmin, studies were carried out where the toxin was fed directly to sheep with the same or similar lesions developing (Done *et al.*, 1961; Leaver, 1968).

The liver appears blotched and discoloured due to the retention of bile pigments, and there is thickening and partial, or full, occlusion of intra-hepatic bile ducts (Clare, 1952; Di Menna *et al.*, 2009). The left (ventral) lobe of the liver, which is commonly more affected, is often atrophied, and the whole liver may be cirrhotic and distorted (Clare, 1952). An increase in the weight of hepatic lymph nodes and the presence of oedema were reported by Smith (2000) following sporidesmin intoxication in sheep. It was suggested that this may be due to injury to the extra- and intra-hepatic biliary system.

Sporidesmin is highly active and produces inflammation and destruction of tissues wherever it becomes sufficiently concentrated. This occurs firstly in the bile ducts as they channel the toxin for removal into the intestine. When the toxin becomes highly concentrated during high risk periods of FE, the bile ducts become severely injured with necrosis of the epithelium (Hopkirk, 1936; Mortimer *et al.*, 1962). The damaged areas are infiltrated by granulation tissues during the repair process and this leads to the obstruction of the bile ducts, restricting bile flow, leading to even more concentrated sporidesmin levels, and the retention of phytoporphyrin that then overflows into the bloodstream. Following bile duct obstruction, sporidesmin build-up leads to hepatocellular damage and subsequent repair results in severe liver damage and further retention of phytoporphyrin (Mortimer *et al.*, 1962).

Other lesions include necrosis of liver cells, bile duct obstruction, inflammation of hepatic arterioles and portal vein branches and inflammation of the urinary bladder epithelium (Cunningham *et al.*, 1942). Early skin changes include erythema, swelling and serum leakage in the skin. Some thickening of the skin, as well as scab formation and loss of hair can ensue (Smith & O'Hara, 1978; Wyllie & Moorehouse, 1978), followed by necrosis and sloughing of the affected area in severe cases. This leaves open wounds which are susceptible to secondary infection and flystrike.

1.1.9 Treatment and prevention of facial eczema

There is essentially no effective treatment for FE once cellular damage and photosensitivity have occurred; all that can be done is alleviating the pain and discomfort to the animals, providing shade and reducing chlorophyll intake (provision of hay or silage).

Ideally, prevention of this disease is the goal, with a number of methods presently available, including pasture management or modification, avoidance/removal strategies, alternative crop use, fungicide application to pasture, zinc prophylaxis, and genetic selection for resistance. Progress has been made in these areas over the years, but none of these are 100 % effective and are often costly and time consuming for farmers, adding to the cost and frustration created by this disease.

The earliest control methods for FE involved the avoidance of suspected toxic pastures during high risk times of the year. The identification of such pastures is simplified by pasture and/or faecal spore counting (Towers, 1986). Studies on pasture spore counts have revealed that they are closely correlated to the severity of intoxication (Barr, 1998). Animals generally become affected when spores reach levels greater than 50,000 g fresh grass and will show clinical signs after several weeks of grazing at this level. Animals grazing on pastures with counts of 200,000 to 300,000 spores/g fresh grass become affected after only a few days of exposure (Barr, 1998). Spore counts have been suggested to give inaccurate estimations of pasture toxicity, so immunoassays were developed to detect sporidesmin in pasture, to improve monitoring of pasture toxicity (Collin *et al.*, 1995). Once high spore counts have been identified, stock can be moved to less improved pastures on hill country or peat land, both of which are considered to be safer (Towers, 1986). Stock can also be turned onto uncontaminated supplementary crops, such as forage brassica (Clare, 1955). However, the latter raises another issue as photosensitisation, unrelated to FE, has been shown to develop when animals are exposed to certain brassica crops (Collett & Matthews, 2014). Although spore counting is considered to be a useful and simple tool for identifying risk periods, it also has its limitations. For example, often only one or two paddocks across the farm will be chosen for spore counting during the risk season. Because the prevalence of spores can vary between paddocks, implicated paddocks may be missed completely. In addition, there are breed and individual animal variations in response to levels of sporidesmin (Smith, 2000). So although spore counts may be at a minimum in the measured pastures, certain animals may still become affected, especially with regards to the development of subclinical FE. It has been shown by Mortimer *et al.* (1978b) that if animals are housed and given complete protection at the first sign of photosensitisation, the mortality can be halved, but this is not always a viable option for many farmers, and is only helpful to clinical animals, not subclinical cases which can develop further. The use of alternative pasture species may reduce the number of *P. chartarum* spores in pasture, however this is still a method of control which is under investigation (Collin *et al.*, 1998b).

Benzimidazole fungicidal spraying at 140 - 280 g/hectare every four to six weeks prior to and during the risk period has been shown to be successful in suppressing the growth of *P. chartarum* and

therefore reducing the number of toxin-containing spores in the pasture (Di Menna *et al.*, 2009; Smith & Towers, 2002). However, the growing ineffectiveness and expense of these methods makes them less favoured now.

The introduction of an atoxigenic strain of *P. chartarum* to outcompete or displace naturally occurring toxic strains with the aim of reducing toxin levels in pasture has been trialled. Laboratory investigations found that toxin production is decreased when sporidesmin-producing strains are co-cultured with non-sporidesmin-producing strains (Collin & Towers, 1995a). Preliminary field trials established the same results early in the summer (Fitzgerald *et al.*, 1998). However, the untreated plots also showed minimal spore counts, so further trials were required to determine the efficacy of this method as a biological control (Fitzgerald *et al.*, 1998). As far as I am aware, no further work on this has been published.

The administration of high doses of zinc (15 - 30 mg/kg liveweight/day) to animals via zinc oxide drenching , the addition of zinc sulphate to drinking water supplies (Smith *et al.*, 1983), or controlled release of zinc oxide through intraruminal devices, otherwise known as zinc boluses (Collin *et al.*, 1998b; Grace *et al.*, 1997; Munday *et al.*, 1997), either at or before the risk period of exposure, has been shown to reduce liver injury and production losses by 60 - 90% (Smith & Towers, 2002). The zinc boluses have become popular, primarily due to their consistent release of zinc over long periods, which additionally helps to overcome deficiencies in zinc administration (Munday *et al.*, 1997; Munday *et al.*, 2001). The exact mode of action of zinc supplementation is unclear. It is commonly considered that zinc forms a stable thiolate with the reduced dithiol group of sporidesmin which prevents this entering the auto-oxidation cycle, thereby inhibiting the generation and release of the hepatotoxic ROS (Collin *et al.*, 1998b; Munday, 1984a). The prophylactic effect of zinc is suggested to be related to its ability to inhibit intestinal absorption of copper which strongly catalyses the reaction (Munday, 1982). A decrease in copper limits the catalysis of zinc, and may also bind with reduced sporidesmin preventing its autoxidation (Munday, 1984b; Munday & Manns, 1989). Zinc is toxic at high doses and it has been suggested that products such as zinc sulphate should not be used due to the narrow margin between therapeutic and toxic doses (Smith *et al.*, 1978). For best protection, zinc doses should be provided daily. Drenching of large herds is not practicable; however, slow-release boluses do provide protection for 4 - 6 weeks. This does mean that bolus administration is needed more than once during a risk season, and although reasonably effective this again is costly. The application of zinc sulphate to the water supply has been shown to be effective; however, the dose of zinc ingested by each animal depends on the amount of water consumed and this is difficult to control. In addition, each animal, due to varying susceptibility and

metabolism, should require appropriate doses of zinc to provide adequate protection, which cannot be assured with water trough applications.

Immunisation against sporidesmin has been investigated. However, it is non-antigenic, and any attempts to combine sporidesmin with larger molecules to induce antibody production have given weak protection against toxicity (Fairclough *et al.*, 1984).

The response of individual animals to sporidesmin challenge varies greatly, which suggests that some animals are inherently resistant to sporidesmin while others are less so (Smith & Towers, 2002). It has been shown that there is a significant genetic component in resistance to facial eczema (Duncan *et al.*, 2007). Studies have indicated that facial eczema resistance or susceptibility is a heritable trait in sheep (0.42 ± 0.09) (Morris *et al.*, 1995), and three dairy industry studies have also shown this for cattle (Morris *et al.*, 1991a; Morris *et al.*, 1990). Cattle are usually less susceptible to facial eczema than sheep. Heritability in Friesian cattle has been reported to be 0.29 ± 0.15 while estimates in Jersey cattle lie in the range of 0.77 ± 0.13 (Morris *et al.*, 1998). The performance or heritability tests for resistance use the response of serum GGT activity to sporidesmin dosing to detect and quantify the severity of subsequent liver damage (Collin *et al.*, 1998a; Smith & Towers, 2002).

1.2 Metabolomics and biomarkers

In recent years, studying biological systems in a holistic way has become more prevalent. Referred to as systems biology, this approach focuses on the study of interactions between the components of biological systems and how these give rise to the function and behaviour of that system in response to internal and external signals. These biological processes are complex, but can be understood by studying the structures and properties of specific molecules that are the building blocks of living organisms. These building blocks, in combination with information storage structures, such as organelles, cells and tissues, can be divided into four main biochemical components, the genes, transcripts, proteins and metabolites (Dunn *et al.*, 2011b). Genomics (the study of all genes present in a system), transcriptomics (the study of the expression of genes and how this is affected by genotype, environment, and disease), proteomics (the study of the expression and activity of proteins and how this is affected by genotype, environment and disease), and metabolomics (the identification and quantification of all metabolites and their relationships in a biological sample) are the main analytical technologies used to study systems biology.

Metabolites are unique in that they are the building blocks for all other biochemical species and structures including proteins (amino acids), genes and transcripts (nucleotides), and cell walls (Dunn

et al., 2011b). The metabolome is the final downstream product of the genome and is defined as the quantitative collection of all small molecular weight compounds (metabolites < 1500 Daltons [Da]) present in a biological system (Kouskoumvekaki & Panagiotou, 2011; Psychogios *et al.*, 2011). Metabolites can therefore provide information about the ultimate biochemical outcome of changes in the genome, transcriptome and proteome. As opposed to genomics, metabolomics can therefore more closely reflect the disease phenotype of an animal at a physiological level (Ellis *et al.*, 2007; Zheng *et al.*, 2012). Metabolic profiling can lead to higher diagnostic sensitivity and specificity for biomarker discovery and disease diagnosis.

Metabolomics is the study of all metabolites in a biological system, the metabolome, and the changes in these metabolites in relation to genetic and environmental perturbations (Dunn *et al.*, 2011b). Metabolites can be divided into two general groupings, primary and secondary, based on their various functions. Primary metabolites, of which there are more than 3,000 known, are directly involved in normal growth, development, reproduction and function, whereas secondary metabolites are not directly involved in these processes, but rather have important ecological functions, for example pigments as well as exogenous compounds such as antibiotics (Kouskoumvekaki & Panagiotou, 2011). Secondary metabolites are produced by a number of plants, bacteria, fungi, and animals, and can play a role in the overall biological state of a living organism. In some cases these metabolites can influence the vital functions of an organism and can represent serious risks to its integrity and health (Holcapek *et al.*, 2008). There can also be interactions between the metabolisms of two different organisms, such as those seen with the symbiotic relationship between the microflora of the mammalian gastrointestinal tract and the mammal itself (Dunn *et al.*, 2011b). Many of the secondary metabolites are unidentified, but could represent markers for disease state and provide a deeper understanding of the mechanisms of disease (Kouskoumvekaki & Panagiotou, 2011). Metabolomics is playing a huge role in the discovery of biomarkers and/or risk factors associated with specific diseases as well as enabling scientists to gain a greater understanding of the pathogenesis of diseases (Dunn *et al.*, 2011b).

The terms metabonomics and metabolomics are used interchangeably throughout the literature, with distinctions being more a matter of historical usage than meaningful scientific reasoning (Beger *et al.*, 2010; Robertson *et al.*, 2011; Zhang *et al.*, 2011). Some articles specifically distinguish between the two terms (Dunn *et al.*, 2005; Robertson *et al.*, 2011), but this distinction appears to be trivial, and for this reason as well as for simplicity, the term metabolomics will be used throughout this thesis and will be considered synonymous to metabonomics.

1.3 Analytical platforms

All of the techniques used to date for investigating photosensitivity diseases are not definitive . In addition, there are a large variety of these diseases seen in livestock, many of which have unknown causes, making it even more difficult to distinguish individual cases. These factors combine to complicate the issue and make it difficult to identify causes of unknown photosensitivities. This highlights the need for more specific, well-defined analytical techniques which are able to identify and distinguish disparity within and between the different types of photosensitivities and for discovering causative agents.

At the forefront of methods of choice for the early detection and evaluation of severity of disease is metabolomics, used to study, identify and map metabolites (Bruce *et al.*, 2009; Goldsmith *et al.*, 2010). Metabolomics technology applies advanced separation and detection methods to capture the collection of small molecules, present in biofluids, that characterise the metabolic pathways in a system (Kouskoumvekaki & Panagiotou, 2011). It can permit the potential identification and quantification of all metabolites in a system.

A number of analytical techniques, individually or combined, are routinely used to gather a vast amount of metabolite information quickly, with little sample preparation, to allow the profiling (types, quantities, ratios) of the metabolites. Data can then be assessed via statistical methods, such as principal component analysis (PCA), enabling differences in groups of metabolite profiles to be detected, and ultimately the identification of the metabolites responsible for these changes. Commonly used analytical techniques include the following (or a combination of):

- Fluorescence analysis
- Nuclear magnetic resonance (NMR) – primarily ^{1}H-NMR
- Mass spectrometry (MS) – including tandem MS (MS/MS)
- Chromatography (single and multidimensional – gels, gas phase chromatography, high pressure liquid chromatography (HPLC))

The majority of studies apply either MS or NMR spectroscopy as the analytical instrument of choice (Dunn *et al.*, 2011b). Mass spectrometry techniques are often coupled with chromatography to separate the metabolites. A brief description of each of these techniques follows. Additionally vibrational spectroscopy techniques such as Fourier transform infrared spectroscopy and Raman spectroscopy are utilised for metabolic profiling (Ellis & Goodacre, 2006; Madsen *et al.*, 2010). However, these techniques are not discussed here as the scope of the research didn't require the use of these methods.

1.3.1 Fluorescence

Current detection of photodynamic agents, including phytoporphyrin, that aid classification of photosensitivity diseases as either primary (type I) or secondary (type III), has relied on basic, well established analytical techniques like fluorescence spectroscopy.

Most photodynamic agents have functional groups, known as fluorophores, which absorb light energy of specific wavelengths and re-emit this energy at different, but specific wavelengths. Photodynamic agents have absorption spectra in the ultraviolet-A and the visible region (315 – 750 nm), bestowing them with their coloured or fluorescent nature (Galitzer & Oehme, 1978). Fluorescence spectroscopy is able to detect fluorophore-containing photodynamic agents that have been clearly identified as indicative or causative of a disease. These qualities have meant that fluorescence spectroscopy can be utilised to quantify emissive photodynamic agents present in a variety of biological fluids such as serum, plasma, urine and bile (Campbell *et al.*, 2010; Scheie *et al.*, 2003b).

While fluorescence spectroscopy has proven to be a reliable and rapid method for quantifying fluorophores present in biological samples, it does have its limitations. The fluorophore of interest must be known already to allow for excitation at a specific wavelength and it should be the only emissive species responsible for the emission peak being measured. The spectra should not be complicated by the emission(s) from other fluorophores present, thus hindering reliable extrapolation of data in these complex biological matrices. An example of these limitations would be from the present study where difficulties with phytoporphyrin (excitation 425 nm, emission 644 nm) analysis exist. Campbell *et al.* (2010) showed that the haemolysis of serum/plasma samples due to inadequate or unsatisfactory handling conditions, following collection, produces free haemoglobin (excitation 425 nm, emission 600 nm) (*Figure 1.4*). In addition, the complex protein matrices of serum/plasma show very large emission peaks that can obscure the analyte peak. The analysis of such spectra has to rely on complex extrapolation techniques to obtain quantitative data from the shoulder of the peak envelope, as seen in *Figure 1.5*.

It is also almost impossible to quantitate the molecules responsible for a particular spectral emission (Campbell *et al.*, 2010). This poses some limits for disease differentiation and the identification of unknown or novel compounds, hence other techniques need to be utilised. In addition it is still unknown whether phytoporphyrin is protein-bound in serum or plasma.

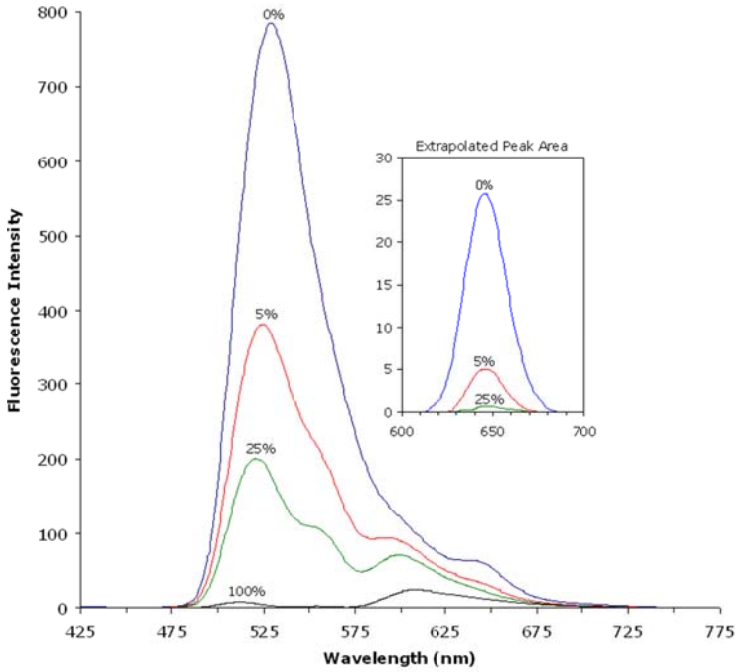

Figure 1.4 Fluorescence spectra of serum samples subjected to varying levels of haemolysis (0%, 5%, 25% and 100%) showing the effect of haemolysis (~600 nm) on the protein peak (~525 nm) and the phytoporphyrin peak (~ 647 nm). Insert: shows the extrapolated phytoporphyrin peak at varying levels of haemolysis (used with permission from Campbell *et al*., 2010) .

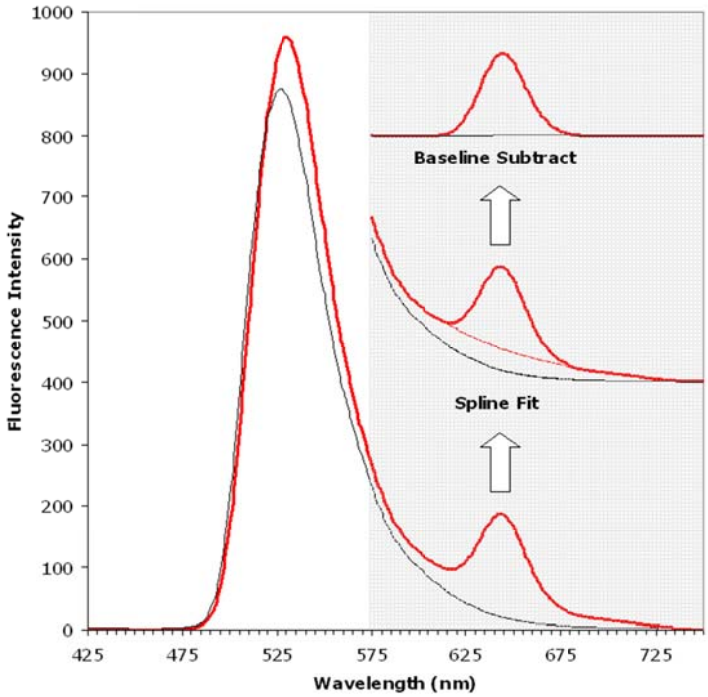

Figure 1.5 Fluorescence spectra of serum showing a normal (control) cow (black) and a FE affected cow (red) where the phytoporphyrin peak at 645 nm can be seen. The spline fitting and baseline subtraction of the phytoporphyrin peak is shown in the insert (used with permission from Campbell *et al*., 2010).

1.3.2 ^{1}H Nuclear magnetic resonance

^{1}H Nuclear magnetic resonance (NMR) is considered to be one of the most common analytical platforms for metabolic profiling (Beger *et al.*, 2010; Dunn *et al.*, 2005). NMR is based on the measurement of the radio frequency (RF) energy absorbed by an atomic nucleus in a strong magnetic field. Each nucleus has a charge and certain nuclei also have an intrinsic angular momentum called 'spin'. The combined spin and charge generate a magnetic dipole along the spin axis. When a sample is placed in a magnetic field these dipoles align to produce a net magnetisation parallel (for ^{1}H nuclei) with the magnetic field (Jacobsen, 2007). In the simplest case, a short pulse of RF energy is applied to the sample. This causes the sample magnetisation to rotate away from the equilibrium position and precess (change the orientation of rotation) around the axis of the spectrometer's magnetic field. The precessing magnetisation generates an oscillating voltage in a coil placed around the sample. Differing chemical environments will cause signals with differing frequencies (chemical shifts) to be detected. The intensity of a signal is directly proportional to the concentration of the atomic nuclei. These features are the basis for detecting, differentiating and quantitating different metabolites in a biofluid sample.

NMR has the capacity to detect hundreds of metabolites in biological samples. Its major advantages are: a) no requirement for the separation of analytes allowing simple sample preparation, b) ability to simultaneously quantify multiple classes of metabolites, c) high analytical reproducibility, and d) non-selectivity (Beger *et al.*, 2010; Goldsmith *et al.*, 2010; Klein *et al.*, 2010). It is also non-destructive allowing samples to be used for further analysis. Its main disadvantage is a relative lack of sensitivity, especially when compared with mass spectrometry. For example, for NMR if a metabolite is present in a sample at less than micromolar concentration then it will not be detected, while mass spectrometers using electrospray or MALDI ionisation could detect 0.01 – 0.025 mg/ml of 500 Da molecules in 20 - 50 μM of sample (Siuzdak, 1996).

The chemical shifts of some metabolites overlap, making them difficult to resolve with a high degree of certainty (Beger *et al.*, 2010). This can often be remedied using two dimensional (2D) NMR, with optional sample spiking using known standards.

Quality control with NMR is based primarily on: the use of buffers to reduce pH dependent chemical shift changes, measurement under identical conditions (especially temperature) and the referencing of peak positions to a signal from chemical shift standards such as 4, 4-dimethyl-4-silapentane-1-sulfonic acid (DSS) or 3-(trimethylsilyl) propionic acid (TSP) which are added to each sample (Beger *et al.*, 2010). Consistent sample and measurement conditions help to ensure that peaks from a particular metabolite always appear at the same chemical shifts.

1.3.3 Mass spectrometry

Mass spectrometers measure the masses and relative concentrations of molecules in a sample, and are therefore useful for quantifying changes in concentrations of metabolites, making this an invaluable analytical tool for metabolomics. MS has high selectivity and sensitivity and is able to provide molecular formulae (Goldsmith *et al.*, 2010). It works by separating molecular ions according to their mass-to-charge ratio (*m/z*) (Siuzdak, 1996). There are essentially four steps to the general process of MS. Step 1 is the ionization of molecules, where ions are generated by inducing either a loss or a gain of charge. Step 2 involves the acceleration of these ions. Step 3 is the separation of the ions based on their unique *m/z*. The final step is the detection of the ions via electron multipliers or scintillation counters (Siuzdak, 1996). A mass spectrometer therefore contains an ion source, a mass analyser and an ion detector. For metabolomic research, MS is often coupled with different separation techniques such as liquid chromatography (LC) and gas chromatography (GC) (Beger *et al.*, 2010), which are applied to the sample prior to entering the MS system. Furthermore, modern mass spectrometers often permit MS/MS analysis which allows fragmentation of parent ions and the subsequent mass analysis of the fragment ions (Siuzdak, 1996). Fragmentation of parent ions allows for the positive identification of metabolite species by obtaining structural information. There are many methods used to fragment the ions which can result in different types of fragmentation and thus different information about the structure of a molecule.

Quality control is important during data acquisition, especially when chromatography is utilised, to ensure consistency of results. Quality control ensures correct chromatographic retention times and identifies drifts in peak placement in chromatograms due to equipment. In general, changes in LC retention times are monitored by internal standards spiked into each sample, or periodically running a specific quality control sample (Beger *et al.*, 2010). The latter can be either a synthetic sample, or a pooled sample of all of the samples used in the analysis. Carry-over of sample or solvent from one to the next can be detected by the running of blanks at regular intervals (Beger *et al.*, 2010).

Contrary to ^{1}H NMR, mass spectrometry analysis usually involves some form of sample preparation prior to analysis and is also a destructive technique. This can limit its application for samples of small volume.

1.3.3.1 Separation techniques

Chromatography is a term used to describe analytical techniques that physically separate complex sample mixtures. These techniques can be used alone or in combination with MS and NMR

instruments (Liland, 2011). The major chromatographic classes are GC, high performance LC (HPLC) and ultra performance LC (UPLC) (Beger *et al.*, 2010).

In GC the mobile phase is a gas. Gas chromatography has very high chromatographic resolution, and is both sensitive and efficient for metabolomics studies. However, GC is limited to volatile compounds, before and after derivatisation (Qiu & Ree, 2014). Therefore, non-volatile compounds which do not derivatise, and large or thermo-labile compounds are not observable in GC-MS (Zhang *et al.*, 2012a). Although, a large portion of small molecular metabolites are within the range of separation for this procedure, some potential markers may be below the detection limit. In contrast, LC techniques use columns which are packed with a porous stationary phase, and involve the movement of a mobile phase across the stationary phase. The mobile phase can either be a liquid sample directly injected into the column, or a sample extract dissolved in a liquid. The separation of sample components is based on the differential interaction of the components with the respective stationary and mobile phases as they pass through a particular column. The different components of a sample elute at different times from the column, allowing easier identification. The choice of column is based on composition of the stationary phase, defined by the sought after constituent(s) i.e. polar, semi-polar, or non-polar compounds. The mobile phase is usually divided into two subclasses, normal-phase (NP) LC and reverse-phase (RP) LC, based on the polarity of the mobile and stationary phases. Liquid chromatography has a lower chromatographic resolution compared to GC, but has the advantage of having a wider range of potentially measureable metabolites.

1.4 Data analysis

Like other functional genomic techniques, metabolomics produces high-dimensional data sets represented as complex matrices with several hundred or more peaks originating from various metabolites (Kouskoumvekaki & Panagiotou, 2011; Ramadan *et al.*, 2006). Often sample numbers are much smaller than the number of variables, i.e. metabolite peaks, making it difficult to produce strong training sets with known classifiers and to select suitable features for prediction. Metabolomic data sets can also be distinguished by the presence of correlation among markers, primarily due to chemical similarities in the metabolites (Zuber & Strimmer, 2009). For example, an increase in one metabolite causing an increase or decrease in another, or simultaneous changes due to the specific mode of action of a toxin. Chemometrics is the application of mathematical and statistical methods to chemistry (Lavine & Workman, 2008) and is necessary to develop data reduction and statistical pattern recognition models, achieve optimal characterisation, and detect

biomarkers from these complex data sets (Beger *et al.*, 2010). The aim of chemometrics is to assign and classify spectral peaks from analytical techniques (Goldsmith *et al.*, 2010).

The raw data produced by the analytical techniques used for metabolomics are complex and are often large (a typical MS data set can be 10 - 1000 MB). The raw data is generally converted to a more suitable format for importing into a range of analytical software packages before pre-processing steps are applied (Dunn *et al.*, 2011b). This conversion also reduces the size of the data files by reducing the complexity of the data. The next step in pre-processing is alignment of the data. Drifts occur in the data which do not reflect any real sample variations. These drifts are seen in retention time, migration time and accurate mass in MS and are due to changes in pH or osmolarity in NMR causing changes in chemical shifts (Dunn *et al.*, 2011b). Drifts can lead to multiple reports for a single feature, such as one metabolite being reported as two individual metabolites in different samples. Alignment is done using signal reference peaks (NMR) or standards (MS). Baseline correction and normalization of the data follows. These strategies need to be applied to account for biological and equipment variability, and depend on the method used and the matrix of data. In addition, frequency binning (bucketing) is applied with NMR spectra. This process divides the spectra into a defined number of bins, usually ranging from 0.01 to 0.04 ppm, over a total chemical shift range of ~ 10 ppm, and sums all the measurements inside each bin to 'group' peaks and produce fewer variables (Liland, 2011). This can partially account for a degree of shift in peak locations by reducing the spectral resolution (Zhang *et al.*, 2010). Additionally, this process acts to smooth the spectra.

Following pre-processing, a number of statistical modelling techniques are available to analyse the data, ranging from univariate statistical testing, like analysis of variance (ANOVA), to multivariate regression methods such as principal component analysis (PCA), partial least squares-discriminant analysis (PLS-DA), orthogonal partial least squares-discriminant analysis (OPLS-DA), non-linear methods, and many more. Kouskoumvekaki and Panagioutou (2011) produced an informative review of data analysis and database tools and a concise description of different data analysis tools is provided. Principal component analysis, PLS-DA, and OPLS-DA will be discussed briefly in sections 1.4.1, 1.4.2, and 1.4.3, respectively; as they are the most commonly used and easily applied techniques.

In general one, or both, of two approaches are applied when measuring the metabolome; non-targeted (unfocused) and targeted (focused) metabolic profiling (Beger *et al.*, 2010; Dunn *et al.*, 2011b). Robertson *et al.* (2011) also define a third approach which they term metabolomic fingerprinting. All three will be defined briefly here.

Non-targeted metabolomics (global profiling) usually involves chemometric analysis of data from NMR and/or MS to determine spectral patterns of biomarkers that can be related to toxicity or health status (Beger *et al.*, 2010; Teahan *et al.*, 2006). This strategy seeks to assign as many individual peaks as possible to acquire data relating to a wide range of metabolites in the metabolome (Dunn *et al.*, 2011a) and produces a quantified list of metabolites (Robertson *et al.*, 2011). Once metabolites are identified, statistics can be used to determine new biomarkers of health or disease status (Beger *et al.*, 2010). Limited sample preparation is required and these studies are performed with little or limited *a priori* information on the composition of the sample used (Dunn *et al.*, 2011a).

With targeted metabolomics, chemical classes or specific analytes/metabolites, such as amino acids, bile acids and lipids, are pre-selected, usually to address specific biological questions within a study, and are assessed (Beger *et al.*, 2010; Robertson *et al.*, 2011). Typically less than 20 metabolites are evaluated at a time with this approach, but a greater level of resolution is required with these studies to separate the targeted metabolites from other metabolites and sample matrix components (Dunn *et al.*, 2011b). Targeted studies will often develop from untargeted studies where there is a desire for more information on specific molecules.

Metabolomic fingerprinting is a rapid biochemical snapshot from minimally prepared peripheral biofluids, such as blood, where changes from normality are detected in a diseased sample and correlated with disease progression or recovery (Ellis *et al.*, 2007; Robertson *et al.*, 2011). In this strategy, the result is obtained without the requirement to quantify or identify individual metabolites (Madsen *et al.*, 2010). Without this data acquisition limiting step this approach is a rapid global technique. This allows it to be utilised as a screening tool to quickly discriminate between samples from different biological status, such as diseased versus healthy subjects (Ellis *et al.*, 2007; Robertson *et al.*, 2011).

The approaches above represent a continuum moving from qualitative to quantitative methodologies, and ideally most metabolomics studies would seek to provide information from all three approaches.

1.4.1 Principal component analysis

Principal component analysis (PCA) is a procedure that reduces a spectrum produced by NMR or MS which may contain several hundred variables (NMR chemical shift buckets or MS masses) to typically, two or three variables that still represent as much of the variance from the original spectrum as possible (Halouska & Powers, 2006). This is a well-established statistical technique that

determines the directions of the largest variations in a data set, where the data set is composed of spectra collected from numerous samples. The data are usually represented as a two or three dimensional plot, the scores plot, where the coordinate axis corresponds to the principal components. In its simplest form PCA usually requires the spectrum to be divided into a number of equally spaced regions (binning) and the area of the signal in each of these regions to be measured (Goldsmith *et al.*, 2010). The regions with the biggest variation are used for the scores plot.

Principal component analysis acts to simplify the data set of complex metabolite mixtures that have been obtained from biological samples that may be composed of hundreds or thousands of chemical components. It allows a large number of observed values to be modified into a reduced number of artificial values (principal components) that account for most of the variance in the observed variables. Principal component analysis is primarily used to identify the relative change in concentration of metabolites to identify trends or characteristics within data that permits discrimination between various samples that differ in their source or treatment (Beger *et al.*, 2010).

1.4.2 Partial least squares discriminant analysis

Partial least squares discriminant analysis (PLS-DA) is a linear regression method that can be applied to data to establish a predictive model, even if the variables are highly correlated (Kouskoumvekaki & Panagiotou, 2011). This technique generalises and combines features from PCA and multiple regression. The principal components (*X* variables), which are the predictors, are used to predict the scores of *Y* variables (the dependants), which are also reduced to principal components. The *Y* component scores are used to predict the actual values of the *Y* variables (Kouskoumvekaki & Panagiotou, 2011). This technique therefore models relationships between sets of observations by means of latent variables.

1.4.3 Orthogonal partial least squares-discriminant analysis

PLS-DA allows greater class separation between scores in space, however variation not directly related with Y is still present (Worley & Powers, 2013). This complicates the interpretation of PLS-DA scores and loadings. Orthogonal partial least squares (OPLS) is an extension of PLS, where the variable data is separated into predictive and uncorrelated information, which leads to improved diagnostics. This improves the interpretability, by effectively separating the information related to the class separation from the unrelated information. OPLS does not bestow any predictive performance advantages over traditional PLS (Tapp & Kemsley, 2009). OPLS-discriminant analysis

(OPLS-DA) is the classification variant of OPLS. This is applied when working with discrete variables and maximises the separation among the defined groups by maximising the covariance between the *X*- and *Y*-variables. OPLS-DA has the ability to separate between-class variation from within-class variation, improving the visualisation of the data (Bylesjo *et al.*, 2006; Trivedi & Iles, 2012).

1.5 Objectives of this project

Although elevated activities of GGT and GDH enzymes, as shown in earlier literature, are indicative of sporidesmin challenge, they are not specific for the disease, and have not been shown, on their own, to be sensitive enough to identify subclinical and non-responder cows in a herd. They are not representative of early stage disease, and therefore of the pathways and processes occurring in the lead-up to liver damage. Commonly, animals are not able to be removed from toxic pastures and/or treated until clinical signs are observed, meaning severe liver damage has already occurred. There is a need for more information on the pathological changes occurring following sporidesmin challenge, and introduction of robust and early stage markers for this disease.

The intent of this project was to induce subclinical facial eczema in dairy cows through the administration of a one off dose of sporidesmin. Samples gathered from the cows were to be used to identify specific early risk biomarker(s) of sporidesmin intoxication, by comparing conventional diagnostics for clinical facial eczema (liver enzyme activities), to results from metabolomics analyses, using various detection platforms including fluorescence spectrometry, NMR spectroscopy, UPLC/MS, and UPLC/MS-MS.

The project was divided into the following parts:

- The first stage was to dose cattle with a low dose of sporidesmin (anticipated to cause subclinical disease) and analyse traditional measurements, including liver enzyme activities in serum, and measure bodyweight, and milk yields
- The second step was to measure phytoporphyrin concentrations in these cattle, to see when this marker reaches the threshold of "normal" following sporidesmin challenge.
- The third step was to use NMR spectroscopy and UPLC/MS in an attempt to identify an ideal metabolomic biomarker that appears prior to changes in liver enzymes and phytoporphyrin following sporidesmin challenge.

CHAPTER 2

SPORIDESMIN CHALLENGE IN DAIRY CATTLE

2.1 Introduction

In susceptible dairy cattle, facial eczema (FE) is accompanied by a drop in milk production (Cullen *et al.*, 2006; Morris *et al.*, 1990; Towers & Smith, 1978), which usually leads to drying off and large losses in profit. It is well recognised that this milk production loss can occur with subclinical FE, and it is a widely-held belief that liver injury is a contributing, if not a causal factor, of many metabolic problems and unexplained deaths encountered in dairy cattle at or near calving (Towers, 1978). In addition, live weight losses and consequently a decrease in body condition and decrease in growth rates, the cost of veterinary call-outs and treatments, preventative techniques, altering feeding regimes, as well as individual survival within a herd (Morris *et al.*, 2002), add to the cost, losses and negative impact on animals.

Some deaths occur with clinical FE, but the greatest losses arise from increased culling rates following outbreaks of this disease (Smith & O'Hara, 1978). Many affected animals incur further losses due to hide damage, and carcass and liver condemnation at abattoirs (Smith & O'Hara, 1978).

Both natural and artificial FE challenges have been studied in cattle; however, the majority of research on this topic has been conducted on sheep. Much of the literature focusing on cattle has involved natural challenges, where the animals have already become clinical before recording begins. Therefore, developments during the preclinical period, as well as baseline measurements for affected cattle have not been obtained.

Literature reports of artificial sporidesmin challenges in cattle utilise varying doses ranging from 0.14 mg/kg up to 3.0 mg/kg. The size of the sporidesmin dose chosen does not seem to be related to whether the studied animals were calves or adult cows. The responses to these challenges varied, but most showed some clinical signs when doses were > 0.5 mg/kg. In one study, where calves were split into three groups and each group given single oral doses of either 3.0 mg/kg, 1.0 mg/kg or 0.8 mg/kg, of sporidesmin concentrate, all groups showed some signs of photosensitivity. All animals within the highest dose group died, the second group showed either serious illness, photosensitivity or death, while the third group had 50% of the calves showing transient photosensitivity (Mortimer, 1963). In another study using calves, weight loss, but no accompanying photosensitivity was observed following a single oral dose of 0.5 mg/kg. An increased dose of 1.0 mg/kg showed variable effects, with one calf dying showing no signs of photosensitivity 18 days after dosing, another calf showing photosensitivity at 19 days, and all the others showing significant weight losses of approximately 25 kg by 5 weeks post-dosing (Mortimer, 1971). These studies demonstrated the difficulty in predicting responses and trends of individual treated animals, and supported the hypothesis that animals differ in their susceptibility to sporidesmin toxicity. A summary of published

trials of artificial sporidesmin challenges and natural exposures in cattle, giving details of the age, breed, method of application, dose and tests applied, where applicable, is given in *Table 2.1*.

With this information in mind, and following consultation with Neville Amyes, at AgResearch, Ruakura, it was decided to administer a single oral dose of 0.24 mg/kg sporidesmin. It was anticipated that this dose would be too low to produce clinical disease.

2.1.1 Aim

To induce subclinical facial eczema in lactating dairy cows using a single oral low dose of sporidesmin, anticipated to be insufficient to cause clinical disease, and monitor the cows production parameters, and sample biofluids (serum, urine, and milk) for biochemical and metabolomics analyses in order to discover biomarker(s) of early stage and/or subclinical sporidesmin intoxication.

2.1.2 Objectives

- Administer a single low sporidesmin dose to most of the cows with some serving as un-dosed controls
- Sample blood, urine, and milk from all cows three times weekly for serum biochemistry and storage for subsequent metabolomics studies
- Sample livers for histology when the cows are slaughtered at the end of the trial and score liver lesions for severity
- Look for statistical correlations between liver enzyme activities, and milk yield and body weight changes

Table 2.1 Summary of published trials of artificial sporidesmin challenges and natural exposures in cattle

	Type[1] of FE challenge	Breed[2]	Age	Sex	Number	Method of application	Dose (if given)	Analys Diagno
h	A	M (mainly J and J x)	Mixed (late lactation)	Female	20 + 10 control	Intra-ruminally on 3 consecutive days	a) total = 0.26 mg/kg b) total = 0.63 mg/kg	GGT, OCT, BSP clea grading, live weig a) no observab b) increase G
)	A	J	Mixed age 7 months in-calf	Female	12 (8 dosed, 4 control)	Orally. Total dose given over 5 days	4 = 1.0mg/kg 4 = 0.5 mg/kg	Gross obs, live wei injur
7)	A	F, J	Bull calves	Male	?	Oral (2 doses, 1 month apart)	a) 0.14 mg/kg b) 0.16 mg/kg	PCV, GGT, GDH, G
)	A	J	Calves		42	Oral	a) 3.0 mg/kg b) 1.0 mg/kg c) 0.8 mg/kg	Gross obs animal & c a) dea b) serious illnes c) 50% trans
0)	N	J (LIC SPS[4])		Female 1st lactation	571	N/A	N/A	GGT
8)	N	F, J	Calves 7 months	Male	132	N/A	N/A	GGT
8)	A	F, J	calves	Male	61	Oral. Split dose 1/3 on 3 consecutive days	0.2 mg/kg	
8)	A		?	Male	335	Single oral dose	0.14 mg/kg	GGT, G
	A		Calves	Mixed	74	Oral, 4-day period, 25% per day	Total 0.3 mg/kg	GGT at weekly inter post ad
6)	A and N	F, J	Mixed	Mixed	4,333	Natural pasture & Oral	0.1-0.18 mg/kg	GGT, G
	N	X	M	Mixed	1357	N/A	N/A	GGT, conditio

[1] A= Artificial challenge, N = Natural challenge [2] J = Jersey, F = Friesian, X = cross

[3] GGT = gamma-glutamyl transferase, GDH = glutamate dehydrogenase, OCT = ornithine carbamoyl transferase, BSP = Bromsulphthalein (liver dye used to measure hepatic dysfunction), GST = glutathione S-transferase, PCV = packed cell volume (test used to measure the amount of cells in the blood).
4 LIC = Livestock Improvement Corporation, SPS = Sire proving scheme

2.2 Materials and methods

2.2.1 Animals and diet

In March 2011, 20 adult Friesian and Friesian x Jersey non-pregnant and lactating dairy cows of mixed-age, with a mean live-weight of 441 kg, were purchased from a commercial dairy herd in Eketahuna, Wairarapa, New Zealand. These animals had been recorded in the LIC system. The animals were tested prior to purchase for enzootic bovine leukosis, Johne's disease, and bovine viral diarrhoea antigen, with all results being negative, clearing the cows for transport and introduction to a new farm.

Additionally, prior to purchase, blood samples from all animals were submitted to the New Zealand Veterinary Pathology (NZVP) diagnostic laboratory at Massey University, Palmerston North, for a liver panel analysis (bilirubin (bil), GGT, GDH, albumin (Alb), globulin (Glo), total protein (TP) and albumin/globulin ratio (AGR)). All chemistry tests were performed on a Roche/Hitachi Modular P800 clinical chemistry analyser using standard Roche reagents (Roche Diagnostics GmbH, Sandhofer Strasse 116, Mannheim, Germany) following NZVP standards (Schmidl, 1986).

The cattle arrived at Massey University Dairy No. 4 on the 30th March 2011. All animals were weighed and blood samples were collected on arrival. The cow ID, breed, age and weight on arrival are recorded in *Table 2.2*. The cows had been accustomed to a herringbone milking shed system, whereas the Massey Dairy No. 4 milking system consisted of a 60 bale rotary platform. Therefore, the first five days on the farm involved normal, twice-a-day milking, but no sampling, to allow the cows to adapt to the new farm and milking routines before commencement of the trial on the 4th of April.

All animals were grazed on ryegrass/white clover mix pastures and were given access to water *ad libitum*. Four paddocks, closed off from the Dairy No. 4 herd, were allocated for use in this trial. The paddocks were sprayed with Goldazim 500 sc (Adria New Zealand Ltd, Auckland), with the active ingredient carbendazim, a fungicide used to control fungal growth on pastures, applied at 300 ml/ha.

The animals were front and back fenced and given a new break every morning. This allowed the cows to utilise the available pasture, grazing the sward to maintain the farms post-grazing pasture residuals, and decreased the amount of trampling of the pasture. Each paddock was able to be rationed to ~ 2 weeks of grazing. The fencing was setup to ensure that the cows had access to natural (trees) or artificial shade (shade cloths) in all paddocks.

The cows were monitored before and after each of the two daily milkings, and any out-of-the ordinary behaviours and/or physical changes were recorded.

The study was approved by the Massey University Animal Ethics Committee, Palmerston North (protocol no. 11/23).

Table 2.2 Cow details.

ID No.	Breed*	Age†	Weight (kg) (30.03.2011)
22	F4J4	8 yrs 7 months	432
64	F8J8	3 yrs 7 months	387

152	F13J3	2 yrs 8 months	445
195	F	3 yrs 11 months	494
222	F	3 yrs 6 months	388
239	F6J2	3 yrs 6 months	395
244	F	8 yrs 7 months	502
282	F8	3yrs 7 months	403
298	F2J2	6 yrs 7 months	426
312	F	2 yrs 7 months	405
317	F8J8	3 yrs 7 months	413
374	F	6 yrs 7 months	468
384	J12F4	6 yrs 8 months	464
393	F8J8	3 yrs 7 months	396
395	F8	4 yrs 7 months	430
420	F	8 yrs 0 months	548
424	F8	8 yrs 6 months	410
440	F	3 yrs 7 months	397
448	F12	7 yrs 8 months	495
450	F12J4	7 yrs 7 months	526

* F8/J8 = first cross Holstein-Friesian and Jersey; F4J4 = second cross Holstein-Friesian and Jersey; F = 16/16 Friesian; F12/J4 = 12/16 Holstein-Friesian, 4/16 Jersey; J12F4 = 12/16 Jersey, 4/16 Holstein-Friesian; F13J3 = 13/16 Holstein-Friesian, 3/16 Jersey
†Age at 31st March 2011

2.2.2 Experimental design

This experiment was designed as a 60 day trial, where all cows were subjected to a 14 day baseline control sampling period prior to dosing (Day -14 to Day -1) and 44 days of toxin response testing, so that all cattle could act as their own controls during the study. *Table 2.3* shows the trial timeline.

Table 2.3 Trial timeline.

Date	Period	Sampling
Day -19 to Day -14	Delivery and habituation	Blood testing and weighing on Day -19
Day -14 to Day 0	Control testing	Monday – blood, milk, urine, weight and faeces Wednesday and Friday – blood, milk, urine
Day 0	Sporidesmin challenge and final control testing	Blood, milk, urine, weight and faeces (pre-dosing)

Day 0 to Day 44	Sporidesmin challenge testing	Monday – blood, milk, urine, weight and faeces Wednesday and Friday – blood, milk, urine
Day 45	Culling	Liver sampling

Of the 20 cows, three were randomly chosen as untreated controls and the remaining 17 were challenged with sporidesmin. On the day of sporidesmin administration (Day 0), the 17 cows were administered a measured sporidesmin dose (0.24 mg/kg) intra-ruminally. The measured dose was calculated based on the weight of all cows on arrival to Dairy No. 4. The control cows were subjected to the same regimen, excepting the sporidesmin dose was replaced by the equivalent volume of water. The sporidesmin doses are given in *Table 2.4*.

The liver enzyme activities and the presence or absence of clinical signs enabled the separation of cows into four sample groups at the end of the trial, namely controls, non-responders, subclinicals and clinicals.

2.2.3 Sporidesmin administration

The sporidesmin was a crude extract from spores of *P. chartarum* dissolved in 96 % ethanol, prepared by AgResearch, Ruakura, Hamilton, New Zealand. The night before administration the sporidesmin/ethanol solution was diluted 1:10 with Milli-Q water (Millipore Corporation, Billerica MA, USA), at Massey University, Palmerston North, NZ.

Table 2.4 The sporidesmin doses administered on Day 0. The sporidesmin dose was per animal based on its weight on arrival on 30.03.2011 (Day - 19).

ID No.	Weight (kg) (30.03.2011)	Sporidesmin dose (mg)	Group
22	432	-	Control
64	387	92.88	Treated
152	445	-	Control
195	494	118.56	Treated
222	388	93.12	Treated
239	395	94.8	Treated
244	502	120.48	Treated
282	403	96.72	Treated
298	426	102.24	Treated
312	405	97.2	Treated
317	413	99.12	Treated

374	468	112.32	Treated
384	464	-	Control
393	396	95.04	Treated
395	430	103.2	Treated
420	548	131.52	Treated
424	410	98.4	Treated
440	397	95.28	Treated
448	495	118.8	Treated
450	526	126.24	Treated

Sporidesmin doses were administered via intra-ruminal intubation, using an intra-ruminal pump consisting of an alkathene tube with a nose clip and funnel. The alkathene tube was fed down the oesophagus of each cow. Once the tube was in position, the sporidesmin dose (*Table 2.4*), was administered. The dose was followed by 1 litre of water to rinse the funnel and tube, ensuring all sporidesmin was administered to each treatment cow. The three control cows were administered a volume of water only, equal to the expected volume of the sporidesmin solution based on their weight.

2.2.4 Sampling procedures

Samples were collected three times a week (Monday, Wednesday and Friday), during (milk) and after (blood and urine) the morning milking. Milk yields were initially recorded during sampling in the morning, but after the two control weeks this was re-evaluated, and from here on, were recorded daily for all cattle, during morning and afternoon milking. Every Monday, one red topped vacutainer (BD Vacutainer®, 6.0 mL, 13 x 100 mm), from each cow was sent to NZVP for liver panel analysis, primarily to monitor any changes in GGT and GDH enzyme activities. Cows were weighed and condition-scored each Monday and weekly faecal samples were submitted to NZVP for *P. chartarum* spore counts. Pasture samples were sent to NZVP for spore counting when the cows were moved into a new paddock. Additionally, daily observations were made and recorded to detect any behavioural changes or clinical signs of photosensitisation. Clinical signs were defined as reddening and swelling of the skin and/or additional peeling of unpigmented skin. Behavioural changes were defined as obvious shade-seeking, inappetence, or any irritability or discomfort at milking.

The milk, serum, and urine samples were divided into smaller aliquots in the laboratory post-sampling, and frozen at -80 ^{o}C pending analysis.

2.2.4.1 Milk collection

The test cows were milked before the main herd to ensure the cups were clean for sampling and no contamination could occur. Milk samples were collected using herd testing equipment loaned for the duration of the trial from Dairy No. 4. Bales 1 to 20 were assigned as the ones to be used for sampling days. Each herd test sampling container was labelled with its corresponding bale number. During milking, a proportionate volume of the cow's milk (from start to finish) was collected. At the end of milking a sample from each animal was transferred into sterile 60 mL plastic containers labelled with the cow ID tag number and date, and were placed on ice in a polystyrene container for the duration of testing. In the laboratory, the samples were separated into four 4 mL styrene tubes and these, along with any spare sample, were stored at -80 ^{o}C until required for analysis.

2.2.4.2 Blood collection

Blood samples were collected via venipuncture, either from the tail (coccygeal) vein or from the jugular vein in the neck. The tail vein was the first choice, however some cows proved difficult to obtain enough blood for analytical purposes, in these cases the jugular vein was used. The inconsistency of sampling sites didn't appear to have had any effect on the results. For tail bleeding the animals were moved into a herringbone race, away from the milking shed, and positioned so they were restrained by the other animals in the race. The tail was raised to be approximately horizontal to the ground. An 18 gauge hypodermic needle held by a plastic holder was inserted perpendicular to the skin surface into the groove lying in the ventral midline of the tail (approximately 100 – 150 mm from the base of the tail). For jugular bleeding, the animals were restrained in a head bale. The head was elevated, pressure was applied at the base of the jugular groove, and the needle was inserted. Three red top plastic (serum) vacutainers of blood were withdrawn from each animal, per sampling, where possible. Samples were stored in a light-protected plastic container until transported to the laboratory. Samples were left at room temperature for between 2 and 6 hours to allow the blood to clot. The serum was separated and the clot was removed by spinning down the tube at 3000 rpm for six minutes, using a Heraus Multifuge centrifuge. The supernatant was transferred into 5 mL polypropylene tubes and stored at -80 ^{o}C until required for further analysis.

Every Monday, one blood sample per cow was submitted to the NZVP laboratory for 'liver panel' screening. The blood samples were spun down at 3000 rpm for 6 minutes and assayed at 37 ^{o}C. The two major liver enzymes measured were serum GGT and GDH, which are non-specific, but useful, indicators of bile duct damage and hepatocyte leakage, respectively.

2.2.4.3 Urine collection

The cows were coaxed to void themselves by gently massaging/stroking the escutcheon below the vulva, stimulating the cow to urinate. At each sampling 50 - 60 mL of mid-stream urine was collected in sterile plastic sampling containers from each cow. Urine samples were placed in a polystyrene container on ice until all sampling was completed. In the laboratory, aliquots of the urine samples were transferred into three 4 mL polypropylene tubes and these, along with any spare urine in the sampling containers, were stored at -80 ^{o}C.

2.2.4.4 Faecal and pasture spore counts

Faecal spore counts were measured to confirm that the cattle were not subjected to any natural sporidesmin challenges during the trial. A random sampling of faeces was taken from 10 cattle during every Monday sampling session. The 60 mL samples were pooled at the NZVP laboratory for analysis. The NZVP staff then followed laboratory protocol for faecal spore counting (Smeaton, 2003a).

Whenever possible, pasture spore counts were measured prior to the cows moving onto a new paddock. Although pasture fungal spraying was carried out prior to animal utilisation, these counts verified that the spraying was successful, and the chance of a natural sporidesmin challenge was minimal. Thirty cuts of 'grass' were taken from several places per paddock, to average any variation across the paddocks. Each sample was cut at the base of the sward using shears and placed into paper bags labelled with the paddock number and date. These samples were submitted to NZVP for spore counting. Again, NZVP staff followed laboratory protocol for pasture spore counting (Smeaton, 2003b).

Additionally, the pasture spore count records of the Massey University Equine and Farm Services Clinic, which give an average spore count of Dairy No. 1 and Dairy No. 4, were monitored.

2.2.4.5 Abattoir sampling

The cattle were transported to Silver Fern Farms Pacific processing plant in Hastings two days after the cessation of the trial (Day 42). On Day 45, the cattle were routinely slaughtered by complying with all relevant government regulations relating to the processing of beef. All livestock were inspected by a government employed veterinary officer and all animal welfare regulations were met. At the offal removal stage, the offal was checked for any sign of parasites, bacteria or infection by

qualified meat inspectors, and graded. Liver sampling was then carried out, in a room to one side of the killing floor, for subsequent histological analysis.

Liver samples for histopathology were removed from the ventral and caudate lobes (2x2x1 cm sections). The samples were placed directly into 10 % formalin within 20 minutes of slaughter, and transported back to Palmerston North for analysis.

Formalin-fixed liver samples were then trimmed into blocks and processed routinely, using a series of alcohol solutions and a clearing agent before drying for staining. Sections were cut at 3 µm and were stained with haematoxylin and eosin (H&E) for examination with a light microscope.

2.2.5 Statistical analysis

The data were analysed using a combination of programmes, including Microsoft Excel (2007) and RStudio (Version 0.97.449, RStudio, Boston, MA, USA). Multiple regression analyses and generalised additive models (GAM) were used to compare groups and variables. Typically, the activity of GGT following sporidesmin challenge was skewed, since individual cows, within a group, could exhibit highly variable levels of response, in which case, $\log_e$ transformed data were used.

To assess how the different variables, weight, milk yields, and GGT and GDH activities, changed over the trial period, a GAM was fitted to the data (df = 7), allowing for each group to have a separate smooth average, taking into account the initial weight of the animals. The model fitted was as follows:

$$\log(X_t) = \log(X_0) + f_G(t) + e_t$$

where X_t was the variable at time t, X_0 was the variable at time 0, $f_G(t)$ is a smooth curve for each group, and e_t is the residual, distributed normally. The mixed GAM computational model (mgcv) package (Wood, 2006, 2011) within the Rstatistics environment (R Development core team (2012)) was used to fit this model, with the smoothness of the function f_G estimated by cross-validation. To assess whether there was a difference between groups, this model was compared to one where $f_G(t) = f(t)$ for each group G, i.e. a model where the change through time was similar for all groups. Model comparison was done by computing the Akaike Information Criterion (AIC) for each model, which trades model goodness of fit against model complexity. The model with the lowest AIC was deemed the most appropriate. Using the logarithm of the variables means that the average change for a group was considered as a proportion of the animal's initial value, so that, for example with weight, the heavy animals would lose more absolute weight, but the same proportion of their weight as lighter animals.

2.3 Results

During the trial, five cows had to be euthanased because of, clinical facial eczema (*n = 3*), lameness (*n = 1*) or mastitis (*n = 1*). The remaining cows were slaughtered at an abattoir on the 2nd June 2011 (Day 45). A number of cows developed diarrhoea, but this was not restricted to post-dosing or to treated cows, so was not considered to be diagnostic of the sporidesmin challenge. Alternatively, this could have been due to differing pasture from their original farm.

2.3.1 Spore counts

2.3.1.1 Faecal spore counts

According to Smeaton (2003a) , the risk levels of a natural FE challenge, associated with faecal spore counts in dry faeces are: low < 600,000, moderate 600,000 – 1,000,000, and high > 1,000,000. On Day 0, the pooled faecal spore count was 666,000 spores/g (a moderate spore risk). The faecal spore levels dropped to < 400,000 the following week and continued to drop to 0 on Days 28, 35 and 42. The risk of natural challenge was considered to be moderate on Day 0, and the animals were monitored closely at this time. A significant drop on Day 7 and thereafter, returned the risk of natural challenge to low. The changes in the dry faecal spore counts measured over the trail period are shown in *Figure 2.1*.

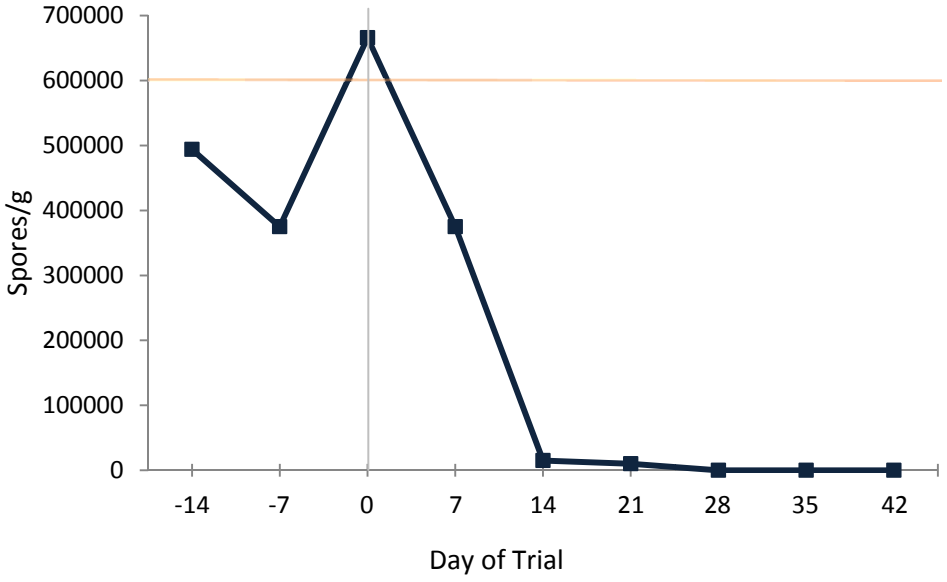

Figure 2.1 Line graph showing dry faecal spore counts (Days -14 – 42). The horizontal line (—) represents a 'moderate' risk level of natural FE challenge for dry spore counts (600,000 – 1,000,000 dry spores/g), where preventative measures should begin to be considered. The vertical line corresponds to the day of sporidesmin dosing (Day 0)

2.3.1.2 Pasture spore counts

Pasture spore counts were determined by NZVP for Days 15 (03.05.2011) and 21 (09.05.2011) giving measurements of 5000 spores/g and 10,000 spores/g of pasture, respectively. NZVP grade spores as low being 0 - 30,000 spores/g, moderate being 35,000 – 100,000 spores/g, and highly elevated being > 100,000 spores/g. Spore measurements from pastures available to the cows during this trial had low levels of spore counts. The low pasture spore count on Days 15 and 21 correlate well with the faecal spore counts.

Pasture spore counts, recorded by Massey Equine and Farm Services for Massey Dairy Farms No. 1 and No. 4 combined are shown in *Figure 2.*2.

Massey Equine and Farm Services defines spore counts over 100,000 spores/gm pasture to be considered dangerous for cattle, although spore counts of only 40,000 can be equally dangerous if the paddock is grazed down low. Moderate risk was assumed for Day -14 based on NZVP grading; however, the slightly elevated levels were averaged recordings from a number of paddocks across the farm, and probably were not representative of the paddocks where the trial cows were kept, as these paddocks had been sprayed with fungicide.

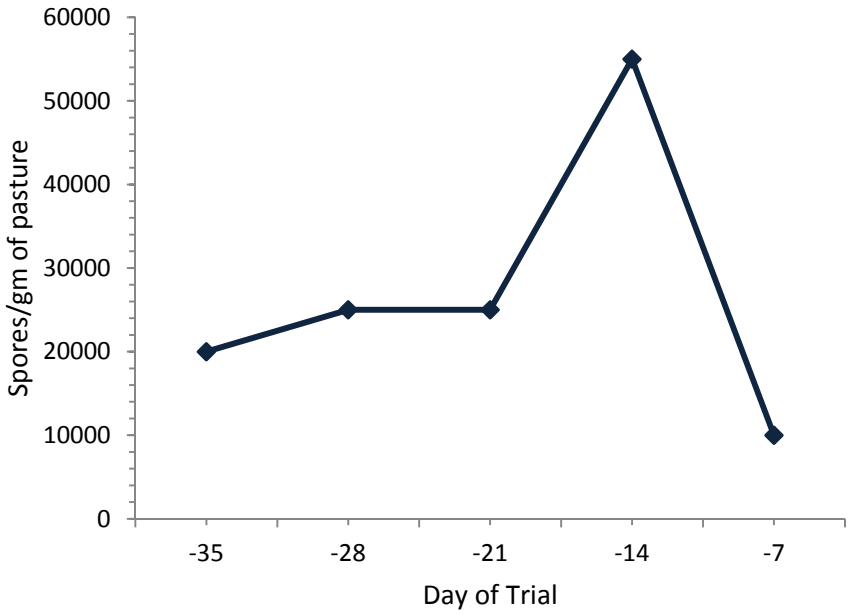

Figure 2.2 Pasture spore counts measured by Massey Equine and Farm Services for Massey Dairy No. 1 and Dairy No. 4, prior to commencement of the trial and during the control weeks. Measures above 100,000 spores/gm pasture are considered dangerous for cattle (Smeaton, 2003b).

2.3.2 Categorisation of cow groups

Liver enzyme activity in serum is widely used as a measure of biliary tree and/or hepatocyte damage in the liver. GGT and GDH are therefore often used as indicators of response to sporidesmin challenge. In this trial, cows that were treated and whose GGT activity remained within the normal ranges (0 - 36 IU/L) throughout the monitoring period post-dosing were classified as non-responders, while cows with elevated GGT activities were considered to be 'responders'. The responders were then further categorised as subclinical or clinical based on visual observations of photosensitivity. Photosensitivity signs were considered to be excessive reddening, swelling and peeling of unpigmented or exposed skin and these cows were categorised as clinical (*Table 2.5*). Of the 17 treated cows, 10 did develop photosensitivity, i.e. they were non-responders or subclinically affected, however, seven cows did develop clinical signs.

It should be noted that the greater than expected values for GDH for the control and non-responder groups are due to two outlier values of 59 IU/L and 65 IU/L which occurred on Day 35 for cow 384 (control) and Day 42 for cow 195 (non-responder) respectively. With these two outliers removed, the remaining GDH activities remain within the 'normal' range for cattle, with maximum values of 39 IU/L and 38 IU/L for the two groups, respectively. Since these abnormal values appeared so long after the dosing date, they were assumed to be due to other unrelated events.

Prior to purchase, four cows (No. 312, 393, 395, and 420) had slightly raised GGT activities, ranging from 40 IU/L to 70 IU/L. Nine cows had elevated GGT activities during pre-dosing weeks, with cow 393 having the maximum GGT activity of 1097 IU/L and GDH activity of 850 IU/L. Cows 239, 282, 312, 317, and 424 had elevated GGT activities between 56 IU/L and 495 IU/L on Day 0. Cows 239, 282, 317, 395 and 424 had elevated GDH activities between 72 IU/L and 360 IU/L on Day 0. These results did not affect the choice of treated and control cows.

The first clinical cases (*n = 2*) occurred on Day 9 following sporidesmin dosing, thereafter two more cases at Day 10, and Day 22, after dosing. The first signs of photosensitivity were shade-seeking, irritability in the milking shed, red and swollen teats and leathery shoulders for one cow. Of the clinical animals, cow 282 exhibited shade-seeking behaviour on Day 10 following morning milking, and the skin on her shoulders began to thicken and become leathery to the touch. At Day 14 all teats had become leathery and sensitive to touch. Cow 298 had developed reddening of her right fore teat and a small blister was apparent on Day 22, but did not develop any further than this, even though she experienced GGT activities above 1000 IU/L. The teats of cow 317 showed faint reddening on Day 9, slightly thickened wither and rump skin at Day 14 and by Day 21 had become sensitive to touch in the milking shed. At Day 25 cow 317 showed a small blister on her left rear and

left fore teats, but did not develop further photosensitivity and showed signs of recovery. Cow 440 displayed reddening of teats at Day 9 and shade seeking at Day 10. No further photosensitivity development was seen until Day 14 when her vulva swelled and her condition dropped considerably. From here reddening and thickening of the skin was seen to be affecting her teats, udder, rump, brisket, and nose, developing into small scabs on the nostrils, muzzle, left rear, and right rear teats. All animals exhibiting early signs of photosensitivity had teat balm applied to all teats in the milking shed and zinc ointment applied to all exposed or unpigmented areas of skin.

Although GGT and GDH activities in serum were elevated in all subclinical and clinical cows, bilirubin levels remained within the normal range (0 - 13 µmol/L) during the trial. There did not seem to be any correlation between GGT or GDH activities and the time when clinical photosensitivity became evident, for example one cow had a GGT activity level of 863 IU/L three days prior to clinical signs emerging, while a second cow only experienced a level of 116 IU/L two days prior to the signs appearing.

In *Figure 2.3* changes in GGT activities for individual cows, calculated by GAM, are shown, while *Figure 2.4* shows the average, within-group, model fits, across time. It can be seen clearly that GGT activities remained well within the normal range for controls and non-responders, while they increased between Days 7 and 14 for subclinical animals, followed by recovery after around Day 21. Clinical animals had elevated levels through the entire trial (*Figure 2.4*).

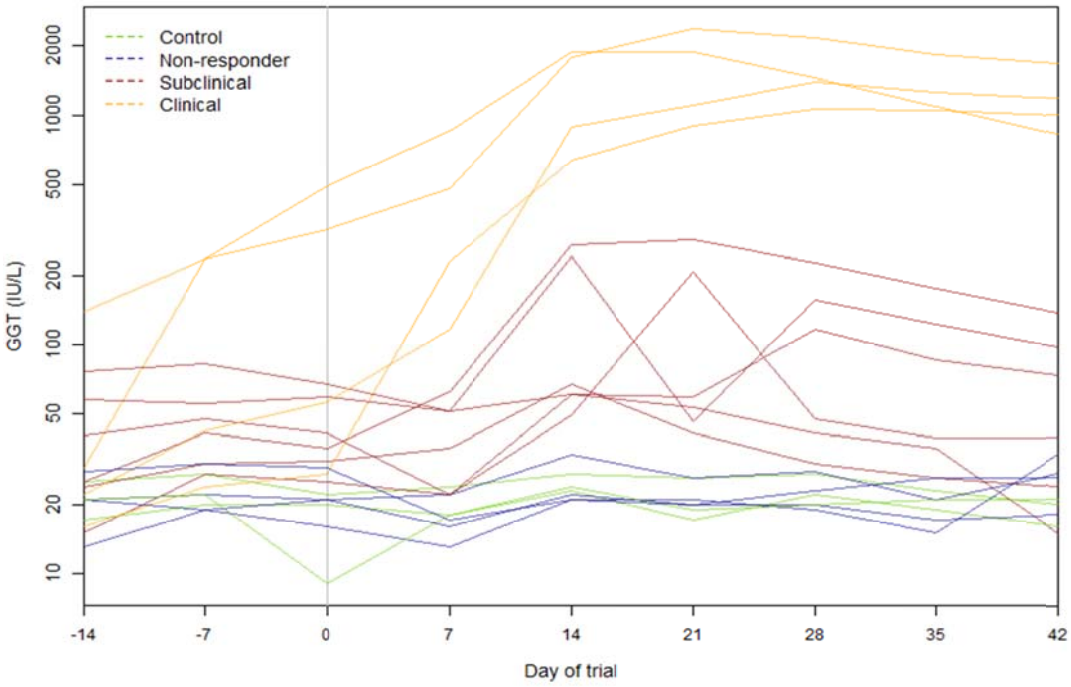

Figure 2.3 GGT activities for individual cows, calculated using GAM, coloured by their defined group. Day 0 refers to the day of dosing.

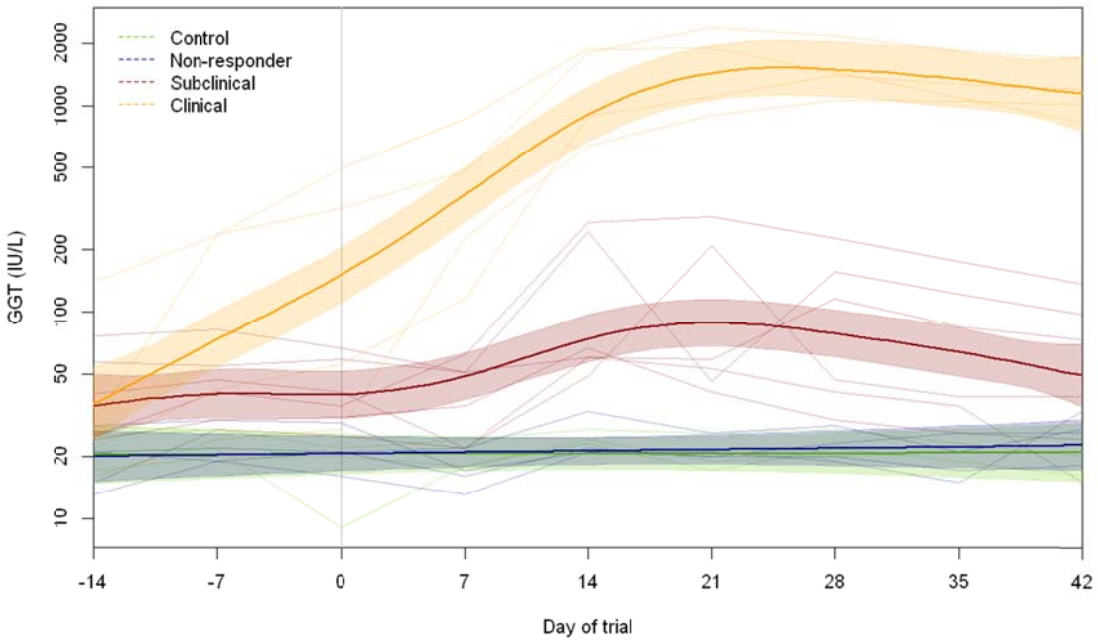

Figure 2.4 GGT activities for each of the four defined groups, with within group models fit, calculated using GAM. Day 0 refers to the day of dosing. Shaded areas represent the 95% confidence bands for that group.

The same pattern can be seen for GDH activity before and after dosing (*Figure 2.5* and *2.6*), except that the raised activities begin to decrease earlier than with GGT activities, around Day 14.

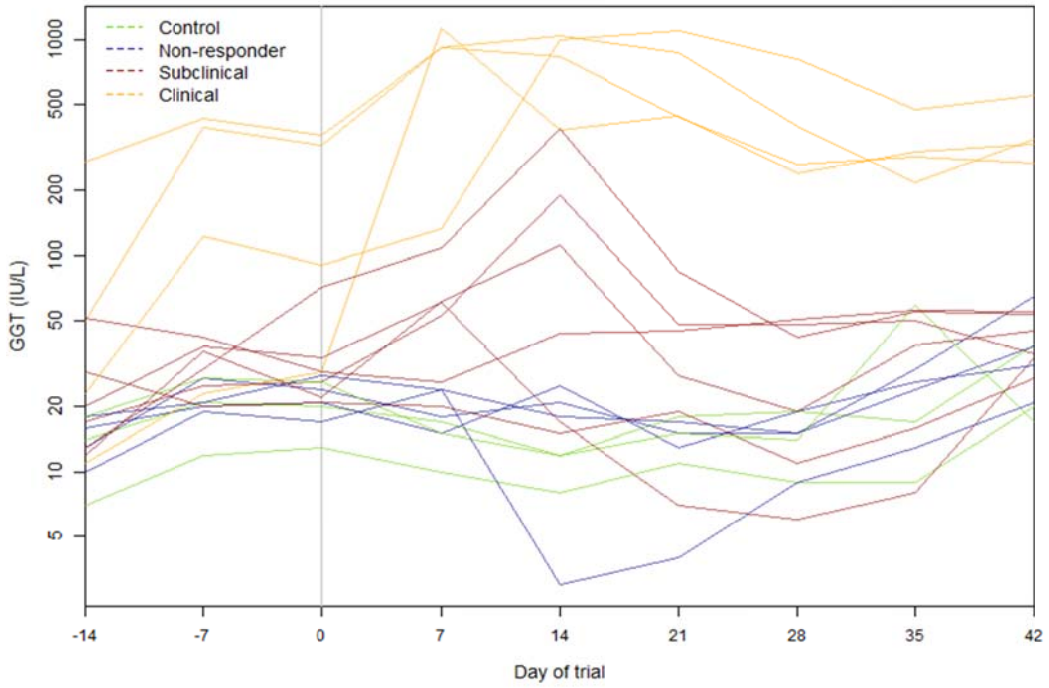

Figure 2.5 GDH activities individual cows, calculated using GAM, and coloured by their defined group. Day 0 refers to the day of dosing.

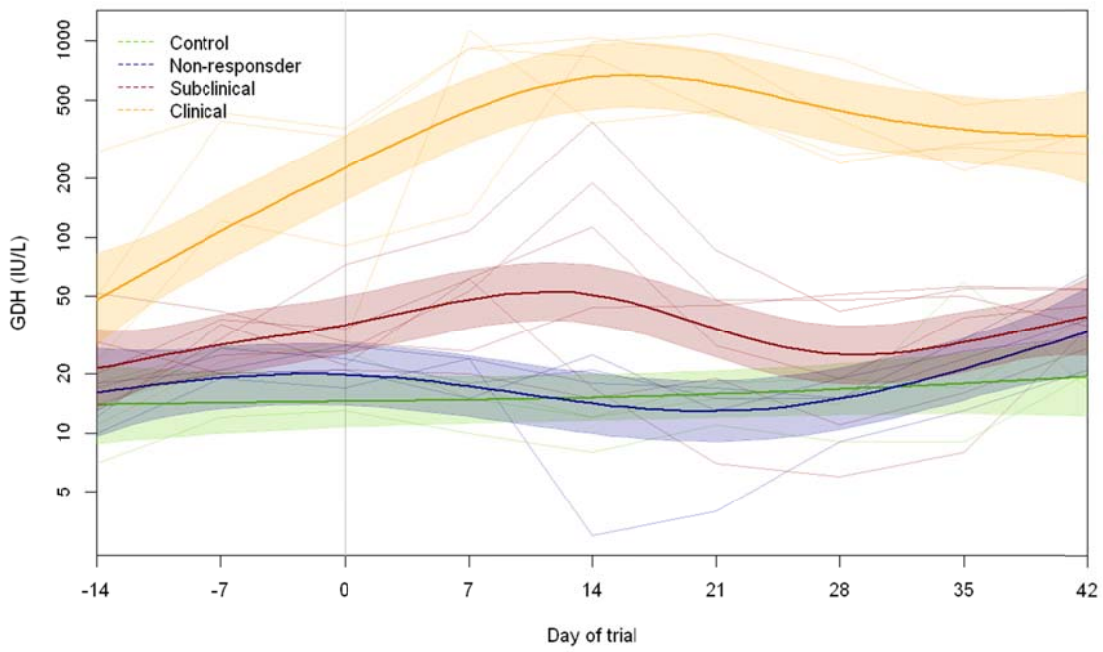

Figure 2.6 GDH activities for each of the four defined groups over time with within-group models fit, calculated using GAM. Day 0 refers to the day of dosing. Evidence for a difference in the shape of the curve between groups was observed ($p < 0.005$). Shaded areas represent the 95% confidence bands for that group.

2.3.3 Liver histopathology

The ventral and caudate liver lobes from each cow were subjectively graded on a scale 0 (normal), 1 (mild), 2 (moderate), and 3 (severe) for each of the following histological lesions:

- peribiliary concentric fibrosis and/or oedema
- ductular hyperplasia
- arteriolar hyperplasia
- portal fibroplasia
- portal inflammation, and
- parenchymal necrosis

The total score was the sum of all of the grades for both lobes. This meant that the minimum score was 0 with a possible maximum of 36. The liver lesion scores for each of the respective cow response categories are shown in *Table 2.5*. The liver lesion scores for individual cows are shown in *Appendix 1*. The mean lesion scores of 0.67 for controls, 2.75 for the non-responders, 7.0 for the

subclinicals, and 22 for the clinical cows, served to confirm the group categorisation that was defined by liver enzyme changes.

Of the control cows, mild peribiliary concentric fibrosis was seen in the ventral lobes of cows 22 and 152. Variable lesions were seen in the animals that were given a sporidesmin dose. Non-responders showed mild peribiliary fibrosis in the ventral and caudate lobes. The non-responder, cow 244, showed moderate to severe portal inflammation and peribiliary concentric fibrosis in the right (dorsal) lobe. This lobe is not commonly affected by sporidesmin and is likely to have been caused by exposure to other causes of inflammation. No other lesions were seen. The maximum GGT activities for this group ranged from 30 – 38 IU/L, including cow 244.

The subclinical cows all had mild to moderate peribiliary fibrosis in the ventral and caudate lobes. Cow 424 showed no other damage to the ventral and caudate lobes, but like 244 showed significant damage to the right lobe, with portal fibroplasia being severe and arteriolar and ductular hyperplasia being mild. Cow 395 showed moderate to severe damage in the caudate lobe, while cow 222 showed mild arteriolar and ductular hyperplasia, portal fibroplasia, and portal inflammation in both ventral and caudate lobes.

All clinically affected animals had severe lesions in the ventral and caudate lobes of the liver. No parenchymal necrosis was seen with any of the cows, other than in 244 which had moderate damage to the right lobe.

Table 2.5 Categorisation of groups based on elevated liver enzyme activities following sporidesmin dosing and visual signs of photosensitivity. Measured GGT and GDH activities are presented as median (range) for the group from the trial, after Day 0. Histological grading was performed post-trial on liver samples collected after euthanasia/slaughter so was not used to define the initial groups, but served as a confirmation of the status of each cow (discussed in 2.3.2).

Category		n	Cow ID	GGT* (IU/L 37°C)	GDH** (IU/L 37°C)	Clinical signs	Liver lesion score ***
Normal	Control	3	22, 152, 384	21 (16 – 27)	15 (7 – 59)	None	0.69 (0 - 1)
	Non-responder	4	195, 244, 374, 448	21 (13 – 33)	18 (3 – 65)	None	2.75 (2 – 4)
Responders	Subclinical	6	64, 222, 312, 395, 420, 424	56 (15 - 288)	44 (6 – 389)	None	7 (2 - 13)
	Clinical	7	239, 282, 298, 317, 393, 440, 450	1102 (116 – 2377)	440 (11 – 2420)	Abnormal irritability, shade seeking, increased sensitivity, reddening of non-pigmented skin, peeling of skin	22 (20 – 24)

* γ-Glutamyl transferase; normal range is 0-36 UI/L at 37 °C
** Glutamate dehydrogenase; normal range is 8-41 UI/L at 37 °C
*** Mean (range) of six different ventral and caudate liver lobe lesions subjectively graded on a scale from 0 (normal) to 3 (severe)

2.3.4 Body weights

The overall starting weight of the subclinical and clinical cows was lower than that of the controls and non-responders during the control period (*Figure 2.7*), and the range was greater for the subclinicals and clinicals, especially for the subclinicals, where one cow (ID 420) was much heavier at 548 kg. *Figure 2.7* illustrates this.

Following dosing, losses in body weight for the clinical cows ranged from 32 kg to 67 kg. Subclinical cow body weights were variable with only two of six cows showing large drops in body weight of 36 kg and 69 kg at Day 7 and Day 21 after dosing, respectively. Two non-responders showed large decreases in body weight of 29 kg and 57 kg at 7 and 21 days after dosing, respectively, while the other two cows (195 and 244) gained weight initially after dosing. Drops of 25 kg to 44 kg were observed with the three control cows 7 to 28 Days after dosing. Individual changes can be seen in *Figure 2.8.*

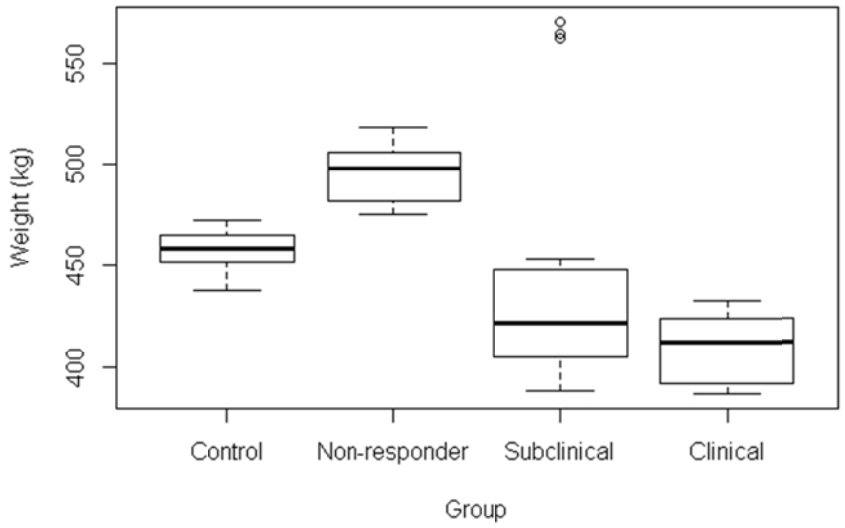

Figure 2.7 Box plot showing weights for the four trial groups during the control weeks. There is some heterogeneity between the groups, with subclinical and clinical groups having larger within-group variation and a lower average weight compared to the other two groupings. The large variation in the subclinical group is primarily due to a single heavy cow (No. 420).

To assess how weight changed during the trial a GAM was fitted to the data. The model fit and raw data for each animal is shown in *Figure 2.9*. There is some suggestion of slight drops in body weight over the trial period. While the average weight of control and non-responders is relatively constant over time, there appears to be a small initial drop in the subclinical group and a larger drop in the clinical group. The clinical group continued to lose weight until after week two (Day 14), but this drop was recovered by the end of the trial. However, there was no evidence of the separate curves between groups being statistically significant, suggesting that the differences in weight observed

may have arisen by chance. This may be partially due to the amount of variation within each group. For example, in the non-responder group there are two cows whose weight was relatively stable, and two whose weight dropped in the first two weeks. Similarly, in the subclinical group the heaviest cow showed no evidence of weight loss.

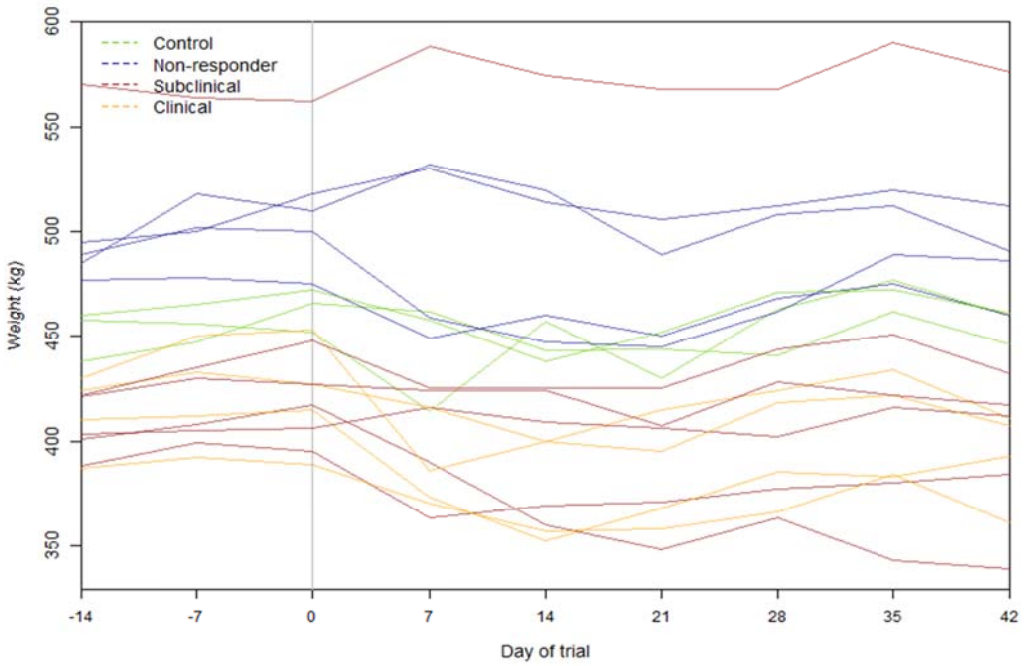

Figure 2.8 Bodyweight over time for individual cows, using a generalised additive model (GAM), coloured by defined groups. Day 0 refers to the day of dosing.

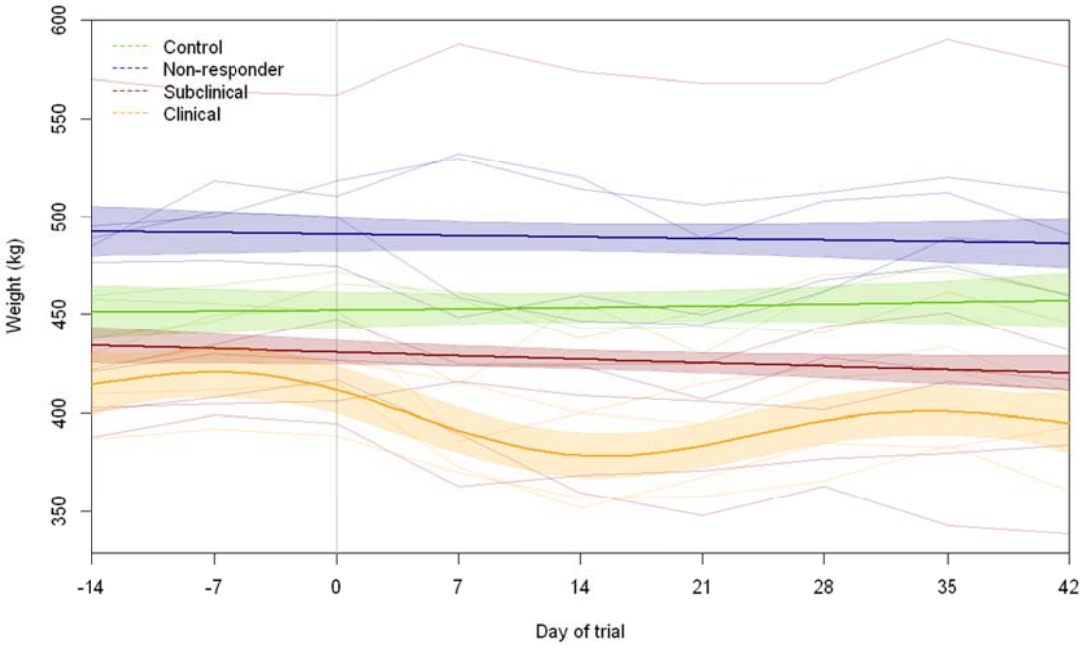

Figure 2.9 Bodyweight over time using a generalised additive model (GAM), with within-group model fits (bold lines) and individual weights shown. The clinical group showed a slightly bigger decrease in bodyweight up to Day 14 compared to the other groups, but this was not significant. Shaded areas represent the 95% confidence interval for that group.

2.3.4 Morning milk yields

A difference can be seen in the milk production of each group during the control weeks (*Figure 2.10*). It appears that the overall starting yield of non-responder, subclinical and clinical cows was lower than that of the control cows, however the range was greater for subclinical and clinical, especially for subclinical where one cow had higher levels of milk production than the rest. The clinical group included one cow that produced the lowest milk yield on the morning of Day 0 (cow 440, 3.3 L).

The milk yield data was further analysed using GAM to assess how milk yields changed over the trial period. This modelling allowed for each group to have a separate smooth average milk yield, taking into account the initial weight of the animals. The model fit and raw data for each animal is shown in *Figure 2.11*.

The average milk production for all cows, including the control cows, varied over time; however, a consistent drop in milk yield can be seen in the dosed cows, with the non-responders showing the smallest drop, and clinical animals having the greatest drop in morning milk yields.

All treated cows showed a transient drop in morning milk production in the days following dosing (Day 0) (*Figure 2.12).* By around Day 7, the milk production of the non-responders and subclinicals had dropped to their lowest level, while the clinical cows continued to drop, reaching their lowest average milk production around Day 11, post-dosing.

In *Figure 2.12* a decreasing trend can be seen in the controls, non-responders and subclinicals after around Day 20, with these levelling out again towards the end of the trial. The clinicals responded in the same way, but less obviously due to the slow increase from the minimum at Day 11.

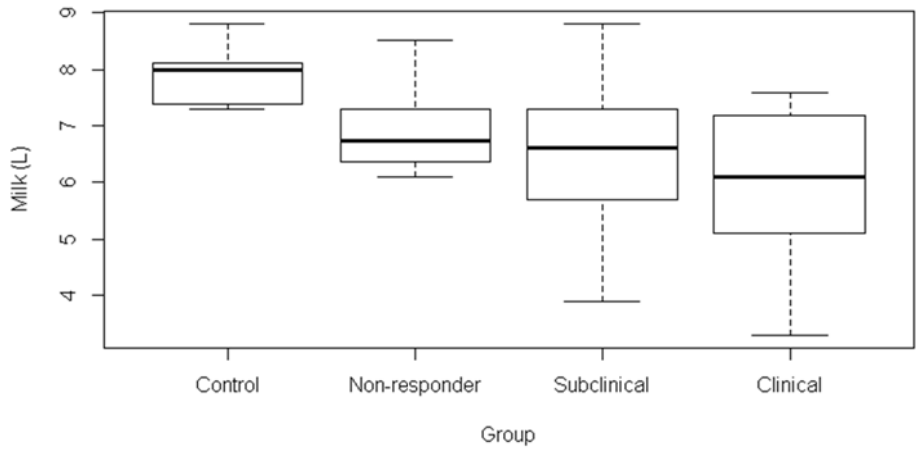

Figure 2.10 Box plot showing the range in milk yields for all groups during the control weeks

Through this analysis a clear drop in milk yields can be seen following dosing, but by Day 42 these are close to their original levels as at Day -14. However, when weight is taken into account, using another GAM model (not shown), this drop in milk production appears to be the same for all groups. The correlation between weight and milk production is analysed in more detail in the next section.

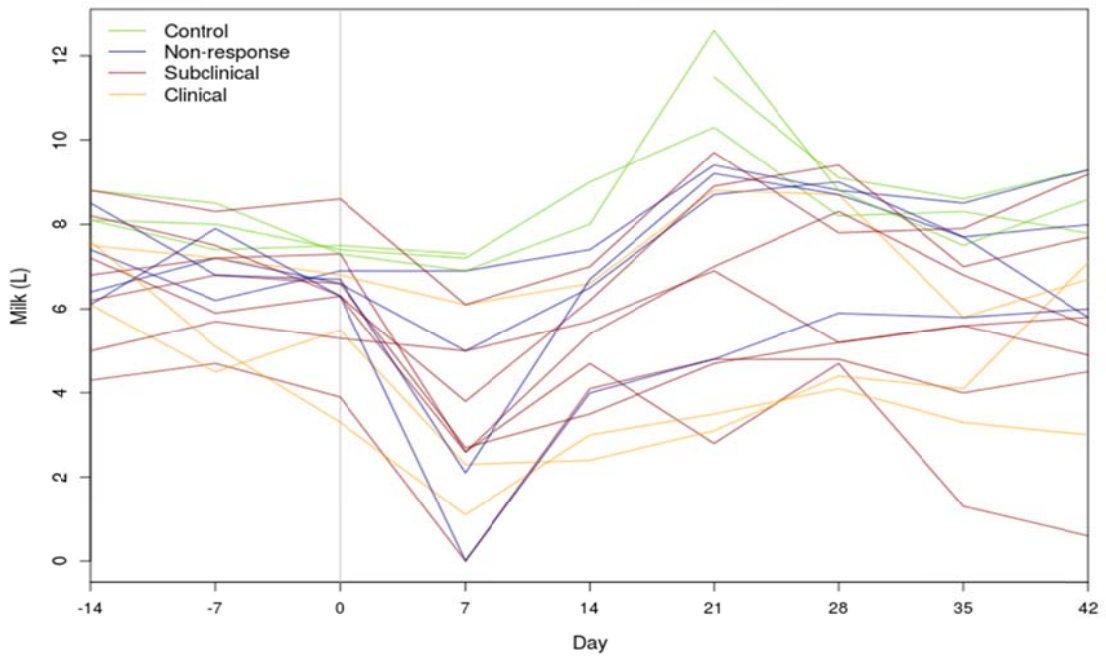

Figure 2.11 Milk yields of individual cows over time, calculated using a generalised additive model (GAM), coloured by defined groups. Day 0 refers to the day of dosing.

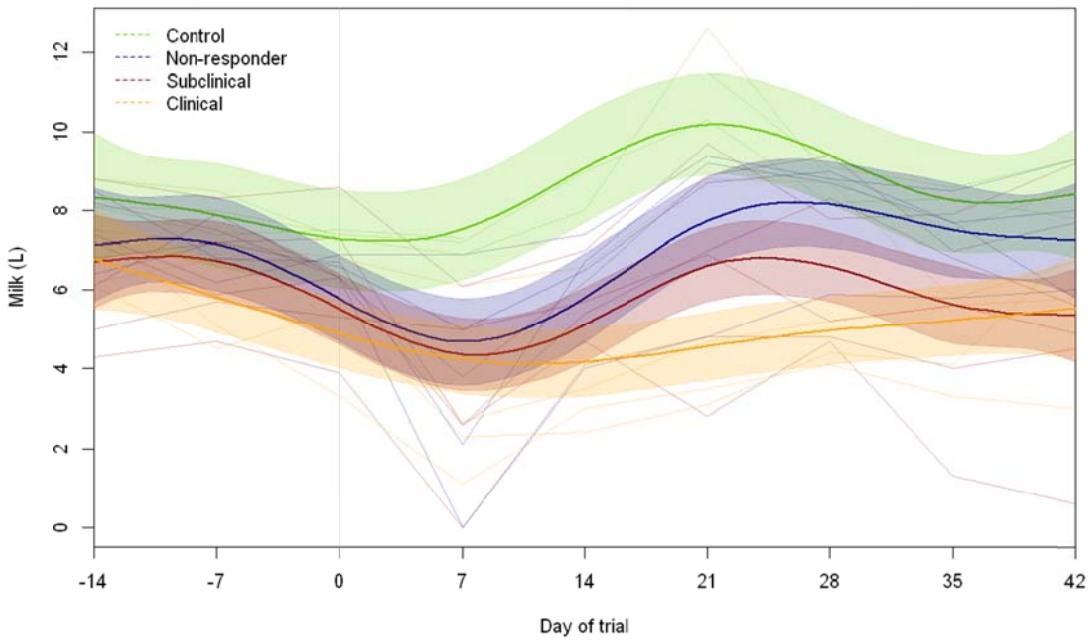

Figure 2.12 Milk yields of cows over time, calculated using a generalised additive model (GAM), with within-group model fits shown. No evidence of a difference in the shape of the curve between groups was seen. Shaded areas represent the 95% confidence intervals for that group.

2.3.6 Descriptive analyses of liver enzyme activities with milk yields and body weights

Scatterplots were used to identify whether variables were related and how much influence they had on other variables. The GGT and GDH activities appear to be positively correlated (*Figure 2.13*), therefore for an overall increase in GDH activities there would be a subsequent increase in GGT activities. This appears to be a within group effect, where the observations with high GGT and GDH correspond to the clinical group, and observations with low GGT and GDH with controls and non-responders. The activity of GGT is proportional to the activity of GDH for individual cows, and these are in the order, for the groups, of clinical > subclinical > non-responder = control. It can be seen that the non-responder and control groups show very little change in GGT activities ($\log_e$GDH range 2-4 IU/L), however, show greater within-group spread in GDH activities ($\log_e$GGT range 2.5 - 3.5 IU/L). This is also apparent, but less-so, in the subclinical and clinical groups, with GGT changes occurring between groups, while GDH spread occurs within groups. This suggests that GGT activities may be more indicative of the degree of liver damage following sporidesmin challenge occurring within individuals, compared to GDH activities.

GGT and GDH activities were both negatively correlated with weight over the trial period (*Figures 2.14 and 2.15*). Subclinical and clinical groups showed overall lower weights than controls and non-responders, except for one subclinical cow (420) which had the highest weight over all, but still lost

weight after dosing. The controls and non-responders stayed well clustered over the trial period, while the subclinicals and, more extremely, the clinicals showed a change in GGT activities following dosing.

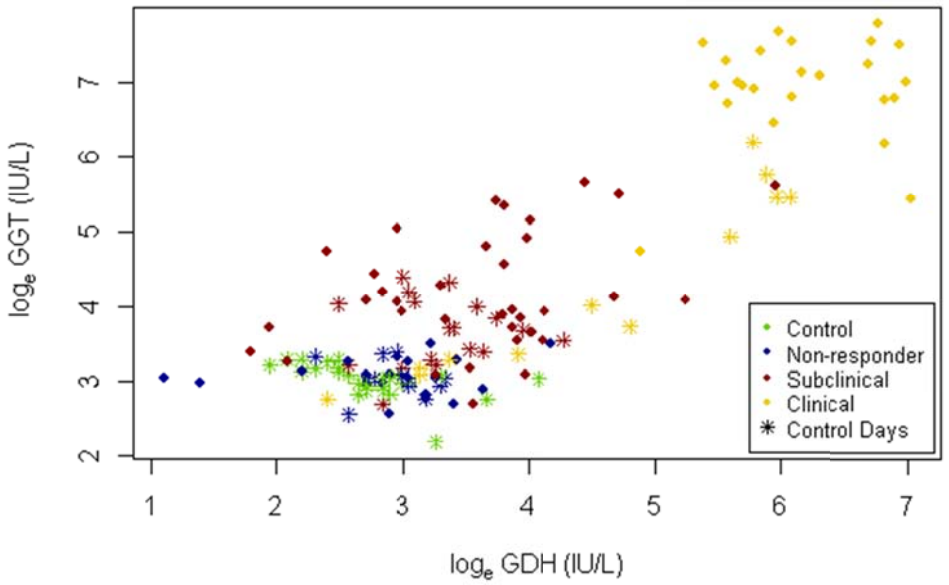

Figure 2.13 Scatterplot showing the relationship between the log$_e$ of GDH and GGT activities for all cattle, over the entire trial period.

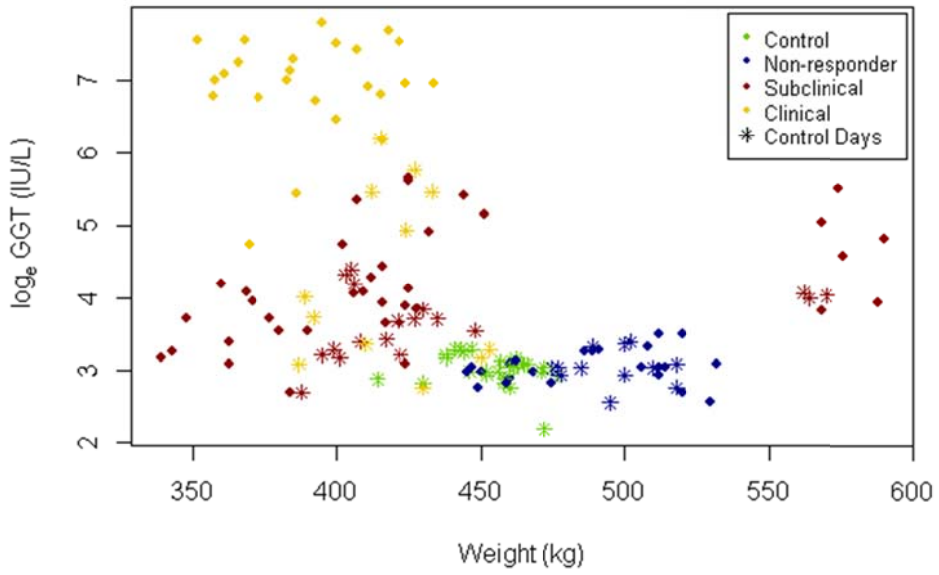

Figure 2.14 Scatterplot of all groups over the entire trial period showing a negative relationship between log$_e$GGT activities and weight.

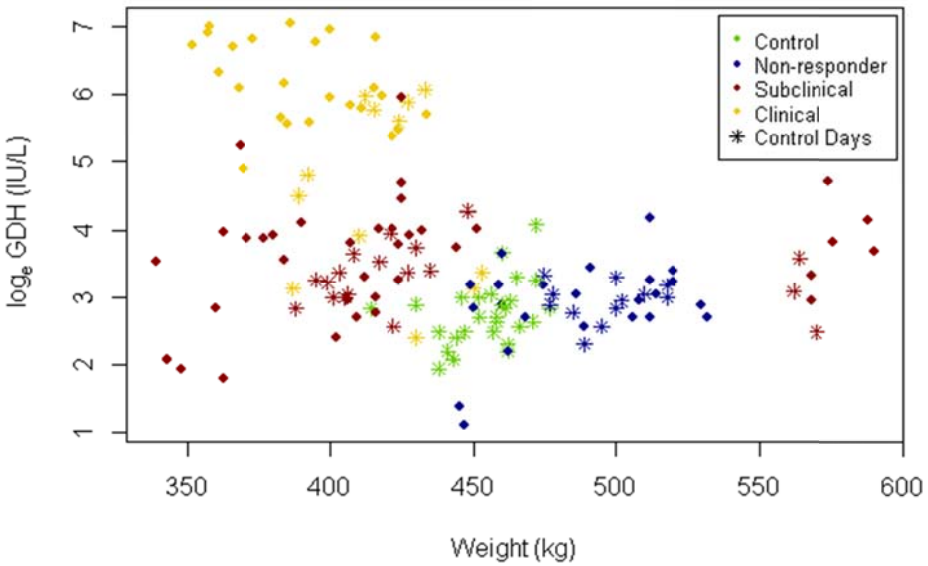

Figure 2.15 Scatterplot of all groups over the entire trial period showing a negative relationship between $\log_e$GDH activities and body weight.

Body weight and milk yields were shown to have a positive relationship (*Figure 2.16*).

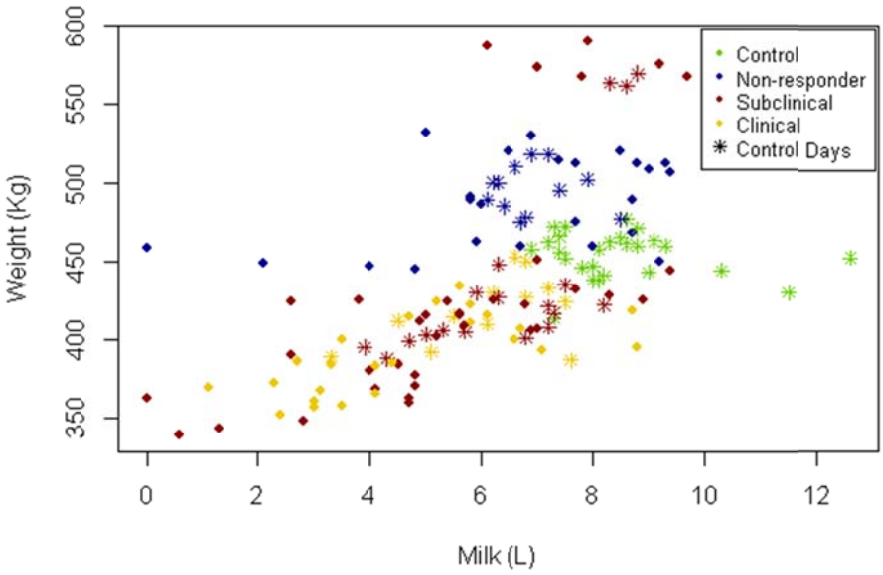

Figure 2.16 Scatterplot of all groups showing a positive relationship between body weight and milk yield. Non-responders and controls over the whole trial, and subclinicals during the control period, showed higher weights and milk yields over all.

A negative relationship was seen between milk yields and $\log_e$ of GDH activities (*Figure 2.17*). No relationship was found between GGT activities and milk yields. Note that observations with a high GDH tend to be samples from the clinical group that correspond to the weeks immediately following sporidesmin dosing (e.g. Days 7 and 14), while those with low GDH tend to correspond with control

weeks (Days -14, -7 and 0) and late stages of the trial (Days 35 and 42) where activities were returning to normal.

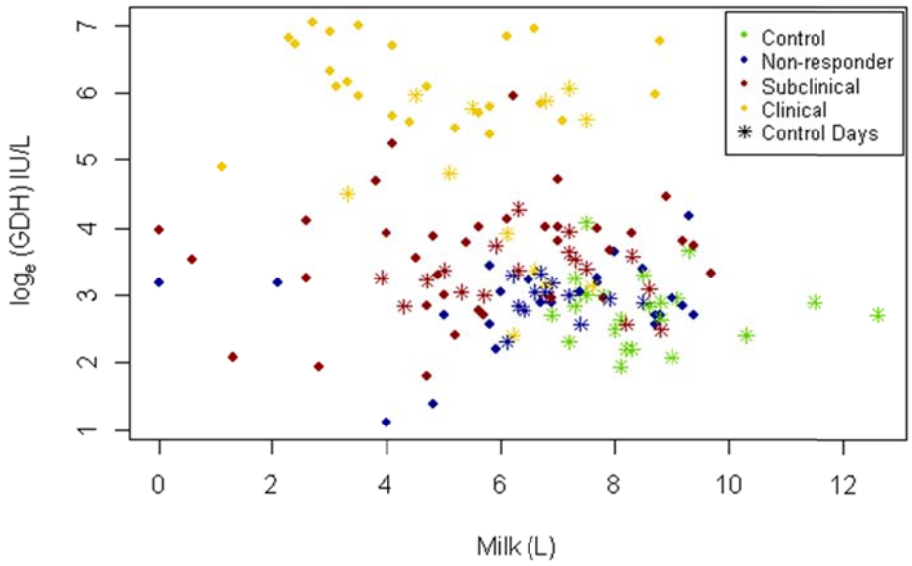

Figure 2. 17 Scatterplot of all groups over the entire trial period showing a negative relationship between milk yields and log$_e$ of GDH activites.

2.4 Discussion

The current study was designed to minimise the risk of natural exposure to *P. chartarum* spore challenge. Despite the application of fungicide sprays on the paddocks used in the trial, a moderate spore count was measured on two separate days during the trial period. Moderate counts were also recorded by the Massey Equine and Farm Services Clinic on Day -14, however, these samples were taken from random paddocks, and therefore are not strictly comparable to the paddocks grazed in the trial. However, a moderate measurement at this time in the pastures does correspond well with the moderate faecal spore counts (666,000) that were measured on Day 0. Moderate spore counts usually indicate the need to consider corrective measures. However, because the faecal spore counts dropped significantly by Day 7, they were not considered to affect the trial results. Additionally, spore counts taken directly from the paddocks that were grazed in the trial were low, so were not considered to be a risk to the trial results. Furthermore, the only evidence of any response to a natural sporidesmin challenge in the cows was a drop in weight after Day 0 for the control group, which did not receive the artificial challenge. In New Zealand, sporidesmin production is reported to be directly related to the number of spores in pasture (Di Menna & Bailey, 1973). This means that low pasture spore counts imply low levels of sporidesmin in pastures and therefore minimal chance of a natural challenge.

The liver enzyme activities combined with the clinical observations, allowed for the division into categories according to the response to sporidesmin challenge by the cows. These results, along with changes in body weight and milk yield, allowed for general time lines to be identified. For example, the three weeks after dosing could be identified as a stage of response to the sporidesmin exposure, while the following (final) three weeks could be seen as a recovery stage, where liver enzyme activities were beginning to decrease, and body weight and milk yield began to, and in some cases did, return to levels seen in the pre-trial control stage.

Of the 17 dosed cows, 41.2% (7/17) presented as clinical, 35.3% (6/17) as subclinical, and 23.5% (4/17) were non-responders. This could imply that in the typical North Island herd of approximately 332 dairy cows (*New Zealand Dairy Statistics*, 2012-2013) exposed to a sufficient sporidesmin challenge, approximately 117 would be subclinically affected, depending on susceptibility and heritability. This trial shows that subclinicals would be losing some weight, show some deterioration of condition, and be producing less than expected milk yields, without any outward signs of photosenstisation. Previous studies have confirmed that liver lesions, like those seen in this study when animals are orally dosed with sporidesmin, are similar to those seen in naturally challenged animals. (Mortimer, 1963, 1971).

Although at first glance, body weight differences could be seen between the groups with a loss of weight visible directly after dosing, especially for the clinical cows, these differences were not considered to be significant. One reason for these changes not showing significance may be due to the small population size for the trial. This finding conflicts with much of the literature on facial eczema. Studies by Towers and Smith (1978) and Morris (1991a) showed that both adult Jersey cattle and mixed breed bull calves revealed significant weight losses following large doses of sporidesmin during artificial challenges. Other studies, using sheep as the study species, also showed marked losses in body weight in animals with severe clinical FE proportional to the dose rates given over a short period (Smith, 2000), and the magnitude of the GGT activities were positively correlated to the losses (Towers & Stratton, 1978). Morris (1991a) also reported that live weight gain showed a significant negative regression with $\log_e$GGT. This was also found in the present trial.

The insignificant drop in body weight, for all four groups, from the start of the trial until the end may be due to some indirect environmental or physiological effect, unrelated to FE, such as paddock changes, the change in pasture composition from the original farm to the trial farm, or because the cows were nearing the end of lactation. Since less energy is required to maintain milk production at the end of lactation, more energy is required to build body condition to act as an energy reserve for

the next lactation (Harzia *et al.*, 2013; Klein *et al.*, 2010). During the trial no changes were made to the quantity of feed and this may have influenced the loss of weight towards the end of lactation.

Although it is a commonly discussed theory by farmers and veterinarians that one of the effects of clinical FE is a sudden pronounced depression in milk production following sporidesmin dosing (Smith *et al.*, 1983; Steffert, 1970; Towers & Smith, 1978), there are few studies with data on this. In addition, the effects of subclinical FE generally go unnoticed (Morris *et al.*, 1991a), which makes studying these animals, and attributing these decreases in milk production to sporidesmin challenge, difficult. In this study, all treated cows showed a transient, but significant, drop in milk production in the days directly following dosing. The cows within the non-responder and subclinical groups recovered reasonably quickly, and returned to close to their initial milk yield at around Day 16, however, the subclinical cow production level remained below that of the non-responders. Clinical cows never recovered their initial levels of milk production. This pattern of recovery or non-recovery is consistent with the level of liver damage that each group had. This is in agreement with previous reports on artificial sporidesmin challenges. Towers and Smith (1978) gave sporidesmin on two occasions to groups of Jersey cows, where one group was given preventative zinc, while the other was provided with no preventative strategies. Although they did not report on non-responders or subclinical cattle as such, they demonstrated that clinically photosensitive cattle showed significant drops ($p < 0.001$) in milk production immediately after both the initial and secondary doses. Additionally, the clinical cows in the 1978 study were shown to increase milk production above their minimum at 4 - 5 days post dose, at a rate equal to those cows that received zinc, but then levelled off and never returned to initial production by the end of the trial. This lowered milk yield, at the end of the trial, was still significantly lower than the control or zinc-dosed cattle. The same pattern was seen in the present study. However, all cattle, including the control cows, showed a drop in milk yield towards the end of the trial. This could be due to the cows reaching a late lactation stage, where their mean daily milk yield would naturally diminish anyway.

Individually, there was wide variation in the response to sporidesmin within groups. However, the immediate and significant drop in milk production, following a single dose of sporidesmin, does indicate that ingestion of this mycotoxin significantly decreases milk production. These results also show that the speed of recovery of milk production to normal or original levels is in some way dependant on the susceptibility of the cow to this toxin, and the level of damage caused following ingestion. It is still unknown whether this is caused by a direct effect of the sporidesmin toxin on the mammary gland, or whether the decreased production is a transient effect caused by other

metabolites or metabolic factors. Towers and Smith (1978) believe that it is likely that a direct effect on the mammary gland is the cause of reduced milk yields following sporidesmin intoxication.

The significant increase in GDH and GGT activities for subclinical and clinical cattle following one dose of sporidesmin seen in the present study is consistent with previous studies (Ford, 1974; Towers & Stratton, 1978). Morris *et al.* (1990) state that in their study, which was investigating a natural challenge, elevated GGT activities of > 30 IU/L were considered indicative of liver damage associated with FE.

The non-responders, although dosed at the same rate, showed no or very little change in liver enzyme production. These cattle clustered closely with the control samples, especially when looking at the correlation of GGT and GDH, which were highly positively correlated. The findings of the non-responders are similar to what would be expected of animals that have been administered zinc preventatives before and/or after a sporidesmin challenge (Towers & Smith, 1978).

Both GDH and GGT activities stayed elevated after sporidesmin dosing until the end of measurements (Day 42), with the GGT activities reaching a maximum, on average, between Days 21 and 28, while the GDH reached a maximum around Day 14. Previously it has been shown in bulls that a sporidesmin dose led to maximum GGT activities after Day 23 post-dose (Morris *et al.*, 1991a). This is all in agreement with what is known of FE where GDH enzyme production precedes GGT enzyme production, and the GGT activities stay elevated for longer following liver damage (Morris *et al.*, 1998). Additionally, GGT and GDH activities are positively correlated and were both higher in subclinical and clinical cows after dosing when compared to the control weeks, prior to dosing. These two groups also show significantly higher activities of both liver enzymes when compared to control and non-responder cows. There is also a greater spread in GDH levels within groups, for all groups, than seen with GGT levels. This is suggestive that GGT is a better indicator of severe liver damage after sporidesmin challenge.

GGT and GDH activities were both negatively correlated with weight. Subclinical and clinically affected cows showed lower weights overall and the biggest drop in weight measurements following dosing. The one exception was cow 420 that had a higher than average weight initially, which skewed the results somewhat. The control and non-responder cows clustered well, demonstrating that there were similarities between the two groups, and suggesting that, using these analysis techniques, non-responders change very little, if at all, in response to sporidesmin challenge. However, this relationship may be largely driven by the grouping. For example, the clinical group typically weighed less than the others throughout the trial, while having higher GGT and/or GDH activities.

While milk yields and GGT activities showed no significant correlations, milk yields and GDH activities were negatively correlated. A higher GDH activity correlated with a lower milk yield in subclinical and clinical groups. The subclinical and clinical cows did already have lower milk yields than controls and non-responders in the control period; however, the former groups showed a greater range in the measurements as well.

Body weights and milk yields were shown to be positively correlated, with control and non-responder cows having higher milk yields and higher weight measurements than the subclinical and clinical cows. The one outlier was again cow 420, which had the highest weight and one of the highest milk yields of the herd throughout the entire trial. Cow 420 did follow the same pattern of milk yield decline, immediately following dosing, as seen with all other subclinical and clinical cows. Subclinical and clinical cows showed a decrease in both milk yield and weight following dosing; however the latter was not considered to be significant. These results do not provide conclusive evidence as to whether this correlation is significantly related to sporidesmin challenge or not.

Although elevated GGT and GDH enzymes as well as liver damage shown in the earlier literature and in the present study are considered to be indicative of FE challenge, they are not specific for FE, and cannot be used on their own to identify clinical, subclinical and non-responder cows in a herd. These enzymes are well known to be affected by diseases and injury in other organs as well as various causes of injury to the liver (Moreira *et al.*, 2012). These parameters are therefore unreliable as the only indicators of FE; they are not representative of early stage damage, and therefore of the processes occurring in the lead-up to liver damage. In addition, the indication that even cattle showing no signs of sporidesmin challenge, including normal liver enzyme activities, can have depressed milk production, suggests that significant milk production losses on farms may not be recognised or could even be wrongly attributed to other causes. Furthermore, very little is known about the 'carry-over' effects of sporidesmin intoxication, including the effect on conception and gestation. It has been suggested that continual small doses of sporidesmin, over time, although not initially causing clinical signs, may cause enough damage to produce a 'build-up' effect, meaning in time, an animal which could have been considered a non-responder, may escalate to a subclinical and a even clinical case eventually. This not only demonstrates how easy it can be to overlook non-responders and subclinical facial eczema, but also signals the need for more definitive identification strategies.

CHAPTER 3

MEASURING PHYTOPORPHYRIN CONCENTRATIONS IN THE BLOOD OF PHOTOSENSITIVE CATTLE USING FLUORESCENCE SPECTROSCOPY

3.1 Introduction

Liver and bile duct damage caused by the ingestion of sporidesmin during late summer and autumn months leads to the retention of phytoporphyrin (phylloerythrin) in the bloodstream of susceptible ruminants. With increased retention, the concentrations of this compound increases in dermal capillaries, and when exposed to light of certain wavelengths it becomes excited through photochemical reactions (Scheie *et al.*, 2002). The excited molecules react with oxygen, producing cytotoxic reactive oxygen species (ROS) (Scheie *et al.*, 2003b). These cytotoxic products cause reddening and swelling of the skin, and these natural acute inflammatory responses result in the initial clinical signs of clinical facial eczema (FE). Phytoporphyrin has also been found to be localised in Golgi and/or mitochondria which may act to enhance its cytotoxic effect (Scheie *et al.*, 2002).

It is unknown how long phytoporphyrin remains photoactive in the body or how its activity is eventually lost. There are reports that some photosensitising molecules can be degraded and/or modified by light (photodegredation) (Moan *et al.*, 1988). This can be seen as a loss of fluorescence in both tissues and solutions during light exposure. However, no form of photodegradation has been reported, to date, for phytoporphyrin when exposed to light (Scheie *et al.*, 2003b).

The fluorescent spectra of phytoporphyrin have previously been characterised spectrophotometrically in serum, bile (Perrin, 1958a, 1958b), and urine (Ford & Gopinath, 1974). Phytoporphyrin can be excited at 425 nm and has an emission peak at approximately 644 nm. *Figure 3.1* shows an example of the emission peak, which appears on the shoulder of a protein peak in serum samples, and the procedure used to extract the phytoporphyrin peak for further analysis.

Quantification of phytoporphyrin in biofluids came across early difficulties due to the compounds insolubility in water. It was found to be only partially soluble in calibration solutions, or precipitated within minutes at room temperature at concentrations > 5 µM (Campbell *et al.*, 2010). Campbell *et al.* (2010) subsequently determined that solutions were able to be prepared in methanol at concentrations up to 3.7 µM, and these were stable for several weeks when stored at room temperature in the dark.

Another limitation to phytoporphyrin measurements includes the coagulation of serum proteins which can alter the position of the phytoporphyrin peak. In addition, the presence of other fluorophores, such as haem, which has a peak at 600 nm in haemolysed blood samples, can mask the phytoporphyrin peak and/or quench some signals, making extrapolation of the peak difficult (Campbell *et al.*, 2010; Dunn *et al.*, 2011b). It was suggested that phytoporphyrin in bile and serum at pH 7.4 is maintained by adsorption on colloidal micelles (Perrin, 1958b). These factors may mean

that fluorescence measurements are not a true representation of the concentration of phytoporphyrin present in blood of an animal at any one time. It may, however, give a snapshot of changes between disease stages, such as non-responder, subclinical and clinical cows following sporidesmin challenge.

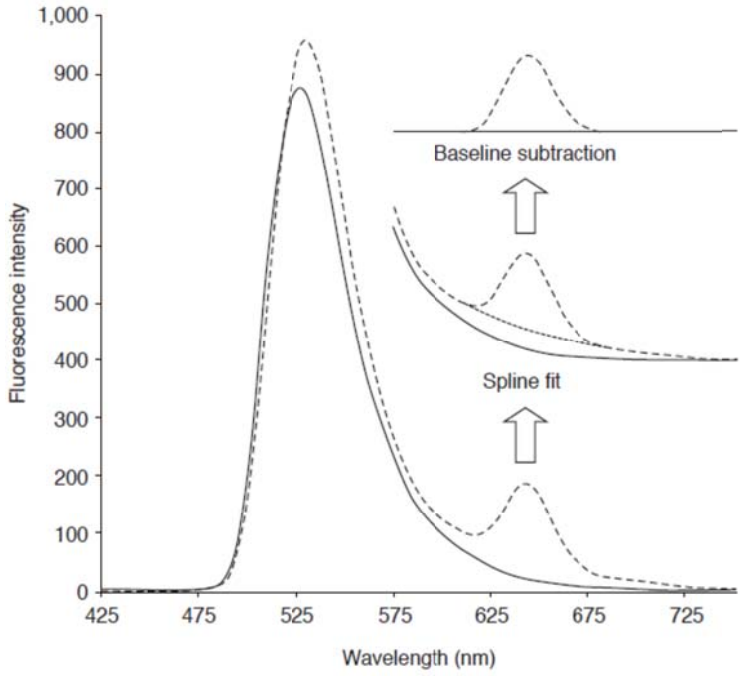

Figure 3.1 Fluorescence spectra of serum from a control cow and diseased cow showing the appearance of the phytoporphyrin peak at approximately 644 nm on the shoulder of the protein peak, and the spline fitting and baseline subtraction of this peak for further analysis (used with permission from Campbell et al. (2010)).

Scheie *et al.* (2003b) determined that the concentration of phytoporphyrin in the plasma of sheep dosed with sporidesmin (0.25 mg/kg) was between 0.08 to 4.90 µM for photosensitised animals, while control animals ranged between 0.01 and 0.09 µM. The average concentration of phytoporphyrin in healthy cattle was calculated as 0.05 (SD 0.03) µM (Scheie & Flåøyen, 2003).

Campbell *et al.* (2010) determined levels of phytoporphyrin in cattle (n = 5) to range from 0.4 to 1.8 µM. Another study followed these same methods (Cullen *et al.*, 2014), however none of the cattle measured in their 2012 study (n = 50) showed signs of clinical FE, even though they reported activities of GGT > 600 IU/L. All 50 animals challenged were reported to have phytoporphyrin concentrations of < 0.4 µM following a sporidesmin challenge of 0.27 mg/kg. No studies measuring phytoporphyrin levels have presented data on subclinical cattle.

3.1.1 Aim

To detect variations in concentration of phytoporphyrin in serum following sporidesmin challenge, and identify whether changes occur before or after changes in liver enzyme activities.

3.1.2 Objectives

- To detect the variations in concentration of phytoporphyrin in serum of all categorised groups following sporidesmin challenge.
- To identify whether different categories of response to sporidesmin challenge, can be identified using phytoporphyrin concentrations in serum, i.e. non-responders, subclinical and clinical cases.
- To determine the stage at which phytoporphyrin concentrations in serum increase above the 'normal' threshold, following a single sporidesmin challenge.
- Identify how changes in phytoporphyrin concentrations relate liver enzyme activities and clinical signs.

3.2 Materials and Methods

3.2.1 Standard solution preparation

A standard solution of phytoporphyrin (~95%, batch # JB04-233; Fontier Scientific Inc. Logan UT, USA) was prepared according to the method of Campbell *et al.* (2010), by dissolving the phytoporphyrin in methanol (99.8%, Merck KGaA, Darmstadt, Germany) with the aid of ultrasonication at 50 ^{o}C for 45 minutes. The solution was made to a final concentration of 3.549 µM using Milli-Q water (Merck Millipore Inc. Billerica, MA, USA). Phytoporphyrin has been shown to adsorb on to glass surfaces (Campbell *et al.*, 2010), and therefore the standard solution was prepared and stored in polypropylene containers. The final solution was stored at room temperature, in the dark, and was ultrasonicated prior to use if unused for several weeks.

Calibration curves were generated using the standard solution and control sera from cattle of various species and age cohorts, including adult cattle as well as calves. The method of Campbell *et al.* (2010) was replicated here, where different ratios of methanol and standard phytoporphyrin solutions (5, 10, 20, 40, 80, 160, 320, 350 µL) were added to sera to give a desired concentration in a total volume of 750 µL. Serum samples were diluted with water (1:1) before the phytoporphyrin/methanol solution could be added to eliminate (or minimise) coagulation of

proteins in the solution (Campbell *et al.*, 2010). Additionally, cuvettes were cleaned thoroughly with water followed by methanol using cotton swabs, between each measurement to remove any remaining phytoporphyrin.

3.2.2 Sample source

The samples were sourced from the sporidesmin challenge trial in dairy cattle described in *Chapter 2*. Venous blood samples were collected into vacutainers containing no anticoagulant (BD vacutainer, Franklin Lakes NJ, USA). Samples were sent to the New Zealand Veterinary Pathology (NZVP) Ltd, in Palmerston North, for liver panel testing and then forwarded to our group for further testing. The liver panel test included γ-glutamyl transferase (GGT) and glutamate dehydrogenase (GDH) activities, bilirubin, total protein, albumin and globulin measurements. Blood tubes were kept in the dark by being wrapped in aluminium foil and/or placed in enclosed polystyrene or black plastic containers to protect against light.

Full detail sampling procedures for the collection of blood samples for fluorescence analysis from the facial eczema challenge are explained in *Chapter 2*. Samples were stored at -80 ^{o}C until required for analysis.

3.2.3 Fluorescence measurements

All measurements were made with a Perkin Elmer LS-50B luminescence spectrophotometer (PerkinElmer Inc., Norwalk CT, USA) equipped with a red-sensitive photomultiplier tube (R928; Hamamatsu Photonics, Hamamatsu, Japan), using quartz semi-micro cuvettes (0.8 ml, 4.75 x 4.75 x 33 mm, PerkinElmer Inc., Beaconsfield, Bucks, UK).

On the day of analysis sample tubes were thawed on ice. Thawed samples were centrifuged at 3000 rpm for 6 minutes, and then 200 µL of the serum supernatant was transferred to a quartz cuvette before adding 200 µL of Milli-Q water and 350 µL of HPLC grade methanol. The sample was mixed by inverting several times.

For the measurement of phytoporphyrin the spectrophotometer was set to measure emissions between 425 and 750 nm, at an excitation wavelength of 425 nm. The excitation and emission slit widths were set at 15.0 nm and 20.0 nm, respectively, with an emission filter cut-off of 515 nm and scan speed of 100 nm/minute. The red-sensitive photomultiplier tube (R928) was employed. A standard calibration block was measured at the beginning of every sample batch to ensure consistency of the equipment performance.

3.2.4 Data analysis

All fluorescence data, including calibration curves, were processed using OriginPro graphing software (OriginLab Corporation, Northampton MA, USA). The following methods, based on those of Campbell *et al.* (2010), were used to process the data. The peak areas were found by spline-fitting a baseline in the region of 575 – 750 nm. The phytoporphyrin peak is seen at 644 ± 5 nm. The baseline was subtracted and the resulting peak was fitted with a Gaussian-Lorentzian cross-spectral peak fit to measure the area of the extrapolated peak and to ensure that no potential underlying spectral peaks were present. The area under the curve was compared to the phytoporphyrin calibration curve and from this the concentration of the phytoporphyrin in the serum was determined. A second order polynomial was fitted to compensate for slight deviations from linearity at higher phytoporphyrin concentrations. At low concentrations (< 0.05 µM) of phytoporphyrin in sera (< 0.05 µM) the reliability of the method decreased appreciably, therefore Gaussian -Lorentzian areas under the peak measuring less than 2 were deemed too low to be determined accurately (limit of detection S/N ratio > 2). Gaussian-Lorentzian areas under the peak measuring less than 2 were deemed to be too low to determine phytoporphyrin concentration accurately so were considered to be noise in the spectra, and were removed from the data analysis accordingly. This was regarded as the lower limit of the spectrophotometer sensitivity.

Biplots were produced to look for correlation patterns between phytoporphyrin, GGT, and GDH activities. Common linear regression analyses, mixed effect models, ANOVA analyses and Generalised Additive Models (GAM) were conducted using RStudio statistical software (Version 0.97.449, RStudio, Boston, MA, USA). An explanation of the GAM process can be found in *Section 2.2.6.*

Mixed effect models were used to take into account that individual cows may have differences between each other and within themselves due to the temporal nature of the data. The models also allowed for varying slopes and intercepts for each group (control, non-responder, subclinical and clinical). These models, including the common regression model, are nested, and thus were compared using an F-test to identify the best model. Furthermore, it was established whether the regressions were group dependant or whether cow random effects were important. To assess the relationships between phytoporphyrin and liver enzymes (GDH and GGT) a mixed effects linear regression model was used. This took the form:

$$Phyto_{ij} = \alpha_j + \beta_j(\log_{GGT_{ij}}) + Cow_{ij} + \varepsilon_{ij}$$

where cow_{ij} was a random per-cow effect, accounting for the fact that multiple observations on each cow over time were unlikely to be independent; α_j was the per-group intercept; and β_j the

per-group slope. Thus, the model fits separate regressions for each group. In addition, a common regression across all groups (by setting common $\alpha_j = \alpha$ and $\beta_j = \beta$) was used to determine the overall relationship across all groups. The conditional R^2 was then computed. Additionally, Cook's distance was inspected in residual versus leverage plots to identify any outliers. Cook's distance measured the effect of deleting a given observation. Samples with large residuals may strongly bias the accuracy of the regression. Any outliers were removed and the regression re-calculated.

3.3 RESULTS

3.3.1 Serum phytoporphyrin concentration in cows dosed with sporidesmin

Serum from clinically healthy animals (controls, non-responders, and all animals during the control weeks) generated either a weak fluorescence signal or no signal at all, at 644 nm. Serum from all cows that developed clinical FE showed spectral features matching those of phytoporphyrin during the experimental period, namely an emission band at 644 nm when excited at 425 nm. The concentration of serum phytoporphyrin from clinically affected animals, taken after dosing, ranged from < 0.05 to 1.33 µM, while those from subclinical cows ranged between < 0.05 and 0.18 µM, and non-responders between < 0.05 and 0.25 µM. In control cows, the phytoporphyrin concentrations in serum ranged from < 0.05 to 0.12 µmol/L over the 44 day trial period. During the control weeks for all of the sporidesmin-dosed cattle the phytoporphyrin concentration ranged between < 0.05 and 0.16 µmol/L. One cow from the subclinical group (No. 395) presented higher than expected values on two days during this period, while all other phytoporphyrin concentrations for this cow remained in the normal range. These two days were considered to be outliers, with values of 0.79 and 0.57 µM on days -5 and -3, respectively. The phytoporphyrin concentrations shown on the days before and after these measurements were 0.11 and 0.1 µM, respectively. Because of this, these values were excluded from further analysis.

As with the traditional metric measurements reported in *Chapter 2*, the phytoporphyrin data were further analysed using GAM to assess how the concentrations changed over the trial period, and whether changes were related to groups and therefore the degree of damage caused by sporidesmin. See *Chapter 2, section 2.2.6*, for details on how the model was fitted to the data. The model fit and raw data for each animal are shown in *Figure 3.2*. The model showed that there is evidence for a difference in the shape of the curve between groups ($p < 0.001$). Looking at the plot it can be seen that this difference is caused by an increase in phytoporphyrin concentration in the clinical cows, while all other groups remained relatively constant. Phytoporphyrin concentrations in

clinically affected animals began to increase at Day 4. The time line for these increases was inconsistent between individuals, with the first increase for each animal seen between Days 2 and 9. Although minimal, a slight increase did occur for the subclinical cows following dosing, however this was not significant.

3.3.2 Phytoporphyrin concentrations and the onset of photosensitisation in clinical cows

All clinical cows exhibited elevated levels of serum phytoporphyrin and the range within this group was large (*Table 3.1*). Cow 298 showed its first obvious change in phytoporphyrin concentration at Day 7, but did not show the first clinical signs of the skin of the right fore teat becoming red and blistering until Day 22. Furthermore this cow did not develop any other obvious photosensitivity signs, despite having one of the higher serum phytoporphyrin concentrations. Conversely, cow 317 developed reddening of the udder at Day 9 and thickening of the withers and rump at Day 14, while increases in phytoporphyrin concentrations were only seen on Day 14. Cow 440 also developed the first signs of clinical photosensitivity before increases in phytoporphyrin concentrations were measured.

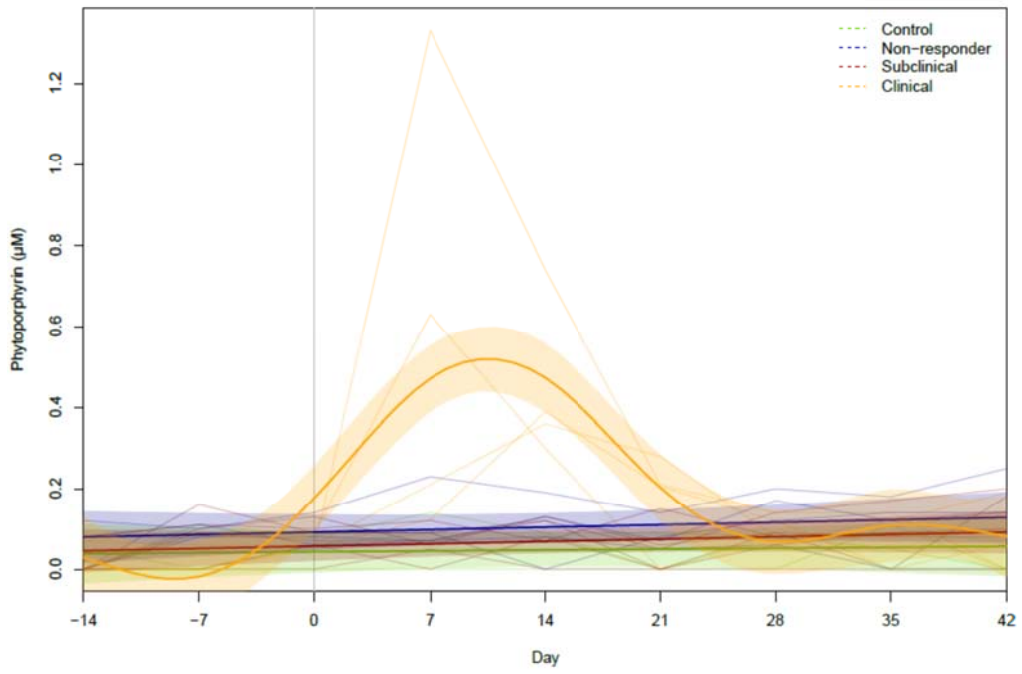

Figure 3.2 Phytoporphyrin concentrations of cows over time using generalised additive model (GAM) analyses with within-group model fits shown. The model determined that a significant difference could be identified between groups ($p < 0.001$). This difference was due to the clinical cows, which were the only group to show an obvious increase after dosing (Day 0).

Table 3.1 The day of first signs of increase in phytoporphyrin concentrations (μM), GGT and GDH activities (IU/L) and the day that clinical photosensitivity signs first appeared, for four of the clinical animals following dosing (Day 0).

Animal ID	282	298	317	440
Phytoporphyrin	7	7	14	11
GGT	7	7	7	7
GDH	7	7	7	7
Clinical photosensitivity	10	22	9	9

3.3.3 Relationship of serum phytoporphyrin concentration to liver enzyme activities

There were no clinical signs of photosensitisation in the cattle prior to dosing with sporidesmin. Some of the clinical cattle did, however, show elevated GGT and GDH activities prior to dosing (*Figure 3.3*).

In all of the clinical cows serum concentrations of phytoporphyrin increased following dosing. As mentioned above there were inconsistencies in days of onset (*Table 3.1* and *Figure 3.*3). Bilirubin concentrations all remained within the reference range of clinically healthy animals.

Given that the groups of varying response to sporidesmin challenge is known, and the GGT and GDH activity at set times during the trial, it was questioned whether phytoporphyrin concentrations could be predicted. This was tested using common linear regression analyses (*Figures 3.4 and 3.5*). Both GGT and GDH activities produced significant p-values when correlated with phytoporphyrin. However, GGT presented a low R^2 (12 %) for the regression model. This implies that, although a relationship can be seen between phytoporphyrin and GGT, only a small percentage of the variation in the dependent variables can be explained by the independent variable. GDH produced a higher R^2 value (35 %); however this was still low, and again was not the major contributor to increases in phytoporphyrin. This implies that although a relationship can be seen between phytoporphyrin and the two enzyme activities, only a small percentage of the variation in the dependent variables can be explained by the independent variable.

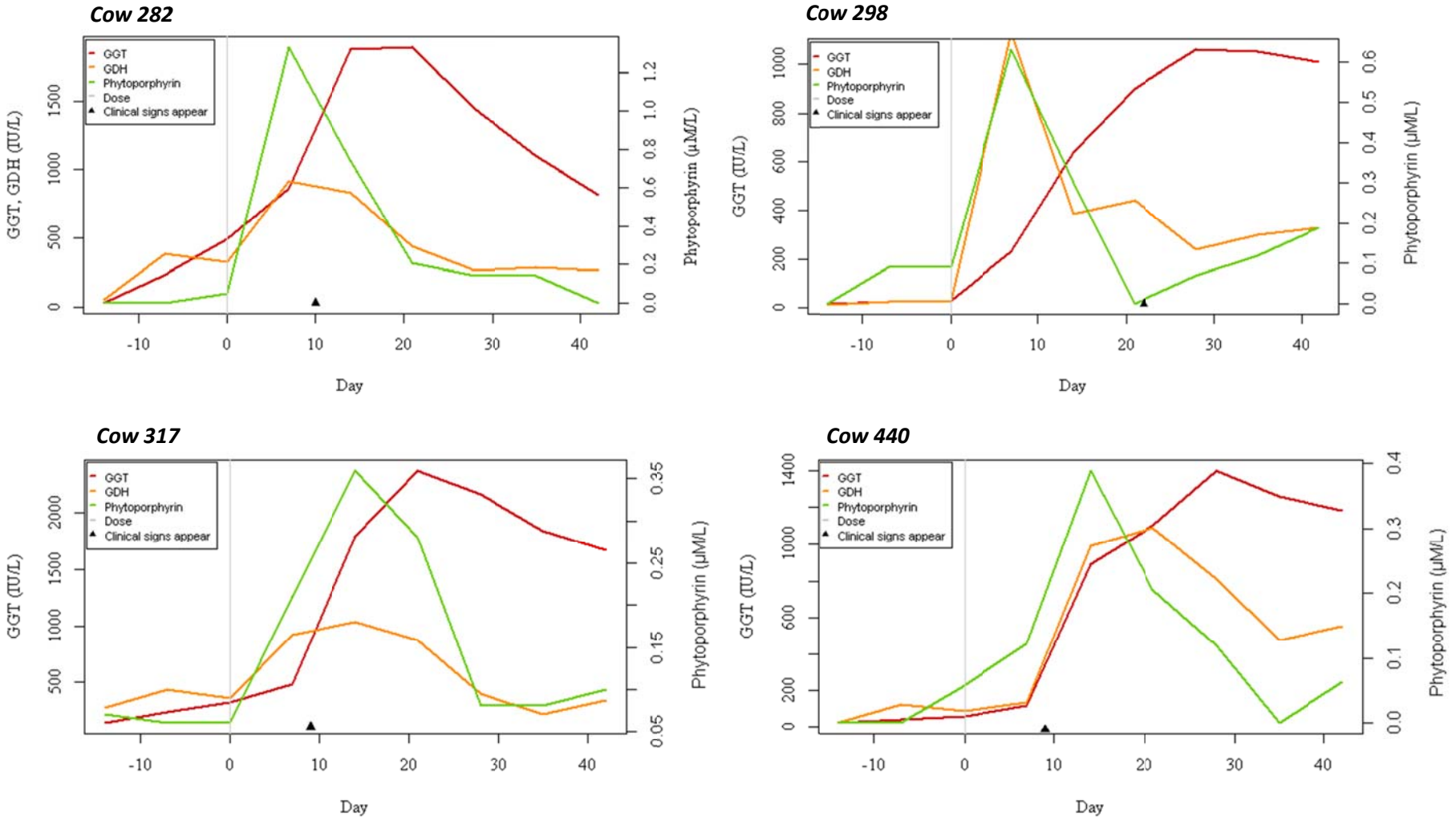

Figure 3.3 GGT and GDH activities, phytoporphyrin concentrations, and the day that clinical signs were observed, for four clinical cattle over the 42 day trial period

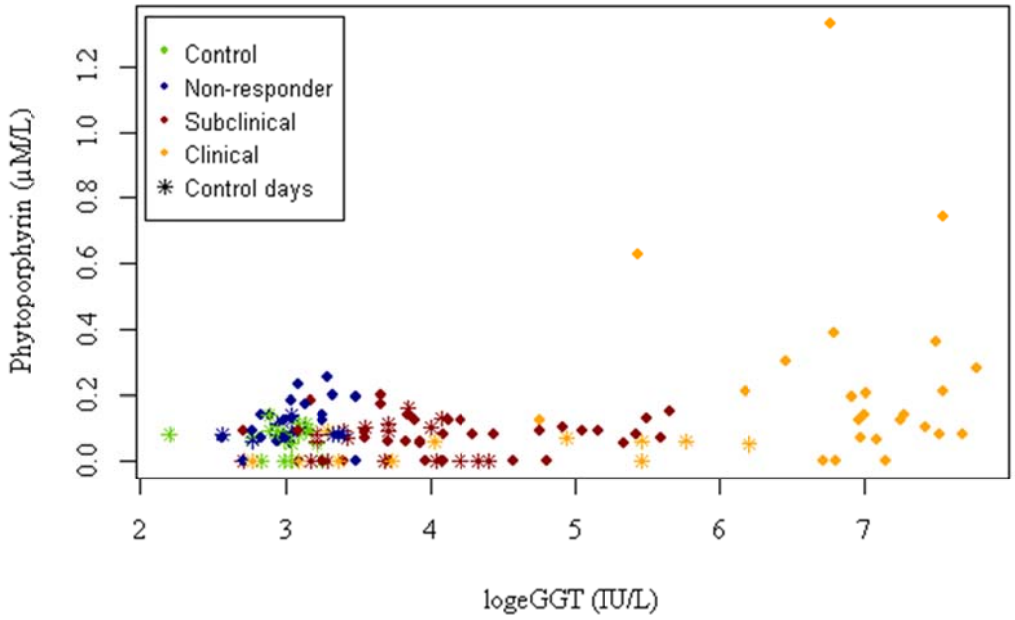

Figure 3.4 Common regression scatterplot showing phytoporphyrin and $\log_e$GGT over the trial period for all groups. The model produced a low p-value (< 0.001) and a low R^2 of 12%.

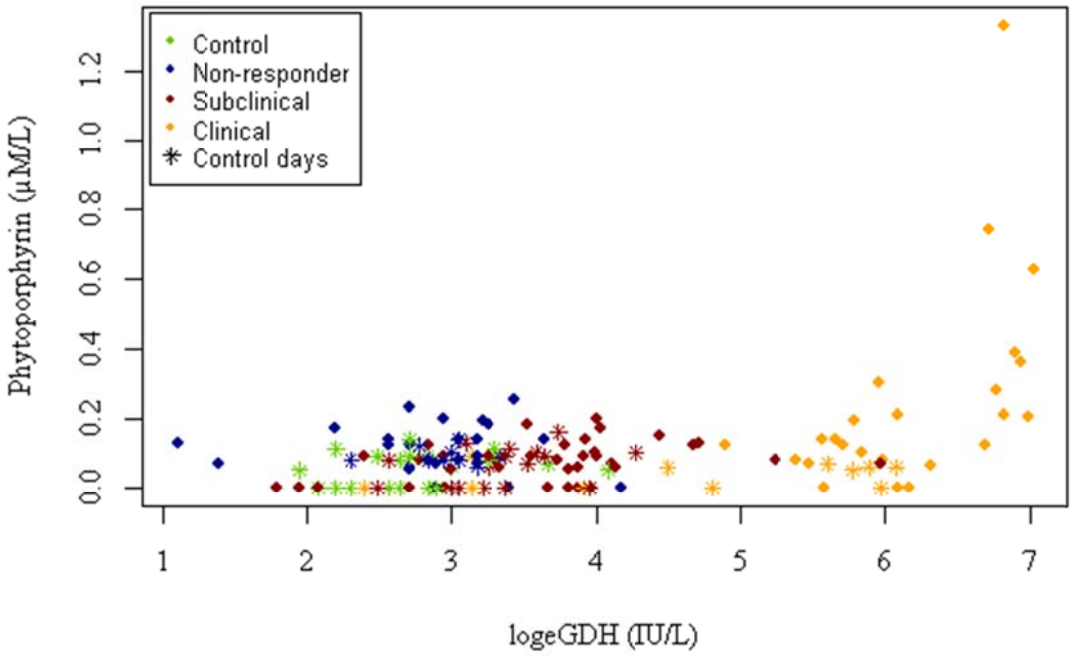

Figure 3.5 Common regression scatterplot showing phytoporphyrin and $\log_e$GDH over the trial period for all groups. The model produced a low p-value (< 0.001) and an R^2 of 35%.

Mixed effect models were used to take into account that individual cows may have differences between each other and within themselves due to the temporal nature of the data. The models also

allowed for varying slopes and intercepts for each group (control, non-responder, subclinical and clinical).

Any outliers were identified with residuals versus leverage plots, using Cooks distance, which measures the influence of individual samples in the data set.

A significant positive relationship was identified between phytoporphyrin and GGT (p = 0.0262) as well as between phytoporphyrin and GDH (p = < 0.0001). The difference was recognized as being caused by the clinical group for both variables (GGT p = 0.0014 and GDH p < 0.0001). However, most of the relationship in the clinical group seen between GGT and phytoporphyrin appears to be driven by two observations from cow 282 (Days 7 and 14). This is also seen with GDH, but with the addition of a sample from cow 298 (Day 7). When these observations are excluded from the relevant models, the relationship between GGT/GDH and phytoporphyrin in the clinical group remains significant (p 0.0197 and p < 0.001, respectively). The conditional R^2 for GGT increased to 27 % while for GDH it remained at 35 %.

3.4 Discussion

In general, the literature on the spectrofluorometric analysis of phytoporphyrin appears to focus on comparing clinically healthy animals with those exhibiting clinical photosensitivity, primarily in sheep. These studies have shown that significantly raised phytoporphyrin concentrations clearly relate to hepatocyte and bile duct damage due to sporidesmin intake in ruminants (Morris *et al.*, 2009; Scheie & Flåøyen, 2003; Scheie *et al.*, 2003a; Scheie *et al.*, 2003b). There have been no reports of phytoporphyrin concentrations in subclinical cattle or in those that have not responded to sporidesmin dosing.

In the present study, it was expected that non-responders would present the same as clinically healthy (control) cattle, and this was found to be true. It was thought that subclinical cattle may show a slight increase in phytoporphyrin concentrations, to match the slight increases seen in the liver enzyme activities in response to sporidesmin administration; however, this was not apparent in the results.

Previous studies have shown that clinically healthy animals grazing pasture do contain small concentrations of phytoporphyrin in their serum (Scheie *et al.*, 2003a; Scheie *et al.*, 2003b), but these levels remain reasonably stable over time in comparison to those exhibiting clinical photosensitivity. Therefore, as expected, the control cows and all cows during the control weeks of the present study showed phytoporphyrin concentrations ranging from < 0.05 to 0.16 µM. However,

the levels recorded are above the threshold for control levels recorded in sheep and cattle from previous studies (Scheie & Flåøyen, 2003; Scheie *et al.*, 2003a). These differences may be due to different sample preparation used in the present study, and/or variances in breed.

Although showing little to no change over time following dosing, the non-responders and subclinicals, did have maximum concentrations above those recorded in previous studies as 'clinically healthy' (0.05 µmol/L ± 0.03) (Scheie & Flåøyen, 2003). None of these values were considered to be significantly different from the control cattle, and therefore were considered to be within the clinically healthy range for this trial. Differences between the studies may have resulted from variations in sampling procedures, sample preparation, and/or fluorescence analysis.

Very little change was seen in bilirubin concentration in any group, including the clinical cows. This contradicts many previous studies which have shown clear increases in bilirubin concentrations following dosing with sporidesmin. As most of these studies focused on sheep (Perrin, 1958a; Scheie *et al.*, 2003b), these differences may be due to a variation in response to sporidesmin intoxication between the two species. One study did show increased concentrations of bilirubin in both sheep and calves, however this was following bile duct ligation (BDL) rather than sporidesmin dosing (Ford & Gopinath, 1976). Another study found phenotypic correlations of $\log_e$ bilirubin levels with $\log_e$ GGT activities, even though the bilirubin concentrations did not rise appreciably (Morris *et al.*, 1998).

When regression analyses were applied to the data it was shown that GGT and GDH explain the variation in phytoporphyrin. This is somewhat expected, as increases in phytoporphyrin occur due to the retention of compounds in the blood, as a secondary effect of damage to the liver, by sporidesmin and further immune-mediated reactions.

Scheie *et al.* (2003b) concluded that plasma or serum fluorescence can be used to demonstrate the elevation of phytoporphyrin concentrations in lambs prior to hepatogenous photosensitisation, and that phytoporphyrin is a sensitive indicator for this, when combined with GGT analyses. The present study went against this, showing disparities between the onset of photosensitivity and phytoporphyrin increases and maximums. Phytoporphyrin concentration increased prior to increases in GGT activity for all of the clinical cows, which was expected (refer to *Figure 3.3*). This is in contrast to a study in sheep dosed with sporidesmin, carried out by Scheie *et al.* (2003b), where plasma phytoporphyrin measurements were shown to increase between 3 and 5 days after the beginning of the rise in GGT activities, and the increases could be related to the onset of clinical signs. In the present study, phytoporphyrin concentrations increased after GDH for three of the clinical cows (282, 298 and 317), while the other cow (440) showed an increase before GDH increased. It is well known that GDH has activities rise earlier than GGT activities following liver

damage (Morris *et al.*, 2013), and that GGT remains elevated for longer. It is unknown why cow 440 deviated from this.

In the present study, it was recognised that clinically affected cows showed significant increases in phytoporphyrin concentrations following dosing, and that the timing of maximum correlated well with other studies. However, the increases in phytoporphyrin did not match days of onset recorded by other trials. It was expected that subclinical cows would present an intermediate between non-responders/controls and clinical cows, with phytoporphyrin concentrations mirroring this. However, this was not found. All of the 'non-clinical' groups (controls, non-responders, and subclinicals) showed high levels of overlap in the concentration ranges over the dosed period. Fluorescence analysis of phytoporphyrin, using these conditions, does not appear to be an efficient technique for identifying early onset changes in relation to sporidesmin challenge, and is not suitable to be used to identify differences between the degrees of effect in relation to susceptibility to sporidesmin.

Serum is a complex matrix and contains large numbers of proteins which may mask the phytoporphyrin, as seen in the fluorescence peaks where the phytoporphyrin appears on the shoulder of the protein peak. Additionally, phytoporphyrin has been theorised as being protein-bound in the blood. If this is the case, what is being measured is likely to be a small fraction of what is truly present in the blood. Additional work on separating phytoporphyrin from protein molecules, such as processes utilising protein degradation, while ensuring phytoporphyrin molecules remain intact, is required.

Conceivably, phytoporphyrin seeps into the extravascular connective tissue and this could help explain why serum maxima do not always correspond with the onset of photosensitisation. The ideal test would assist early detection of facial eczema, particularly in subclinical animals. However, the concentration of phytoporphyrin at an early stage would be below the threshold for many fluorimeters. The identification of a specific biomarker, specific to a sporidesmin challenge, is desirable, although fluorescence analysis as used in the present study is unlikely to prove useful for this. For that reason phytoporphyrin is not likely to be a good biomarker for subclinical or early onset FE.

Chapter 4

Nuclear magnetic resonance spectroscopy based metabolomics

4.1 Introduction

Despite significant advances in analytical technologies, the accurate discovery of biomarkers in biological fluids remains a significant challenge. Traditional markers of sporidesmin exposure, specifically γ-glutamyl transferase (GGT) and glutamate dehydrogenase (GDH) enzyme activities are not disease-specific. Many of these markers only increase significantly after serious liver injury has already occurred, as is seen in cases of facial eczema (FE). In the previous chapter it was seen how phytoporphyrin, although slightly more specific to FE, does not generally reach a maximum until clinical signs appear. By this time, decreases in milk yields and bodyweight are already apparent. These are therefore not useful for early stage diagnosis of FE. More sensitive early-onset markers are therefore needed to indicate exposure to sporidesmin.

Metabolic profiling using nuclear magnetic resonance (NMR) spectroscopy as the analytical platform, followed by multivariate statistical analysis (MVA), of blood serum and/or plasma, urine and other fluids and tissues has been effective for studying a wide range of diseases and/or nutritional states. In contrast to mass spectrometry (MS), NMR has the benefit of better reproducibility, can be quantitative, and metabolite identification can be reasonably straight forward. However, NMR does suffer from a lack of sensitivity.

Applications for NMR metabolomic profiling continue to grow rapidly, and more specifically the methods for data extraction and interpretation. Using the Web of Knowledge database and searching for the keywords 'NMR AND metabolomic*' and 'NMR AND metabonomic*', a total of 9,739 publications were found, spanning from the year 1999 through to March 2015. A review by Larive *et al.* (2015) showed that the number of publications on this topic had increased around 41 fold from the year 2000 to 2013. NMR has provided an unprecedented level of understanding of how organisms (plants, animals, and single cell organisms alike) respond to environmental and internal factors, such as disease, toxins, nutrition, ageing, and exercise. A few specific examples of studies showing the application of NMR-based metabolomics are mentioned below.

Serum metabolite profiling has been used to reveal differences between chronic lymphocytic leukaemia molecular subgroups (MacIntyre *et al.*, 2010); to differentiate between control animals and animals treated with a model hepatotoxin (α-naphthylisothiocyanate (ANIT)) to investigate hepatoxicity (Beckwith-Hall *et al.*, 2003); to identify distinct metabolic fingerprints for cerebral and non-cerebral malaria (Ghosh *et al.*, 2012, 2013); and to detect epithelial ovarian cancer (Odunsi *et al.*, 2005).

Urine metabolite profiling has been used to identify markers of cholestasis. Ishihara *et al.* (2009) concluded that bile acids, (BAs) valine, and methyl malonate could possibly be urinary biomarkers of cholestasis. Urine has also been used for the elucidation of metabolic changes during diabetes disease progression in rats, and for identifying potential metabolic markers to help understand the mechanisms underlying the development of diabetes (Guan *et al.*, 2013).

The number of studies focusing on the biochemical milk profile of dairy cows has increased in recent years (Klein *et al.*, 2010). Studies have demonstrated the relationship between the milk metabolic profile and the health status of the cow. In particular this has been used to identify imbalances during early lactation (Duffield *et al.*, 2009). In addition, high levels of ketone bodies, such as acetone, acetoacetate, and β-hydroxybutyric acid (BHBA), have been measured and related to subclinical ketosis in dairy cattle (Enjalbert *et al.*, 2001; Geishauser *et al.*, 2000). However, these findings have been limited to measuring metabolites that are already well known, rather than identifying new metabolites. Milk metabolic profiling using ^{1}H NMR allows for the complete metabolomic spectrum to be examined, and has been utilised in nutritional science as well as for determining disease status and identifying the stage of lactation. Sundekilde *et al.* (2011) have used NMR-based metabolomics to identify small molecules in milk which may be involved in bovine milk coagulation. Two years later, they demonstrated the potential of NMR metabolomics to assess changes in metabolite composition of bovine milk, associated with changes in milk somatic cell count (SCC) (Sundekilde *et al.*, 2013b). They identified eight metabolic compounds to use as novel indicators for elevated SCC in bovine milk. These metabolites have potential in the diagnosis of mastitis in cows. Additionally, ^{1}H NMR has been used to identify prognostic biomarkers for risk of ketosis in dairy cattle, using milk samples. Klein *et al.* (2012) demonstrated that high milk glycerophosphocholine (GPC) levels, and high ratios of GPC to phosphocholine may be able to be used as markers to identify cows that cope well with metabolic stress, and thereby serve as an indicator of ketosis risk in dairy cattle.

Combining the analysis of multiple biofluids in NMR-based metabolomics can also be beneficial, for example Jiang and co-workers (2013) showed that changes in the metabolic profile of serum, urine and liver tissue extracts can shed light on the different stages of disease in hyperlipidaemia. Maher *et al.* (2013) have established metabolic correlations between blood and milk in Holstein dairy cows.

In this study ^{1}H NMR spectra were recorded using 1D nuclear overhauser effect spectroscopy (NOESY), diffusion-edited, Carr-Purcell-Meiboom-Gill (CPMG) spin echo, and 2D J-resolved (JRES) methods. The JRES spectra were projected on their chemical shift axis to generate proton-decoupled projected 1D spectra (p-JRES) for MVA. Additionally, 2D ^{1}H – ^{1}H total spin correlation

spectroscopy (TOCSY) and ^{1}H – ^{13}C heteronuclear single quantum coherence (HSQC) methods were utilised to produce spectra from each biofluid to aid metabolite identification.

NOESY experiments are typically used to determine the spatial proximity of pairs of H atoms. As used in the present study, this 1D experiment simply provides a robust method to suppress the unwanted water peak when combined with a low power presaturation pulse. 1D-NOESY spectra are useful for biofluids that contain low levels of macromolecules, such as urine, and any metabolite extracts which are devoid of macromolecules. Blood serum and plasma samples have high concentrations of macromolecules such as proteins and lipids, and therefore for metabolite studies, require spectral editing to obtain the spectra, or alternatively altered sample preparation techniques such as centrifugal filtration or solvent precipitation. The latter two options are often expensive, and more time consuming, especially for the large sample numbers commonly utilised in metabolomics investigations. The CPMG method attenuates macromolecule signals and provides high-resolution spectra for low molecular weight metabolites. This method exploits the fact that the signals from the macromolecules decay much faster, due to their slower tumbling, enhancing T_2 relaxation, than those of the small metabolites. The CPMG experiments incorporate a spin echo pulse train which 'locks' the observable magnetisation in the transverse plane, relative to the magnetic field direction during a delay in the order of 60 – 100 ms. The slow tumbling rate of macromolecules in solution leads to faster relaxation of the transverse magnetisation (short $T_{2,}$ ~50 ms) (Richardson *et al.*, 2012), while the T_2 relaxation of the fast tumbling small metabolites is less efficient (~ 1 s) which allows their signals to persist well beyond the spin-lock delay.

While effective, the CPMG method is not completely infallible and residual signals from the macromolecules are commonly present and, unfortunately, this can obscure some of the metabolite peaks. In addition, going beyond 100 ms for the CPMG spinlock can cause the generation of heat, which can damage the probe.

When macromolecules are the desired species, a diffusion-edited experiment is used. This method relies on small molecules diffusing faster than macromolecules. Pairs of pulsed magnetic field gradient pulses, in conjunction with an appropriate delay, can be used to scramble the magnetisation of molecules which have diffused significantly, whilst retaining that of the larger molecules, which have remained in their original positions, thereby allowing the measurement of the macromolecules, while disregarding the small molecules.

JRES spectroscopy is traditionally applied to obtain a 2D NMR spectrum where the chemical shifts are shown on one axis and peaks corresponding to the J-coupling (spin – spin splitting) are shown on the other. When used for metabolomics studies the rows of the 2D spectrum matrix are summed to

give a 1D spectrum showing just the chemical shifts. Each multiplet in the conventional 1D spectrum collapses in to a single line. It therefore provides a means of increasing the spectral resolution. The data processing typically applied to these spectra is also very effective at removing any macromolecule peaks.

Although 1D NMR has typically formed the basis of metabolomics studies, it is hampered by signal overlap, which limits the unambiguous identification of metabolites (Ludwig & Viant, 2010). This is where two-dimensional (2D) NMR methods come in to play. These methods retain many of the benefits of 1D NMR, but spread the overlapping resonances into a second dimension, which reduces congestion and increases metabolite specificity. Two dimensional methods, such as TOCSY, help overcome this problem, but at the expense of long acquisition times making them impractical for studies involving large numbers of samples. A full JRES spectrum can be acquired in approximately 20 minutes, however. The separation of chemical shifts and J-couplings along different spectral dimensions significantly increases peak dispersion versus 1D NMR facilitating spectral assignments and accurate quantification. The application of 2D JRES ^{1}H NMR spectroscopy to metabolomics was first reported in 2003 (Viant, 2003; Wang *et al*., 2003). However, the usual practice when used for metabolomics is to project the 2D spectrum onto the chemical shift axis and use the resulting 1D spectrum, which shows only the chemical shifts.

To the author's knowledge, the only NMR procedures to be applied to the topic of FE are those determining the structure of sporidesmin (Blunt *et al.*, 1979; Woodcock *et al.*, 2001). In the present experiments, a combination of NOESY, CPMG, diffusion-edited and JRES spectra were recorded.

4.1.1 Aim

To discover a potential metabolic biomarker of sporidesmin challenge in cows, which can be used to identify cows at all stages of disease (i.e. subclinical or clinical), prior to changes in liver enzyme activities, phytoporphyrin concentrations, and the presentation of clinical signs.

4.1.2 Objectives

- To utilise ^{1}H NMR spectroscopy to investigate whether or not samples of serum, urine and milk could be differentiated into groups (e.g. non-responders, subclinical and clinical) based on differences in their NMR spectra in response to sporidesmin challenge.
- To tentatively identify metabolites responsible for any differentiation based on their chemical shifts and peak multiplicities.

4.2 Materials and methods

All samples were randomised before preparation. This randomisation was used to prevent systematic errors in spectrum measurements caused by any drift in spectrometer performance or sample degradation over the total duration of data collection.

The identity of each sample was recorded using a code containing: the animal's ID, the date a sample was taken, the biofluid and the assigned "disease" grouping, for example S_C/022/001, which reads as serum sample, control group, cow 22, and date code 1 referring to the first measurement day (Day -14 of the trial: 04/04/2011). These codes were entered in to Excel and randomised using an inbuilt function for this purpose.

4.2.1 Buffers

The pH of samples can have a significant impact on the chemical shifts observed in the NMR spectrum, therefore it is important to minimise variation of this parameter. Serum is naturally buffered *in vivo*, however individual variation can still occur. Because of this samples were diluted with a phosphate buffer stock solution. A di-sodium hydrogen phosphate buffer (Na_2HPO_4, 0.2 M, pH 7.4) was made up in D_2O, with the addition of 3-trimethylsilyl-(2,2,3,3,-d4)-propanoic acid (TSP, Sigma-Aldrich) as an internal reference compound, and sodium azide (NaN_3, 0.02 % in the final solution) to prevent bacterial growth.

The pH of urine can vary more than the blood. The blood is regulated closely by homeostasis, whereas urine is not. Urine is the vehicle for a number of by-products of metabolism and any excess water or salts in blood will also be removed into urine to help keep the pH of blood balanced. Because of this the urine can become more, or less, concentrated and the pH can change rapidly. For this reason buffering of urine is important to insure consistency across samples. Milk pH can also vary over the day and between animals, and therefore also requires buffering. For both urine and milk samples a monopotassium phosphate buffer (KH_2PO_4, 1.5 M, pH 7.4), with the addition of 0.1 % TSP and ~ 0.2 % (*w/v*) NaN_3, was made up in D_2O.

4.2.2 Sample preparation

4.2.2.1 Raw serum

Samples were stored in 1.5 mL cryovials at -80 °C pending analysis. The samples were placed on ice to thaw (~ 90 min), and once thawed were mixed briefly by vortex (30 s), then centrifuged at 13,400

rpm at room temperature for 10 min. A 300 µL aliquot of the supernatant was transferred to a second tube. If there was to be a delay in sample preparation for the NMR, post-thawing, all samples were placed on ice until preparation could be continued.

A 300 µL aliquot of Na_2HPO_4 buffer was added to the serum, then inverted 5-6 times to combine the solutions and transferred into a standard 5 mm NMR tube, labelled with the sample code for analysis. Inversion rather than vortex was used to limit frothing.

4.2.2.3 Urine

The urine samples were removed from the -80 °C freezer and thawed over ice (~ 60 min). Once thawed the urine samples were mixed briefly (10 s vortex) and centrifuged at 13,400 rpm for 10 min at room temperature. A 540 µL aliquot of this urine was transferred into a new Eppendorf tube. A 60 µL aliquot of KH_2PO_4 buffer was added to the urine, mixed, and then centrifuged again for 2 min to remove any additional precipitate. The sample was transferred into a standard 5 mm NMR tube.

4.2.2.4 Milk

Milk samples were removed from the -80 °C freezer and placed on ice to thaw (~ 60 min). Samples were mixed by inverting, and were then centrifuged at 13,400 rpm for 10 min at room temperature.

Following centrifugation the milk samples, separated into (generally) three distinct layers, namely the cream (fat), the whey proteins, and caseins. The fat was removed by skimming. This was repeated to ensure any remaining fat was removed. The casein clumped at the bottom of the tube, so the whey, required for metabolomic analysis, was pipetted from the top. This whey was precipitated to remove the proteins, leaving the remaining metabolites in milk for analysis. A 1:4 (v/v) precipitation was used, with 540 µL of whey transferred to a 15 mL Falcon tube and 2160 µL of acetonitrile (ACN, HPLC grade) was added to this. The combined solution was mixed briefly (vortex 30 s) and left to extract for 15 min at room temperature. The solution was then vortexed briefly, again, and centrifuged at 3,400 rpm for 2 min. The supernatant was transferred to a second 15 mL Falcon tube and stored at -80 °C in preparation for freeze drying. The frozen milk:ACN (1:4, v/v) samples were placed into 1.2 L flasks, and onto a freeze dryer. Samples were left to dry overnight, and once the solvent mixture was entirely evaporated the tubes were stored in the -80 °C freezer until required for NMR analysis.

When required, the samples were reconstituted with 540 µL of Milli-Q water, ultrasonicated (10 min) to mix the dried material completely, and centrifuged to settle any remaining solid. A 60 µL

aliquot of KH_2PO_4 buffer (1.5 M, pH 7.4), was added to the supernatant, mixed briefly (10 s vortex), then 600 µL of sample was aliquoted into a standard 5 mm NMR tube, labelled with the sample code, ready for NMR data acquisition.

4.2.3 Spectrum acquisition parameters

All spectra were recorded using a Bruker Avance 700 MHz NMR spectrometer (Bruker-Biospin, GmbH, Rheinstetten, Germany) operating at 700.25 MHz equipped with a standard four channel inverse detection probe. The temperature for all measurements was 299.2 K, which was calibrated using the separation of the residual ^1H signals from a standard sample of deuterated (d_4)-methanol.

Water suppression was achieved during the recycle delay in all serum, urine, and milk experiments. This was done via pre-saturation at the water offset frequency (4.7 ppm), using a field strength of 50 Hz for serum and urine. All milk spectra used a field strength of 49 Hz. All methods used a recycle delay of 2 s at the end of each scan.

1D NOESY and 2D JRES spectra were recorded for all samples. The 1D NOESY spectra were recorded using the standard Bruker 'noesygppr1d' pulse sequence, with a spectral width (SW) of 11.16 kHz (15.94 ppm) and 32 k points, with an acquisition time of 1.468 s, and averaged for 32 scans, with 4 dummy scans for serum, 128 scans and 4 dummy scans for urine, and 256 scans and 4 dummy scans for milk. A mixing time of 10 ms was used for the serum and urine samples, while 100 ms was utilised for the milk samples.

The 2D JRES spectra were recorded using the standard Bruker 'jresgpprqf' pulse program with a SW of 11.68 kHZ (11.68 ppm) in the F2 domain, and 16 k points, SW of 60 Hz (0.086 ppm), and 40 points in the F1 domain, using an acquisition time of 0.7 s. Four scans were used for serum and urine samples, and 8 scans for milk. All spectra were preceded with 8 dummy scans.

In addition, 1D CPMG and 1D diffusion-edited measurements were carried out for all of the serum samples. The 1D CPMG spectra were recorded using the Bruker 'cpmgpr1d.comp' pulse sequence, with a SW of 9.765 kHz (13.95 ppm) and 64 k points, with an acquisition time of 3.35 s, and averaged for 128 scans. The CPMG spectra were recorded using a refocusing delay of 78.6 ms with an inter-pulse spacing of 0.6 ms.

The 1D diffusion-edited spectra were recorded using the standard Bruker LED sequence ('ledbpgppr2s1d.comp'), using a big delta of 60 ms and a little delta of 3 ms. A SW of 9.765 kHz (13.95 ppm) using 32 k points was used and averaged for 32 scans, with 4 dummy scans, an acquisition time of 1.68 s, and a pulsed field gradient strength of ~ 50 G cm^{-1}.

4.2.4 Spectrum and data processing and data analysis

All NOESY spectra and the CPMG serum spectra were apodised using an exponential function with line broadening of 1 Hz, and zero filled to 128 k points. Diffusion-edited spectra were apodised using an exponential function with a line broadening of 3 Hz, and zero filled to 128 k. All JRES spectra were apodised using a sine bell in both dimensions and Fourier transformed in magnitude mode, zero filled to 16 k points in the F2 dimension, and 256 points in the F1 dimension.

Prior to statistical analysis all spectra were referenced, phased, and baseline corrected using Topspin (version 2.5; Bruker-Biospin, GmbH, Rheinstetten, Germany).

All serum spectra were referenced to formate (8.475 ppm) after trialling other peaks, including TSP (~ 0.0 ppm) and glucose peaks (5.3 ppm and 4.7 ppm), as this gave the best overall alignment of the spectra. Although TSP is a standard reference for biological samples, it has a tendency to bind to blood proteins, leading to a change in its chemical shift, and thus can cause inaccuracies in referencing. It is however, an ideal reference for urine samples (Lindon *et al.*, 2007). Urine and milk spectra were referenced to the TSP standard at 0.00 ppm. All spectra were manually phased and baseline corrected if required.

For the data to be utilised for MVA, following initial spectrum processing, the spectra needed to be amalgamated into a unified format, and exported as either a text or Excel-format file. Although the drifting of peak positions between spectra was largely controlled by pH buffering and maintaining a stable temperature during data acquisition, it was inevitable that a small amount of variability remained. This was accommodated by dividing the spectrum into a series of 'buckets' (typically ~250). The intensities of all the points in a particular bucket are summed together (Beger *et al.*, 2010; Liland, 2011). It is these bucket intensities which are then exported into text or Excel files and used for subsequent processing and statistical analysis. For this study standard rectangular buckets of 0.04 ppm width were employed from 0.2 ppm to 10 ppm for all serum and urine spectra, and milk *p*-JRES spectra. Other bucket widths gave no noticeable improvement. For milk NOESY and serum diffusion-edited spectra, a width of 0.08 ppm was used due to the presence of broad macromolecule peaks. For the production of the bucket tables the TSP peak (-0.2 - 0.2 ppm) and the water peak (4.6 - 5.2 ppm) were excluded for the serum and milk samples, and with urine, the urea peaks were also excluded (4.5 - 5.98 ppm).

Two methods of normalising the bucket intensities of each spectrum were investigated: normalising to total intensity, and normalising to a reference peak (TSP). The first method involves dividing each bucket intensity by the sum of all the bucket intensities in the spectrum. The second method uses

the intensity of the reference peak as the divisor. Both methods moderate inconsistencies in spectrum intensity from sample to sample caused by drift in measurement conditions such as probe tuning. The former method will also compensate for variable dilution of the original sample. However, this method can fail when the spectrum is dominated by an intense peak with large intensity variance across the sample population. In practice both scaling methods produced better results than no normalisation, and total intensity was chosen for subsequent data analysis. For initial data interpretation bucket tables were produced using AMIX (version 3.8.4, Bruker-Biospin).

NMR spectra often have peaks with a large dynamic range. This can cause problems where the random variance of an intense peak masks the non-random (i.e. important) variance of smaller peaks. This effect can be reduced by scaling each column of buckets (van den Berg *et al.*, 2006). Two methods are typically employed: scaling to unit variance, where each bucket intensity or variable, at a particular chemical shift, is divided by the standard deviation of all the bucket intensities at this chemical shift (meaning that each variable has a variance equal to one); and Pareto scaling where the square root of the standard deviation is used as the divisor. The former method can be more effective, but it also magnifies measurement errors such as imperfect baselines leading to spurious results. Pareto scaling is often used as a compromise, and acts to minimise the impact of noise and artefacts on the models, which helps the models' predictive ability (van den Berg *et al.*, 2006; Worley & Powers, 2013). Because small and medium variations in the data may be important, Pareto scaling was chosen.

Even with the bucketing process, a typical NMR bucket table from biological studies produces complex datasets which are hard to summarise and visualise. Chemometrics tools such as principal component analysis (PCA), partial least squares discriminant analysis (PLS-DA), and orthogonal PLS-DA (OPLS-DA) are utilised for modelling this information (Holmes *et al.*, 2000; Worley & Powers, 2013). PCA is an unsupervised multivariate analysis technique. It is based only on the explanatory variables of a dataset, so no information on group identity, for example diagnosis, is used to construct the model. PCA can be used to identify strong subgroupings and trends in the data (Beger *et al.*, 2010). However, it is susceptible to the effect of instrumental drift, artefacts, and other experimental variation - information which is not important to the dynamics of the system and diverts the focus from the scientific question of interest. Additionally, it is difficult to match the observed separation (if any) back to the original variables. Therefore, it is more commonly used for exploratory data analysis, to reduce the dataset and for the assessment of quality and homogeneity of the dataset (outlier identification). PCA reduces data into principal component 'scores' which are weighted averages of the original variables. These scores are presented on a scatter plot. By

projecting the data in this way, the variables (~ 250 buckets) of the original spectrum can be reduced to a much smaller number of variables (principal components (PC)) while still maintaining the majority of the information content (bucket intensity variance) of the data.

In the present study, PCA was used primarily to identify any major outliers in the datasets. This was done by utilising the Hotelling's T^2 plots produced from these models, which identify the strongest outliers. The ranges in these plots measure how far away an observation is from the centre of a PC or PLS. The T^2 critical (99 %) line represents the 99 % tolerance for the data in each model. A T^2 critical line, based on a 95 % tolerance is also represented in the scores plot as the ellipse surrounding most samples. Any observations situated outside this ellipse or outside the T^2 critical line are outliers (Trivedi & Iles, 2012). These observations were checked for their sample ID, and the raw spectra were examined to try and identify a reason for this. Not all samples outside the T^2 tolerances were excluded from further analysis, as these may symbolise significant changes associated with the degree of effect of a sporidesmin challenge. Rather, observations were excluded from further analysis when the spectra showed poor water suppression and/or a failed measurement. The remaining data were used to produce PLS-DA and OPLS-DA models.

The data matrix, imported into SIMCA (version 13.0.2.0, Umetrics AB), consisted of all the observations or predicted variables (NMR buckets), which are defined as *X*'s (or *X*-block), and the variables, such as group, defined as *Y*'s (or *Y*-block). PLS-DA finds a linear regression model by projecting the predicted variables (*X*), and the observed or response variables (*Y*) to a new space to develop a relationship between them (Wheelock & Wheelock, 2013). PLS is more suited to biological data, as it is often large and comprised of heavily inter-correlated parameters, and the matrix of predictors often has a large number of variables in relation to the observations. PLS-DA more clearly exposes separations between classes in the scores space than what PCA can (Liland, 2011). However, variation not directly correlated with *Y* is still present, and any strong confounding or opposing variables can weaken or even obscure the underlying group separation or correlation, which complicates the interpretation of the scores and loadings (Worley & Powers, 2013). OPLS-DA addresses these problems by incorporating an orthogonal correction filter which distinguishes the variations in the data that are useful for the prediction of a quantitative response, from the variations orthogonal to the prediction (Bylesjo *et al.*, 2006). Therefore, OPLS-DA separates the variance of interest, for example clinical diagnosis, from the variance that is unrelated (orthogonal) to the defined *Y* variables (Bylesjo *et al.*, 2006). This results in the rotation of the original PLS model so the variance important for the defined group separation is focused on the predictive components (*X*-axis), thus providing an easier interpretation of the models (Liland, 2011).

With PLS-DA and OPLS-DA, different classes are used to determine whether differences can be identified between these classes. For example, in the present study, in order to adapt the data for analysis using these standard MVA techniques, samples were categorised into binary classes such as dosed versus non-dosed, those presenting clinical signs versus non-clinical response, those which responded to dosing in some way (both subclinical and clinical) versus those which did not (dosed, non-responders, and controls), and also by the four groups based on clinical response (control, non-responder, subclinical, and clinical). Additionally, days of trial, cow ID, and control weeks were used as quality control classes to determine whether separations in the data were based on true responses to the dosing of sporidesmin and the presence or absence of FE, rather than random environmental or individual cow effects.

Over-fitting of the data is an inherent risk in PLS-DA and OPLS-DA analysis, and validation of the models is required to ensure the data is reliable and can stand true as a predictive model (Westerhuis *et al.*, 2008). The degree of over-fitting is related to the number of components used to construct the model (Trivedi & Iles, 2012; Wheelock & Wheelock, 2013). The PLS-DA model is therefore used to validate the OPLS-DA models. All PLS-DA models were validated using permutation testing, which works best for binary data. Permutation testing is a randomisation-based cross-calibration technique where the experimental data is split into equally-sized blocks, and different combinations (permutations) of these are used to create a permuted response which can then be compared to the original (true) response (Szymanska *et al.*, 2012). This is repeated 999 times. A permutation plot is produced, which displays the correlation coefficient between the original *Y*-variable and the permuted *Y*-variable on the *X*-axis, versus the cumulative R^2 and Q^2 on the *Y*-axis, and draws a regression line (*Figure 4.1*). The R^2 is the goodness of fit and indicates how well the model explains the dataset, while Q^2 represents the predictability of the data. If the R^2 and Q^2 values are greater than that of the permuted models, it implies that the observed statistics (observed classing) is significantly better than it would be if data were assigned randomly to the classes. In an ideal model, the R^2 and Q^2 should be similar (Wheelock & Wheelock, 2013; Worley & Powers, 2013). This would mean that each of the subjects contribute equally and uniformly to the observed group separation. However, in reality the Q^2 is normally lower than the R^2. If this difference is too big though, the robustness of the model is poor, which implies over-fitting. The authors of SIMCA define the 'ideal' difference between these two values as being no greater than 0.2. Others have stated that Q^2 just needs to be above 0.4 (Westerhuis *et al.*, 2008), or that R^2 and Q^2 just need to be close to each other (Lundstrom *et al.*, 2012; Wheelock & Wheelock, 2013). There is no hard and fast rule to this though, and it is highly dependent on the data, especially with

biological data as the number of variables is often large in relation to sample number. This was therefore only used as a starting point. Only validated models have had their results reported here.

All PCA, PLS-DA and OPLS-DA models were produced in SIMCA.

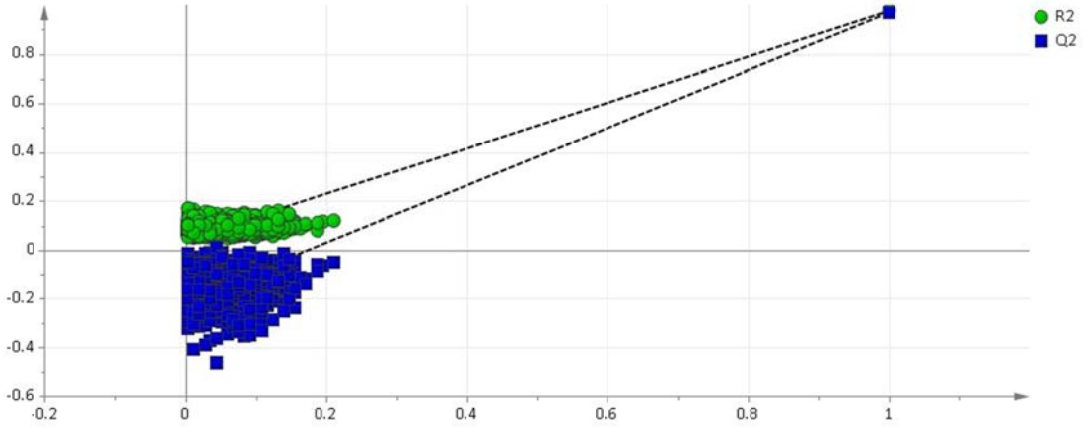

Figure 4.1 Example permutation validation plot of binary data, after 999 permutations, showing that the R^2 (0.97) and Q^2 (0.96) of the original models are situated well above those of the permuted models (line intercept R^2 0.05, Q^2 – 0.23), which cluster around the origin, proving the original defined classing for the model, fits the data best, and the model is robust. The R^2 and Q^2 values for the original models are similar meaning that each subject contributes equally and uniformly to the class separation.

Dividing the samples into classes, such as those described above, allowed the data to be analysed using the standard practice for metabolomics studies. However, in doing so the temporal component of the data is masked. A method was developed whereby the time profiles of each spectral bucket (ideally each peak) could be compared across the sample population. This allowed the examination of changes in relation to described classes while taking into account the profile of the metabolites over the entire trial period, in the hope that interaction of the component(s) could reveal more of the mechanism regulating sporidesmin dosing.

The same bucket tables as used with MVA above were used to produce bucket intensity vs. time curves for each cow, to identify how the specific bucket intensities change throughout the trial period. The time profile of each bucket was extracted for each cow, and then this was used to calculate the average time profile for the groups to which they had been assigned. If necessary, missing time points were substituted by linear interpolation for internal points, and replicating of the nearest data for missing end points. This information was then used to see which NMR buckets show large differences in the shape of the time curves when comparing groups, while taking into account how much variation there is between cows within each group. This was done as follows:

The difference between each cow at each time point was computed using Euclidean distance squared, between the measurements of the $i-th\ cow$ and $j-th\ cow$. The distance in the curves between cows *i* and *j* for time *t* is: $\mathrm{d}_{ij} = \sqrt{\sum_t \left(cow_{it} - cow_{jt-}\right)^2}$

The total variation within a group (sum of squares) was then calculated. This was given by:

$$\mathrm{group}_{\mathrm{variation}} = \frac{1}{2\mathrm{n}} \sum_{i,j} \mathrm{d}_{ij}^2$$

The within-group variation is then the sum of all the total variation across each group:

$$\mathrm{Within}_{\mathrm{variation}} = \sum_{groups} \mathrm{group}_{\mathrm{variation}}$$

The between-group variation can be computed as the difference between the total variation in the datatset (irrespective of the group), minus the within-group variation:

$$\mathrm{Between}_{\mathrm{variation}} = \mathrm{Total}_{\mathrm{variation}} - \mathrm{Within}_{\mathrm{variation}}$$

An F-statistic is then computed. This is given by:

$$F = \frac{\frac{\mathrm{Between}_{\mathrm{variation}}}{g-1}}{\frac{\mathrm{Within}_{\mathrm{variation}}}{n-g}}$$

Where *g* denotes group and *n* is sample size. A large F-statistic means there was a lot of variation between the groups, compared to within the groups. The size of the difference was determined by permuting the cows between groups, and recalculating the F-statistic for each permutation. If a difference was present between the groups, it would be expected that the F-statistic from the initial calculation would be larger than that produced during permutation testing. A p-value is also produced, this is the proportion of F-statistics produced by permutating the groups that are larger than the original F-statistics (the true data). These p-values are not corrected for multiple testing, so it would be expected that many p-values < 0.05 would arise even if there was no difference between the populations. Thus a p-value < 0.05 was not regarded as statistically significant. However, ranking by p-value does allow the identification of buckets which are more likely to separate the groups. A small p-value suggests that the results identified from the data are unlikely to arise by chance, whereas a large p-value suggests the differences between the groups were similar in the permuted models to the original models and therefore could have arisen by chance. The data is ranked by p-value, as well as by shrinkage discriminant analysis (SDA) ranking. The SDA ranking determines a ranking of predictors by computing correlation-adjusted t-scores (CAT) between the

group centroids and the pooled mean. These ranks are combined to produce a new rank. This is done using $New_{rank} = SDA^2_{rank} + P^2_{rank}$. The data is then plotted in the order of this new rank.

All time series analyses were produced using RStudio (Version 0.97.449, RStudio, Boston, MA, USA) statistical software.

4.2.5 Interpretation of the data

Scores plots (*Figure 4.2 a*) are a way to visualise the new, reduced, variables, often called coordinates, for the study observations. With OPLS-DA, two-class scores plots are built from one predictive component, and one orthogonal component. The scores present the variation in the sample direction allowing for pattern recognition (e.g. class assignment/separation). However, the scores do not give any information on the metabolic nature of the class separations/clustering.

A major difficulty with MVA is the interpretation of the data, especially the identification of variables of interest. Unlike many univariate statistical techniques, general rules for 'cut-offs', such as $p < 0.05$, have not been established for MVA (Wheelock & Wheelock, 2013). However, some techniques prove to be common in publications, and are used in combination to provide some reliability to the interpretation (Wheelock & Wheelock, 2013). A combination of loadings scatter plots, loadings column plots (with jack-knifed confidence intervals), and S-plots with Variable Influence of Projection cross validation (VIPcv) colouring were used in the present study to aid in the identification of variables of interest.

Loadings scatter plots are used to give a graphical summary of the clustering in scores plots, by presenting the correlations between the original variables in *X* and the new variables (scores) in *Y* (*Figure 4.2 b*). Each variable (NMR bucket) is represented as a point in the loadings plot. The plot is used to investigate which component peaks have the greatest contribution to the differentiation of the sample sets. Comparing the loadings plot to the scores plot enables some understanding as to how the variables relate to the observations (Worley & Powers, 2013). Variables located distally on the *X*-axis are important for between-group (class) separations, while those located distally on the *Y*-axis contribute to within-group variance.

Loadings column plots are another way to visualise the data (*Figure 4.2 c*). The plots are displayed with the loadings column vector, pq1 for OPLS-DA models, on the *Y*-axis, and the variables, e.g. NMR buckets, on the *X*-axis. The variables with a large pq1 (more influence) are situated further away from the origin on the *Y*-axis. With a loadings column plot, jack-knifing is used to estimate the bias, and standard errors (variance), which are displayed as error bars at the end of each column.

Columns where the jack-knifed confidence interval includes the origin (zero) are considered to have low reliability for class separation. These variables were excluded from further analysis in the present study.

S-plots provide a visualisation of the OPLS-DA predictive component loading to facilitate model interpretation. It is a scatter plot that combines both the covariance (p[1]) and the correlation (p(corr)[1]) structure between the *X*-variables and the predictive score (t[1]) (Wiklund *et al.*, 2008). These two vectors produce an S-shape when plotted (*Figure 4.2 d*), unless there is uniformity in the discrepancy of the variables. The covariance in the S-plot is shown on the *X*-axis, and is the contribution or magnitude of the model variables, while the correlation is shown on the *Y*-axis and demonstrates the reliability of the model variables with respect to the component scores. The variables situated far out on the wings of the S-plot combine high model influence with high reliability and are of relevance to the class separation. As seen in *Figure 4.2 d*, with the 1.18 ppm bucket in the top right hand corner of the plot showing a high p(corr)[1] value (0.89) and one of the higher p[1] values (0.19) for the plot, meaning high reliability for class separation. The 1.34 ppm bucket in the bottom corner has a low p(corr)[1] (– 0.21), so has low reliability for class separation, while the 4.62 ppm bucket is located in a region of ambiguous significance, as it is close to the origin, and has a low p(corr)[1] (0.29), and would not be selected as an important variable. Often a p(corr)[1] > 0.4 – 0.5 is used as a cut-off, however there is no real consensus on this (Kohler *et al.*, 2013; Lundstrom *et al.*, 2012).

The use of VIPcv colouring in loadings and S-plots is commonly utilised to deduce which variables are relevant to the class separation (*Figure 4.2*). VIPcv summarises the importance of each variable in driving the class separation. A standard score of > 1 is often used to imply a greater than average contribution to the model, but the higher the VIPcv score, the more significant the contribution is to the class separation. This cut-off (> 1) often still results in up to 50 % of the variables being selected as important (Wheelock & Wheelock, 2013).

All of these techniques only have general rules when determining which variables are significant and relevant to class separation. Therefore, a combination of all of these visualisation techniques is required to ensure reliability. In the present study, a VIPcv score of > 1, a p(corr)[1] generally > 0.4, and loadings columns with jack-knifed confidence intervals not crossing the origin were used as the 'cutoff' points for relevant variable selection.

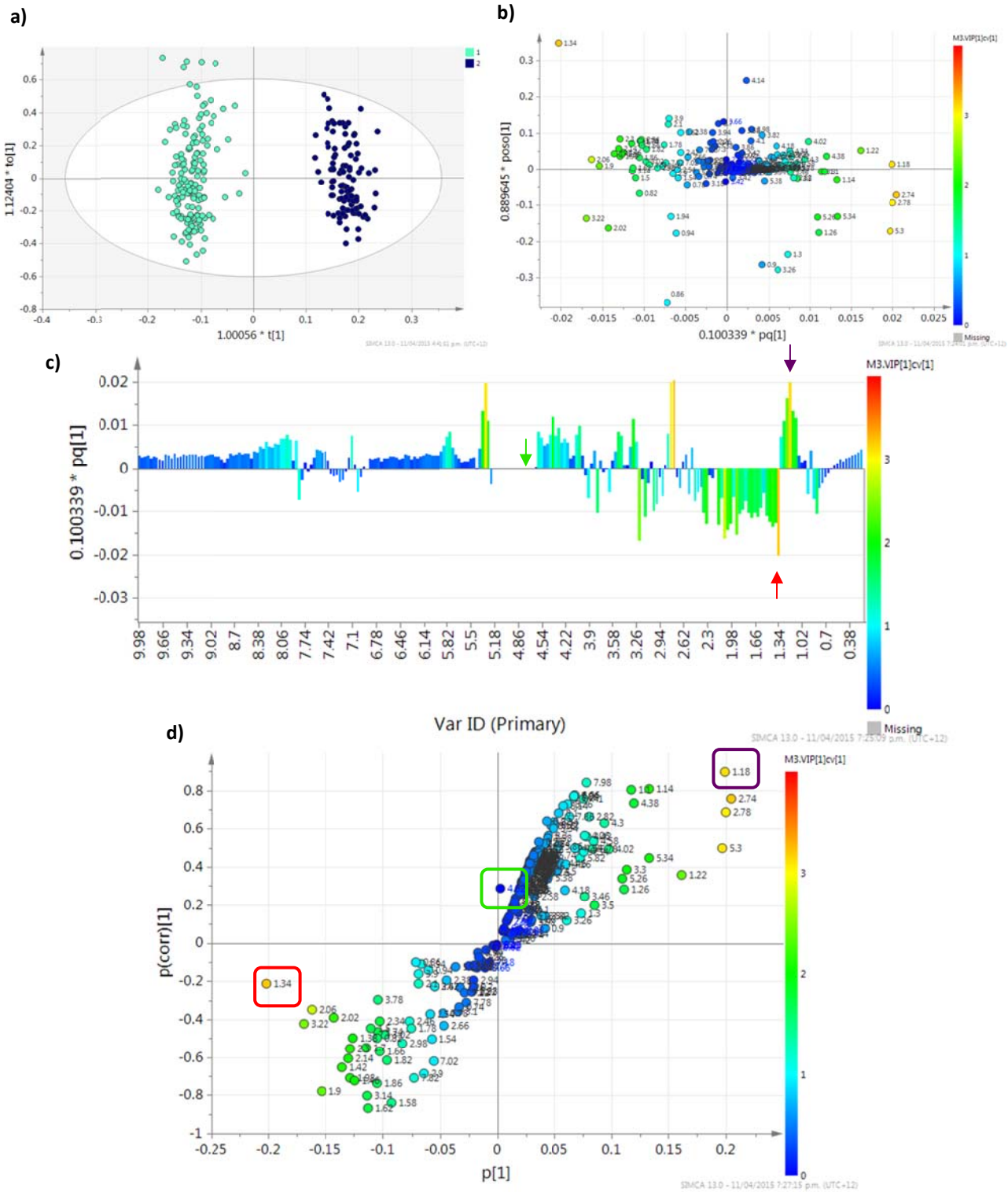

Figure 4.2 MVA example plots ***a)*** OPLS-DA scores plot visualising the separation of the classes. The model was constructed with 1 predictive + 3 orthogonal components, resulting in a clear separation between classes along the predictive component (*X*-axis; R^2 = 0.97, Q^2 = 0.96, p[CV-ANOVA] = 0). Within-group variation is displayed in the orthogonal direction (*Y*-axis); ***b)*** Loadings scatter plot showing the influence of the NMR bucket variables on the class separation. Those located along the *X*-axis are important for between group separation, while those along the *Y*-axis contribute to the within class separation; ***c)*** Loadings column plot representing the variables along the *X*-axis, and the degree of variance (change) on the *Y*-axis (pq 1). Those which are positive show an up-regulation in one class and those which are negative show a down-regulation in this class. The arrows indicate the metabolites shown in the S-plot below; and ***d)*** S-plot showing three metabolites situated in different regions of the plot, with varying contribution and reliability to class separation.

Once the important variables (NMR buckets) were identified, for both the MVA models, and the time series models, the raw spectra were examined to identify whether the buckets contained true peaks, rather than noise, and to determine the chemical shift of the peaks present in the bucket, as more than one peak may be contained. In addition, one peak may span more than one bucket. Once the peaks were identified, a combination of spectral annotation from HSQC and/or TOCSY spectra using Metabominer (Xia *et al.*, 2008), publications, multiplicity of peaks, and metabolite databases, such as the Human Metabolome Database (HMDB) (Wishart *et al.*, 2013) were used to identify the likely metabolites producing the peaks.

4.3 Results

4.3.1 Multivariate data analysis

4.3.1.1 Serum

Suppression of broad protein signals by the CPMG experiment is rarely perfect, and in the present case the residual signals were of sufficiently variable intensity as to compromise reliable extraction of the overlying metabolite peak intensities. It was found that the projected p-JRES spectra performed much better in this regard and so these were used for the subsequent multivariate analysis. *Figure 4.3* shows an example of the quality of the spectra recorded.

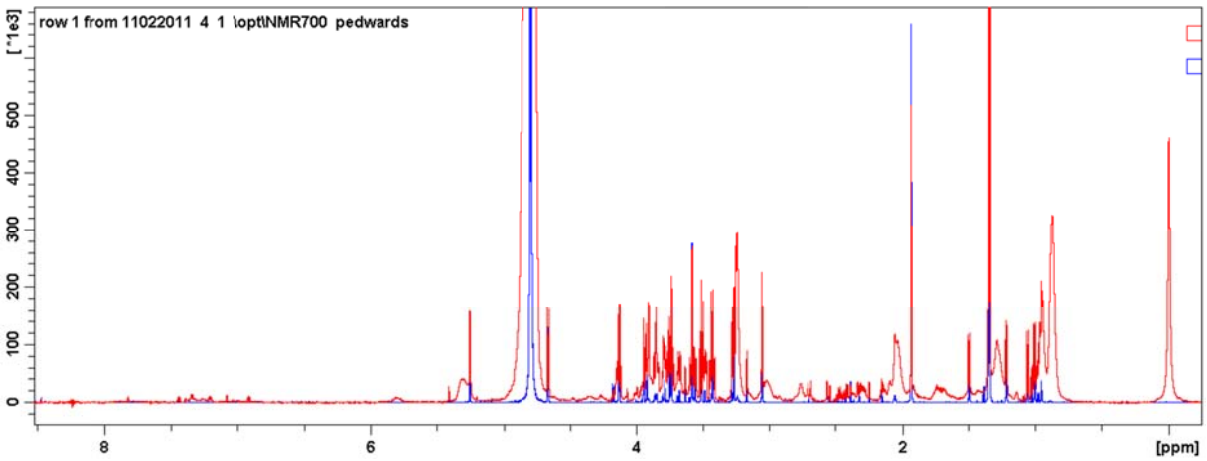

Figure 4.3 One dimensional ^{1}H NMR spectra of serum, showing the difference in resolution between the CPMG (red) and p- JRES (blue) spectra, recorded following a sporidesmin challenge in dairy cattle, showing -0.5 – 8.5 ppm.

Due to limitations in available spectrometer time directly after the trial, it was not possible to record spectra for every sample. Initially, samples from trial Days -14, -7, 0, 7, 14, 21, 28, 35, and 42 (Mondays) were run following the trial in 2011, as these days coincided with sampling of weights,

liver panels, and faecal spore count measurements. In order to produce a larger dataset, additional samples were run in 2013, focusing on the Wednesday and Friday samples during one week before and after dosing (trial Days -5, -3, 2, and 4). The samples recorded in 2013 also included samples from day -7 and day 7 for quality control comparison between 2011 and 2013 run samples.

4.3.1.1.1 The effect of sample storage: analysis of serum p-JRES spectra recorded in 2011 and 2013

If data recorded in differing years was to be combined it was important that it could not be differentiated based on the year in which the NMR data was collected. This was tested by classing the spectra by the year in which they were run, and testing whether the two groups could be separated using OPLS-DA (*n* = 264). The scores plot revealed a clear differentiation between the two groups (R^2 0.939, Q^2 0.885), and the R^2/Q^2 values for the original models were similar, meaning the model was robust (*Figure 4.4 a*). Furthermore, when the samples from days -7 and 7 (which had their spectra recorded in both 2011 and 2013) were compared in the same way, a clear differentiation was also seen in the scores plot (R^2 0.899, Q^2 0.677). The difference between R^2 and Q^2 exceeded the criterion for model robustness of 0.2, but this may be due to the small number of samples or observations used for this comparison (*n* = 62) in relation to the number of variables. The original models were still situated well above the permuted models (intercepts R^2 0.318, Q^2 -0.376), so the defined class was a better fit to the data than any random grouping. It was hoped that by excluding the small number of buckets which were responsible for most of the separation (1.34, 4.14, 4.18, 3.66, 3.86, 3.26, 3.46, 3.54, 3.5, 3.87, and 3.74 ppm) the combined data could still be used for further analysis. However, when these buckets were excluded, and the analysis repeated, the data remaining from the different years were still clearly separated. Therefore it was decided that it was better not to enlarge the dataset by combining the data run in the differing years. The main buckets responsible for the separation can be identified from the extremes in *Figure 4.4* and are listed in *Appendix 1*.

It can be seen from the loadings and S-plots that the main buckets, relevant to the separation seen between years of recording samples, contain peaks related to lactate (1.34 and 4.14 ppm) and to glycerol, glucose, and amino acids (3.26 – 3.86 ppm).

Since the data collected in 2011 formed the larger dataset this was used for all subsequent analyses.

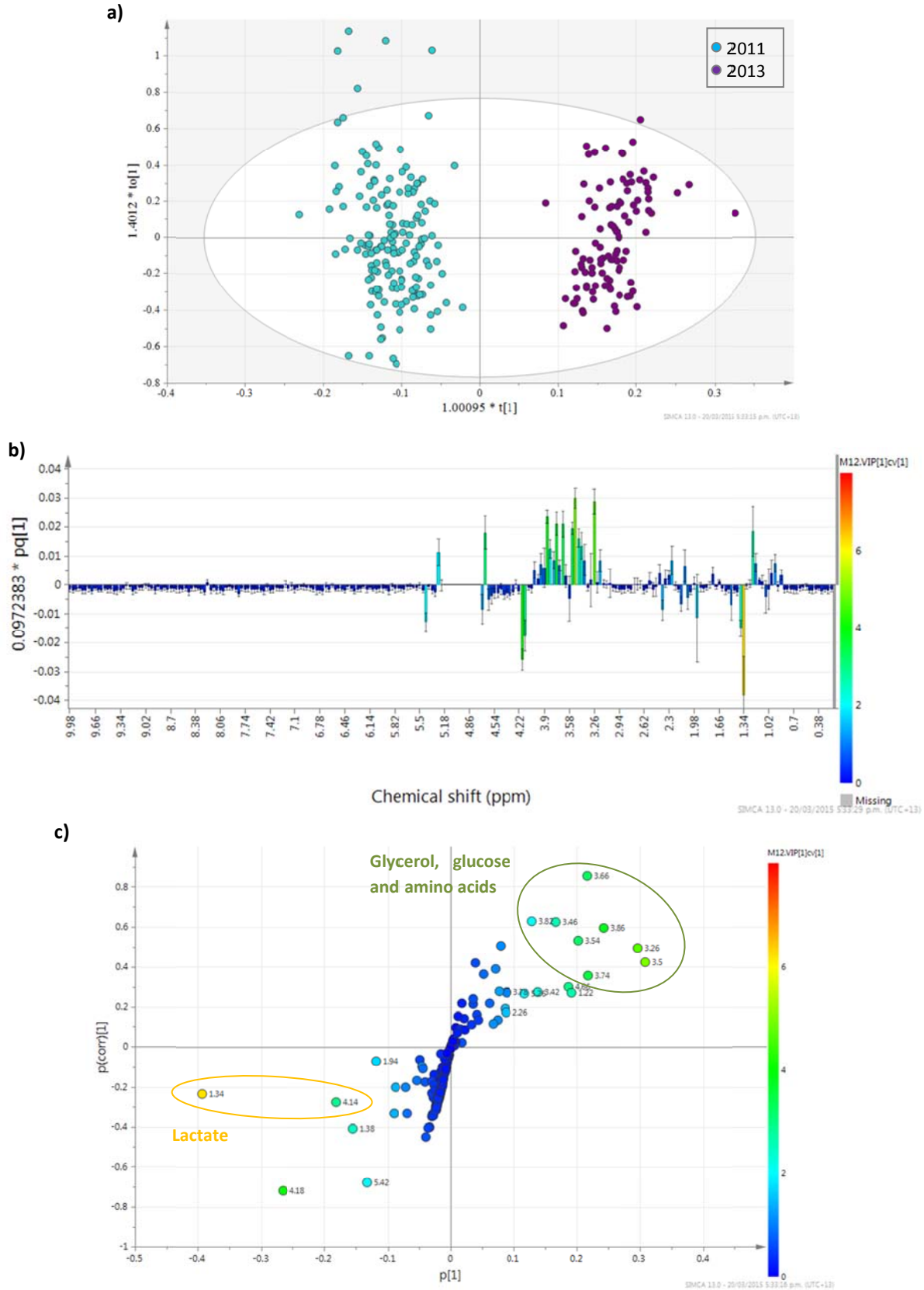

Figure 4.4 OPLS-DA of combined serum p-JRES data classed by NMR run dates (2011 vs 2013); ***a)*** the scores plot shows a clear division between the two years; ***b)*** the loadings column plot; and ***c)*** the S-plot, both coloured by variable influence of projection cross validation (VIPcv), show that lactate is higher in the 2011 samples, while glycerol, glucose, and amino acids are higher in the 2013 samples.

4.3.1.1.2 Orthogonal partial least squares discriminant analysis of ^{1}H p-J resolved spectra used to classify blood serum data

The aim here was to test the differentiation of the samples based on various categorisations using their p-JRES spectra. The comparisons included, (a) samples collected before (Days -14 to 0) and after dosing (Days 7 – 42), (b) samples from the clinical group versus all others, (c) responders (clinical and subclinical) versus non-responders (control cows, all cows in the control period and samples from the non-responder group), and (d) clinical cows starting from their first clinical signs versus all other days and all other cattle. Additional comparisons, including classing by day which compares the buckets between each day of the trial, classing by cow ID, analysing data from control cows over the whole 42 days (classed by cow ID and day), and comparing samples from all cows during the control weeks (classed by day and group). These were performed as a means of testing that the samples could not be differentiated based on criteria unrelated to the presence or absence of FE. A summary of the attempted sample classifications and whether the models were considered valuable for biomarker identification of sporidesmin dosing are given in *Table 4.1*. Details of the noteworthy comparisons are given below.

Initial PCA models, using all samples, identified five outlier samples sitting outside the Hotelling's T^2 critical 99 % line. However, when the raw spectra of these samples were checked, only one spectra showed abnormalities, related to poor water suppression during the NMR experiment. The NMR spectrum from this sample (cow 440, Day 7) had poor resolution and line shapes, and was therefore excluded from further analysis.

4.3.1.1.2.1 Classification based on samples from dosed cattle (Days 7 – 42) versus non-dosed cattle (control), and control days (-14 – 0)

Samples clustered into two groups when OPLS-DA was applied to samples classified according to whether or not they were derived from a cow that had received a dose of sporidesmin. The scores plot for this comparison is shown in *Figure 4.5 a.* The PLS-DA model was validated, with a difference between the goodness of fit (R^2 0.678) and the predictive ability (Q^2 0.472) of 0.206. All random models (intercept R^2 0.331, Q^2 -0.272) were situated below the original models, so the OPLS-DA model was considered to be reliable. The S-plot combined with VIPcv colouring (*Figure 4.5 b*) indicated 13 buckets which had a major influence on the separation of the classes. Four of these showed a down-regulation in dosed samples (1.94, 3.18, 3.22, and 3.3 ppm), while nine showed an up-regulation (1.34, 1.38, 2.06, 2.26, 2.38, 3.58, 3.78, 4.14, and 4.18 ppm). Of these, one produced a

jack-knifed confidence interval in the loadings column plot which crossed zero (3.58 ppm) and wasn't considered to be a reliable indicator for this classing.

Table 4.1 Summary of the sample classes used for multivariate analysis of serum data obtained from p-JRES NMR analysis. The R^2 and Q^2 reported are from the original class models used in PLS-DA, produced during validation tests using 999 permutations.

Sample classification	N	No. of components†	R^2	Q^2	*p*[CV-ANOVA]	Validated
Dosed versus non-dosed	158	5	0.678	0.472	1.009×10^{-15}	Yes
Clinical group versus all others	158	3	0.621	0.456	5.989×10^{-14}	Yes
Responders (clinical + subclinical) versus non-responders (Control and non-responder group)	158	5	0.611	0.384	2.029×10^{-9}	Yes
Day of clinical signs for the clinical group versus all other days and groups	158	4	0.618	0.477	1.203×10^{-16}	Yes
Group	158	4	0.217	0.082	0.0002	No
Trial day	158	5	0.265	0.176	4.335×10^{-20}	No
Cow ID	158	0	N/A	N/A	N/A	N/A
Control group only by trial day	26	0	N/A	N/A	N/A	N/A
Control group only by cow ID	26	0	N/A	N/A	N/A	N/A
Control weeks (Days -14 to 0) only by trial day	52	4	0.601	0.413	7.739×10^{-6}	Yes
Control weeks exclude Day -14, by day	35	6	0.965	0.621	0.138	No*
Control weeks only by group	52	0	N/A	N/A	N/A	N/A

† Produced during PLS-DA modelling using Pareto scaling
* Permuted models were situated close to original models on both axes

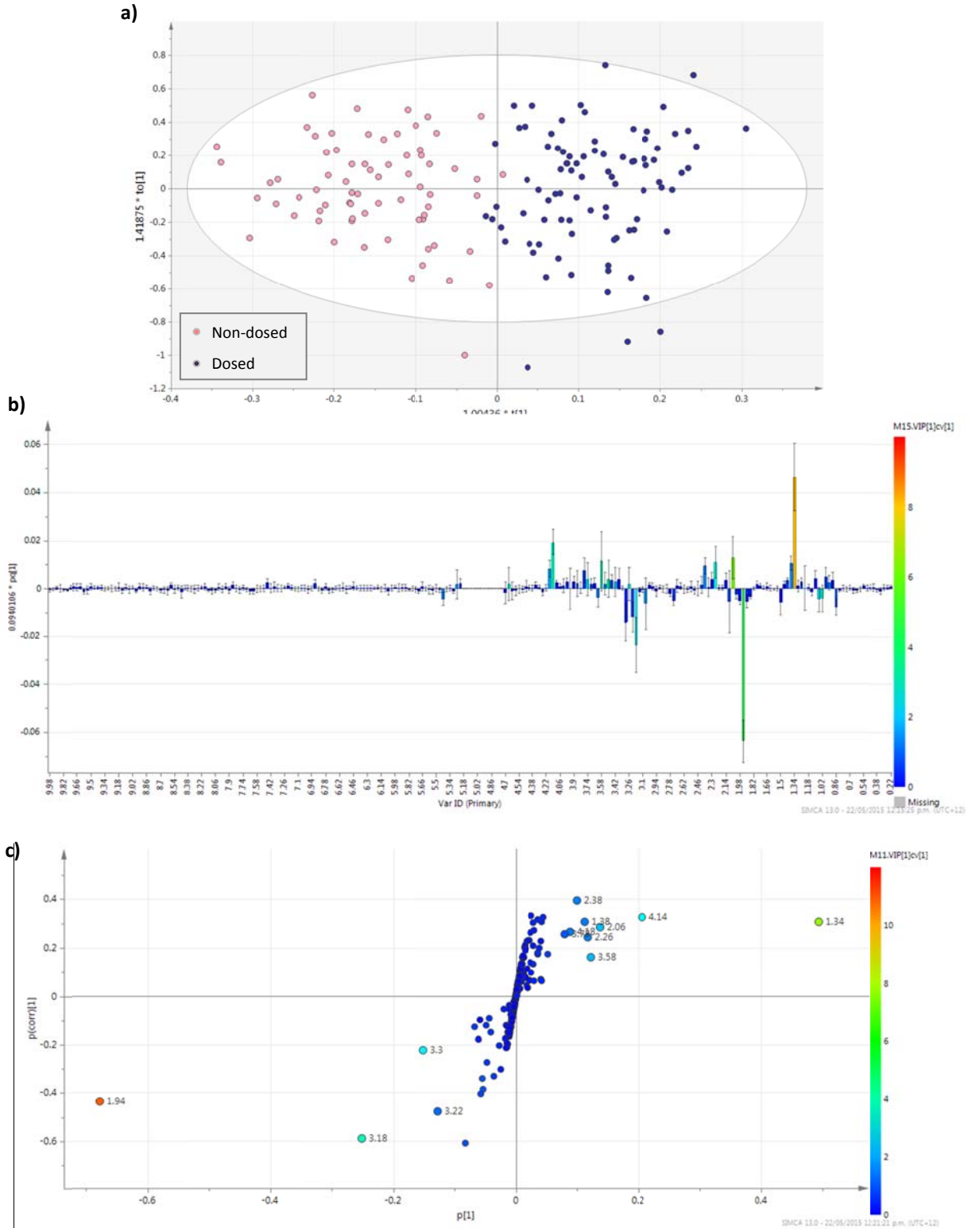

Figure 4.5 OPLS-DA of p-JRES serum samples, defined by samples taken from dosed cows versus those taken during the control weeks and from control cows over the whole trial period; ***a)*** scores plot showing separation between the classes. Some dosed samples do orientate close to the non-dosed, in the centre of the plot. However, these represent samples from the non-responders and from subclinical cows at early or late stages of the trial (Days 7 or 42); ***b)*** the loadings column plot; and ***c)*** the S-plot with major buckets involved in the separation labelled (VIPcv > 1).

The NMR spectra showed two of the buckets (1.38 and 3.22 ppm) to include primarily noise, or very low intensity peaks, coinciding with only half of a peak in the CPMG spectra. Therefore, a total of 10 buckets were considered important in the separation of dosed from non-dosed cows. These buckets contained a total of 11 peaks, with bucket 2.38 ppm containing a single peak and a multiplet, while all other buckets contained one peak only.

4.3.1.1.2.2 Classification based on clinical cattle

Two comparisons were made for the clinical samples. The first (model A) was comparing samples from the clinical group (Days 7 - 42) versus samples combined from all other groups and all control days (-14 – 0). The second (model B) was comparing samples from Days that the individual clinical cows showed clinical signs, versus all other groups and Days. Differentiation could be made between these classes, using OPLS-DA (*Appendix 2 Figures A2.1, A2.2*). The PLS-DA models were validated, with differences of 0.186 and 0.141 between R^2 and Q^2 for the models A and B, respectively. The S-plots, using only buckets with a VIPcv > 1, revealed 26 (A) and 25 (B) buckets which contributed to the separation between the classes. All except three peaks were identical between the models. However, only one bucket was considered reliable for class separation with a p(corr)[1] greater than 0.4 (2.06 ppm), although in model B the 1.34 ppm showed a high contribution (p[1] of 0.47), and was considered important even with a p(corr)[1] of 0.2. Both of these buckets showed an increase in clinical cows. All other buckets from both models had large confidence intervals in the loadings column plot and/or orientated quite close to zero in the S-plot, and were not considered reliable for class separation. The 2.06 ppm bucket is likely to be attributed to changes in glycoprotein concentrations, while 1.34 ppm is caused by changes in the lactate doublet peak.

4.3.1.1.2.3 Quality control analyses, comparing samples from control cows only, and during control weeks for all cows

Quality control analyses were carried out, determining if differences could be found in relation to variables unrelated to the sporidesmin challenge. No variation could be found between control cows during the 44 day trial (n = 26) when defined by day or by cow ID. Using PLS-DA, all samples from control weeks (n = 52), classed by day, showed Day -14 to have significant variation from Days -7 and 0 (R^2 0.751, Q^2 0.629). When Day -14 data was removed, the groups could not be separated with statistical significance. When Day -14 was removed from all other analyses, e.g. all samples classed by dosed versus non-dosed, a slight decrease in R^2 and Q^2 was found, however, the

difference was < 0.05 and was not considered important, so this day was retained in the dataset for all analyses. No separation was found when the control week data was classed by group. Therefore, it was concluded that any differences identified between classes, such as dosed and not dosed, would likely be due to changes relevant to FE, rather than a non-related cause.

Additionally, no differences could be found when control, non-responder, or subclinical groups were individually compared to all other groups. All metabolites identified as being important in the separation of classes are reported in *Table 4.2*.

Table 4.2 Summary of serum metabolites, analysed by ^{1}H NMR p-JRES methods, involved in the separation of groups affected at different degrees following sporidesmin challenge.

^{1}H Shift (δ)	Direction of change *	Multiplicity†	Metabolite
1.35	↑	d	Lactate
1.94	↓	s	Acetate
2.06	↑	broad s	Glycoprotein
2.25	↑	s	Acetoacetate
2.36	↑	m	Proline
2.39	↑	s	Pyruvate
3.17	↓	s	Choline
3.28	↓	s	TMAO
3.79	↑	q	Alanine
4.14	↑	q	Lactate
4.18	↑	dd	3-hydroxybutyrate

† Taken from the CPMG spectra of the serum samples; s, singlet; d, doublet; dd, doublet of doublets; q, quartet; m, multiplet.

*Up - or down- regulation in the sample in relation to the control class

4.3.1.1.3 Investigating the behaviour of serum macromolecules using diffusion-edited ^{1}H NMR

Figure 4.6 shows a random selection, from all groups, of the ^{1}H NMR diffusion-edited spectra recorded using serum samples collected from dairy cows during the sporidesmin trial. The broad resonances from the larger macromolecules are clearly visible in these spectra.

As with the p-JRES dataset, the effect of sample storage was investigated using OPLS-DA for the serum samples recorded using diffusion-edited methods in 2011 and 2013. The initial PCA showed five major outliers in the Hotelling's T^2 plot (99 % critical), and all five outliers showed poor water

suppression, and were excluded from further analysis. The data was then classed by NMR run date (*n* = 266). The years were definitively separated, and the model was supported by a strong validation (R^2 0.956, Q^2 0.922). The main buckets responsible for the separation are listed in *Appendix 2*. Following this, all 2013 data were excluded from further analysis.

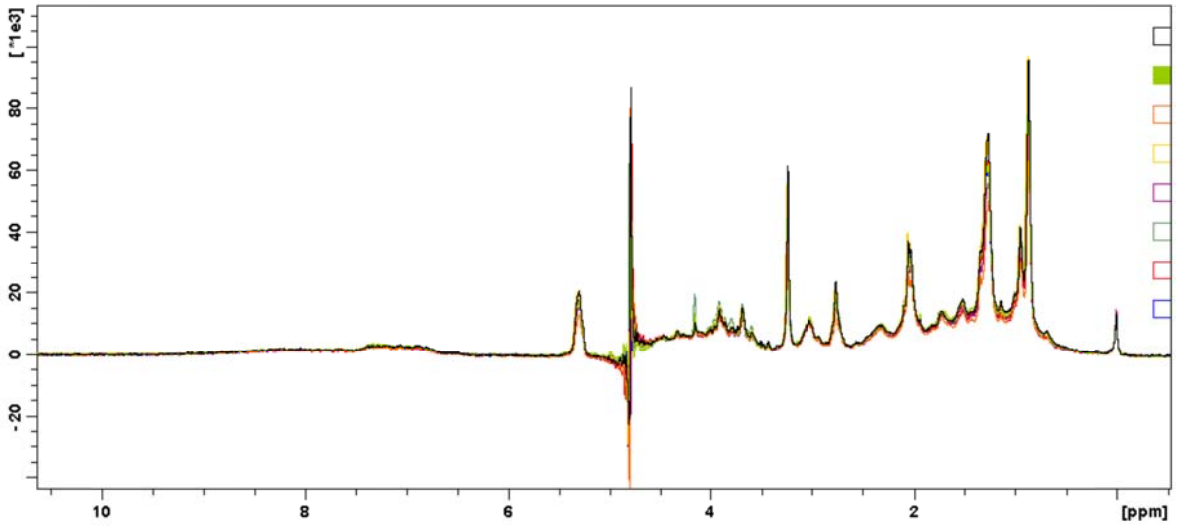

Figure 4.6 One-dimensional diffusion-edited 700 Hz ^{1}H NMR spectra of a random selection of serum samples, across all groups, recorded following a sporidesmin challenge in dairy cattle, showing 0 – 10 ppm.

A summary of the variable classes used to model the diffusion-edited NMR data recorded in 2011 is shown in *Table 4.3*.

4.3.1.1.3.1 Looking for differences in macromolecules for all groups dosed with sporidesmin

The serum diffusion-edited samples could be differentiated by cows which were dosed versus those that were not (control cows) and the control days of the dosed cows (model C; R^2 0.357, Q2 0.342) and by those which responded to dosing (subclinical and clinical) versus those which did not (non-responders and control) (model D; R^2 0.580, Q2 0.461). Although the permutation values of the dosed class are low, the R^2 and Q^2 values of the original models sit well above the permuted models, and are close to each other, so this model was cautiously considered as being reliable. Additionally, the 24 buckets identified by the S-plot (VIPcv > 1) for model C, were identical to those identified in model D. All of these buckets had p(corr)[1] values > 0.5, and small confidence intervals in the loadings column plots, so were considered reliable for class separation. Nine of these showed a down-regulation in samples from dosed cows, while 18 showed an up-regulation. The scores plot and S-plot for model B are shown in Figure 4.7.

Table 4.3 Summary of the sample classes used for multivariate analysis of serum data obtained from diffusion-edited NMR analysis. The R^2 and Q^2 reported are from the original class models used in PLS-DA, produced during validation tests using 999 permutations.

Sample classification	N	No. of components	R^2	Q^2	*p*[CV-ANOVA]	Validated
Dosed versus non-dosed	156	1	0.357	0.342	1.258×10^{-14}	Y
Clinical group versus all others	156	3	0.716	0.493	1.265×10^{-14}	Y
Responders (clinical + subclinical) versus non-responders (control and non-responder group)	156	2	0.580	0.461	2.319×10^{-19}	Y
Day of clinical signs for the clinical group versus all other days and groups	156	3	0.651	0.465	4.779×10^{-13}	Y
Group	156	3	0.237	0.141	2.889×10^{-9}	N
Trial Day	156	4	0.173	0.097	5.271×10^{-7}	N
Cow ID	156	17	0.428	0.0468	1	N
Control group only by trial day	25	0	-	-	-	-
Control group only by cow ID	25	1	0.327	0.172	0.0365	N
Control weeks (Days -14 to 0) only by trial Day	51	1	0.347	0.301	3.463 x10-6	Y
Control weeks exclude Day -14, by Day	35	2	0.533	0.375	0.013	Y
Control weeks only by group	51	1	0.109	0.056	0.097	N

In the scores plots, those which responded more strongly to the dosing orientated further from the centre of the plot as well as from control cows and days (Figure 4.7 a). This implies that these samples showed a larger response to dosing in specific buckets of the NMR spectra and suggests the ability to distinguish between the degrees of damage in response to sporidesmin. This was also seen with the weeks following dosing, with weeks 2, 3, and 4 for the clinicals sitting further away from the other samples, while weeks 5 and 6 were closer to the centre of the plot, near to week 1. These weeks correspond with increases in GGT and GDH activities, and phytoporphyrin concentration. The observations orientating amongst the opposite class, in the scores plot, are related to subclinical cows in the later stages of the trial (Days 35 and 42), and non-responders from Days 7 and 14. This

implies that the non-responders may show low-level changes in compounds such as lipids in the first two weeks after dosing. The S-plot recognised 24 main buckets involved in this differentiation.

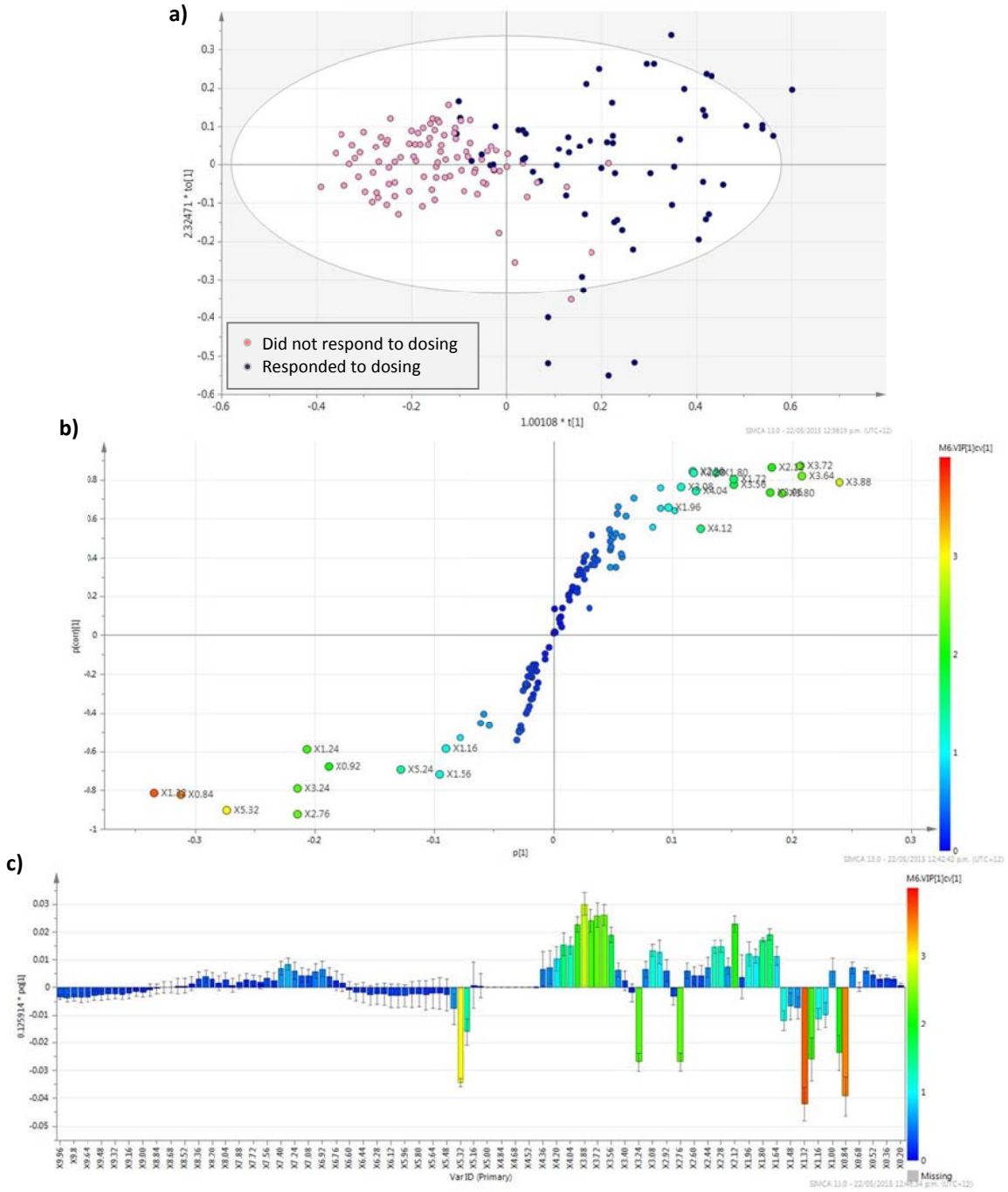

Figure 4.7 OPLS-DA of diffusion-edited NMR serum samples comparing all cows, defined by those which responded, showing ***a)*** scores plot where it can be seen that the samples further from the centre of the plot and further from control cows/days are weeks 2, 3 and 4. Weeks 5 and 6 appear to move back towards the centre for most samples; ***b)*** S-plot showing the main buckets involved in this separation (VIPcv > 1), and ***c)*** 1-D loadings column plot.

4.3.1.1.3.2 Classification of clinical cows

A clear separation was seen between samples taken from clinical cows, after clinical signs were recognised, and all other samples (model E; R^2 0.651, Q^2 0.465), as well as between the clinical group (all samples after Day 0) and all other groups and Days (model F; R^2 0.716, Q^2 0.493). It can be seen in the scores plot for model E (*Figure 4.8 a*) that two samples from non-clinical days are distributed amongst the clinical days. These samples belong to cow 298 (clinical), and cow 222 (subclinical), from Day 14. The clinical samples orientating close to the non-clinical observations, are from samples measured late in the trial (Days 35 and 42), suggesting a degree of recovery. The S-plots identified 24 (model E) and 25 (model F) buckets which contributed to the differentiation between classes (model E shown in *Figure 4.8 b*). One of the buckets (0.92 ppm), was only seen with model E, but had a jack-knifed confidence interval that included zero, and was excluded as a significant bucket. Additionally, two buckets in model F (2.36 ppm and 4.04 ppm) were unique to the clinical group, suggesting changes in earlier weeks after dosing. Of the remaining 23 buckets, two buckets (1.72 and 1.24 ppm) had p(corr)[1] values < 0.04 in both models and were not considered reliable for class separation. All other buckets had p(corr)[1] values > 0.04, and had significant confidence intervals in the loadings column plots. Of the remaining 21 buckets, 10 of these showed a down-regulation in cows showing clinical signs, while 11 buckets showed an up-regulation in those showing clinical signs.

No clear separations could be found when the other individual groups were modelled against the control group and days, and all other groups.

4.3.1.1.3.3 Quality control analyses, comparing samples during control weeks for all cows and samples from control cows only

Control weeks were modelled to identify if any changes occurred, within, or between animals and days, unrelated to sporidesmin challenge. No validated differences were found when control weeks were defined by group, but when defined by Days (-14, -7, and 0) validated differences were found between Day -14 and the other two control Days (R^2 0.619, Q^2 0.545). When Day -14 was excluded from the model, no validated separations could be found between Days -7 and 0. This casts doubt on the models comparing control Days to dosed Days, however, when models were produced on the control group only, over all Days of the trial, no difference was found between Days. Additionally, when control weeks were excluded from the models, the same outcomes were obtained for all previously validated models.

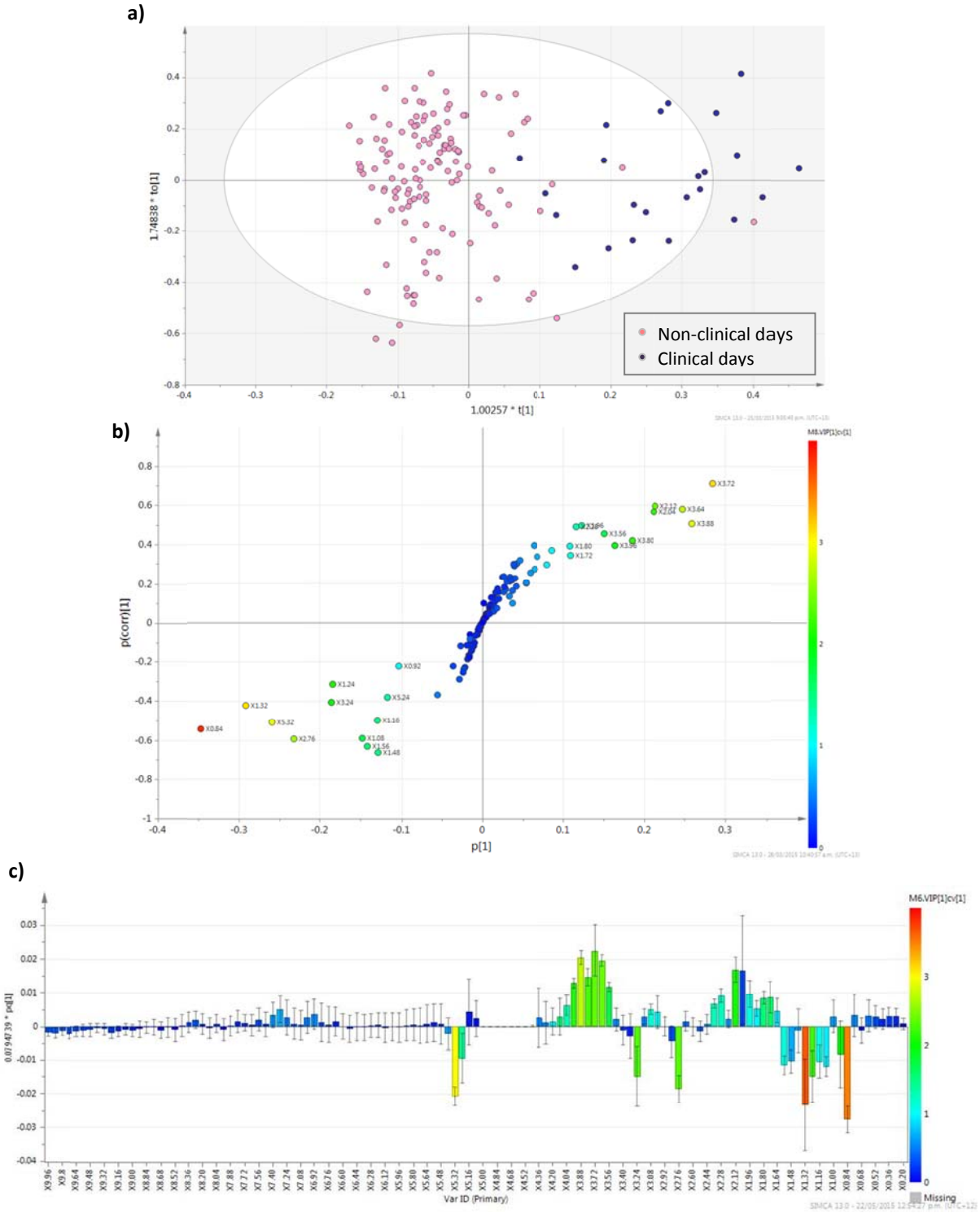

Figure 4.8 OPLS-DA of all serum diffusion-edited NMR samples defined by the samples collected after clinical signs were observed; ***a)*** scores plot demonstrating an orientation to the right of X = 0 for samples measured after clinical signs were observed; ***b)*** S-plot showing the buckets which contributed to the separation in the scores plot (VIPcv > 1); and ***c)*** loadings column plot showing all buckets, coloured by VIPcv.

The diffusion-edited method focuses on recording the presence of macromolecules in the sample, meaning the generated spectra contain broad peaks. Although the bucket width used (0.08 ppm) was larger than that used for CPMG and p-JRES spectra, not all peaks are encompassed within one bucket, and may span two or three buckets. On the other hand, more than one peak may be present within a bucket. When the buckets were checked in the raw spectra, a total of 22 peaks were identified. These peaks and the likely metabolites producing these peaks are shown in *Table 4.4*.

Table 4.4 Summary of serum metabolites identified, using diffusion-edited ^{1}H NMR, as being involved in the separation of cattle dosed with sporidesmin from those which were not, and from those which responded more strongly to the dosing (subclinical and clinical).

^{1}H Shift (δ)	Direction of change *	Multiplicity†	Metabolite
0.87	↓	Broad	CH_3 protons of fatty acyl chains of lipoproteins [cd]
0.94	↓	Broad	Lipids [ab] / CH_3 (lipoproteins)[d]
1.27	↓	Broad	Lipids $(CH_2)_n$ / lipoproteins (mainly VLDL and LDL)[ad]
1.52	↓	Broad	Lipid (CH_2CH_2CO)[cd]
1.73	↑	Broad	Unknown
2.03	↑	Broad	Lipoproteins[a] $(=C.CH_2)$[d]
2.06	↑	Broad s	Glycoproteins[ad]
2.09	↑	Broad	N-acetyls of glycoproteins[d]
2.32	↑	Broad	CH_2CO[d]
2.76	↓	Broad S	CH_2 citrate[d]
3.24	↓	S	$N(CH_3)_3$Choline / lipoproteins[ad]
3.59	↑	m	Unknown
3.69	↑	Broad S	Unknown
3.79	↑	m	Unknown
3.91	↑	m	Unknown
3.96	↑	m	Unknown
4.15	↑	Broad S	CH_2glycerol[d]
5.30	↓	Broad s	Lipid (CH=CH)[a]

* Up - or down- regulation in the sample in relation to the control class

† Taken from the CPMG spectra of the serum samples; s, singlet; m, multiplet.

Tentative identification from: [a] (Tang *et al.*, 2004); [b] (Beckwith-Hall *et al.*, 2003); [c] (Nicholson *et al.*, 1995), [d](Liu *et al.*, 2002), [e](Liu *et al.*, 1997).

4.3.1.2 Urine

Figure 4.9 shows a random selection of spectra, from all groups, of the urine samples from dairy cows collected during the sporidesmin trial, recorded using the ^{1}H 1D NOESY experiment.

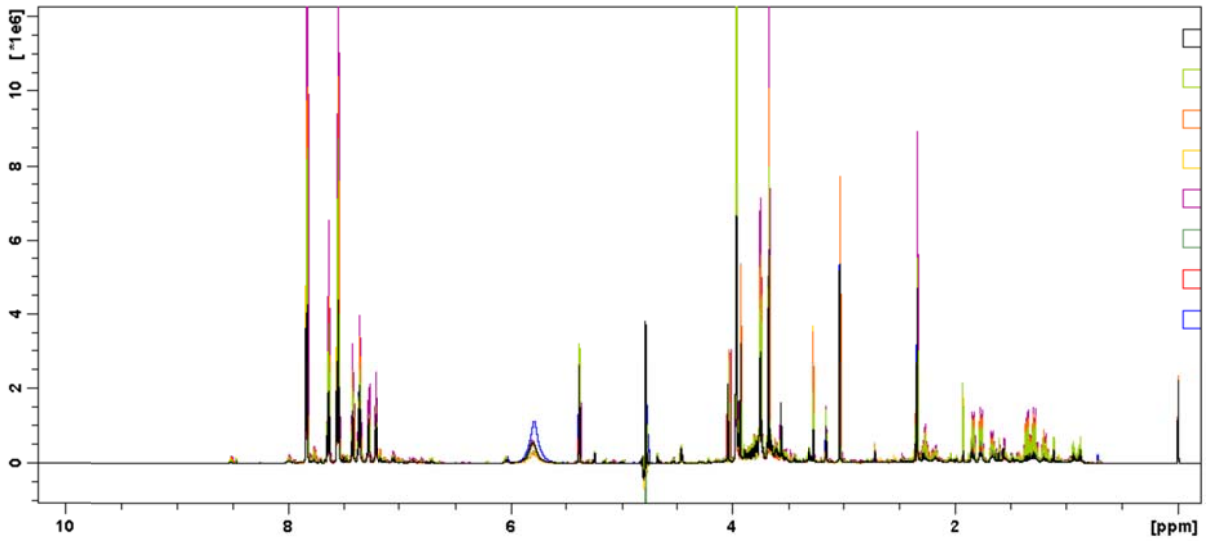

Figure 4.9 One dimensional NOESY ^{1}H NMR spectra of a random selection of urine samples, across all groups, recorded following a sporidesmin challenge in dairy cattle, showing 0 – 10 ppm.

All samples were analysed using the same classes as used with the serum samples. A summary of the models reported here are given in *Table 4.5*.

Table 4.5 Summary of the reported sample classes used for multivariate analysis of urine data obtained from NOESY ^{1}H NMR analysis. The R^2 and Q^2 reported are from the original class models used in PLS-DA, produced during validation tests using 999 permutations.

Sample classification	N	No. of components	R^2	Q^2	*p*[CV-ANOVA]	Validated
Dosed versus non-dosed	153	1	0.507	0.474	1.232×10^{-21}	Y
Trial Day	153	16	0.699	0.281	0.918	Y*
Control group only by trial Day	28	0	-	-	-	N
Control weeks (Days -14 to 0) only by trial Day	48	6	0.838	0.608	1.80×10^{-6}	Y

* Although the R^2/Q^2 difference was high, the original models were orientated away from the permuted models. Additionally, with nine different trial Days and a small number of cows a value like this is acceptable

When all samples were used for modelling, no patterns could be identified by cow ID, and although patterns could be identified by clinical using PLS-DA, the model could not be validated. Additionally, no validated differences could be found when the samples were classed by those that responded to dosing (subclinical and clinical) versus those that did not (non-responder and control), no by samples taken after clinical signs were observed versus all other samples.

4.3.1.2.1 Classification based on samples from dosed cattle (Days 7 - 42) versus non-dosed cattle (control) and control days (-14 – 0) from all groups

The urine samples were able to be differentiated by those that were dosed and those that were not (control group and control days), and this was validated giving a difference between R^2 (0.507) and Q^2 (0.474) of 0.033. The OPLS-DA model gave a scores plot which, although it appeared to show some separation by dose, when analysed more closely appeared to follow a day pattern, with control cow samples, after Day 0, orientating to the right of the scores plot, amongst the samples from dosed cows (*Figure 4.10 a*). When groups were analysed individually, by dosed days, the same separations were seen (results not shown). The S-plot identified a number of buckets involved in the separation (*Figure 4.10 b*).

Because there appeared to be something changing the urine profile on a day to day basis, probably unrelated to sporidesmin dosing, additional models were run where the data was classed by day, to analyse this affect in more detail.

4.3.1.2.2 Using OPLS-DA models to identify day effects in urine samples from dairy cattle

The OPLS-DA modelled by day showed some effect, however this model is difficult to validate due to the large number of variables. When the scores plot was coloured by three week clusters (*Figure 4.11 a*) a clear differentiation was seen. All samples from Day 21 were the only samples which didn't follow this pattern. These samples were primarily distributed between the control days and the days from the last three weeks of the trial. The control cow samples were distributed amongst all other samples/groups, following the day of sampling. This implies that urine is influenced by day to day changes and that these changes may have a stronger influence than dose or clinical FE. Because this model contains more than two classes, S-plots cannot be produced to visualise the predictive component loadings, therefore loading plots (*Figure 4.11 b*) combined with VIPcv column plots were used to identify buckets involved in the separation of the samples.

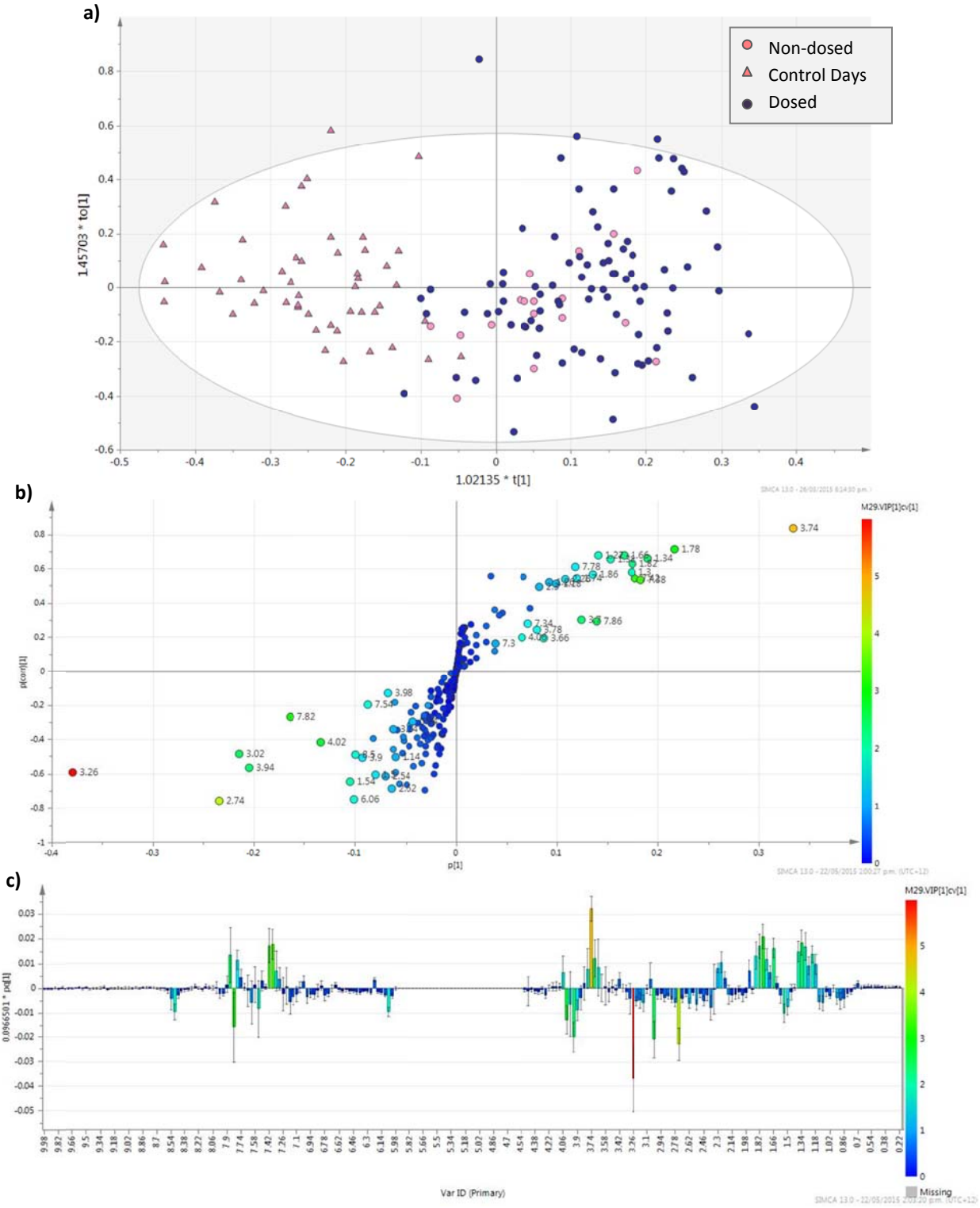

Figure 4.10 MVA of urine classed by dosing; ***a)*** OPLS-DA scores plot of urine samples from all cows. It can be seen that all control day samples (Days -14, -7 and 0) are left orientated, and all the other days are right orientated, including control cattle during Days 7 through to 42; ***b)*** S-plot showing buckets influencing the differentiation of samples (VIPcv > 1); and ***c)*** loadings column plot of all buckets

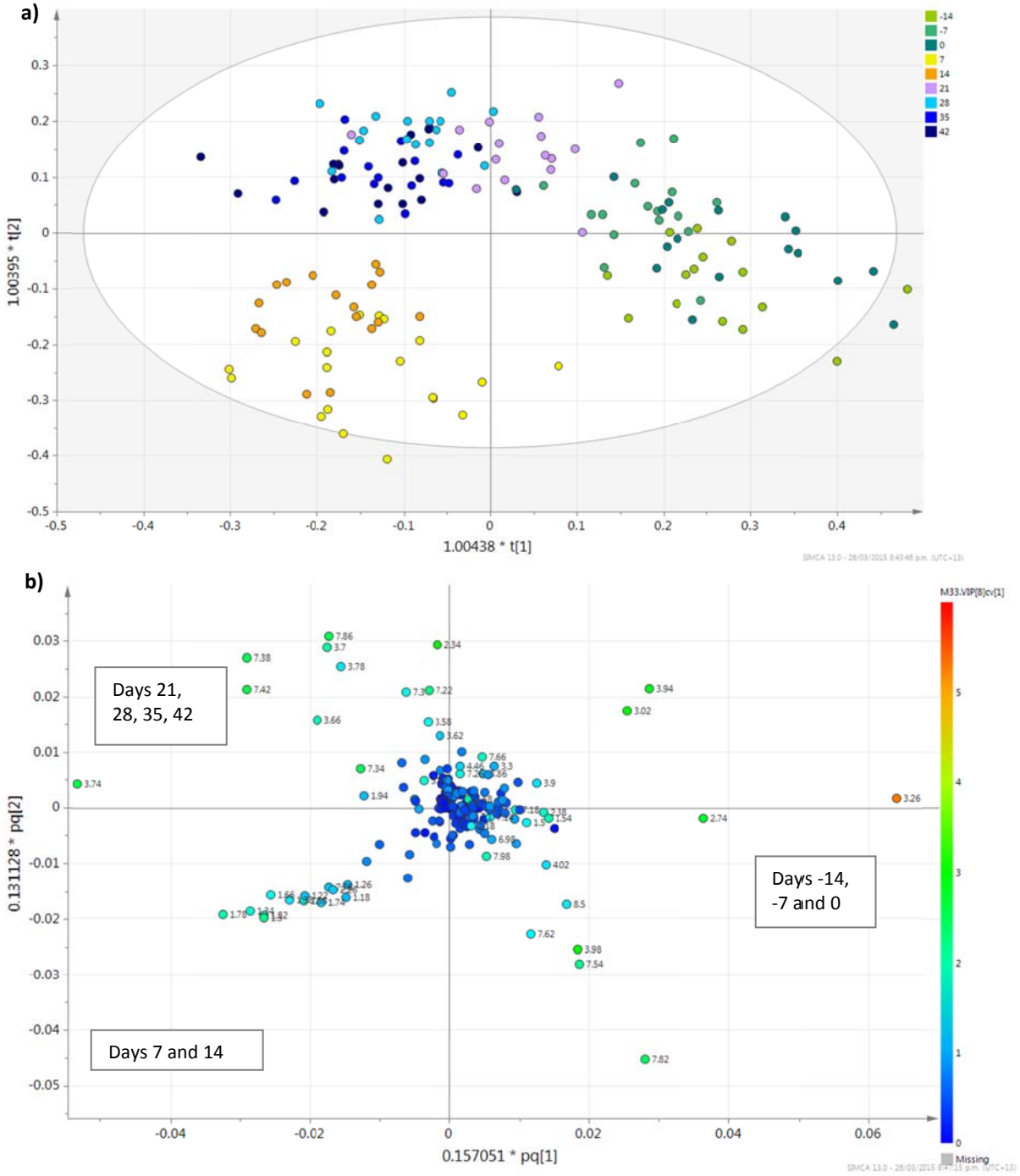

Figure 4.11 OPLS-DA of urine NMR 2011 samples, classed by day. ***a)*** Scores plots showing that all samples, including those from the control group, seem to be affected strongly by a day/week effect. A clustering of control days can be seen to the right of the plot, while Days 7 and 14 orientate to the left, and Days 21 to 42 orientate to the top of the plot; and ***b)*** loadings plot showing the buckets influencing this effect

A total of 54 buckets were identified with a VIPcv > 1. Of these, 26 buckets had confidence intervals in the loadings column plot that included zero, and were excluded. Ten of the remaining buckets showed higher intensities on Days -14, -7, 0, and 21, and lower intensities in 18 buckets. However, only two of these buckets, 3.26 ppm and 3.74 ppm, had p(corr)[1] values > 0.04, showing an increase

and decrease, respectively, and were the only buckets considered reliable for class separation. The NMR spectra show the 3.26 ppm bucket as containing a single peak at 3.27, which may be trimethylamine N-oxide (TMAO), while the 3.74 ppm bucket contained two doublets at 3.758 and 3.744 ppm, which may be attributed to α-glucose, which appears as a doublet of doublets at this chemical shift position (Nicholson *et al.*, 1995).

4.3.1.2.3 Quality control analyses comparing samples from control cows only, and from control weeks for all groups

When the control days (-14, -7, and 0) of all cows were classed by group, no separation was identified, but when classed by day the three days were separated into individual clusters, in the scores plot, for all cows sampled on those days (no shown). The buckets in the loadings scatterplot appeared to cluster considerably around the centre axes. When the loadings scatterplot was coloured by VIPcv, a total of 47 buckets was identified as contributing to the differences seen in the scores plot (VIPcv > 1). The column loadings plot identified 12 up-regulated and 5 down-regulated buckets that had jack-knifed based confidence intervals that did not cross zero. However, the confidence intervals for these were still large, which indicates low reliability for the class separation.

Conversely, no separation could be found between control animals over the nine week sampling period when classed by day or by cow when using PLS-DA. This contradicts the prior models, where all cows, including control cows, could be separated by day. This disparity may be because the number of variables within this class (Days), is high in relation to the number of samples (control cows).

4.3.1.3 Milk

A random selection of ^{1}H NMR p-JRES milk spectra, spanning across all groups and all days of the sporidesmin trial in dairy cattle, are shown in *Figure 4.12*. All samples were classed by: clinical (all days after clinical signs appeared for clinical cattle) versus all other cows and days; dosed versus all others (control cows and days); cows which responded to dosing (clinical and subclinical) versus all others (control cows and days for all groups, and non-responders); classing by group; as well as by individual groups versus all others. Additional quality control analyses, including control cows only, defined by day or by cow ID, as well as control days for all cows classed by group and by day were carried out.

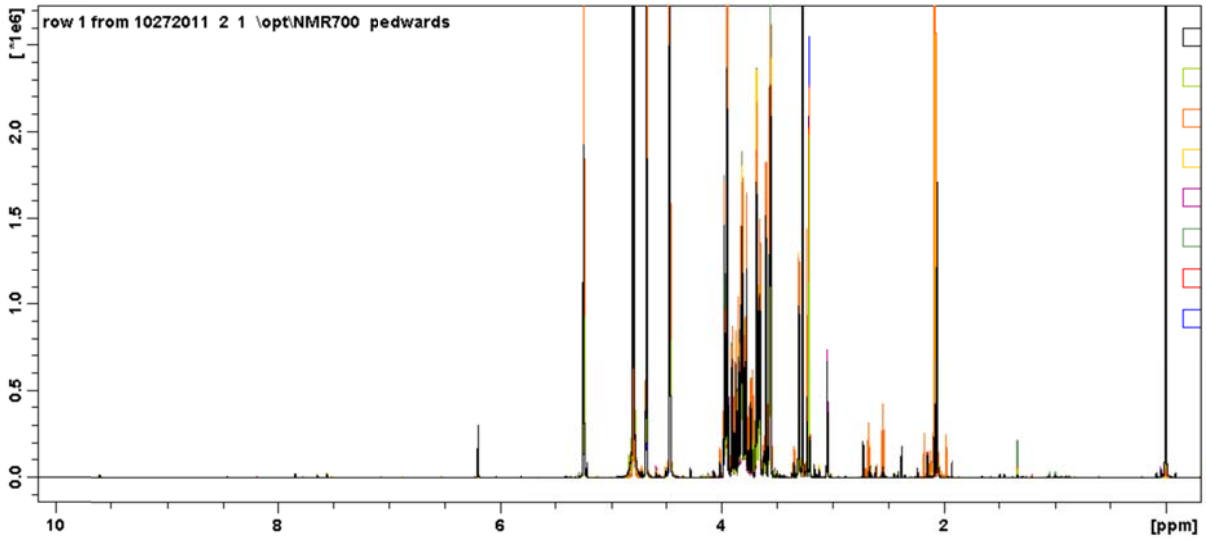

Figure 4.12 One dimensional p-JRES ^{1}H NMR spectra of a random selection of milk samples, across all groups, recorded following a sporidesmin challenge in dairy cattle, showing 0 – 10 ppm.

Initial PCA models, using all samples, identified ten outliers (T^2 critical > 99%). Of these, one of the raw spectra (cow 222, Day 42) showed poor water suppression and was removed from the dataset. One other sample (cow 448, Day 35) showed 'new' peaks, in comparison to others from the trial, in sections of the spectra, at 0.8 – 1.5 ppm and 6.5 – 8.5 ppm. It was not obvious whether this difference was due to experimental failures, but as this was at a later stage of the trial, and therefore not likely to have a significant effect on the response to sporidesmin dosing, it was removed from the dataset. These 'new' peaks may be due to subclinical mastitis or natural changes occurring in late lactation.

Models for clinical days and responders produced 1 component each, but were not able to be validated. No components were produced for classing by group, nor for individual groups versus all other groups. Additionally, the model looking for differences between days over the entire 42 day trial produced 10 principal components, but was unable to be validated. Equally, no discrimination between control cows or control weeks was found.

4.3.1.3.1 Separation of dosed cattle from non-dosed cattle using OPLS-DA

Some differences could be seen between the dosed and non-dosed samples, and this was validated giving a difference between R^2 (0.567) and Q^2 (0.433) of 0.134. Although the R^2 and Q^2 values are low, the permuted models were orientated definitively away from the true models on the *Y*-axis, so were considered viable. As can be seen in the scores plot, shown in *Figure 4.13 a*, a number of samples from both classes overlap in the centre of the plot. The overlapping non-dosed samples

predominantly belong to control cows, measured after Day 0. Three other non-dosed samples belong to cows 298 (clinical), 420, and 64 (subclinical), from Days 0, -7, and -7, respectively. The overlapping dosed samples are primarily from Days 28, 35, and 42 of the trial. These dosed samples may be representing a return to 'normal' following dosing. The reason why the non-dosed samples orientated towards the dosed samples is unknown. Albeit, the likely buckets involved in the overall movement of dosed samples away from non-dosed were still investigated. The S-plot (*Figure 4.13 b*) identified 20 buckets contributing to this pattern. However, only six of these had a p(corr)[1] > 0.4. Three of the buckets (2.70, 2.74, 3.10 ppm) had low p[1] values, so although they were considered reliable for class separation, their contribution to the difference was not high. They were still considered for metabolite identification. All six buckets had small jack-knifed confidence intervals in the loadings column plot. Two of these were increased in dosed cows (3.10 and 3.22 ppm), while four were decreased (2.06, 2.10, 2.70, and 2.74 ppm). The p-JRES and NOESY NMR spectra were used to determine if the buckets contained true peaks, and to establish the multiplicity of the peaks. The spectra showed two peaks within the 2.06 ppm bucket at 2.06 ppm, and 2.08 ppm, both single peaks, which could be attributed to CH_3 protons of N-acetylcarbohydrates, and an unknown peak. While the 2.10 ppm bucket had some very low intensity peaks and was considered to be noise. The 2.70 and 2.74 ppm buckets each contained half of a single peak at 2.72 ppm, and this may be the CH_2 protons of citrate. The 3.10 ppm bucket showed a single peak at 3.11 ppm and is thought to be the CH_3 resonances from lecithin. The final bucket contained two single peaks at 3.20 and 3.23 ppm. The peak at 3.20 ppm is likely to be CH_3 protons from choline, while that at 3.23 ppm can be attributed to CH_3 protons from carnitine. These six peaks are represented in *Table 4.6* along with the tentatively identified metabolites for these peaks.

Table 4.6 List of chemical shift values and the tentatively identified metabolites related to the effect identified in the milk of cows following dosing of sporidesmin, using OPLS-DA on 700 MHz ^{1}H NMR p-JRES spectra

^{1}H Shift (δ)	Direction of change*	Multiplicity†	Metabolite
2.06	↓	s	N-acetylcarbohydrates[a]
2.08	↓	s	Unknown
2.72	↓	s	Citrate[ab]
3.11	↑	s	Malonic acid[acd]
3.20	↑	s	Choline / Phosphocholine[b]
3.23	↑	s	Carnitine[b]

*This is the change in the observation seen in the analysis in response to the variable
†The multiplicity is determined from a combination of JRES and NOESY spectra; s, singlet peak
[a] Sundekilde *et al.* (2013a), [b] Sundekilde *et al.* (2011), [c] Hu *et al.* (2004), [d] HMDB online, were used as aids for identification

No differences could be found in the control group when classed by day, and although the PLS-DA identified 6 components when the control group was classed by cowID, this model was not able to be validated.

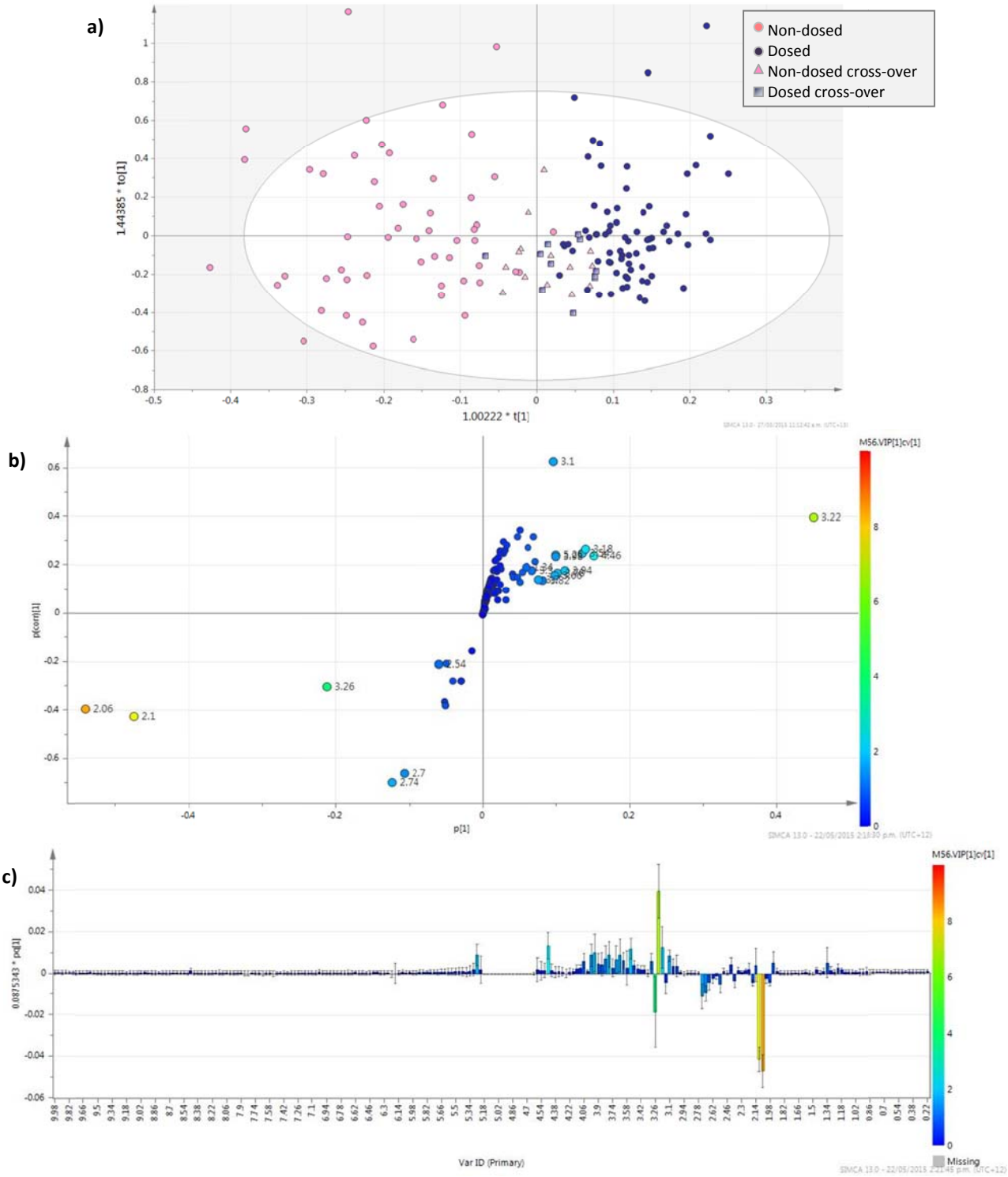

Figure 4.13 OPLS-DA of milk p-JRES spectral analysis, classing by cows which were dosed versus those which were not; ***a)*** Scores plot demonstrating some separation between the classes. However, an overlap of the non-dosed and dosed samples can be seen in the centre of the plot; **b)** the S-plot revealed 18 buckets that were involved in the overall separation of the classes; and ***c)*** loadings column plot of all buckets.

4.3.2 Time-series analysis

Time series modelling, was carried out to try and identify any temporal differences across the trial days, and between the groups of cows. These models produced timeline plots of each bucket for the trial, for all groups. The trace for each group, of a particular bucket, was produced by averaging the bucket intensities of each member of the group, giving four main time profiles per bucket (controls, non-responders, subclinicals, and clinical). Buckets with similar time profiles for each group would not be expected to be relevant to the sporidesmin dosing. On the other hand, buckets with profiles which did differ *could* be important. Therefore, the buckets that differed the most between the groups were identified by ranking, using p-values and SDA. All buckets, identified as being potentially important were checked in the NMR spectra to guarantee these were true peaks, rather than areas of low signal to noise in the spectra. The latter were considered to be false positives, and were excluded from further analysis. Finally the remaining profiles for a particular bucket were assessed subjectively on the extent to which their differences were related to sporidesmin dosing or other factors, for example profiles where large differences were restricted to the control period are unlikely to be important.

4.3.2.1 Serum

Analysis of the p-JRES dataset (0.04 ppm buckets) initially revealed 17 buckets whose time profiles showed some group effect, after dosing. Eight of these buckets appeared to only contain noise in the p-JRES NMR spectra, and were excluded from further analysis. Of the remaining nine buckets, the 2.49 ppm bucket contained only very small peaks at 2.48 and 2.49 ppm. When investigating the CPMG spectra to determine multiplicity it appeared that the bucket contained one outer peak from a quartet, with the quartet centred at 2.47 ppm. It may be that there are peaks underlying the quartet within this bucket, but it would speculative to assume so. Due to the unknown origin of the peak and the low intensity of the peak in the p-JRES spectra, this was not considered useful for group differentiation. The 2.06 ppm bucket contained a peak that was reminiscent of a non-resolved multiplet at 2.06 ppm in the p-JRES spectra, and presented as a broad single peak in the CPMG spectra. It is likely to represent glycoprotein and was only elevated in the clinical following a dose of sporidesmin (*Figure 4.14 a*). The bucket at 6.91 ppm had a peak at 6.917 ppm which matched with a doublet in the CPMG spectra. This peak was elevated in the clinicals and less-so in the subclinicals (*Figure 4.14 b*). It is possibly tyrosine, although no other tyrosine peaks were identified as being important for group separation. This bucket had the greatest combined ranking for separation between groups (*p* 0.003, SDA 27.8). The bucket at 2.02 ppm showed a decrease in

intensity directly after Day 0 for all groups, including controls. The clinical group, although starting higher, did not drop as much as the other three groups, then showed an increase at Day 7, reaching the maximum at Day 21 (*Figure 4.14 c*). This bucket contained a multiplet in the CPMG spectra and may be a lipid or glutamate compound. Although JRES spectra are meant to remove the broader peaks, it may be that a residual peak remained for the compounds in this bucket. Interestingly, the buckets 2.54 and 2.70 ppm showed the same pattern of change of an increase after dosing in non-responders and subclinicals only, to a maximum at Day 7 (*Figure 4.14 d, e*). The amount present in the non-responders then returned to 'normal' at Day 21. The subclinicals also returned back to near 'normal', but at a later date, between Days 28 and 35. The control and clinical cows essentially tracked together for the time period, showing very little change. The peaks in these buckets represented doublets at 2.55 and 2.69 ppm in the CPMG spectra, which may correspond to citrate (Nicholson *et al.*, 1995; Tang *et al.*, 2004). The other three buckets, 0.94, 1.86, and 8.46 ppm, all contained singlet peaks at 0.95, 1.85, and 8.46 ppm, respectively. The 0.95 ppm peak showed very little difference between the groups until Day 14 when the level in the clinical group began to drop until Day 35, and the other three groups increased, until Day 28, then dropped again to Day 35 (*Figure 4.14 f*). In the CPMG spectra this bucket contains a broad peak, with two obvious peaks on top. These peaks may be attributed to isoleucine, leucine, or valine, but it is too difficult to know which without further analysis. The 1.85 ppm peak showed a drop in all groups after Day 0. However, the non-responders plateau at Day 7, while all other groups continue decreasing until Day 14, when they increase to meet the non-responders at Day 21 (*Figure 4.14 g*). This peak has very low intensity in both the JRES and CPMG spectra and was not able to be identified. The final peak (8.46 ppm) appeared to increase slightly in all cows after Day 0; however, the change was greater in the clinical and subclinical cows (*Figure 4.14 h*). This peak can be assigned to formate. The eight peaks identified as showing change after sporidesmin dosing in the NMR spectra are summarised in *Table 4.7*.

The diffusion data was analysed using 0.08 ppm buckets due to the presence of broad peaks from the relatively large molecules selected in this spectral technique. A total of 23 buckets were identified as showing some noticeable change between groups. Eight of these presented as noise in the raw NMR spectra and were excluded from further analysis. Macromolecules produce broad resonances in the NMR spectra, and often span more than one bucket. Of the remaining 15 buckets influencing group differences, eight of these represented four peaks, 1.52, 1.72, 3.02, and 3.69 ppm. 1 bucket had two peaks within it (2.03 and 2.06 ppm), while the other 6 buckets contained only one peak each (0.86, 1.13, 1.81, 2.10, 2.76, and 3.48 ppm).

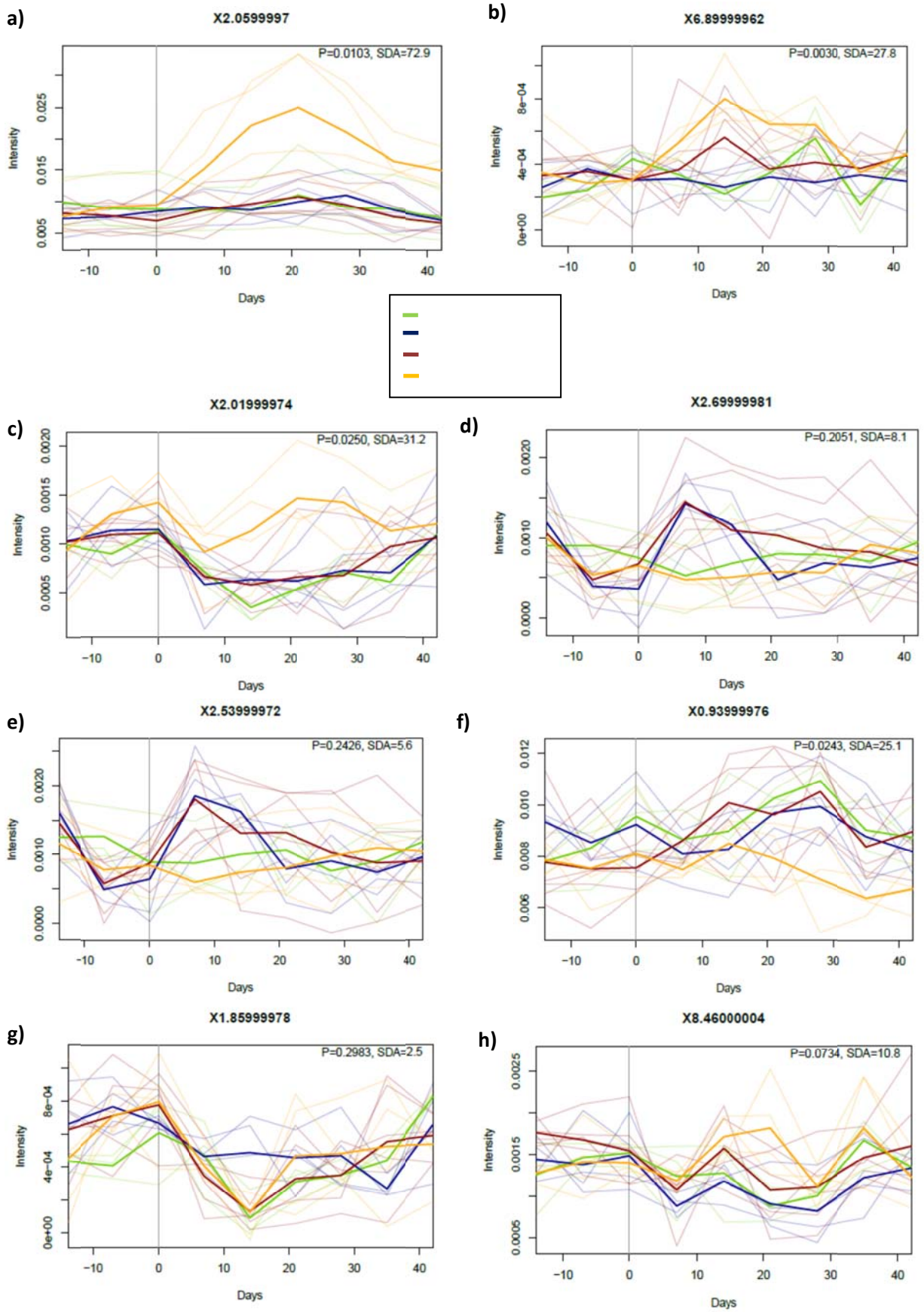

Figure 4.14 Time series plots of serum CPMG ^{1}H NMR data illustrating the peaks recognised as showing differences between groups after dosing; ***a)*** 2.06 ppm; ***b)*** 6.91 ppm; ***c)*** 2.02 ppm, ***d)*** 2.55 ppm, ***e)*** 2.69 ppm; ***g)*** 1.85 ppm; ***h)*** 8.46 ppm.

Therefore, 12 peaks showed an apparent separation of clinical cows from all others, after dosing with sporidesmin (*Table 4.7*). Four of these influenced the clinical group only, with the 2.03 and 2.06 ppm peaks increasing and the 1.52 and 1.13 ppm peaks decreasing after Day 0. Three peaks influenced all dosed groups, with two increasing, 3.48 and 3.02 ppm, and one decreasing, 2.76 ppm, after Day 0. The other five peaks showed the same direction of change in all of the groups however, the changes occurred later for the control group and were minimal. The change showed a greater intensity for the groups that were more severely affected by dosing, clinicals > subclinicals > non-responders > controls. Four of the peaks were elevated after Day 0 (1.72, 1.81, 2.76, and 3.69 ppm), while one was reduced (0.86 ppm). These peaks and their likely metabolites are listed in *Table 4.7*.

Table 4.7 Summary of chemical shift values and likely metabolites identified as showing changes in dosed groups in serum following sporidesmin challenge, from 700 MHz ^{1}H NMR p-JRES and diffusion-edited spectra.

^{1}H Shift (δ)	Direction of Change *	Multiplicity †	Metabolite
0.86	↓	b	Lipid / lipoprotein[abc]
0.95	↓	s	Isoleucine[ab]
1.13	↓	d	Unknown
1.52	↓	b	Lipid (CH_2CH_2CO)[ac]
1.72	↑	b	Unknown
1.81	↑	b/m	Unknown
2.02	↑	m	Lipid / glutamate[ø]
2.03	↑	b	α-hydroxyisovalerate[b] / lipoproteins[ce]
2.06	↑	b/s	Glycoprotein[ab]
2.10	↑	b/m	Unknown
2.55	↑	d	Citrate[ad]
2.69	↑	d	Citrate[ad]
2.76	↓	s	lipoprotein[ab] / CH_2 Citrate[c]
3.02	↑	b	CH_2 lysyl (albumin)
3.48	↑	m	Glucose[ad]
3.69	↑	b	Unknown
6.91	↑	d	Tyrosine
8.46	↑	s	Formate[ab]

*The change in the observation seen in the analysis in response to the variable

† Determined using a combination of p-JRES, CPMG and diffusion-edited NMR spectra; s, singlet peak; d, doublet; m, multiplet; b, broad

ø Very low intensity in the p-JRES

Metabolite identification is tentatively based on [a] Nicholson *et al.* (1995), [b] Lindon *et al.* (1999), [c]Liu *et al.* (2002), [d](Liu *et al.*, 1997), [e](Tang *et al.*, 2004)

4.3.2.2 Urine

Matrix tables of the urine spectra were produced, with buckets at 0.04 ppm, and run through time series analyses. The model produced seven buckets with p-values < 0.05. Two of the buckets (3.259 and 2.739 ppm) showed maximum intensity of peaks at Day 0 (dosing day) and then no obvious difference between groups at any other stage of the trial. These buckets were considered to be unrelated to sporidesmin dosing and were excluded. Additionally, one bucket (9.979 ppm) didn't appear to show any obvious changes in the time series plot, coincided with noise in the raw spectra, and was also excluded.

Four of the plots showed the same general type of pattern of change and shape as each other (7.259, 2.339, 7.219, and 3.419 ppm), with the average clinical cow increasing directly after dosing to a maximum at Day 7, then decreasing briefly to a low at Day 13, and climbing again, along with all the other groups, until the end of the trial (*Figure 4.15*).

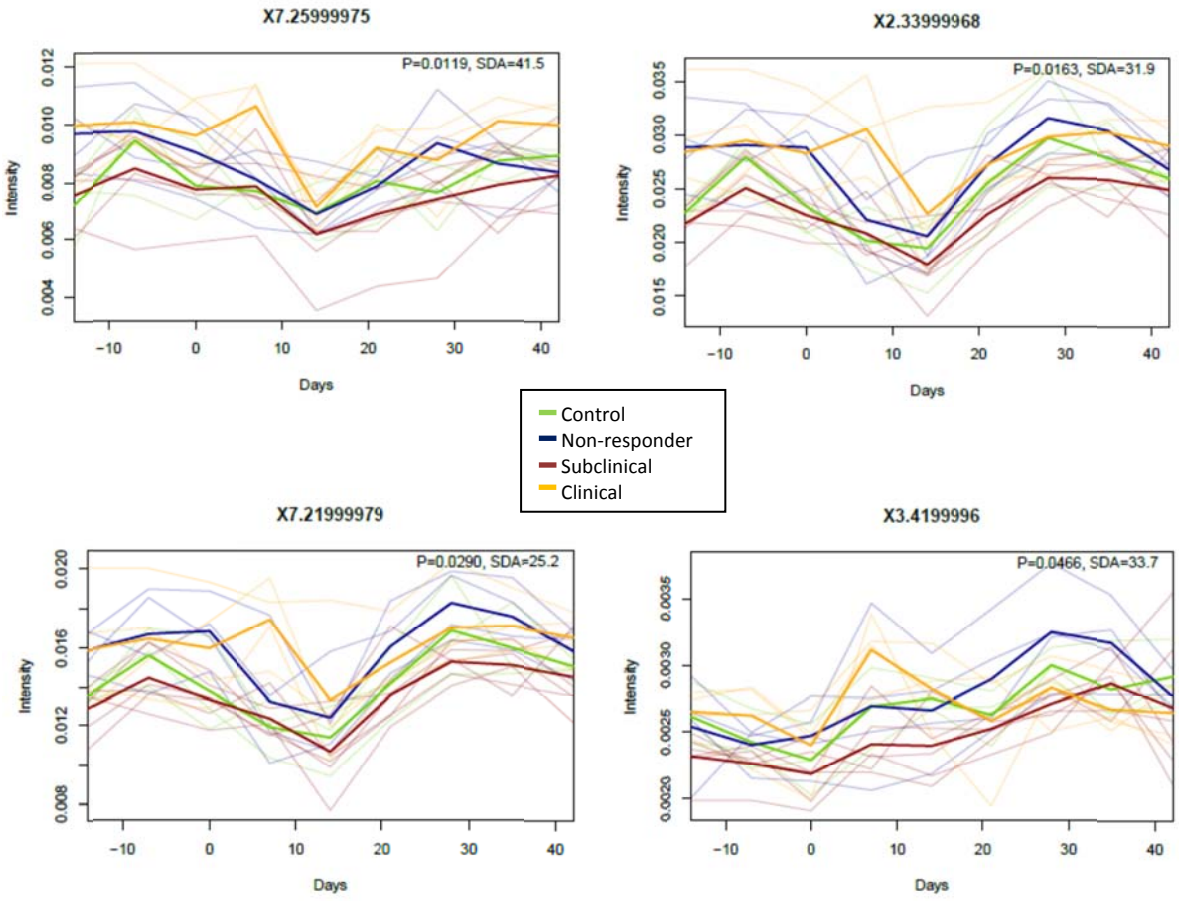

Figure 4.15 Time series plots of urine ^{1}H NMR NOESY data, showing the four buckets which produced the most obvious change in time profile for one or more of the groups following dosing, and were true peaks in the raw ^{1}H NMR spectra. These changes are likely to be due to daily rhythm, or other effects unrelated to sporidesmin.

The 3.419 ppm bucket follows the same pattern – but without the minimum at day 13. This suggests a day or week effect, like that seen in the MVA analyses earlier in this chapter. Due to the changes not being apparently directly relevant to the sporidesmin challenge, these traces were not investigated any further.

4.3.2.3 Milk

As with the multivariate analyses, the 0.08 ppm bucket table was considered to represent the data more closely than the 0.04 ppm bucket table, and was used for further analysis.

The 0.08 ppm buckets showed very little difference between groups on first inspection, and the only p-values < 0.05 obtained were for two buckets (8.6 and 8.76 ppm) which showed no obvious changes in the time series plot for groups after dosing.

In a considerable number of plots individual samples stood out as having excessively large peaks, of unknown origin. The samples contributing to these were identified (cows 424, 448, and 64 from Day 7, and cow 222 Day 42), removed from the dataset, and the model was calculated again. With these extremes removed, none of the buckets produced profiles that were likely to be due to the effects of sporidesmin dosing.

It was concluded that, using the present ^{1}H NMR processing methods combined with time series analyses, milk is not a reliable indicator of sporidesmin challenge.

4.4 Discussion

The present study confirms that, using ^{1}H NMR serum samples could be used to identify dairy cattle that have been given a one-off dose of sporidesmin, at 0.24 mg/kg. Additionally, those that responded more severely to the dose and developed clinical signs, were able to be separated from those that responded less severely, or not at all, following the same one-off dose of sporidesmin. Unfortunately, ^{1}H NMR metabolomics of serum, under the present conditions, was unable to differentiate subclinical cows or non-responders after dosing from their control days. Early changes could not be identified. The urine samples showed changes after dosing, but it appears that these changes were related to a day-to-day change in the urine profile, most likely unrelated to sporidesmin dosing as all control cows exhibited the same changes. These results indicate that urine, under these circumstances, is not a reliable indicator of sporidesmin challenge. Milk was inconsistent between the statistical techniques, with no significant changes identified using time

series analyses, but six metabolites emerged as causing the separation of dosed cows using MVA methods.

To the authors knowledge, this is the first study to have been carried out using ^{1}H NMR for metabolomics analysis for FE diagnosis and biomarker identification. A large number of studies have been carried out assessing FE clinical signs and pathology, using liver enzymes as diagnostic measures of liver damage in relation to sporidesmin ingestion in both natural and artificial challenges. Additionally, measurements of bilirubin and phytoporphyrin in serum and urine have been made, and some of these results have been related to genetic heritability. These include studies by Munday (1982), Clare (1944), Smith *et al.* (1998), Collin *et al.* (1998a), Morris *et al.* (1998), and Di Menna *et al.* (2009). There are also studies on sporidesmin A, identifying the structure and reactivity of the compound, and how ingestion manifests into FE (Done *et al.*, 1961; Flåøyen & Smith, 1992; Hohenboken *et al.*, 2000), however, few have used NMR analysis (Blunt *et al.*, 1979; Woodcock *et al.*, 2001). Conversely a large number of studies have been published on hepatobiliary injury or diseases due to other toxins or heritable traits in humans, rats, and mice, using a combination of biochemical diagnostic tests such as assays and histology, and more commonly now, NMR metabolomics analyses. Examples are studies on non-alcoholic fatty liver disease and acute liver failure (Kotoh *et al.*, 2011), hepatobiliary damage caused by cancer cells, obstructive cholestasis (Allen *et al.*, 2011), damage through artificially administered hepatotoxins (Waters *et al.*, 2001; Wu *et al.*, 2005), as well as using artificial blockages via bile duct ligation (BDL) to identify pathological responses (Froh *et al.*, 2008; Ishihara *et al.*, 2009; Zhang *et al.*, 2012c).

4.4.1 Serum

In the present study, changes in the serum of cows in relation to a single dose of sporidesmin became apparent. Increases in the ketone bodies 3-hydroxybutyrate and acetoacetate, in the amino acids proline, alanine, and histidine, as well as other small metabolites lactate, formate, pyruvate, glutamate, glycerol, and glycoproteins, were seen in these animals. In addition, decreases in acetate, choline, citrate, isoleucine, trimethylamine N-oxide (TMAO), lipids and lipoproteins, cholesterol, and α-glucose were seen. Interestingly, glycoproteins and lactate appeared to be higher in the more severely affected cows, and were able to separate the clinical cows from all others. Citrate was identified as showing an increase in non-responders and subclinicals using time series analysis.

In agreement with the present study, Wu *et al.* (2005) observed similar changes in serum metabolites following intake of three different hepatotoxins in rats. The study showed increases in

alanine, acetoacetate, glycoprotein, and 3-$_D$-hydroxybutyrate. They also observed an increase in low-density lipoproteins and acetate, which was in contrast to the results in the present study, where a decrease in acetate, lipoproteins, and lipids was seen.

An increase in serum lactate concentrations has been observed in samples from patients with acute liver damage compared to those with either no liver damage, or less extensive damage, which is also consistent with the results presented here. For example, Nishijima *et al.* (1997) confirmed an increase in lactate in human patients with malignant hepatobiliary diseases in comparison to healthy adult subjects. Additionally, high levels of lactate suggest an increase in the levels of lactate dehydrogenase (LDH), which catalyses the conversion of pyruvate to lactate and back as it is converting nicotinamide adenine dinucleotide from the reduced form (NADH) to the oxidised form (NAD^+), under anaerobic conditions. LDH has been shown to increase under hypoxic conditions in a range of acute liver diseases (Kotoh *et al.*, 2011). Waters *et al.* (2001) also detected increases in lactate in liver extracts, measured with ^{1}H NMR, in rats exposed to the ANIT hepatotoxin, while Starnes *et al.* (1987) observed a decrease in lactate levels, opposing the present study. Lactate is produced through fermentation, the process of converting pyruvate to lactate in anaerobic conditions. This process regenerates NAD^+, which is then used in a number of energy producing pathways. Lactate levels often increase under anaerobic conditions as a mode of energy production, to be converted to glucose in the liver via gluconeogenesis. However, when the levels of lactate production are higher than lactate removal, such as when the liver is compromised from hepatotoxin ingestion, intracellular acidosis occurs, gluconeogenesis is inhibited through saturation of the lactate transporter, and the liver produces rather than uses lactate (Schade, 1982). Glycolysis becomes the predominant mode of energy production, as the liver is forced to metabolise glucose anaerobically. It has been suggested that lactate may also scavenge free radicals, such as O_2^- and OH (Degroot *et al.*, 1995; Groussard *et al.*, 2000). However, this is a double edged sword for animals that have ingested sporidesmin A, as ROS produced through the reduction and oxidation of the disulfide bridge, cause damage to hepatocytes and the biliary tree. As mentioned, the excess levels of lactate can lead to more damage, hepatic acidosis, inhibition of gluconeogenesis, and continued lactate production. Furthermore, hypoxic conditions, such as those occurring from ROS production and subsequent lactic acidosis, cause endogenous catecholamine to be released in an attempt to support the circulation, but this also increases glycolysis and lactate formation (Schade, 1982). Elevated lactate is indicative of tissue hypoxia, hypoperfusion, and possible tissue damage (Nishijima *et al.*, 1997; Starnes *et al.*, 1987).

During normal, aerobic respiration in cells, pyruvate is transported to the mitochondria to be used in the tricarboxylic acid cycle (TCA). As previously mentioned, during anaerobic respiration, pyruvate is utilised for fermentation reactions, yielding lactate. An increase in pyruvate is therefore required to allow this cycle to continue. For this to happen, an increase in the conversion of glucose derivatives to pyruvate is needed. This could be one of the causes of the decrease in α-glucose seen in the serum of cows dosed with sporidesmin. Additionally, sporidesmin has been shown to increase the permeability of mitochondria *in vitro* (Gallagher, 1964; Middleton, 1974), which leads to leakage of components from the external membrane of the mitochondria. This may add to the high levels of pyruvate and lactate in serum, as these metabolites will readily leak from the mitochondria without any resistance. However, leakage of NADH and NAD^+ will also occur, which would inhibit mitochondrial enzyme systems, including the fermentation of pyruvate to lactate. Therefore, it is likely that much of the lactate and pyruvate, leading to an excess in serum, may be due to production in other areas such as the muscle, and or the cutaneous tissues where additional damage, due to phytoporphyrin, will also be occurring. These metabolites will be removed into the serum for transport to the liver, which is not able to remove them due to compromise, adding to excess concentrations in serum. As with lactate, pyruvate has been shown, in cell culture, to act as a scavenger, specifically of hydrogen peroxide (H_2O_2) (Long & Halliwell, 2009). It may be that, in addition to the increased production of pyruvate to be used in fermentation reactions for energy production in hypoxic conditions, is also generated to control excess ROS levels in the liver, serum, and peripheral tissues in clinical FE cows.

Contrary to the present study, a decrease in serum branched-chain amino acids was observed in BDL rats (Starnes *et al.*, 1987). Other studies have recognised increases in amino acids though, such as 3-methylhistidine (Saitoh *et al.*, 2014), isoleucine and leucine (Waters *et al.*, 2001), glutamine (Amathieu *et al.*, 2014; Kim *et al.*, 2013), alanine (Wu *et al.*, 2005), and proline (Chvapil & Ryan, 1973) which are known to increase with liver injury. A study on obstructive jaundice, however, showed decreases in alanine, glutamine, threonine, and 1-methylhistidine in effected patients (Srivastava *et al.*, 2013). They suggested that lowered levels of amino acids represent ketone body metabolism, and is suggestive of impaired liver function (Srivastava *et al.*, 2013). However, an increase in both ketone bodies and amino acids was seen following sporidesmin-induced damage. The liver plays an important role in amino acid metabolism, protein synthesis, and other detoxification processes. Therefore, any liver-related pathology is prone to affect these metabolic processes and the quantity of these metabolites in the blood at any one time.

Acetoacetate and 3-hydroxybutyrate are ketone bodies, which are produced as an energy source in states of glucose deficiency, often related to hypoxic conditions (Duffield *et al.*, 2009; Marieb, 2004). An increase in ketone body production is well proven to occur following introduction of hepatotoxins to rats (Saitoh *et al.*, 2014; Waters *et al.*, 2001; Wu *et al.*, 2005), as well as in cases of obstructive jaundice (Srivastava *et al.*, 2013). It has been suggested that catecholamine release may be a determinant in the development and maintenance of ketoacidosis, and catecholamines are secreted during almost all major stresses (Schade, 1982). Usually ketone bodies originate from the metabolism of fatty acids via the *β*-oxidation pathway (Amathieu *et al.*, 2014; Wu *et al.*, 2005). This could suggest that sporidesmin has some effect on fatty acid metabolism. Whether this is a direct effect on the fatty acid constituents, or indirect, for example, through increased permeability and damage to mitochondria causing the release of fatty acids and triglycerides stored in the mitochondrial outer membrane, and a breakdown of fatty acid synthesis, could not be determined in this study.

A decrease in serum lipids and lipoproteins was seen in cows following sporidesmin administration in this trial. In contrast, Waters *et al.* (2001) observed an increase in lipids, very low-density lipoproteins (VLDL), and low-density lipoproteins (LDL) following hepatotoxicity in rats. This increase occurred at around 31 hours post dose, and was followed by a decrease to levels below the controls at 7 days. This pattern was not seen in the present study. These changes were accompanied by an increase in TMAO, phosphocholine, and choline at 7 days post-dose, and it was suggested that lipid removal occurred through enzymatic conversion to these intermediate species (Waters *et al.*, 2001). In the sporidesmin challenge, a decrease in choline and TMAO accompanied the lipoprotein decreases, while phosphocholine did not appear as a significant contributing factor to identifying animals that were dosed with sporidesmin. In the present study, the first samples were obtained 48 hours post-dose, and minimum lipid, choline, and TMAO levels were seen around Day 7 of the trial (7 days after dosing). This matches with the timing of decreases seen by Waters *et al.* (2001). In agreement with the present study, a decrease in lipoproteins, specifically high density lipoproteins (HDL), in patients with acute liver failure, was observed (Amathieu *et al.*, 2014). Another study, examining biochemical markers for the diagnosis of malignant biliary obstruction, detected an increase in cholesterol and LDL, but a decrease in HDL (Kurt *et al.*, 2010). Waters *et al.* (2001) and Beckwith-Hall *et al.* (2003) both measured increases in LDL and VLDL levels following a dose of a hepatotoxin, but did not report on HDL levels. Amathieu *et al.* (2014) state that high HDL levels reflect good hepatic function, and that low HDL levels appear to be related to the severity of chronic liver disease in their study. In the present study, it was not possible to distinguish between the lipoprotein types, and it may be that the lipoprotein related peaks showing a decrease in cows after

ingesting a dose of sporidesmin (0.84, 0.94, 1.27, 1.52, 2.02, 2.03, and 5.30 ppm) represent HDL levels. Additionally, differences between studies may be attributed to species differences (rat vs cow) or it may be that the hepatotoxicity of the compounds (ANIT vs sporidesmin) occur via slightly differing pathways. However, in accordance with the current study it has been reported that choline deficiency is connected to the pathogenesis of liver injury (Northfield *et al.*, 2000). Phosphocholine and choline are products of lipid catabolism and can be further metabolised to TMAO. Additionally, choline is also part of the phosphatidylcholine and sphingomyelin phospholipid classes which are abundant in cell membranes. Necrosis of hepatocytes, bile ducts, and mitochondrial cell walls may lead to an increase in these phospholipids and their precursors in serum.

Acetate is an end product of fatty acid oxidation, and Wu *et al.* (2005) stated that elevated levels of acetate illustrate energy metabolism disorders related to increases in ketone bodies, which was recognised after the introduction of three different hepatotoxins to rats. Waters *et al.* (2001) reported results which opposed this when treating rats with a hepatotoxin; where a decrease in acetate alongside an increase in ketone bodies was detected in blood plasma. The latter study supports the results from the present study, where a decrease in acetate levels, alongside an increase in ketone bodies, acetoacetate, and 3-hydroxybutyrate, was noted.

Glycoprotein, was the main metabolite identified, in both MVA and time series analyses, as clearly separating the clinical cows from all others. Glycoproteins are proteins bound to a carbohydrate, usually an oligosaccharide. In agreement with the present study, Wu *et al.* (2005) observed an increase in glycoproteins in rats with two of the three hepatotoxins that were tested. Following this study, it was suggested that high levels of glycoproteins indicated hepatic insufficiency, which could imply that these toxins affected the activities of key enzymes of protein metabolism. Additionally, gycoproteins are important integral membrane proteins. These proteins can be separated from biological membranes using detergents and nonpolar solvents. Bile acids (BAs) act as detergents in the bile to clean up fatty acids in the blood, and sporidesmin inhibits bile elimination, and causes bile leakage from the bile ducts, through damage to the biliary system. This leads to an excess of BAs in the blood. It is possible that the BAs affect the integrity of cell membranes by solubilising the lipid element of membranes, releasing glycoproteins and other membrane elements. Glycoproteins are also part of the major histocompatibility complex (MHC) molecules, which display fragments from pathogens (antigens) on their surface to interact with T-cells as part of the adaptive immune response (Janeway *et al.*, 2001). Additionally, they are present on the surface of the membranes of platelets. Studies have shown that specific P-glycoproteins, otherwise known as multidrug resistant protein 1, are up-regulated in obstructive cholestasis, and the increased expression may represent a

secondary response in an attempt to eradicate toxic substances into the bile (Adachi *et al.*, 1996; Arrese *et al.*, 1998).

Taking into account the increase in production of ketone bodies and lactate, and a decrease in lipoproteins it is to be expected that aerobic glycolysis has shifted towards anaerobic and lipid metabolisms following hepatobiliary damage from hepatotoxins. Glycoproteins appeared as important for the differentiation of the clinical cows. Increases in glycoproteins in the serum of these cows may be due to a combination of reasons, such as high levels of cell membrane damage and an increase in adaptive immune-mediated response. The concentrations present in serum may therefore be indicative of the severity of damage caused by sporidesmin and possibly phytoporphyrin. This suggests that glycoproteins could be important metabolites to investigate further in more targeted analyses. Additionally, the separation of non-responders and subclinicals by elevated concentrations of citrate, identified using time series analyses, indicate the potential for identification of less severe, and possibly early stage, FE.

4.4.4 Urine

In urine, changes due to daily variation appeared to be stronger than those from sporidesmin intoxication. Urine composition is known to vary daily due to diet, lifestyle, and other environmental perturbations (Maher *et al.*, 2007). It has been shown that daily biological variation may affect measurements of albumin-creatinine ratios when diagnosing chronic kidney disease in humans (Naresh *et al.*, 2013). It was concluded that large changes due to disease status would be needed for these to overshadow day-to-day changes. Chen *et al.* (1995) state that urine collection should be carried out over more than 5 days to help reduce errors due to variation in urine output. They also state that day-to-day variation is usually about 10 % of the variation seen. Kim *et al.* (2014) show that most of the variation can be attributed to technical issues such as sample preparation, rather than biological variables, such as meals, in humans. However, they did show that variability was apparent at different times of the day, for example after the morning and evening meals, and that variability was greater in urine than blood. Skotnicka *et al.* (2007) reviewed renal activity in livestock and concluded that most changes in renal activity are due to diurnal rhythms. In the present study, samples were only taken in the morning to avoid this variability.

In spite of these daily affects, a number of studies have shown that some urinary metabolites can be effective biomarkers for the discrimination between diseased and healthy subjects. For example urinary markers have been found in studies on cancer (Bansal *et al.*, 2013; Chen *et al.*, 2011; Zhang *et al.*, 2012b), as well as for preclinical toxicological screening of candidate drugs (Lindon *et al.*,

2003); additionally, markers have proven useful for identifying liver and kidney toxicity in rats and mice (Ebbels *et al.*, 2007; Lindon *et al.*, 2005; Schnackenberg *et al.*, 2007), and diabetes (Guan *et al.*, 2013), and have been used as models for cholestasis (Ishihara *et al.*, 2009; Katsumi *et al.*, 2015) and hepatotoxicity in rats and mice (Holmes *et al.*, 2000; Kim *et al.*, 2013).

Two studies have shown that phytoporphyrin is present in urine following BDL in horses (Ford & Gopinath, 1974), and in sheep and calves (Ford & Gopinath, 1976). In horses, urine samples were taken up to 80 days after BDL, and measurements showed that concentrations of phytoporphyrin in urine rose rapidly following ligation and then fell again between days 15 and 20 (Ford & Gopinath, 1974). However, these concentrations did not return to pre-ligation concentrations. In calves and sheep, measurements were only obtained five days before and after BDL. Ford and Gopinath (1974, 1976) also quantified changes in bilirubin concentration following BDL. In the present study phytoporphyrin concentrations were measured in serum using fluorescence spectroscopy, but not in urine samples. No signs of phytoporphyrin were present in the serum or urine when analysed using ^{1}H NMR.

Additionally, studies have measured sporidesmin in urine in mice, rabbits, and sheep (Briggs *et al.*, 1994; Smith *et al.*, 1999). Briggs *et al.* (1994) analysed samples from animals injected with sporidesmin A and D, and detected sporidesmin metabolites in urine 1 hour after dosing. These levels reached a maximum at 5 hours and could no longer be detected at 48 hours (Briggs *et al.*, 1994). Smith *et al.* (1999) measured maximum levels of immunoreactive metabolites of sporidesmin A at 15 - 30 hours after dosing with this compound. Additionally, urinary levels of the metabolites were not different between resistant and susceptible sheep. In the present study the first urine sample was taken ~ 48 hours after sporidesmin dosing. It is likely that all direct metabolites from sporidesmin would not be detectable at this stage.

Although changes in TMAO, glucose, ketone bodies, and various amino acids, have been identified in urine with cases of liver damage (Feng *et al.*, 2002), it appears that in the present study, changes related to day-to-day variation in cattle were stronger than any variation caused by hepatobiliary damage initiated by sporidesmin. It may also be that by the time the first samples were taken, on Day 2, any direct metabolic changes had already occurred and therefore were not measureable in urine in high enough levels to overshadow day-to-day changes.

4.4.3 Milk

Increases in malonic acid, carnitine, choline, and/or phosphocholine, as well as decreases in N-acetylcarbohydrates, citrate, and an unknown metabolite became apparent in the milk of dosed

cows using MVA methods. Malonic acid is a dicarboxylic acid that is a competitive inhibitor (Hoffman & Brookes, 2009). It has been known to act against succinate dehydrogenase in the respiratory transport chain in mitochondria (Quinlan *et al.*, 2012), and to affect the TCA cycle by inhibiting the oxidation of oxaloacetate to tricarboxylic acid which is a requirement for the cycle (Pardee & Potter, 1949). Malonates, the ionised forms of malonic acid, have been shown to stimulate the synthesis of fatty acids. Additionally, high levels of malonates, in combination with β-ketoglutarate, a ketone derivative of glutaric acid, lead to as much as thirty-fold increases in acetate incorporation into fatty acids (Wakil, 1961). This may explain why a decrease in acetate was seen in serum in cows following sporidesmin ingestion in the present study. It has been shown in rats that malonates and citrate are two factors that can result in inhibition of milk secretion (Levy, 1964). In the present study, the cows dosed with sporidesmin did show a decrease in milk yield, which may correlate with the malonate increase. However, a decrease in citrate was seen in the same cows.

Choline concentrations in milk have been shown to vary depending on the stage of lactation. A decrease in choline levels can be seen at early- to mid-lactation, before rising to their maximum in late-lactation (Artegoitia *et al.*, 2014). Additionally, a correlation between serum free choline concentrations and milk free choline concentrations has been identified (Ilcol *et al.*, 2005). In the present study a decrease in serum choline levels was coupled with an increase in milk choline levels. This suggests that an increase in the uptake of choline into the mammary gland may be the cause of the increase in free choline in milk samples. The requirement for choline in the mammary gland may be elevated due to lower energy availability during states of ketosis, liver damage, or immune attack. Choline is essential for lipid transport, through the synthesis of VLDL, for the synthesis of acetylcholine, and as an important source of methyl groups for biosynthesis. Choline is extensively degraded by rumen bacteria, meaning that dietary choline contributes insignificantly to the main pool of choline in the body (Pinotti, 2012). However, the output of methylated compounds to milk is high, especially at the onset of lactation. Almost all choline present in milk is from *de novo* synthesis in the mammary gland (Klein *et al.*, 2010; Pinotti, 2012). Choline has been suggested to prevent liver and muscle damage, and other health risks in human adults (Zeisel, 2006).

L-carnitine is necessary to transport long-chain fatty acids into the mitochondria to be used as an energy source. Secretion is high during the first 3 - 4 days of lactation in rats, but falls once the young have developed the capacity to synthesise this metabolite themselves (Shennan & Peaker, 2000). It is suggested that the mammary epithelial cells efficiently remove carnitine from the blood (Erfle *et al.*, 1974). An increase in release of carnitine from rat mammary tissue has been observed when cell-swelling is induced by hypo-osmotic shock (Shennan & Peaker, 2000). The biosynthesis of

carnitine occurs primarily in the liver and kidneys from the amino acids methionine and lysine, which are generally considered to be limiting for milk production. An increase in the excretion of carnitine in milk occurs during ketosis (Erfle *et al.*, 1974). This increase was deemed to be due to an increase in carnitine synthesis, rather than catabolism from skeletal muscle. However, the study by Erfle *et al.* (1974) only measured levels during early-lactation. It is unknown, whether this same effect occurs during late-lactation. No obvious changes were identified in serum in cows after sporidesmin dosing, while Erfle *et al.* (1974) observed increases in both serum and milk carnitine concentrations in ketotic cows. In agreement with the present study though, milk carnitine showed a negative correlation with blood glucose, and a positive correlation with ketones. It has been shown that choline deficiency is correlated with carnitine deficiency in rats, suggesting some connection between these two metabolites (Mehlman *et al.*, 1971).

Citrate is an intermediate in the TCA cycle and plays an indirect role in lipid synthesis by providing NADH as a reducing equivalent (Garnsworthy *et al.*, 2006). It was proposed that it could be used as an indicator of the energy status of a cow, being correlated with ketones in the milk (Baticz *et al.*, 2002). However, mammary epithelium is impermeable to citrate in both directions, which means that milk citrate concentrations reflect mammary gland activity rather than that of general metabolism (Linzell *et al.*, 1976). It was shown by Linzell *et al.* (1976) that citrate is concentrated by the Golgi apparatus and these vesicles then transport the citrate to the apical membrane of the cell to be released by exocytosis. This suggests that changes in citrate are not likely to be a direct effect of sporidesmin intoxication, unless the toxin alters mammary gland permeability and/or the Golgi apparatus somehow.

Acetate is required for the production of citrate in the mammary gland mitochondria. A decrease in citrate in milk following sporidesmin challenge may be due to a decrease in acetate in the serum. Additionally, citrate is thought to maintain fluidity of milk through its effects on the structure of casein micelles, as it acts as a calcium chelating agent (Faulkner & Peaker, 1982). It could be that the additional requirements on the body and immune system of cows that have ingested sporidesmin may cause subclinical mastitis, which will lead to changes in milk fluidity. Oshima and Fuse (1981) have reported that citric acid decreases in milk in conditions such as subclinical mastitis, and it does so proportionately to the degree of inflammation. It may also be that changes in milk occur in late-lactation and at drying-off. The cows in this study were in late lactation, and those that had been given sporidesmin may have had less energy available for milk production, causing an early drying off. Citrate has been shown to decrease during the early drying-off period of lactation (Kutila *et al.*, 2003). It would be expected that these changes would be seen in the control cows if that was the

case though. Although the cows dosed with sporidesmin were able to be separated from the control cows using MVA, some samples did intersect in the centre of the scores plot (Figure 4.18). The samples were identified as samples from dosed cows in the later days of the trial, and samples from the control group between days 21 and 35. It may be that the cross-over of these samples represented natural changes due to the stage of lactation, which would support the theory above.

Chapter 5

Mass spectrometry-based metabolomics

5.1 Introduction

Mass spectrometry (MS) has become the major technical platform for metabolomics. Mass spectrometry methods, especially with the addition of chromatography, allow for more selective and highly sensitive studies than does NMR. In addition, MS affords high throughput, has direct applications to complex biological extracts (Cao *et al.*, 2013), and has the potential to identify metabolites (Xiao *et al.*, 2012).

Mass spectrometry can provide both qualitative (structural) and quantitative (molecular mass or concentration) information on analyte molecules following their conversion to ions. Samples containing molecules of interest are introduced into an ionisation source in small aliquots, where they are ionised to acquire positive or negative charges. The charged ions are separated in the mass analyser based on their mass-to-charge ratios (*m/z*). Signals distinguished by their *m/z* values are recorded by computer systems and displayed graphically as mass spectra, showing the relative abundances of signals ordered according to their *m/z* values (Castillo *et al.*, 2011; Ho *et al.*, 2003). A variety of ionisation techniques are available, such as chemical ionisation (CI), electron ionisation (EI), matrix-assisted laser desorption/ionisation (MALDI) and electrospray ionisation (ESI). ESI and MALDI are the primary techniques used in biological sciences as they are suitable for the analysis of thermally labile and non-volatile analytes available in femtomole quantities in micro-litre sample volumes. ESI is a 'soft' ionisation technique, which forms intact molecule-ions, and provides a sensitive, robust, and reliable tool for global profiling of metabolites (Ho *et al.*, 2003; Watson & Sparkman, 2007; Xiao *et al.*, 2012).

The coupling of chromatography techniques with MS has facilitated compound separation using a variety of different chromatographic columns. This has aided in reducing sample complexity and increasing metabolite identification. However there are no universal methods of analysis for metabolomics, and although gas chromatography (GC-MS) and liquid chromatography (LC-MS) are complimentary techniques for metabolomics analyisis, GC-MS does require compounds to be volatile or derivable (Bruce *et al.*, 2008). This means that non-volatile compounds that do not easily derivatise, and large thermo-labile compounds cannot be studied. Additionally, GC-MS instruments usually use hard-ionisation methods, such as EI, which causes large degrees of fragmentation of the subject molecules. This method does allow reproducible fragmentation patterns which are searchable against EI-MS libraries, but does results in the absence of a molecular ion. With liquid chromatography (LC)-MS and the appropriate method of ionisation, derivatisation is not required, and it is possible to analyse an array of compounds which are unable to be analysed by GC-MS. As a result, LC-MS is particularly suited for profiling-type studies, including the global determination of

metabolites and/or identifying patterns of compounds that vary in ratio in relation to a disease. High performance LC (HPLC) allows separation of compounds of a wide range of polarities, and was the main staple choice for metabolomics, until recent developments on ultra-performance LC (UPLC). UPLC brings a higher resolution for analyte separation, improved speed of analysis, and a lower limit of detection for ions, allowing a larger number of metabolites to be detected and better assignment of peaks (Chen *et al.*, 2007; Dunn *et al.*, 2011a). A range of LC columns are available, with varying chemical and physical properties, such as particle sizes and surface chemistries. What affects the separation in LC is column parameters; for example the type of stationary phase such as the material, the size and shape of the material, inner diameter, and length of the column; and the mobile phase, such as the polarity, hydrophobicity, and electrical charge. The physical parameters have the greatest effect on separation, for example determining the retention capacity of the column through surface area, carbon load, pore size, and volume of the packing material. Reverse-phase (RP) columns enable separation of a wide range of polar and non-polar compounds, and due to their broad application are widely applied. The C18 RP columns are commonly used for the separation of semi-polar compounds (phenolic acids, glycosylated steroids, and alkaloids) while normal-phase (NP) columns, such as in hydrophilic interaction chromatography (HILIC), are used to separate highly polar species (sugars, amino acids, vitamins, carboxylic acids, and nucleotides). Both RP and NP can be used for the separation of lipids, however with RPLC, the compounds are separated based on hydrophobicity, and it is often used over NPLC to avoid co-elution of molecular species from the same class (Nie *et al.*, 2010). Applied RP chromatographic gradients begin with a high aqueous content mobile phase, while the stationary phase consists of an organic non-polar material. NP chemistries use a hydrophilic (polar) stationary phase, and therefore the hydrophilic molecules in the mobile phase tend to adsorb to the column, while the hydrophobic (non-polar) molecules elute first. By increasing the polarity of the mobile phase, the less polar molecules are then eluted.

Current metabolomics investigations are generally categorised into untargeted or targeted approaches. Untargeted methods are used for global analysis of metabolic changes, and for hypothesis generation. This method allows for candidate markers to be tentatively identified, by consulting online databases such as the human metabolome database (HMDB) and Chemspider, and using the accurate mass after confirmation of peaks by means of the ion *m/z* ratio and RT (Want *et al.*, 2013). This list is often still extensive, and the raw data still needs to be consulted to assess whether the *m/z* of interest corresponds to the molecule-ion, adduct, or fragment of a molecule. Additionally, without a synthetic standard, the identification remains somewhat speculative. Targeted approaches focus on specific metabolites, groups of metabolites, or a class of compounds,

and often follow untargeted methods for identification and quantification of metabolites relevant to metabolic changes. Targeted methods can help to reduce sample datasets, and increase the confidence in the tentative metabolite identification gleaned from untargeted methods. Tandem mass spectrometry (MS/MS or MS^2) is of particular importance in metabolite identification. The formation of characteristic product ions and/or specific neutral losses can provide structural information, aiding in potential identification of unknown compounds as it provides a characteristic fingerprint for different metabolites, even if these metabolites have the same elemental formula. For targeted analysis, MS/MS coupled to UPLC is required to collect structural information via fragmentation data. MS/MS provides an improved signal-to-noise ratio compared to single-stage mass spectrometry (Want *et al.*, 2010). Another advantage of MS/MS is that structural elucidation can be performed without switching to additional instruments. Using the first MS (MS1) in the series as a scanning device, precursor ions can be selected for fragmentation, using a type of ion dissociation method. Product ion spectra, with high-mass resolution for fragment ions, can then be produced using the second MS (MS2) (Dettmer *et al.*, 2007). One of the most common methods of ion dissociation is collision induced dissociation (CID), which occurs in a cell between the MS1 and the MS2 *m/z* analysers. The wide dynamic range of MS/MS allows both high- and low-abundance molecules and their metabolites to be identified in a single run.

In this study an ESI/MS coupled to UPLC was utilised for untargeted analysis, or global profiling, while a Tribrid mass spectrometer, combining quadrupole, ion trap, and Orbitrap mass analysis, coupled to UPLC was utilised for targeted analysis (MS/MS).

In the previous chapter it was shown that ^{1}H NMR was unable to differentiate subclinical cows from other groups of cows after being dosed with sporidesmin, and was not able to identify early stage markers of sporidesmin challenge. Additionally, analysis of urine, and milk samples was not particularly useful for identification of subclinical cows. In theory, UPLC/MS with its greater sensitivity should generate more information leading to separation of groups using metabolites in serum. Therefore the aims here were to:

5.1.1 Aim

To discover a potential metabolic biomarker of sporidesmin challenge in cows, which can be used to identify cows at all stages of disease (i.e. subclinical or clinical), prior to changes in liver enzyme activities, phytoporphyrin concentrations, and the presentation of clinical signs.

5.1.2 Objectives

- Use UPLC/ESI-MS to determine if the cow groups could be differentiated from one another, and more specifically, identify differences in subclinicals and/or non-responders following a dose of sporidesmin.
- Use tandem MS to tentatively identify the metabolites (potential biomarkers) that were recognised as significantly changing in clinical, subclinical, and/or non-responder cows after the single dose of sporidesmin

5.2 Materials and methods

5.2.1 Standards and reagents

Ultrapure water was obtained from a Milli-Q® system (Millipore, Bedford, MA, USA) at AgResearch, Palmerston North, NZ. Acetonitrile (ACN), methanol, and chloroform, of optima LC-MS grade, were purchased from Thermo Fisher Scientific (Auckland, NZ). Ammonium formate was purchased from Sigma-Aldrich Chemicals Co. (St Louis, MO, USA).

5.2.2 Loadings tests

Loadings tests were carried out using UPLC connected to an ion trap MS (Thermo Fisher Scientific, Waltham, MA, USA) to determine the best analytical method to use. For this, a pooled sample was prepared, which contained 10 µL each of all serum samples collected during the sporidesmin challenge. The solutions for the loadings tests were prepared as follows, using ice-cold (-20 °C) ACN to precipitate the proteins:

1. 5 µL serum + 20µL ACN
2. 10 µL serum + 40µL ACN
3. 20 µL serum + 80µL ACN
4. 50 µL serum + 200µL ACN
5. 80 µL serum + 320µL ACN
6. 100 µL serum + 400µL ACN

Each of these was mixed and left for 15 min at room temperature before centrifugation for 10 minutes at 13,000 rpm (Heraeus sepatech Biofuge A, Thermo Scientific). The resulting supernatant was diluted with analytical grade H_2O to a total volume of 500 µL, and a 200 µL aliquot of each dilution was used for loadings tests.

The UPLC system consisted of an Accela 1250 quaternary UPLC pump, a PAL autosampler fitted with a 15,000 psi injection valve (CTC Analytics AG., Zwingen, Switzerland), a 20 µl injection loop, and a Q Exactive Orbitrap mass spectrometer with electrospray ionisation source (Thermo Fisher Scientific, Waltham, MA, USA). The samples were cooled in the autosampler at 4 °C, and 10 µL was injected on the column which was held at 25 °C, using a flow rate of 250 µL/min. The gradient elution programme consisted of 1 minute of 100 % aqueous 0.1 % formic acid solution and H_2O as a wash, then varying concentrations of acetonitrile : formic acid (99.9 : 0.1, *v:v*) mixture up to 99 % at 10 minutes. The column was held there for 3 minutes, then returned back to the original concentration, and allowed to equilibrate for a further 4 minutes, as a wash cycle, before the next sample injection. Looking at the chromatograms, it was concluded that 50 µL of serum produced the best spectra, with the presence of a high number of peaks, good peak intensities, and high signal to noise ratio. Subsequently, all serum samples were prepared using 50 µL of serum, 200 µL of ACN, and H_2O to a final volume of 500 µL.

A pooled sample, like that used for the loadings test, was used as a repeat sample to be run within each batch run, alongside a water blank, thereby providing quality control. For this pooled sample, correspondingly higher volumes of extraction solvents, as described in *section 5.2.3*, were used to prepare the sample for analysis. The pooled sample was run every 10 samples during all measurements, to be used as a reference sample.

5.2.3 Sample preparation

All serum samples from the sporidesmin challenge trial were used for MS analysis. Details of the sampling procedures are given in *section 2.2.4*. The serum was removed from the -80 °C freezer on the morning of sample analysis, and placed in test tube holders over ice to thaw (~ one hour ± 30 minutes). All sample preparation was carried out at AgResearch, Palmerston North.

5.2.3.1 Serum preparation for C18 and HILIC analysis

Thawed serum samples were mixed briefly by inverting. 50 µL aliquots were transferred to Eppendorf vials, and 220 µL of ice cold ACN (kept at – 25 ^{o}C) was added to each serum aliquot. The samples were mixed (30 s vortex), left to extract for 15 minutes and then spun down at 13,000 rpm for 10 minutes at room temperature using a bench top mini centrifuge (Heraeus sepatech Biofuge A). The supernatant was aliquoted into labelled Eppendorf vials, adding analytical grade water (~ 250 µL) for dilution, resulting in a total volume of ~ 500 µL. The dilution required was determined

during loadings tests (described in *5.2.2*). The combined samples were mixed briefly (10 s vortex) and 200 µL was used for analysis by UPLC coupled to a high resolution Q Exactive Orbitrap mass spectrometer (Thermo Fisher Scientific, Waltham, MA, USA).

5.2.3.2 Serum preparation for lipid analysis

A chloroform ($CHCl_3$) : methanol (CH_3OH) solvent mixture (2:1, v/v) was used to extract lipids from the serum. 50 µL of the serum sample was mixed with 200 µL of the extraction solvent mixture, followed by a brief mixing (30 s vortex), and 15 minutes extraction at room temperature prior to down-spinning at 13,000 rpm for 10 minutes. The solution separated into 3 layers - two liquid and one solid - the top layer being an aqueous liquid containing methanol, water, salts, and sugars, a solid disc of proteins and cell debris in the interphase, and the bottom layer being organic liquid containing dissolved lipids and chloroform (Folch *et al.*, 1957). The top layer was discarded, the disc removed, and the lower layer was transferred to amber vials for ultra performance liquid chromatography electrospray ionisation Orbitrap mass spectrometry (UPLC/ESI-MS).

5.2.4 Ultra performance liquid chromatography electrospray ionisation Orbitrap mass spectrometry (UPLC/ (-) and (+) ESI-MS)

The serum samples were analysed by UPLC/ESI-MS analysis, both in negative (-) and positive (+) modes.

5.2.4.1 Reversed phase chromatography

The analyses of both polar and non-polar species were performed using a C18 reversed phase column (RRHD SB-C18 column, 2.1 mm x 150 mm, 1.8 µm diameter size, Agilent) based on the work by Fraser *et al.* (2013). The UPLC system and Q Exactive Orbitrap mass spectrometer used here is described in section 5.2.2.

The samples were cooled in the autosampler at 4 °C, and 2 µL of each was injected on the column which was held at 25 °C, using a flow rate of 400 µL/min, and the gradient elution programme as described in Fraser *et al.* (2013). The mobile phases consisted of an aqueous 0.1 % formic acid solution (solvent A) and an acetonitrile : formic acid (99.9 : 0.1, *v:v*) mixture (solvent B). Solvent B was held at 5 % from 0 – 0.5 min, 5 – 99 % from 0.5 to 13 min, 99 % from 13 to 15 min, and returned to 5 % from 15 to 16 min and allowed to equilibrate for a further 4 minutes prior to the next injection. Mass spectral data were collected using a mass range of *m/z* 60 – 1200, a resolving power

of 25,000, and a maximum trap fill-time of 100 ms. The samples were run in both positive and negative ionisation modes separately.

5.2.4.2 Hydrophilic interaction chromatography

Small and very polar compounds were analysed by hydrophilic interaction chromatography using a Merck polymeric bead-based ZIC-pHILIC column (SeQuant, 2.1 x 100 mm, 5 µm particle size). The analytical methods and operating conditions for the mass spectrometer were based on work by Fraser *et al.* (2012). The separation was performed at 25 °C, using a flow rate of 250 µl/min, and the gradient elution program as described in Fraser *et* al., (2012). The mobile phases consisted of acetonitrile with 0.1 % formic acid (solvent A), and water : ammonium formate (16 mM, pH 6.3) (solvent B). The gradient elution programme involved solvent A being held at 97 % from 0 to 1 min, 97 – 70 % between 1 and 12 min, 70 – 10 % between 12 and 14.5 min, held at 10 % for 2.5 min, then returned to 97 % for 1.5 min, and allowed to equilibrate for a further 5.5 min before the next injection.

The data were collected in profile data acquisition mode over a mass range of *m/z* 55 - 1100 at a mass resolution setting of 25,000 with a maximum trap fill time of 100 ms.

5.2.4.3 Lipid analysis

The extracted lipids from the serum samples were analysed using a Thermo C1 column (2 mm x 50 mm, 5 µm particle size) in an HPLC system. A Thermo Scientific Finnigan LTQ was used for mass spectrometric detection. The samples were cooled at 4 °C in the auto sampler and an injection volume of 2 µl was used. The mobile phases consisted of an aqueous 0.1 % formic acid solution (solvent A) and a 1:1 mixture of acetonitrile: *iso*-propanol with 0.1 % formic acid (solvent B).

5.2.5 Tandem mass spectrometry coupled to liquid chromatography

These experiments were carried out at the Danish Technical University, Lyngby, Denmark.

5.2.5.1 Serum sample preparation

Pooled serum samples were prepared by combining 100 µL of sera from three clinical cows, numbers 282, 317, and 440, each of which was collected on the date 04.05.2011 (Day 16). 10 ng of the internal standards 2-amino-5-fluorobenzoic acid (MW 155) and AUDA (12-

[[(tricyclo[3.3.1.13,7]dec-1-ylamino)carbonyl]amino]-dodecanoic acid) (MW 392) were added, both of which were obtained from Sigma-Aldrich (St. Louis, MO, USA) with purities of 97 % and 98 %, respectively. The liquid-liquid extraction for metabolites was carried out by adding 1.2 mL acetonitrile (LC/MS grade, Sigma-Aldrich) to the combined sera, followed by vigorous shaking using a vortex machine (Vortex Genie 2, Scientific Industries, Bohemia, NY, USA). The solution was then centrifuged for 10 min at 4 °C applying 12,000 rpm (Fresco 17 Centrifuge, Thermo Scientific, Waltham, MA, USA). The supernatant was collected and dried in a centrifugal evaporator (Savant SC210A SpeedVac, Thermo Scientific). The dried residue was reconstituted in 100 µL of 50:50 (v/v) acetonitrile:water containing 0.1 % formic acid.

5.2.5.2 Analysis

The serum samples were analysed using a Dionex Ultimate 3000 UPLC system (Thermo Scientific), consisting of a pump, a column compartment which was set to 30 °C, and an auto sampler that was held at 10 °C. The chromatographic separation was carried out using two identical Acquity UPLC high strength silica (HSS) T3 columns connected in series to enhance separation. The columns had a particle size of 1.8 µm, and dimensions of 2.1 x 100 mm (Waters Corporation, Milford, MA, USA).

The mobile phases were (A) water with 0.1 % formic acid, and (B) acetonitrile with 0.1 % formic acid. A 20 min gradient was applied as follows: (B) was kept at 5 % for 1 minute, increased to 95 % up to 12 min, and kept at this ratio for 3 min. The reconditioning of the column back to 5 % (B) occurred over 5 min. The sample was injected using a volume of 1 µL at a flow rate of 350 µL min^{-1}. The eluant from the first 0.5 min was diverted to waste.

An Orbitrap Fusion Tribrid mass spectrometer (Thermo Scientific) was used as the mass analyser, and was operated in both negative and positive ionisation mode. The experimental conditions were: sheath gas flow (N_2), 42 arbitrary units; auxillary gas flow (N_2), 12 arbitrary units; sweep gas (N_2), 1 arbitrary unit; ion source voltage 3.5 kV (positive mode) or -2.5 kV (negative mode); and ion transfer tube temperature 338 °C. The mass spectrometer was operated in both full scan mode and data-dependent MS^2 fragmentation mode. The *m/z* range between 150 - 2000 was acquired in the full scan mode using the ion trap with a S-lens RF level of 60 %, and a maximum injection time of 100 ms. An isolation width of 1 *m/z* unit was chosen for the quadrupole mass analyser in the targeted MS^2 scan mode, and the most intensive 20 ions were subjected to CID. A normalised collision energy of 35 % was applied, and the formed product ions were detected by the Orbitrap, the resolution of which was set to 30,000, and the scan range was *m/z* 50 - 1000.

5.2.6 Data extraction and statistical analysis

The eluants in the first 1.5 min and during the last 5 min of the HILIC and lipid runs were considered as waste; the remaining data were extracted and aligned. A similar procedure was performed for the components eluting between 3 and 14 min from the C18 column using in-house proprietary software developed by AgResearch. The resulting peak-area matrix data was normalised against the average of all peak areas to remove any effects from batches or run-orders, as well as to correct for artefacts from the peak detection, using a number of statistical packages as well as the in-house proprietary software.

Raw data was subjected to a peak detection process using PhenoAnalyzer (SpectralWorks Ltd, Manchester, UK) with key parameter settings described previously (Fraser *et al.*, 2014). The resulting peak data matrices were noisy, and necessitated implementation of a series of quality control filtering techniques before statistical analyses could be conducted. These filtering steps included:

1) missing value treatment: the peaks missing in > 90 % of the samples were removed. Any other missing values were replaced by half of the minimum of the non-missing values of that peak.

2) peak de-isotoping and merging: based on criteria that a series of ions, for example for the positive ionisation [M+H], [M+H]+1, [M+H]+2, must be (a) eluting at the same retention time (RT) with ± 0.1 min, (b) within ± 1.005 *m/z* error zone, (c) their peak intensities are highly correlated among samples (Pearsons correlation coefficient > 0.9), and (d) with a measured peak intensity ratio [M]/[M + H]+1 > 2.0, and [M+H]+1/[M+H]+2 > 2.0 (if peak [M+H]+2 is present, 2.0 is only an emipirical threshold). Only the monoisotopic ion [M] of the series was retained for further quality control analysis.

3) run-order correction within each batch was normalized using linear regression (Koulman *et al.*, 2007). This was to account for changes in the instrument response across batches.

4) batch effect was corrected using a parametric empirical Bayes methods (Johnson *et al.*, 2007), and, thereafter, the peaks still showing significant batch effect (F-test, p-values < 0.05) were removed. Peak annotation processes were not relevant for this analysis.

The data were log transformed prior to any multivariate analyses as it did not follow a normal distribution. PCA analyses on raw peak area data showed large variations within and between batches. Re-doing the analysis using the normalised (log transformed) data showed that the normalisation procedure improved the clustering of these features.

After the pre-processing, a total of 450 *m/z*_RT pairs were detected within the (-) ESI chromatograms and 1278 *m/z*_RT pairs in the (+) ESI chromatograms. These pairs were used to create data matrices of peak areas of target 'features' for all samples for each ionisation mode. The matrix tables were produced with the predictor variables (*m/z*_RT values) in the *X*-block and the response variables (group, day, dosing) in the *Y*-block. The resulting matrices were then analysed using SIMCA (Version 13.0.2.0, Umetrics AB) and RStudio statistical software (Version 0.97.449, RStudio, Boston, MA, USA). Initially the data were reduced using principal component analysis (PCA), then further analysis by partial least squares discriminate analysis (PLS-DA), and orthogonal PLS-DA (OPLS-DA). A brief summary of the processes are given below; see *sections 4.2.4* and *4.2.5* for detail descriptions of the multivariate statistics and time series methods.

Hotellings T^2 plots, from initial PCA modelling, were used to identify any outliers in the data. The T^2 critical (99 %) line represents the 99 % tolerance for the data in each model. A T^2 critical line, based on a 95 % tolerance is also represented in the scores plot as the ellipse surrounding most samples (Wheelock & Wheelock, 2013). Any observations situated outside this ellipse or outside the T^2 critical line are outliers. These observations were checked for their sample ID, and the raw spectra were examined to try and identify a reason for this. Not all samples outside the T^2 tolerances were excluded from further analysis, as these may symbolise significant changes associated with the degree of effect of a sporidesmin challenge. Rather, observations were excluded from further analysis when the spectra showed poorly resolved peaks, low signal to noise ratio, and/or a failed injection. PLS-DA and OPLS-DA models were then produced using defined classes to aid in separation of the data based on specific observations. For example, samples were classed by those measured before dosing (Days -14 – 0) compared to those measured after dosing (Days 7 - 42).

RStudio was then used to produce time series analyses. For the time series analyses, plots were produced showing the *m/z*_RT pair intensity versus time curves for each cow, to compare the time profiles across the sample population. The time profile of each *m/z*_RT pair was extracted for each cow, and this was used to calculate the average time profile for the groups to which they belonged. If necessary, missing time points were substituted by linear interpolation for internal points, and replicating of the nearest data for missing end points. This information was then used to see which *m/z*_RT pairs showed large differences in the shape of the time curves when comparing groups, while taking into account how much variation there was between cows within each group. A p-value and SDA-rank were produced for each of these, combined, and then ranked to identify which variables contributed the most to difference between the samples over time. The p-values were not corrected for multiple testing and therefore were only used to rank the peaks.

5.2.7 Interpretation of multivariate statistical analysis results

Brief explanations of the methods of interpretation are given here. For detailed explanations of the multivariate analyses (MVA) and time series interpretation procedures see *Section 4.2.5*.

For the MVA models produced in SIMCA, a combination of OPLS-DA scores plots, loadings scatter plots, loadings column plots, and S-plots using variable influence of projection cross validation (VIPcv) colouring were used to visualise the new, reduced, coordinates for the study observations, and to identify variables of interest which were reliable for any class separation identified. Lists of the *m/z* and RT of likely candidates for the separation of classes were produced from this analysis, and used for data interpretation.

Loadings scatter plots gave a graphical summary of the clustering in the scores plots, and each *m/z*_RT pair was represented as a new point in the loadings plot. These points related directly to the orientation of the scores in the scores plot. Those variables located distally on the *X*-axis were important for between class separations, while those located distally on the *Y*-axis contributed to within class variance. Loadings columns plots were displayed with the loadings column vector on the *Y*-axis and the variables on the *X*-axis. With a loadings column plot, jack-knifing was used to estimate the bias and standard errors of each column (variable), and was displayed as error bars at the end of each column. Columns where the jack-knifed confidence interval included or was close to zero were considered to have low reliability for class separation, and were excluded from further analysis in the present study. The S-plot is a scatter plot of the OPLS-DA predictive component loading that combined both the covariance (p[1]) and the correlation (p(corr)[1]) structure between the *X*-variables and the predictive score (t[1]) (Wiklund *et al.*, 2008). These two vectors produced an S-shape when plotted. The variables situated far out on the wings of the S-plot combined high model influence with high reliability and were of relevance to the class separation. A high p(corr)[1] means the variable has a high reliability for class separation. VIPcv colouring was used in loadings and S-plots to summarise the importance of each variable in driving the class separation. A standard score of > 1 is often used to imply a greater than average contribution to the model, but the higher the VIP score, the more significant the contribution to class separation. This cutoff (> 1) often still resulted in up to 50 % of the variables being selected as important (Wheelock & Wheelock, 2013).

All of these techniques only have general rules when determining which variables are significant and relevant to class separation, and 'cut-offs' appear to vary in the literature based on the type of data used. Therefore, a combination of all of these visualisation techniques is required to ensure reliability. In the present study, a VIPcv score of > 1, a p(corr)[1] generally > 0.4 - 0.5, and loadings

columns with jack-knifed confidence intervals not crossing the origin, were used as the 'cutoff' points for relevant variable selection.

For the time series analyses, the p-values and SDA rankings were used to help determine which molecule ions are likely to show a difference between the groups and which ions are not. Due to the large dataset, the p-values were initially used to reduce the dataset, namely, all those with a value > 0.05 were excluded from further analysis. All remaining plots were examined to identify which groups (control, non-responder, subclinical, or clinical) were responsible for the difference in each significant *m/z*_RT over the trial period. Additionally, the stage at which this difference was seen, i.e. an increase in the intensity of the compound recorded, was also examined, to determine whether changes occurred pre- or post-dosing, and if the changes coincided with increased GGT and GDH activities reported in *Chapter 2*.

Once the important variables (*m/z*_RT pairs) were identified, for both the MVA models and the time series models, the raw spectra were examined to identify whether these variables related to 'true' peaks, rather than noise, were well resolved, and had high signal to noise ratios (S/N > 3). Once the peaks fulfilled the criteria, a combination of metabolite databases, such as HMDB (Wishart *et al.*, 2013) and literature, such as research by Allen *et al.* (2011) and Griffiths and Sjovall (2010), were used to tentatively identify metabolites corresponding to the peaks.

5.3 Results

An initial inspection of the base peak chromatograms demonstrated that the separation using C18 (+/-) RP chromatography derived relatively well-resolved peaks with low levels of noise (*Figure 5.1 a*). However, some of the peaks showed tailing, which could have been caused by several effects, for example, additional retention mechanisms related to residual silanol group interactions.

The HILIC (+/-) derived chromatograms resulted in poor peak resolution and high levels of noise (*Figure 5.1 b*). With the lipid (+/-) samples, it was obvious that there were many failed injections, inadequate peak resolution, and poor peak separation (*Figure 5.1 c*). Therefore, only the results from the C18 column were focused on for further analyses. The RP column data should contain, in theory, all the information from the HILIC and lipid columns. The RP column is suitable for a wide range of polar and non-polar compounds. For global profiling and a first screening of the samples RP columns are acceptable.

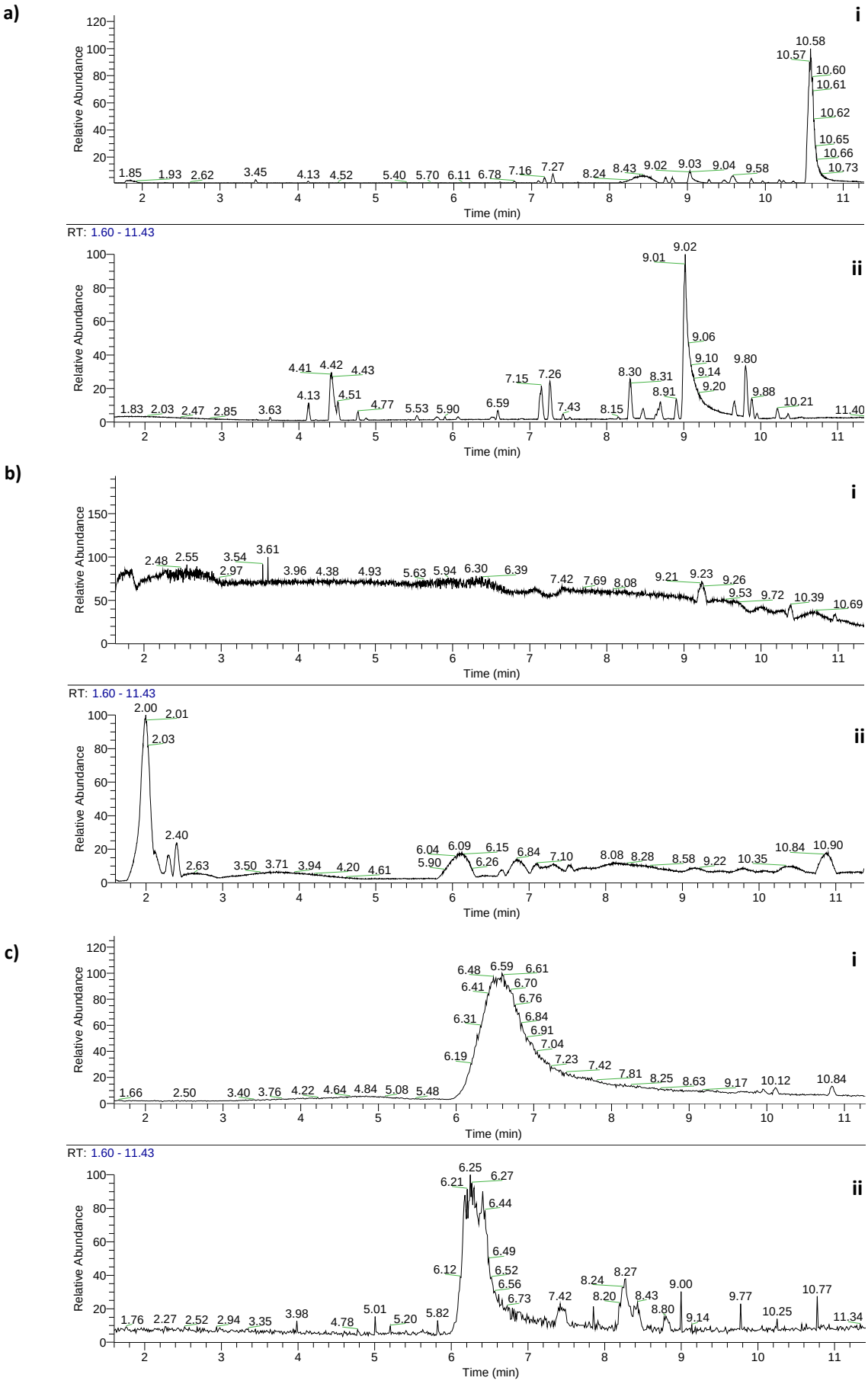

Figure 5.1 Base peak chromatograms of serum samples separated by ***a)*** C18 reversed phase chromatograpy; ***b)*** HILIC; and ***c)*** C1 column, detected in **i.** positive and **ii.** negative mode by Orbitrap mass spectrometry, respectively.

HILIC would be more applicable if some idea of the specific highly polar compounds involved in sporidesmin toxication was known, and that these known compounds may not be well resolved or detected at all using RP chromatography. Additionally, using lipid chromatography to screen for a whole range of lipids is relatively new. Carry-over effects from samples retained in the column from a previous sample, and non-reproducible results are common. Using the latter, would require much more analytical work, such as sample preparation and method optimisation. Unfortunately the timeline of these studies did not allow for this. In theory, the C18 RP column should give a useful overview for untargeted analysis of serum here.

5.3.1 Non-targeted analysis of serum samples using multivariate statistics

Mass to charge ratio / retention time pairs detected were used to generate matrices of features and peak areas for each ionisation mode. The peak areas for each feature were normalised against the average of all the peak areas to account for changes in instrument response across the batches. The data were $\log_e$ transformed prior to any multivariate analyses as they did not follow a normal distribution. PCA analyses on raw peak area data showed large variation within and between batches. Re-analysis using the normalised ($\log_e$ transformed) data shows that the normalisation procedure improved the clustering of these features. Zero values were replaced with a value of half the lowest measured value in the data. Following pre-treatment, for the C18 analyses, there were 450 *m/z* retention time pairs detected within the (-) ESI mode and 1278 *m/*z retention time pairs in the (+) ESI mode.

Hotellings T^2 plots, from PCA analyses, were used to identify any outliers (T^2 crit > 99%) in the data. Initial PCA and Hotellings plots of the C18 negative dataset, using no scaling, identified eighteen spectra above the 99% T^2 crit line; these were considered to be noise in the raw spectra and were excluded from further analysis (*Figure 5.2 a*; see *Appendix 7* for a list of exclusions).

The Hotellings T^2 plot of the C18 positive dataset identified 29 outliers (T^2 crit > 99%; *Appendix 8*). These outliers were excluded, and the dataset re-analysed. The Hotellings T^2 of this dataset still identified a large number of outliers (*Figure 5.2 b*), however when quality control checks of PCA and PLS-DA were carried out on datasets with 31 and 53 exclusions, no differences could be found in the clustering or pattern of the data, nor the points in the loadings. Therefore, the dataset with 31 exclusions was used, for the final dataset, utilising a larger number of samples (*Figure 5.2 b*). *Figure 5.3* shows the PCA scores plot for principle components 1 and 2 for the (-) ESI (*5.3* a) and (+) ESI (*5.3 b*) data, following exclusions, and using no scaling.

Additionally, the effects of normalisation were investigated on both ionisation modes. The data were normalised using Pareto scaling, Pareto scaling without data centering, and univariate scaling. Different normalisation methods emphasise distinct features of the data, for example Pareto scaling reduces the influence of intense peaks while emphasising the weaker peaks that may have more biological relevance (Craig *et al.*, 2006; Wiklund *et al.*, 2008; Worley & Powers, 2013). For this, Pareto scaling is often the method of choice for biological datatsets (Worley & Powers, 2013). Analyses were also carried out using no scaling for comparison. PCA was used to monitor the effect of each transformation. The scaling methods generally improved clustering in the data, however, no clear grouping relevant to the trial could be identified using PCA. This was probably related to the time component in the dataset, as well as the large number of variables. Medium and small features are important in these analyses and therefore Pareto scaling was chosen as the preferred scaling method.

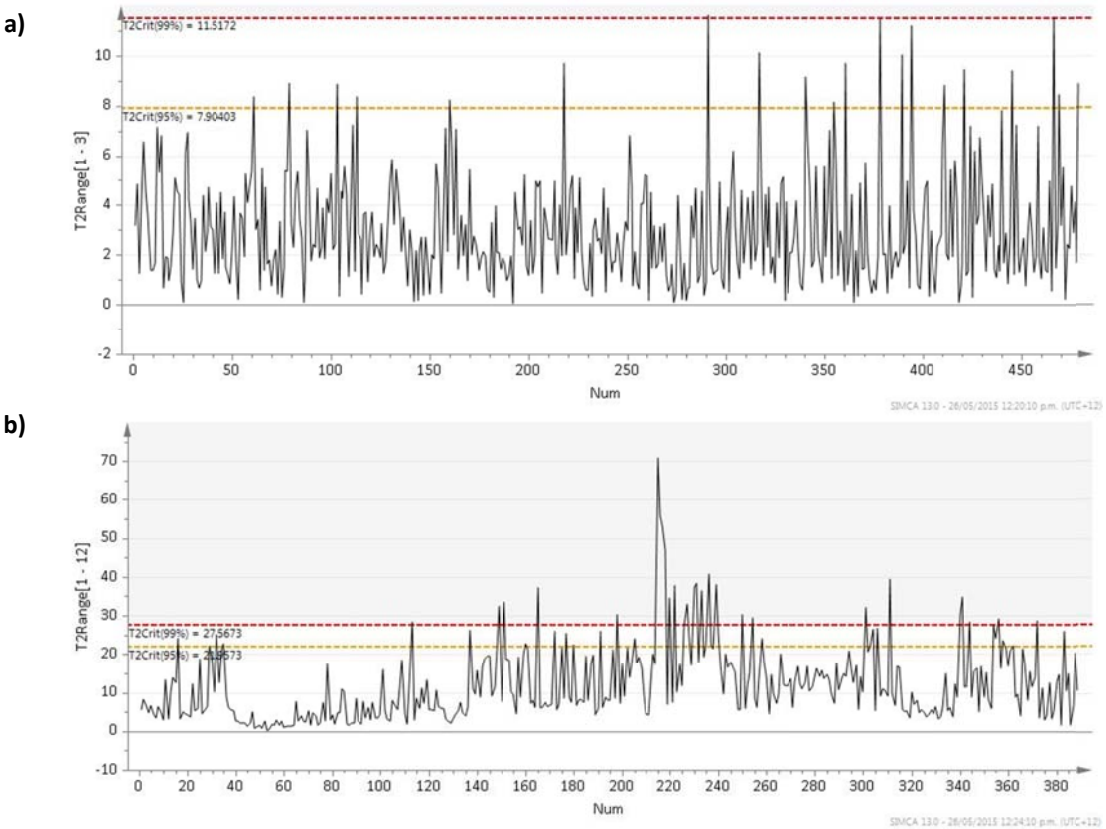

Figure 5.2 Hotellings T^2 of LC-MS C18 column data, after exclusions (T^2 crit > 99%); ***a)*** C18 / (-) ESI MS analysis excluding 18 outliers; ***b)*** C18 / (+) ESI analysis excluding 29 outliers.

Using scaling methods with the negative ionisation data generally identified more outliers. However, these were mainly from one cow (cow 282), a clinically affected animal, and were from sample days following dosing. It may be that this cow showed severe affects of dosing and therefore

these samples were retained in the dataset. The positive ionisation data identified two groups separating on the horizontal plane, however, with further analysis, no connection to the trial (i.e. day effect, dose effect), nor effect of experimental process (i.e. batch or sample run-order effect) could be found to be causing this.

No differences were identified between the groups during the control weeks, nor between control cows over the trial period. Additionally, no differences could be observed between the control cows, and the non-responders or the subclinicals, for C18 (+) and (–) ionisation datasets.

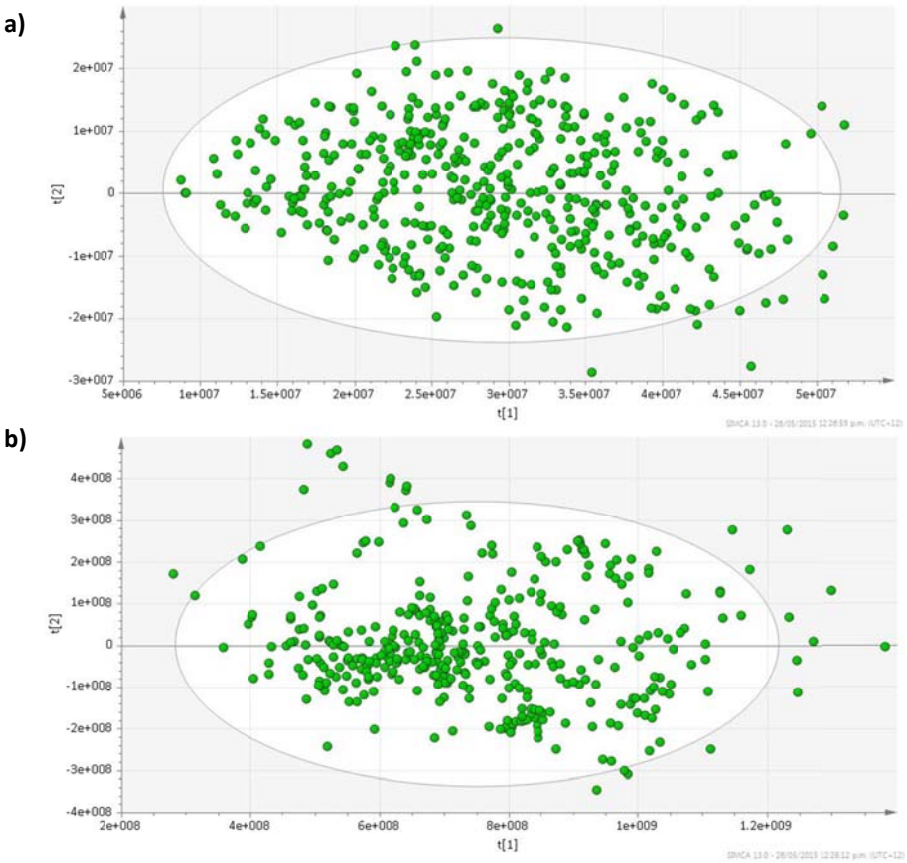

Figure 5.3 Principal component analysis scores derived from UPLC/MS analysis using the C18 reversed phase column in ***(a)*** (-) ESI and ***(b)*** (+) ESI mode, after exclusion of outliers and no scaling application.

Both of the datasets showed significant differences (C18 (+) $p = 4.63 \times 10^{-9}$, C18 (-) $p = 1.88 \times 10^{-28}$) between clinical cattle after dosing and all other animal groups, including control days, (*Figure 5.4 and 5.5*), with the clinical cattle moving directionally away from the other groups following time-trend after sporidesmin dosing, and returning towards the other animal groups in the later weeks of the trial.

The PLS-DA models were validated, with a difference between the goodness of fit (R^2 0.298 and 0.335) and the predictive ability (Q^2 0.201 and 0.249) of 0.097 and 0.086 for the C18 (+) and (-),

respectively. The R^2/Q^2 values were themselves low, and not considered reliable indicators by SIMCA definition; however, because of the nature of large metabolomic datasets of biological origin, and the closeness of these two attributes to each other, these models were accepted (Worley & Powers, 2013). In the scores plots (*Figure 5.4 a and 5.5 a*), those samples sitting outside the grey ellipse (95 % confidence interval), are often considered to be outliers, but here are related to weeks 4, 5, and 6 of the trial, Days 7, 9, 11, 14, 16, and 21 – the latter being closer to zero on the *X*-axis, representing a return to likeness of the other samples, which relate to one, two, and three weeks after dosing. These were the weeks where the cattle had their highest GGT and GDH activities and started showing clinical signs (*see section 2.3.4*). This pattern is expected with disease progression. Furthermore, most of the individual clinical cows appeared to cluster together, whereas cow 282 differentiated the most from all, and were seen to orientate in the bottom right of the OPLS-DA plot (blue ellipse, *Figure 5.4* and *5.5*).

A similar pattern was also seen in the NMR analysis, when samples were classed by the clinical group, except two samples from cow 317 that sat outside the ellipse in the scores plot. The samples for both cows, in the NMR analysis, related to days 14, 21, and 28 after dosing.

The S-plot combined with VIPcv colouring (VIPcv > 1) (*Figure 5.4 b* and *5.5 b*) indicated 34 *m/z*_RT pairs for C18 (-) and 178 pairs for C18 (+) which were relevant to class separation. However, this value only implied that these variables contributed more than average to the class differentiation. The loadings column plots, excluding all variables with a VIPcv > 1, were used as a complementary parameter to determine reliable peaks for class separation. From these, the C18 (-) dataset had 12 peaks with jack-knifed confidence intervals that included zero, and were excluded. Of the remaining 22 peaks, 17 of these showed an up-regulation in the clinical group after dosing, however three of these had a p(corr)[1] < 0.4 and were not considered to be reliable for class identification. The other five peaks were down-regulated and had a p(corr)[1] < - 0.2, so were also excluded from further analysis. Therefore, a total of 14 up-regulated peaks were identified as being relevant to class separation for the C18 (-) dataset. From these, the ions at *m/*z 464.3017 at 7.57 min, 448.3074 at 9.08 min, 465.3047 at 7.57 min, and 449.3105 at 9.08 min contributed heavily to the differentiation between the classes on the *X*-axis. The latter two were identified as isotopes of the former two and were not looked into any further. The former two ions were observed as the most important in the differentiation of clinical cows from all others after dosing, with considerably higher peak areas in the first two weeks after dosing, than in all other samples.

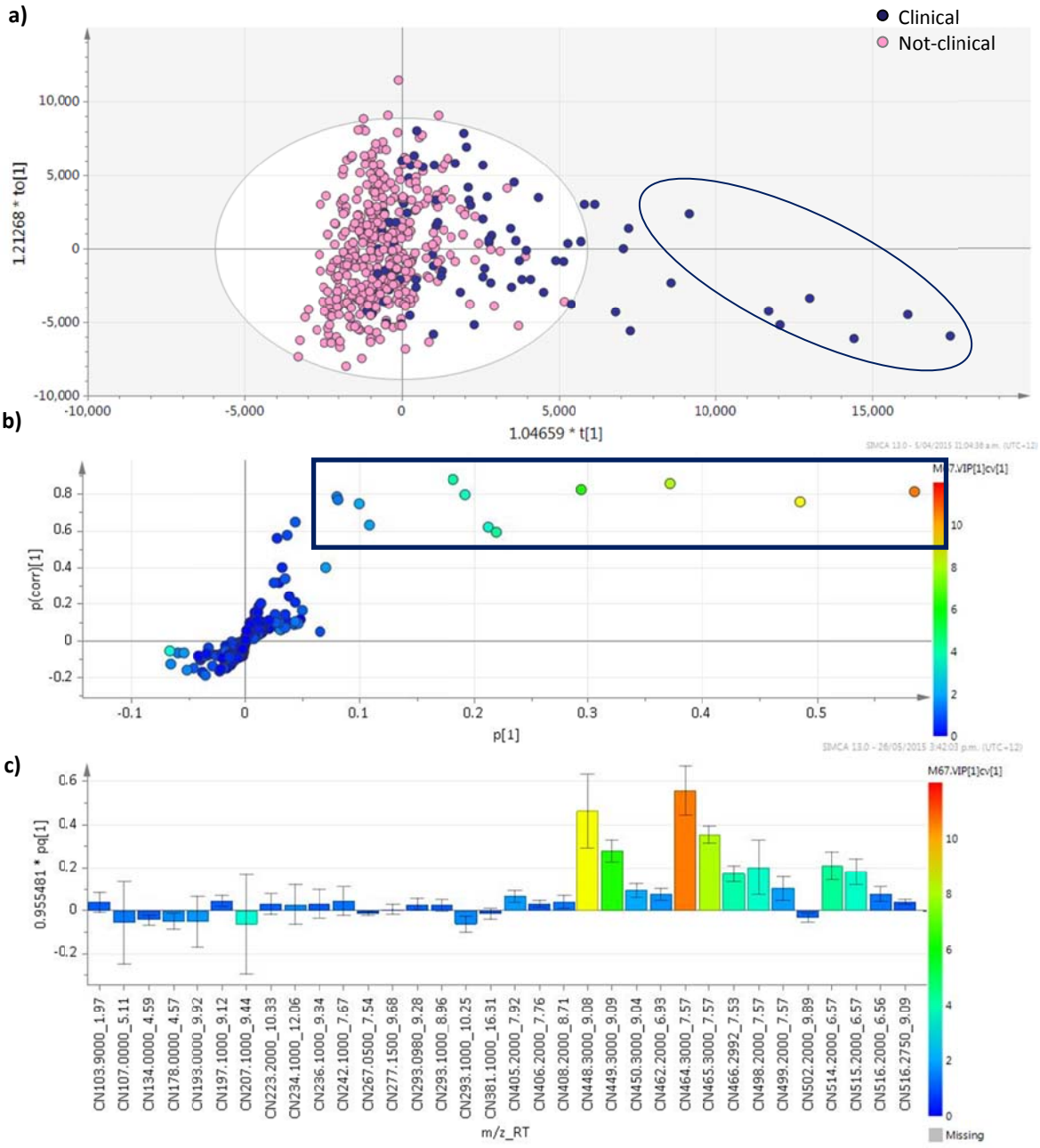

Figure 5.4 Orthogonal partial least squares discriminant analysis (OPLS-DA) of C18 (-) derived data, classed by clinical cows (all days) versus all other cows, using Pareto scaling (R^2Ycum 0.150, R^2Ycum 0.335, Q^2cum 0.249); ***a)*** Scores plot coloured by classes. Cow 282 clustering is shown by the ellipse; ***b)*** S-plot, coloured by VIPcv (box = p(corr)[1] > 0.5; VIPcv > 1); and ***c)*** loadings column plot showing all those with a VIPcv > 1.

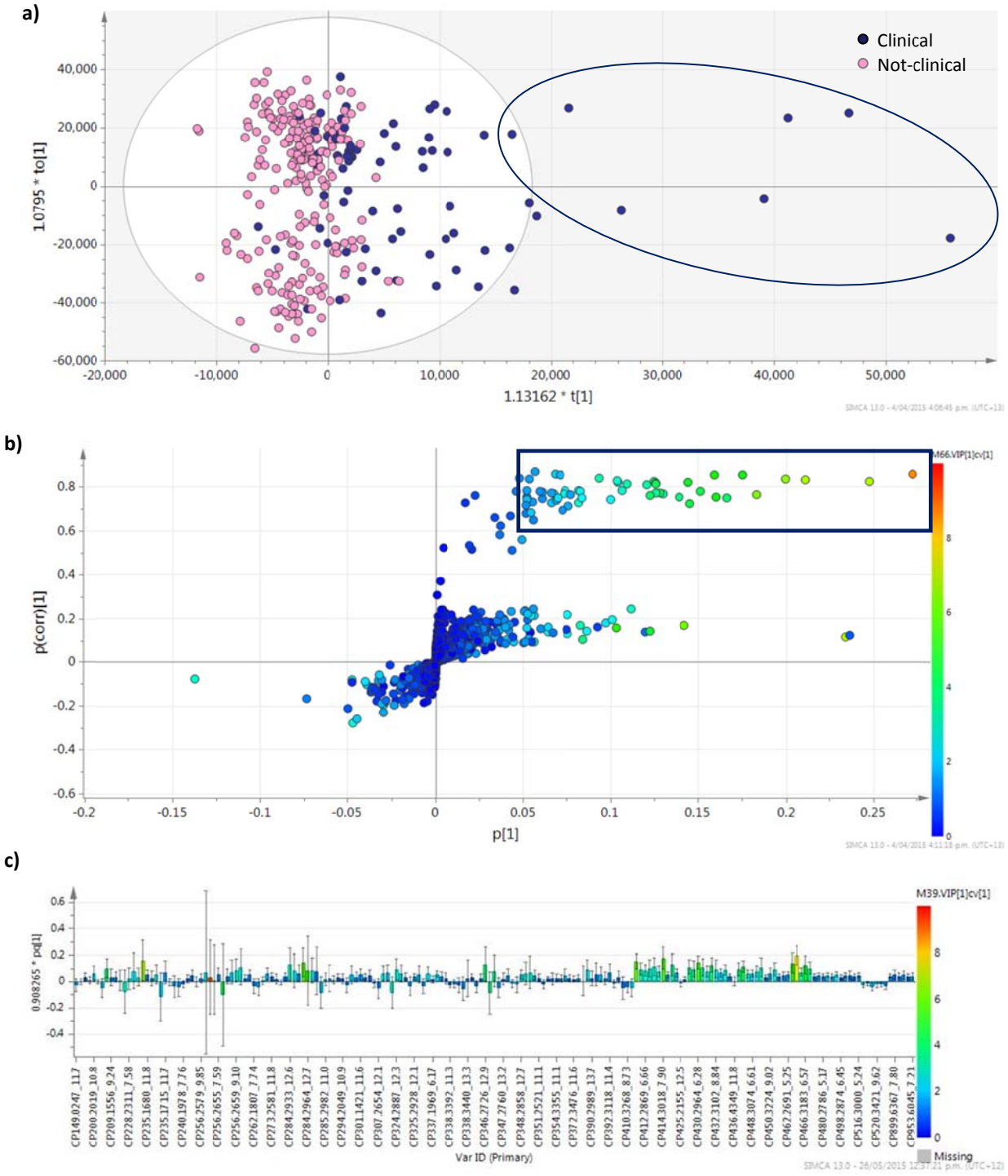

Figure 5.5 Orthogonal partial least squares discriminant analysis (OPLS-DA) of C18 (+) derived data, classed by the clinical cow group, after dosing, versus all other cows and control days, using Pareto scaling (R^2Ycum 0.333, R^2Ycum 0.348, Q^2cum 0.152); ***a)*** scores plot, coloured by classes. Cow 282 clustering is represented by the ellipse; ***b)*** S-plot, coloured by Variable influence of Projection (VIPcv) (box shows p(corr)[1] > 0.5 and VIPcv > 1); and ***c)*** loadings column plot showing all *m/z* with a VIPcv > 1.

These ions could be tentatively identified using accurate mass as glycocholic acid and glycochenodeoxycholic acid, however further analysis using MS/MS was utilised in order to infer more strongly. The results from this are presented in *section 5.3.3*. Both of these metabolites are bile acids which are physiological detergents that facilitate excretion, absorption, and transport of fats and sterols in the intestine and liver, and are essential for the digestion and absorption of hydrophobic nutrients.

Of the 178 *m/z*_RT pairs for the C18 (+) spectra, 102 buckets had large jack-knifed confidence intervals that included zero, and were excluded from the dataset. Of the remaining 76, four showed a down-regulation, and had a p(corr)[1] of < - 0.3, which was corroborated by the points in the S-plot orientating close to zero on both the *X*- and *Y*-axes, so were not considered to be reliable indicators for class separation. The other 72 showed an up-regulation in the clinical cows after dosing. However, the C18 (+) dataset resulted in an unexpected separation in the up-regulated compounds (*Figure 5.5 a, b*). Further data analysis revealed that this separation was neither a result of the trial nor analytical effects, such as batches, sample run order, sampling days, or dosed/not dosed animals. The S-plot of the model duplicated this separation as well, with the points which were up-regulated in those samples taken from clinical cows after dosing (*Figure 5.5 b*). Therefore, of the 72 up-regulated peaks, 15 of these were from the bottom 'group' in the S-plot, with p(corr)[1] < 0.25 and were excluded, while the other 57, in the top 'group', had a p(corr)[1] > 0.5. These 57 up-regulated peaks were considered reliable for class separation for the C18 (+) dataset. Of these, 6 main ions contributed to the class separation. These were at *m/z* 466.3174 at 6.32 min, 414.3018 at 7.90 min, 412.2866 at 6.38 min, 430.2964 at 6.28 min, 466.3155 at 7.31 min, and 448.3075 at 6.31 min (*Table 5.2*). Using the HMDB database these accurate masses were used to tentatively identify the metabolites. This provided more difficulties with the C18 (+) ions, as there are more possible candidates on the database, however a combination of bile acids, for example glycocholic acid and 3-oxo-4,6, choladienoic acid, as well as amino acid derivatives, and minor metabolites of fatty acids appeared to be the likely candidates. MS-MS was used to establish the probable metabolites more reliably. A number of likely isobaric isomers were also detected, including *m/z* 337.2529 (RT 6.31) and 337.2540 (RT 6.53) ($[M+H]^+$).

No other models produced validated results. *Tables 5.1* and *5.2* summarise the peaks which were responsible for the difference between the clinical cattle compared to the other groups, as observed in the OPLS-DA models for C18 (-) and (+) data, respectively.

Table 5.1 Summary of detected compounds from C18 (-) ESI MS analysis of serum, specific for clinical cows as determined from S-plots and loadings column plots.

C18 (-)	
m/z	**RT [min]**
464.3017	7.57
448.3074	9.08
465.3047	7.57
449.3105	9.09
466.2992	7.53
515.2881	6.57
498.2894	7.57
514.2846	6.57
462.2865	6.93
516.2882	6.56
450.3244	9.04
499.2926	7.57

Table 5.2 Summary of detected compounds from C18 (+) ESI MS analysis of serum, specific for clinical cows, as determined from S-plots and loadings column plots.

C18 (+)					
m/z	**RT [min]**	***m/z***	**RT [min]**	***m/z***	**RT [min]**
337.2529	6.31	432.3102	8.84	466.3183	6.57
337.2540	6.53	432. 3124	8.20	466.3199	6.70
339.2683	7.79	432.3131	7.54	472.3031	8.78
412.2866	6.38	432.3134	7.02	472.3039	7.66
412.2842	7.25	448.3048	7.27	480.2786	5.17
412.2869	6.66	448.3075	6.31	483.3442	6.32
414.3005	8.54	448.3047	7.40	488.2975	7.19
414.3018	8.81	448.3074	6.61	488.2989	6.25
414.2997	8.99	450.3209	8.52	498.2874	6.45
414.3018	7.90	450.3226	8.79	498.2888	5.18
414.3005	6.81	450.3219	9.83	500.3057	6.00
414.3019	8.11	450.3224	9.02	516.2988	6.45
415.3063	7.61	450.3233	8.21	516.3000	5.24
430.2953	7.29	450.3235	9.56	533.3275	5.20
430.2950	7.38	451.3262	7.53	899.6367	7.80
430.2964	6.28	462.2691	5.25	921.6201	7.88
430.2976	6.67	466.3155	7.31	931.6240	7.29
432.3105	8.58	466.3174	6.32	948.6482	7.21
432.3126	7.88	466.3166	7.60	953.6045	7.21

5.3.2 Time series analyses

Time series over the trial period for individual *m/z* values were produced to aid in data visualisation for both temporal variations and differences between the animal groups. The time profiles of each *m/z*_RT pair were extracted for each cow; this can be seen as the pale lines in *Figure 5.6*. The individual cow time profiles were then used to calculate the average time profile for the groups to which they belonged; these are shown as the thick lines in *Figure 5.6*. Significant differences from 'normal' (control state) in metabolites recorded using the present methods, were only observed in the clinical cows after dosing, in both C18 (-) and (+) modes (example *Figure 5.6)*. The exclusion of clinical cows resulted in no obvious differences between the remaining groups (control, non-responder, and subclinical). To reduce the dataset, all time series plots with a p-value > 0.05 were considered unreliable for class differentiation, and were excluded from further analysis. The remaining peaks, showing a clear group differentiation, were examined in the raw LC/MS spectra, to avoid false positives. For example, those peaks showing low signal to noise ratio, and/or poorly resolved peaks, were not considered for possible biomarker identification. It was noted whether any compounds were detected in both the negative and positive ionisation modes. *Figure 5.6* shows an example of this, where corresponding *m/z* values were detected.

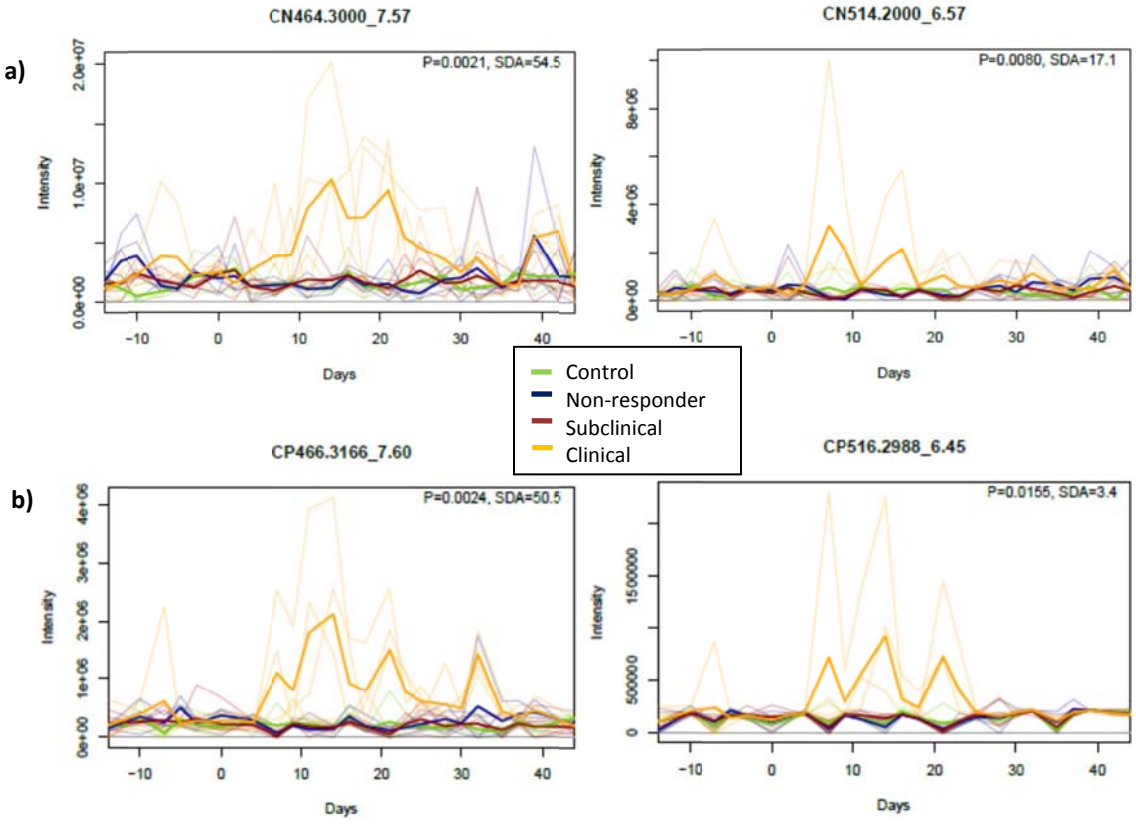

Figure 5.6 Time series of the main two *mz*_RT peaks identified as showing a major difference in the clinical cows, only after dosing (Day 0; $p < 0.05$ and true peaks), derived from ***a)*** C18 (-), and ***b)*** C18 (+) ESI-MS analysis. The observed temporal variations, corresponding RT and m/z values could be attributed to equivalent compounds, i.e. MW 465 (left) and MW 515 (right).

However, more in-depth analysis would be required to confirm this, such as the use of accurate mass measurements, and fragmentation analysis using tandem mass spectrometry. Whether the retention time for the peaks were the same in a selection of different spectra, for example different cows, different days, and different batches, was also assessed. For example *Figure 5.7* shows UPLC/(-) ESI-MS traces for two samples from cow 298 (Day -14 and 14) for the 464 ion in the negative ionisation mode. Additionally, one main peak was detected in negative and positive ionisation mode at retention times of ~7.30 and 7.28 min, respectively, and both showed well resolved peaks, confirming that this was a true peak. Any obvious heavy isotopes of parent peaks were also excluded.

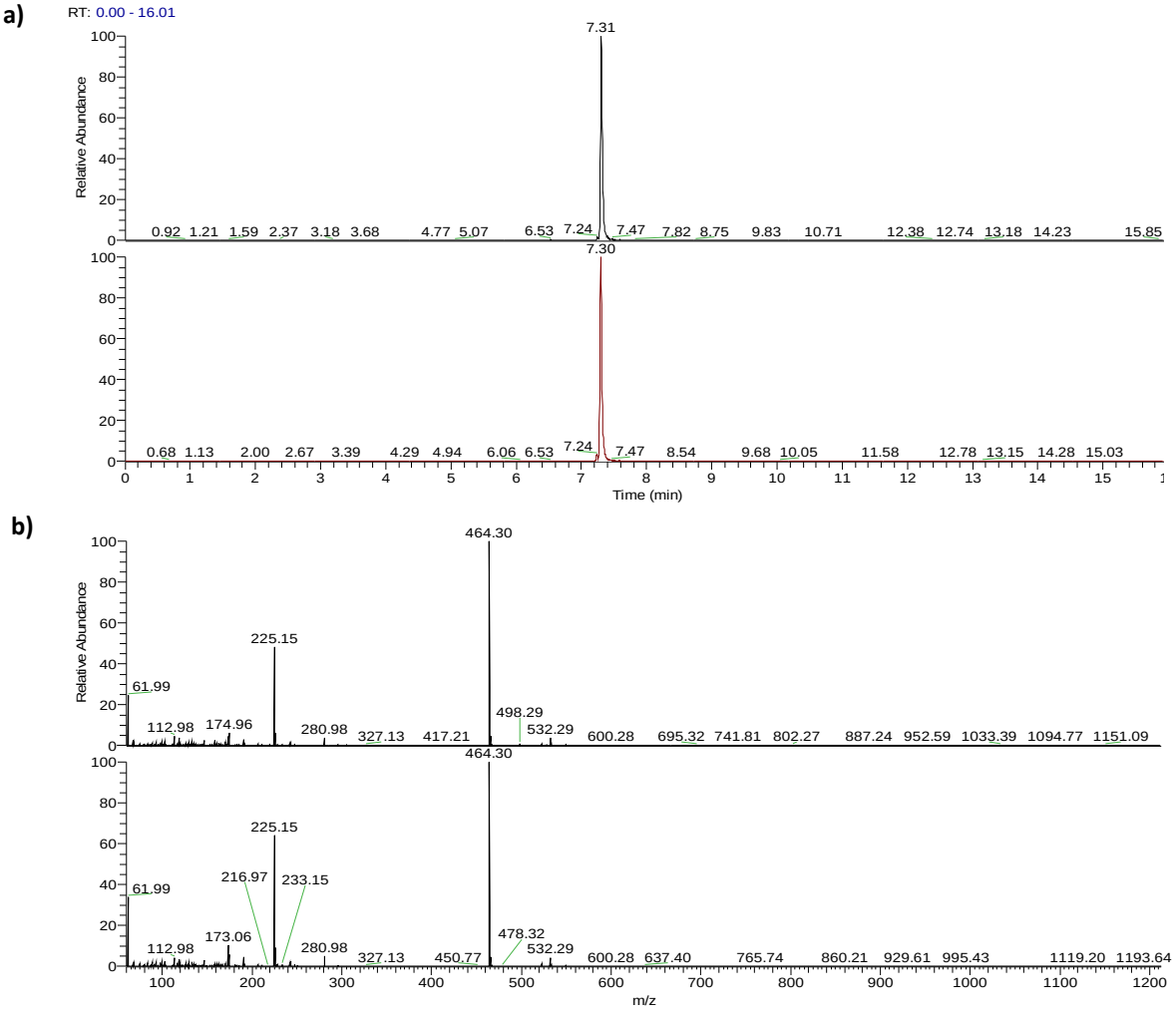

Figure 5.7 Examples of ***a) E***xtracted ion chromatograms of *m/z* 464 detected in the sample from the clinical cow 298 measured on Day 14 (top) and Day -14 (bottom) from C18 (-) ESI-MS analysis, and ***b)*** their corresponding mass spectral data.

In summary, 9 peaks were extracted from C18 (-) and 22 peaks from (+) dataset (*Table 5.3*) that were considered as main components causing the observed differences between clinical and all other cow

groups. Further analysis, using tandem mass spectrometry, was performed to derive further information on their structural properties or identity. *Figure 5.6* shows an example of the two main peaks from (-) and (+) ESI/MS identified as showing a difference in clinical cows after dosing (Day 0). The other 27 recognised peaks are shown in *appendix 9* and *10*, respectively.

Table 5.3 Key components from serum differentiating clinical cows from all other cow groups after sporidesmin dosing, using C18 (-) and (+) ESI-MS. All components were up-regulated in comparison to the other cow groups.

m/z **[M – H]$^-$**	***m/z*** **[M+ H]$^+$**	**RT [min]**	**p-value**
-	533.32750	5.20	0.0216
-	464.28440	5.97	0.1803
-	464.30570	6.15	0.0141
-	337.25290	6.31	0.0047
-	498.28740	6.45	0.0211
-	516.29880	6.45	0.0155
-	337.25400	6.53	0.0063
464.30692	-	6.56	0.0392
514.28452	-	6.57	0.0080
462.28673	-	6.93	0.0018
-	488.29750	7.19	0.0020
-	412.28420	7.25	0.0015
-	448.30480	7.27	0.0017
-	464.28320	7.29	0.0992
-	430.31020	7.38	0.0014
-	500.30390	7.45	0.0292
-	466.31660	7.60	0.0024
464.30175	-	7.57	0.0021
478.31760	-	7.57	0.0138
498.28990	-	7.57	0.0325
-	472.3090	7.66	0.0212
-	450.32090	8.52	0.0042
-	432.31050	8.58	0.0066
-	472.30310	8.78	0.0028
-	450.32260	8.79	0.0046
-	414.30180	8.81	0.0041
-	432.31020	8.84	0.0043
-	414.29970	8.99	0.0028
448.30746	-	9.08	0.0291
516.2750	-	9.09	0.0022
432.31274	-	10.94	0.0476

5.3.3 Orbitrap tandem mass spectrometry

According to VIPcv values, time series combined ranking, and the examination of raw spectra, a total of 9 and 22 variables from C18 (-) and (+) ESI-MS analysis, respectively, were selected for targeted MS^2 analysis (*Table 5.4* and *5.5*).

As an example from the C18 (-) dataset, chromatographic and MS^2 data are shown in *Figure 5.8* for the compound eluting at 9.12 min in the pooled sample. For *m/*z 464, the product ions at *m/*z 420.3159 (loss of 44 amu, 1 x CO_2), 446.2954 (loss of 18 amu, 1 x H_2O), and 402.3050 (loss of 62 amu, H_2O + CO_2) were formed during the MS^2 analysis.

a)

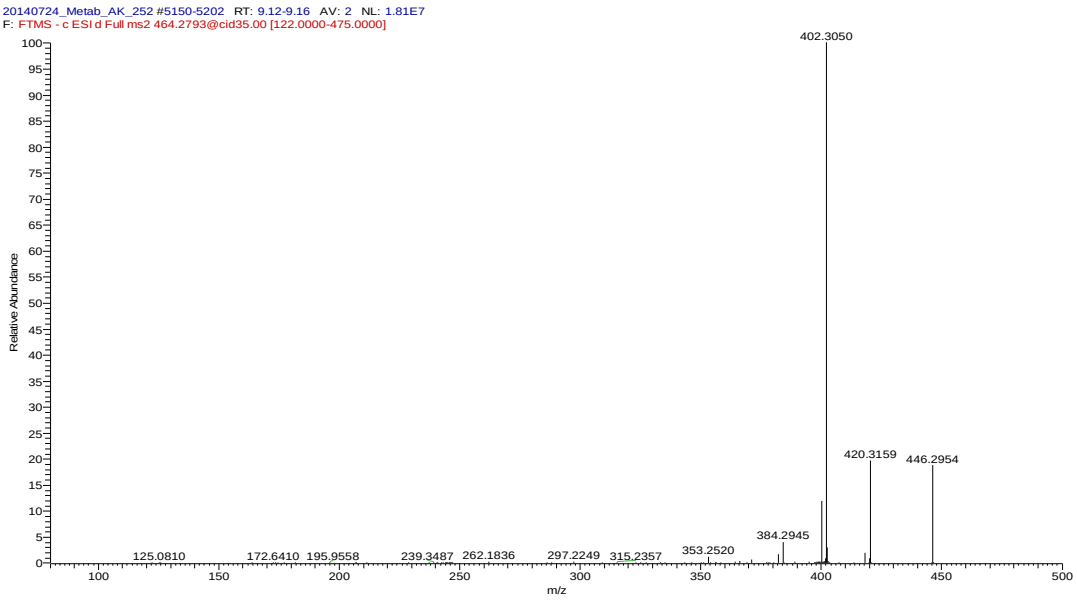

b)

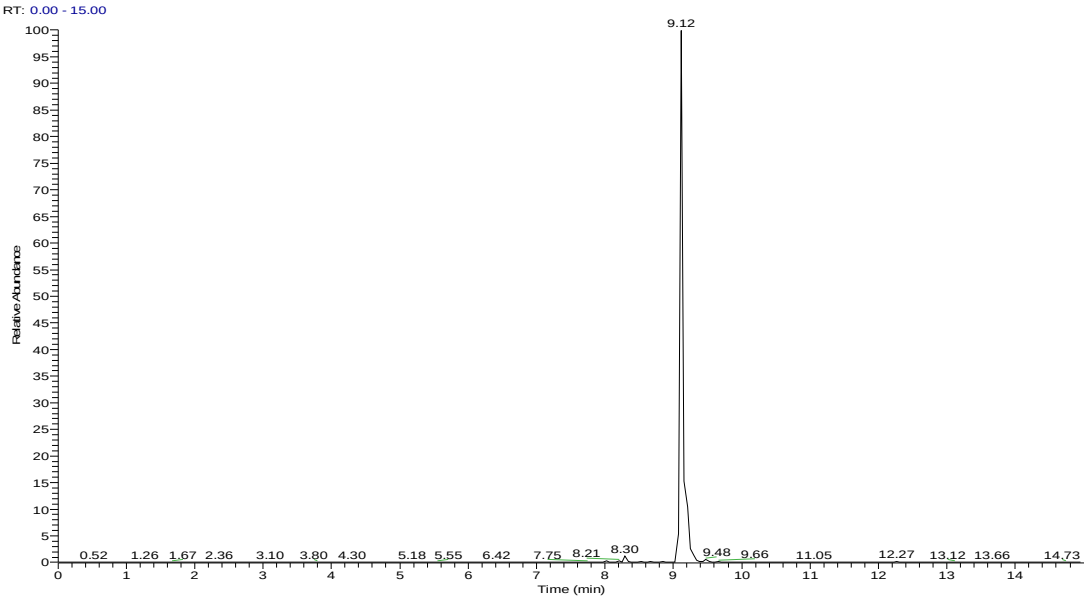

Figure 5.8 C18 UPLC/(-) ESI-MS analysis of serum, showing the *m/z* 464 MS^2 data ***(b)*** eluting at 9.12 min ***(a)***.

A corresponding protonated compound ($[M+H]^+$) was detected at *m/z* 466 at 9.15 min from the C18 (+) ESI-MS analysis (*Figure 5.9*). The product ions at *m/z* 448.3046, 430.2940, and 412.2833 were formed during the MS^2 analysis. Owing to the detection from both (+) ESI-MS and MS^2 analysis, the ions 448.3046 (loss of 18 amu, 1 x H_2O), 430.2940 (loss of 36 amu, 2 x H_20), and 412.2833 (loss of 54 amu, 3 x H_2O) originate from the same compound *m/z* 466.3166, which readily loses water in (+) ESI-MS analysis. Neutral water loss is common for hydroxylated compounds, and the occurrence of multiple water losses lead to the conclusion that *m/z* 466.3166 contains three hydroxyl groups.

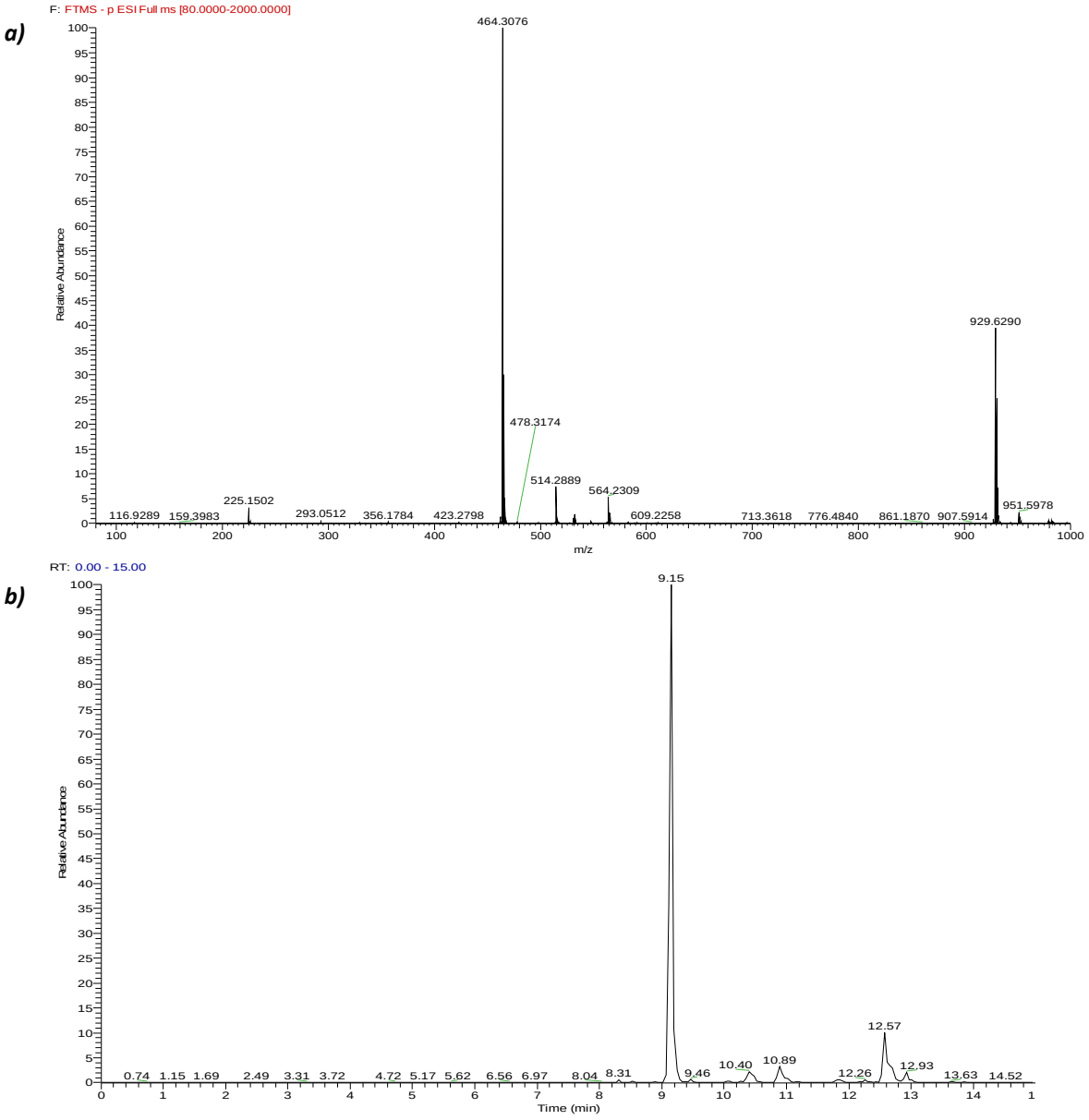

Figure 5.9 *m/z* 466 MS^2 data ***(a)*** eluting at 9.15 min ***(b)*** from C18 (+) ESI-MS analysis of serum.

Accurate mass measurements for both the precursor and product ions are summarised in *Table 5.4 and 5.5* from the C18 (-) and (+) MS^2 analysis, respectively. Online databases, such as the Human Metabolome Database (HMDB) and ChemSpider were used to search for possible candidates based on determined accurate mass and structural features. Many of the compounds were detected both in positive and negative ionisation mode, increasing the confidence for the presence of real peaks and providing complementary fragmentation data for structural identification.

For the *m/z* 466.3166 ($[M+H]^+$) an elemental composition of $C_{26}H_{43}NO_6^+$ (0.612 ppm error) was determined. Taking into account that the molecule contains three OH groups, it is most likely glycocholic acid. For the *m/z* 464.3018 (RT 7.57, $[M-H]^-$) a likely elemental composition of $C_{26}H_{43}NO_6^-$ (-0.024 ppm error) was also determined, and is also likely to be glycocholic acid detected in negative ionisation mode. Another *m/z* 464.30329 (RT 6.56) peak was identified as being instrumental in the difference between clinical and all other cows after dosing. With similar accurate masses and product ions, it is likely that these are isobaric isomers. Other isobaric isomers were detected, including *m/z* 472.30310 (RT 8.78) and 472.30390 (RT 7.66) in the C18 (+) spectra.

The protonated compound ($[M+H]^+$) detected at *m/z* 450.32090 at 8.52 min from the C18 (+) ESI-MS analysis produced two main product ions, 432.3087 and 414.2982. The fragmentation pattern, showing a loss of one and two H_2O molecules, matched with that of glycochenodeoxycholic acid (-3.546 and 0.228 ppm errors, respectively).

The most prominent changes seen between the groups, after dosing, were observable among the compound class of bile acids (BAs). Distinguishing between the different BAs is often difficult, with the only differences being the presence or absence of hydroxyl groups in positions 3, 7, and 12. To be 100 % confident on the assignment of the peaks, serum would need to be spiked with solutions of the pure compounds and MS^2 analysis would be required. This was not done in the present study due to time restraints.

Tentatively 5 bile acids were detected, which were increased in clinical cattle, compared to the other three groups. Glycocholic acid, taurocholic acid, taurochenodeoxycholic acid, and glycochenodeoxycholic acid were detected in both (+) and (-) ESI-MS, giving strong evidence for their presence in clinical cattle following liver damage caused by a sporidesmin dose. Lithocholic acid was only detected in the C18 (-) dataset.

Table 5.4 Summary of accurate mass measurements from C18 (-) ESI-MS/MS analysis of serum from clinical cows.

LCMS *m/z*	LCMS RT	MS^2 *m/z*	LCMS RT	MS^2 product ions (abundance) (loss (amu))	Elemental composition	Error (ppm)	Metabolite identity
462.28673	6.93	462.29218	8.53	444.27602 (30%) (-18); 418.29699 (100%) (-43); 400.28595 (20%) (-62)	$C_{26}H_{40}O_6N$ $C_{27}H_{36}O_2N_5$ $C_{13}H_{38}O_8N_{10}$	3.646 0.818 -0.280	Unknown
464.30175	7.57	464.30758	9.12	446.29515 (20%) (-18); 420.31569 (20%) (-43); 402.30485 (100%) (-62)	$C_{26}H_{42}O_6N$	-0.024	Glycocholic acid
464.30329	6.56	464.30692	9.12	446.29279 (20%) (-18); 420.31555 (25%) (-44); 402.30515 (100%) (-62); 384.29175 (14%) (-80); 353.25220 (5%) (-111); 400.28992 (10%) (-64)	$C_{26}H_{42}O_6N$	3.4	Glycocholic acid
516.27500	9.09	516.29710	10.60	448.30762 (100%) (-67)	Unknown	-	Unknown
514.28452	6.57	514.29800	8.89	496.27597 (10%) (-18); 412.28754 (5%) (-102); 371.26074 (5%) (-143); 353.25009 (8%) (-161);	C26H45O7NS	0.123	Taurocholic acid
478.31760	7.57	478.29720	13.07	281.25035 (100%) (-197); 214.04946 (2%) (-264); 196.03867 (4%) (-282)	Unknown	-	Unknown
448.30746	9.08	448.31360	10.60	430.29821 (15%) (-18); 404.31877 (100%) (-44); 386.30826 (5%) (-62); 355.26639 (5%) (-93)	$C_{26}H_{42}O_5N$	1.368	Glycochenodeoxycholic acid / Deoxyglycocholic acid
432.31274	10.94	432.31779	12.18	388.32431 (100%) (-44); 173.48961 (15%) (-275)	$C_{26}H_{42}O_4N$	1.869	Lithocholic acid glycine conjugate
498.29104	7.57	498.29105	10.74	355.26587 (100%) (-143); 414.30334 (5%) (-84)	$C_{26}H_{45}NO_6S$	3.127	Taurochenodeoxycholic acid / Taurodeoxycholic acid

Table 5.5 Summary of accurate mass measurements of C18 (+) ESI-MS/MS analysis of serum from clinical cows.

LCMS *m/z*	LCMS RT	MS^2 *m/z*	MS^2 RT	MS^2 product ions (abundance) (loss (amu))	Elemental composition	Error (ppm)	Metabolite identity
337.2529	6.31	337.25287	9.15	319.24057 (100%) (-18); 209.13165 (30%) (-128); 227.14209 (15%)(-110); 255.17326 (5%) (-82)	$C_{24}H_{32}O$	0.824	Unknown
337.2540	6.53	337.25215	10.26	319.24057 (-100%) (-18), 295.20441 (5%) (-42), 255.17326 (5%) (-82), 227.14209 (20%) (-110), 209.13164 (30%) (-128)	$C_{24}H_{32}O$	4.174	Unknown
412.2842	7.25	412.28617	9.15	337.25126 (100%) (-57); 319.24081 (40%) (-18); 394.27252 (5%)(-18)	$C_{26}H_{38}O_3N$	-1.02	Glycocholic acid (minus 3 H_2O)
414.2997	8.99	414.30113	10.62	339.26704 (100%) (-75); 396.28846 (10%) (-18); 321.25657 (50%) (-93); 243.19294 (10%) (-171); 229.17335 (10%); (-185); 215.17716 (10%) (-199); 203.15636 (8%) (-211); 278.17416 (8%) (-136); 304.18975 (8%)(-110); 158.08091 (5%) (-256);	$C_{26}H_{40}O_3N$	2.074	Glycochenodeoxycholic acid (minus 2 H_2O)
414.3018	8.81	414.30013	10.40	339.26663 (100%) (-75), 321.25616 (40%) (-93), 396.28793 (10%) (-18); 215.17857 (10%) (-199); 201.16306 (8%) (-213); 238.14275 (8%)(-176); 252.15826 (5%)(-162);	$C_{26}H_{40}O_3N$	-0.339	Glycochenodeoxycholic acid (minus 2 H_2O) (possible hydroxyl isomer of 414.29970)

				278.17380 (5%)(-136); 304.18930 (5%)(-106); 158.08073 (5%)(-256)			
430.2950	7.38	430.28617	9.15	412.28302 (100%) (-18); 337.25148 (25%) (-93); 319.24093 (10%) (-111)	$C_{26}H_{39}O_4N$	-0.43	Glycocholic acid (minus 2 H_2O_
432.3102	8.84	432.31054	10.62	414.29910 (100%) (-18); 339.26773 (5%) (-93)	$C_{26}H_{42}O_4N$	-0.683	Glycochenodeoxycholic acid (minus 1 H_2O)
432.3105	8.58	432.30972	10.40	414.29867 (100%) (-18); 339.26699 (4%) (-93)	$C_{26}H_{42}O_4N$	-2.580	Glycochenodeoxycholic acid (minus 1 H_2O) (possible hydroxyl isomer of 432.31054)
448.3048	7.27	448.30625	9.15	412.28342 (100%) (-36); 430.29377 (95%) (-18); 337.25185 (15%) (-111); 319.24137 (5%) (-129)	$C_{26}H_{41}O_5N$	-2.119	Glycocholic acid (minus 1 H_2O)
450.3209	8.52	450.32011	10.40	432.30872 (100%) (-18); 414.29825 (40%) (-36)	$C_{26}H_{44}O_5N$	-3.546	Glycochenodeoxycholic acid
450.3226	8.79	450.32096	10.62	414.29913 (100%) (-36); 432.31009 (40%) (-18); 339.26782 (3-5%) (-111); 357.27844 (3-5%) (-93)	$C_{26}H_{44}O_5N$	0.229	Glycochenodeoxycholic acid (possible hydroxyl isomer of 450.32011)
464.2832	7.29	464.28152	10.89	339.26670 (100%) (-125); 321.25624 (40%) (-143); 382.20298 (20%) (-82); 354.17178 (15%) (-110); 302.14073 (10%) (-162); 229.15784 (10%) (-235); 215.17861 (10%) (-249); 368.18733 (10%) (-96); 328.15623 (15%) (-136); 446.27033 (5%) (-18); 203.14236 (5%) (-261); 257.18898 (4-5%) (-207);	$C_{30}H_{34}N_5$ $C_{18}H_{38}O_7N_7$ $C_{22}H_{38}O_2N_7S$ $C_{26}H_{42}O_4NS$ $C_{22}H_{46}ON_3S_3$ $C_{29}H_{38}O_4N$ $C_{19}H_{42}O_2N_7S_2$	1.394 -2.591 2.799 -2.985 3.809 4.275 -4.462	Unknown (possible positional isomer of 464.3057)

				288.12519 (4-5%) (-176); 208.06305 (5%) (-256);			
464.2844	5.97	464.29910	8.53	446.28802 (100%) (-18); 428.27751 (20%) (-36); 410.26707 (10%) (-54); 335.23522 (~5%) (-129); 535.24573. (~5%) (+70)	$C_{26}H_{42}O_6N$	-3.37	Glycocholic acid
464.3057	6.15	464.28235	10.40	339.26673 (100%) (-125); 321.25628 (40%) (-143); 382.20308 (20%) (-82); 208.06306 (15%) (-256); 288.12520 (15%) (-146); 354.17181 (15%) (-110); 254.17181 (10%) (-210); 268.18747 (8%) (-196); 302.14077 (8%) (-162); 215.17867 (8%) (-249); 201.16312 (15%) (-263); 243.20968 (8%) (-221); 446.27017 (5%) (-18); 257.18896 (5%) (-207); 229.15788 (5%) (-235) ; 157.14759 (5%) (-307); 276.12521 (5%) (-188)	$C_{18}H_{38}O_7N_7$ $C_{26}H_{42}O_4NS$ $C_{19}H_{42}O_2N_7S_2$ $C_{30}H_{34}N_5$ $C_{27}H_{38}N_5S$ $C_{22}H_{38}O_2N_7S$	-0.803 -1.197 -2.674 3.182 -4.078 4.586	Unknown (possible positional isomer of 464.2832)
466.3166	7.60	466.31739	9.15	430.29407 (100%) (-36); 412.28338 (85%) (-54); 448.30464 (40%) (-18); 337.25194 (10%) (-129); 355.26244 (4%) (-111); 373.27326 (3%) (-93)	$C_{26}H_{43}NO_6$	0.612	Glycocholic acid
472.3031	8.78	472.30255	10.62	454.29074 (100%) (-18); 397.26953 (80%) (-75);	$C_{24}H_{38}O_3N_7$ $C_{23}H_{42}O_7N_3$	.-1.089 1.742	Unknown
472.3039	7.66	472.30177	10.35	454.29050 (100%) (-18);	$C_{24}H_{38}O_3N_7$	0.091	Unknown

				397.26932 (30%) (-75); 396.28526 (5%) (-76)	$C_{23}H_{42}O_7N_3$	-2.741	
488.2975	7.19	488.29848	9.11	470.28532 (100%) (-18), 452.27529 (10%) (-36), 413.26427 (80%) (-75)	$C_{24}H_{38}O_4N_7$	1.026	Unknown
498.2874	6.45	498.28852	8.93	462.26558 (100%) (-36); 480.27590 (70%) (-18)	$C_{26}H_{44}NO_6S$	-4.105	Taurocholic acid
500.3039	7.45	500.30223	10.89	464.28088 (100%) (-36); 482.29153 (40%) (-18);	$C_{26}H_{46}NO_6S$	-0.27	Taurochenodeoxycholic acid
516.2988	6.45	516.29890	8.93	498.28625 (100%) (-18); 480.27571 (70%) (-36); 462.26520 (60%) (-54);	$C_{26}H_{46}NO_7S$	-0.29	Taurocholic acid
533.32750	5.20	533.32548	8.93	516.29672 (-100%) (17), 498.28634 (65%) (-35), 480.27570 (-20%) (53), 462.26510 (-5%) (71)	$C_{18}H_{45}O_{10}N_8$	0.308	Unknown

5.5 Discussion

The intention of the work presented in this chapter was to differentiate between cows responding variably to a one-off sporidesmin dose, using UPLC/ESI-MS and UPLC/MS^2 of serum. The ideal outcome was to be able to identify subclinicals and/or non-responders. However, much like the NMR analysis, the subclinicals and non-responders could not be uniquely identified using any of the techniques presented here. Nonetheless, the clinical cows were able to be clearly differentiated using C18 RP column chromatography coupled to ESI-MS in both positive and negative ionisation modes. Tandem MS was able to tentatively identify nine of the twenty peaks which were relevant to clinical cows after dosing. All of the identified peaks were a mixture of taurine- and glycine-conjugated secondary BAs.

Glycocholic acid, taurocholic acid, taurochenodeoxycholic acid, as well as one peak which was narrowed down to two likely bile acids, being glycochenodeoxycholic acid or deoxyglycocholic acid appeared in both (-) and (+) ESI/MS as being elevated in clinical cows. A lithocholic acid-glycine conjugate was identified in the C18 (-) only. All of these metabolites were elevated in the clinical cows, when compared to the control days of these cows, the control cows, and all other groups after dosing.

It is well established in the literature that concentrations of BAs increase in the liver and blood during cholestasis due to leakage of bile into the parenchyma of the liver (Fickert *et al.*, 2002; Woolbright *et al.*, 2014; Zhang *et al.*, 2012c). It is often assumed that the increases in cytotoxic BAs are the cause of, or at least involved in, the progressive hepatocellular injury that occurs during cholestasis. In harmony with the present study, Zhang *et al.* (2012c) indicated that the concentration of BAs was elevated in serum after bile duct ligation (BDL) in rats. They found that the main BAs involved were TCA, β-maurichолic acid, and tauro-β-maurichолic acid. Other studies have shown that increases in taurolithocholic acid, deoxycholic acid, glycodeoxycholic acid, and glycochenodeoxycholic acid cause necrosis of hepatocytes. Chenodeoxycholate is well known to be directly cytotoxic for hepatocytes (Miyazaki *et al.*, 1984). In addition, lithocholic acid, a bacterial metabolite of chenodeoxycholate, produced in the intestinal tract, has been implicated as a possible hepatotoxin (Miyazaki *et al.*, 1984). Glycochenodeoxycholic acid is the most toxic known form of chenodeoxycholate, it is the major BA present in the serum of cholestatic human patients, and has also been shown to induce hepatocellular injury in a dose-dependent manner (Siviero *et al.*, 2008; Spivey *et al.*, 1993; Trottier *et al.*, 2012; Woolbright *et al.*, 2015).

The main contention between studies on cholestasis is the mechanism of action of the BAs on the hepatocytes. Initial studies recognised BAs as having a direct effect on hepatocytes. However, the method by which this occurs was also in contention, with some studies stating necrosis, and others stating apoptosis, leading to cell death (Woolbright *et al.*, 2015). Other recent studies have suggested that BAs are not directly hepatotoxic, but instead increase the expression of proinflammatory mediators, such as cytokines, which promote hepatic inflammation and significant liver injury through the recruitment of neutrophils and macrophages (Allen *et al.*, 2011; Woolbright *et al.*, 2015; Zhang *et al.*, 2012c).

It appears that the mechanism is dependent on the species of animal, as this determines the composition of BAs in the bile, and therefore the likely BA derivatives that will increase during cholestasis. Woolbright *et al.* (2015) demonstrated the effect of glycochenodeoxycholic acid on human hepatocytes in culture as well as identifying this BA form as the most common to increase in patients with obstructive cholestasis, *in vivo*. This study recognised an increase in damage-associated molecular pattern molecules, which are molecules that can initiate the immune response in non-infectious immune responses. They also showed that human hepatocytes die via necrosis *in vitro*, through a direct cytotoxic effect on cells, when exposed to BAs. In rodents on the other hand, studies have shown a mixture of results. In mice it has been shown that neutrophil recruitment occurs after the onset of BA-induced necrosis (Woolbright *et al.*, 2014). However, the mice were fed a diet with lithocholic acid, as the main BAs present in mice are not cytotoxic, and direct toxicity would not be expected. Spivey *et al.* (1993) showed that, *in vitro,* glycochenodeoxycholic acid cytotoxicity in rat hepatocytes occurs through the impairment of mitochondrial oxidative phosphorylation, causing ATP depletion, and inhibiting mitochondrial function. Allen *et al.* (2011) identified BAs as inflammagens in mice, both *in vitro* and *in vivo*. The BAs stimulated the production of pro-inflammatory mediators by hepatocytes, which promoted neutrophil accumulation, extravasation, and activation. Additionally, the increased production of cytokines, stimulated by BAs, promotes the accumulation of other immune cells which could also influence changes to the liver.

Most studies focus on glycochenodeoxycholic acid and taurocholic acid, with some mention of taurochenodeoxycholic acid, glycocholic acid, and lithocholic acid. However, no mention of deoxyglycocholic acid is made. It may be that this BA is more species specific, and is common in cattle. One study determined that biliary BAs in bovids consisted mostly of three types: cholic acid, chenodeoxycholic acid and deoxycholic acid (Hagey *et al.*, 1997). It has been suggested that glycine-conjugated BAs are more cytotoxic than those which are taurine-conjugated; however this may

partly be due to the stronger prevalence of glycine-conjugated BAs (Woolbright *et al.*, 2015). An even mix of glycine- and taurine-conjugated BAs was identified in the serum of clinical cows in the present study.

Irrespective of the method of action, it appears that the increase in BAs seen in cows which became clinical after a single dose a sporidesmin, a known hepatotoxin, is secondary to primary lesions to bile ducts. The damage to bile ducts by sporidesmin causes necrotising cholangitis, which manifests as cholestasis in severe cases. In addition to initiating cholestasis, sporidesmin has been shown to inhibit BA uptake into hepatocytes (Cordiner & Jordan, 1983). Furthermore, previous work by Gallagher (1964) and Middleton (1974) demonstrated sporidesmin-induced mitochondrial swelling, suggesting that sporidesmin acts on hepatocyte membranes, may increase permeability, and efflux of BAs from the cytoplasm.

Although MS was not able to identify unique metabolites as potential biomarkers of sporidesmin intoxication, it did provide more information on the latter stages of the clinical disease process in dairy cattle. Sporidesmin damage, at the dose given in this study, appeared to manifest itself quickly in those cows which were more susceptible to the toxin.

It is hypothesised that any metabolites produced directly from sporidesmin, and/or other compounds, during the initial attack on the bile ducts would have been removed from the blood before the first blood sample was taken, 48 hours after dosing.

CHAPTER 6

General discussion

6.1 General overview

Facial eczema (FE) is a hepatogenous (type III) photosensitisation disease of ruminant livestock. It is caused by the ingestion of the mycotoxin, sporidesmin A, held within the spores of the fungus *Pithomyces chartarum* which grows on pasture litter. This toxin causes damage to the biliary system in susceptible animals resulting in the retention of phytoporphyrin, a natural metabolite derived from the degradation of chlorophyll *a* by anaerobic microbial fermentation in the rumen. Retention of phytoporphyrin leads to visible clinical photosensitivity signs which are identifiable features of FE. Therefore, the photosensitivity develops secondarily to, and as a direct result of, hepatobiliary damage, causing disturbances in bile flow and hepatic function.

Very little is known about the detection of subclinical FE, nor the early stages of the disease. Additionally, metabolomics analyses have not been applied to FE until now. The main objective of this study was to investigate metabolomics platforms for early onset and subclinical stage biomarkers for FE detection, utilising traditional biochemical measurements, fluorescence of phytoporphyrin, ^{1}H NMR spectroscopy, UPLC/MS, and UPLC/MS/MS methods for metabolomics analysis.

6.2 Project review

To do this, a 60 Day study was designed, where blood, urine, and milk samples were collected from 20 dairy cows, and analysed using the above mentioned platforms. Two weeks of control sampling preceded the administration of a single low dose (0.24 mg/kg) of sporidesmin A toxin to 17 cows, followed by seven and a half weeks of sampling to investigate metabolic changes in the cows. It was anticipated that this dose would cause subclinical disease. Three cows remained as controls. At the end of the trial it was found that the cows could be separated into four groups using liver enzyme activities, and the presence or absence of clinical signs that manifested as reddening, swelling and/or peeling of the skin. These groups were named the controls, non-responders, subclinicals, and clinicals.

The results of the study, using traditional biochemical measurements, and changes in milk yield and body weight, confirmed many of the effects of sporidesmin intoxication previously reported in both cattle and sheep. For example, increases in GGT and GDH activities, with increases between Days 7 and 14, following the dose of sporidesmin. These increases were greater for more severely affected animals, while non-responders remained within the normal range for clinically healthy animals. Milk yields decreased in all treated cows, indicating that sporidesmin may affect all cows in a herd to

some extent irrespective of their level of resistance. This suggested that sporidesmin may interact directly with the mammary gland, or it may purely be that the mycotoxin insult, leading to an increase in the immune system activities, alters the use of energy within the body by limiting processes which are less essential at the time, such as milk production.

An increase in phytoporphyrin concentration was detected in cows that developed clinical signs of FE. These concentrations reached a maximum between Days 7 and 14 after dosing with sporidesmin. There was variability in the time line of clinical signs appearing in relation to phytoporphyrin concentration and elevations in GGT and GDH activities. Phytoporphyrin reached a maximum prior to GGT in all of the clinical cows, while GDH activity and phytoporphyrin concentrations reached their maxima at around the same stage. Maximum concentrations of phytoporphyrin occurred at Day 7 for two cows and Day 14 for the other two, while clinical signs appeared around Day 9 and 10 for three of the cows, and not until around Day 21 - 23 for the fourth. Although more work is required on techniques for phytoporphyrin measurement in serum, it doesn't appear that this compound will be a useful biomarker for subclinical cases nor early stages of FE.

The ^{1}H NMR metabolomic methods used for the serum samples were not able to individually differentiate non-responders and subclinicals from all others, but were able to distinguish all cows that had been dosed from those which had not, as well as identify cows that developed clinical signs. The metabolites that were tentatively identified as being relevant to the differentiation of dosed cows were increases in lactate, pyruvate, formate, glutamate, glycerol, the amino acids proline, alanine, and histidine, and the ketone bodies β-hydroxybutyrate and acetoacetate. Decreases in acetate, choline, isoleucine, trimethylamine N-oxide, lipids and lipoproteins, cholesterol, and α-glucose were also seen. Glycoproteins were highly elevated in clinical cows and allowed their separation from all other cows. Citrate, on the other hand, appeared to be higher in non-responders and subclinicals only. The latter was only found using the time series analyses.

Urine analysis was not able to differentiate between groups, nor samples taken before or after dosing. There was a pronounced day-to-day variation in urine samples which may have masked any sporidesmin-related changes. Some components of milk varied following the sporidesmin dose, with increases in malonic acid, carnitine, choline and/or phosphocholine, and decreases in citrate, N-acetylcarbohydrates, and an unknown metabolite, in cows which were dosed. The latter was only observed using MVA methods; no obvious change was visible in the time series traces.

Similar to the NMR results, UPLC/ESI-MS using C18 columns in (-) and (+) ionisation modes was not able to differentiate the serum samples of subclinical cows or non-responders from those of control cows and days, following the single dose of sporidesmin. However, unlike NMR, the MS was not

able to differentiate between all cows that were dosed and those that were not dosed. Mass spectrometry was able to differentiate the serum metabolites of clinical cows from those of the remaining cows. Using UPLC/MS/MS the molecular ions in serum differentiating the clinical cows from all others could be tentatively identified as the bile acids (BAs) glycocholic acid, taurocholic acid, glycochenodeoxycholic acid or deoxyglycocholic acid, lithocholic acid-glycine conjugate, and taurochenodeoxycholic acid or taurodeoxycholic acid. Concentrations of these BAs all became elevated in the clinical cows after a single dose of sporidesmin. It is well known that BA concentrations increase during cholestasis due to damage to bile ducts and leakage of the bile into the liver and blood (Fickert *et al.*, 2002; Woolbright *et al.*, 2014; Zhang *et al.*, 2012c). Additionally, when hepatocyte damage compounds this, the uptake of BAs from the blood is decreased as well. The changes seen here are likely to be caused by the hepatotoxin; however, they do not represent the early onset changes directly related to sporidesmin damage. Nonetheless, although it was not the intended aim of the study, as far as I am aware, this is the first study to report the main bile acids that become elevated in cows during cholestasis.

It is possible that the changes in metabolites, identified as differentiating between sporidesmin-dosed cows and control cows, are secondary to the initial sporidesmin damage caused at the site of the bile ducts. Sporidesmin is believed to cause bile duct damage through the production of reactive oxygen species (ROS) owing to the oxidation of the disulfide bridge of the piperazine ring by means of interaction with thiols (Barr, 1998; Jordan & Pedersen, 1986; Munday, 1982). This bile duct damage manifests as a necrotising cholangitis, which is only visible through histological analysis, and through biochemical tests. This cholangitis causes inflammation, cell death, and blockage of bile ducts, causing the bile acids to leak into the liver and blood, culminating in cholestasis and additional hepatocyte damage. ROS continues to be produced by the sporidesmin however, so that the hypoxic conditions and the addition of macrophages and leukocytes, as well as platelets act to increase the toxic effect in hepatocytes. Energy is still required for normal functioning and needs to be produced via anaerobic pathways, which culminate in the production of pyruvate and lactate (Kotoh *et al.*, 2011; Schade, 1982). This can lead to acidosis and additional ROS production and damage to cells. The BAs augment this already toxic process by damaging hepatocytes. The mechanism of damage in cattle is unknown, however, three possible mechanisms are proposed based on studies in humans (Woolbright *et al.*, 2015), mice (Woolbright *et al.*, 2014), and rats (Zhang *et al.*, 2012c). The first and second involve interaction with hepatocyte and mitochondrial membranes which leads to loss of membrane potential and decreased efficiency of the cells. Where these two mechanisms differ is in the mode of cell death, either by apoptosis or necrosis. The third

mechanism entails BAs acting as inflammagens; recruiting inflammatory agents through the activation of immune-mediated pathways.

No similarities in serum metabolites were identified between the NMR and MS techniques. There could be a large number of reasons why these differences occurred, for example they are both very different analytical techniques and use different parameters to analyse the samples, and sample preparation and pre-treatments also affect the outcome.

The sample preparation of serum for analysis using the C18 column for UPLC/ESI-MS involved the coagulation of proteins using ice-cold acetonitrile. This is likely to remove any glycoproteins and lipoproteins from the sample, rendering them undetectable using this technique.

Small carboxylic acids, such as lactic acid, formic acid, and citric acid, are too small to interact with the stationary phase of reverse-phase LC columns sufficiently to enable good separation. This means they are eluted early with the salts in the sample. These salts can clog the capillary and disturb the ionisation of compounds, which is why the first eluants in these types of samples are removed as waste. The time period for removal, i.e. the first 2 minutes, depends on parameters such as the sample type and the column used.

Additionally, alcohols such as glycerol are not easily ionisable in MS, and in general, low molecular weight compounds that are polar/hydrophilic are difficult to analyse with chromatography and MS; more method optimisation is required to scan for smaller masses. The HILIC columns retain more hydrophilic compounds and would have enabled analysis of low molecular weight metabolites such as amino acids. Furthermore, lipidomics is a reasonably new area of science, and the analysis of lipids can be complicated, especially due to overlap of ions. Well tested, time-consuming method development is essential.

The NMR was not able to detect BAs. This could be due to the BAs being present in serum at a low enough concentration that the NMR was not sensitive enough to detect them (the detection limit for NMR is ~ 1 μm). Additionally, the NMR samples were not deproteinised, unlike the MS samples, so the composition of the samples are likely to differ. Furthermore, BA structures are relatively complicated, and one of their main roles in the body is to bind lipids to facilitate removal. It may be that the signals of the BAs were removed in the CPMG and p-JRES methods, and the broad resonances recorded in the diffusion-edited analysis are likely to mask any sharper peaks from the BAs. However, this would also mean that most of the BAs would be removed during deproteinising methods for MS analysis.

It is difficult with non-targeted analysis to obtain the optimum conditions for all compounds in a sample simultaneously, particularly when using different analytical techniques and sample preparations. Therefore, while the results from application of the two analytical techniques should not conflict, they do not necessarily have to confirm each other.

The ideal biomarkers for sporidesmin intoxication should be able to identify clinically and subclinically affected animals at an early stage. Facial eczema is heritable in nature, but present day resistance breeding involves introducing sporidesmin to animals and measuring liver enyzme activities. The identification of an easily measurable (less invasive) marker for resistance could also be helpful to identify animals for breeding. Work has and is being carried out on genes associated with the ABC transporter family, specifically ABCG2 which has been identified as a candidate gene for resistance to FE (Babu *et al.*, 2012; Duncan *et al.*, 2007). However, no work has focused on the metabolomic aspects of resistance until now.

This work has expanded the FE knowledge-base by introducing alternative approaches to the discovery of early detection markers of sporidesmin intoxication. This is the first study to investigate metabolomic changes in serum, urine, and milk using ^{1}H NMR, and in serum using UPLC/MS and MS/MS. Additionally, this is the first study to apply time series statistical analyses to the topic. Although the time series method did not prove fruitful for the identification of metabolite groups related to sporidesmin intoxication in this context, it could prove to be highly beneficial for similar studies where metabolic profiles are to be differentiated by their evolution with time. It is possible that there were too few cows per group in the present study for the time series method to be reliable. The number of cows studied impacted somewhat on the results in this research; however, this only became apparent after the trial, and sample analysis. It was not expected that the treated cows would respond so differently and the single dose of sporidesmin was not intended to cause clinical FE. Additionally, financial constraints would not have permitted a larger study set, and ethics approval for a study of larger magnitude, would have been problematic.

6.3 Future work

If an experiment of this type was to be repeated, sampling should begin within a few minutes and hours of the administration of the sporidesmin dose. One limitation of the present study was that the metabolomic changes detected probably transpired after hepatobiliary damage had occurred. Ideally, identifying the metabolites directly related to the ingestion of sporidesmin will provide more insight on the mechanism of action of this toxin.

A long-term study of natural FE, following one or two dairy herds, is required to investigate the 'carry-over' effects of sporidesmin, including the effect of low concentrations of sporidesmin across the seasons and how this accumulates. For example, understanding the accumulative liver damage in subclinicals and non-responders, and how this affects the susceptibility of the cows, as well as reproduction and lactation. It would also be interesting to measure more components in milk to see whether the composition of milk is changing in cows which are affected by sporidesmin. Identifying whether smaller concentrations of sporidesmin produce decreases in milk yield for more resistant cows is also important. Additionally, interest in the area of lipidomics is increasing substantially. Interpretation of changes in the abundance of individual lipids in serum and milk in animals susceptible to facial eczema would be an area to be further investigated. Lipidomics is reasonably new and techniques for method development are still being refined. Additionally, the urine and milk samples were not able to be analysed using UPLC/MS in the present study due primarily to time constraints. Analysing these samples using this technique is an essential next step.

With new knowledge of the metabolites that become elevated in cows following a sporidesmin challenge, it should be possible to apply more targeted analysis in both NMR and MS, allowing better sample preparation, processing, refinement of equipment parameters, and quantification and more accurate identification of metabolites. This may enable direct comparison between the two analytical systems.

Both subclinical and non-responder cows are essentially undetectable in a herd. Although early stage markers, nor markers for subclinical and nonresponder cows were not able to be identified in the present work, I believe it was demonstrated that with earlier sampling following sporidesmin dosing, the techniques applied here could be beneficial for analysis. Additional work on the action of sporidesmin at an early stage in non-responder, subclinical, and clinical cows is essential. The results obtained in this study will hopefully form a foundation for future breakthrough discoveries.

REFERENCES

Adachi, Y., Miya, H., Okuyama, Y., Kamisako, T., & Yamamoto, T. (1996). Hepatocyte canalicular transport of organic anions in bile duct-ligated rats. *International Hepatology Communications, 5*(6), 326-330.

Allen, K., Jaeschke, H., & Copple, B. L. (2011). Bile acids induce inflammatory genes in hepatocytes: A novel mechanism of inflammation during obstructive cholestasis. *American Journal of Pathology, 178*(1), 175-186.

Amathieu, R., Triba, M. N., Nahon, P., Bouchemal, N., Kamoun, W., Haouache, H., . . . Dhonneur, G. (2014). Serum 1H-NMR Metabolomic Fingerprints of Acute-On-Chronic Liver Failure in Intensive Care Unit Patients with Alcoholic Cirrhosis. *Plos One, 9*(2).

Araya, O. S., & Ford, E. J. H. (1981). An investigation of the type of photosensitization caused by the ingestion of st-Johns wort (Hypericum-perforatum) by calves. *Journal of Comparative Pathology, 91*(1), 135-141.

Arrese, M., Ananthananarayanan, M., & Suchy, F. J. (1998). Hepatobiliary transport: Molecular mechanisms of development and cholestasis. *Pediatric Research, 44*(2), 141-147.

Artegoitia, V. M., Middleton, J. L., Harte, F. M., Campagna, S. R., & de Veth, M. J. (2014). Choline and Choline Metabolite Patterns and Associations in Blood and Milk during Lactation in Dairy Cows. *Plos One, 9*(8).

Atherton, L. G., Brewer, D., & Taylor, A. (1974). *Pithomyces chartarum*: A fungal parameter in the aetilogy of some disease of domestic animals *In Mycotoxins* (I.F.H. Purchase ed., pp. 26-68). Amsterdam: Elsevier.

Babu, K., Zhang, J. B., Moloney, S., Pleasants, T., McLean, C. A., Phua, S. H., & Sheppard, A. M. (2012). Epigenetic regulation of ABCG2 gene is associated with susceptibility to xenobiotic exposure. *Journal of Proteomics, 75*(12), 3410-3418.

Bansal, N., Gupta, A., Mitash, N., Shakya, P. S., Mandhani, A., Mahdi, A. A., . . . Mandal, S. K. (2013). Low- and High-Grade Bladder Cancer Determination via Human Serum-Based Metabolomics Approach. *Journal of Proteome Research, 12*(12), 5839-5850.

Barr, A. C. (1998). Hepatotoxicities of ruminants. In T. Garland & A. C. Barr (Eds.), *Toxic Plants and Other Natural Toxicants* (pp. 51-54): CAB International.

Baticz, O., Tomoskozi, S., Vida, L., & Gaal, T. (2002). Relationship between concentration of citrate and ketone bodies in cow's milk. *Acta Vet Hung, 50*(3), 253-261.

Beckwith-Hall, B. M., Thompson, N. A., Nicholson, J. K., Lindon, J. C., & Holmes, E. (2003). A metabonomic investigation of hepatotoxicity using diffusion-edited H-1 NMR spectroscopy of blood serum. *Analyst, 128*(7), 814-818.

Beger, R. D., Sun, J. C., & Schnackenberg, L. K. (2010). Metabolomics approaches for discovering biomarkers of drug-induced hepatotoxicity and nephrotoxicity. *Toxicology and Applied Pharmacology, 243*(2), 154-166.

Bezille, P., Braun, J. P., & LeBars, J. (1984). First identification of facial eczema in Europe: Epidemiological, clinical and biological aspects. *Recueil de Medecine Veterinaire, 160*, 339-347.

Blunt, J. W., Erasmuson, A. F., Ferrier, R. J., & Munro, M. H. G. (1979). Synthesis of haptens related to the benzenoid and indole portions of sporidesmin A - C^{13} NMR-spectra of indole-derivatives. *Australian Journal of Chemistry, 32*(5), 1045-1054.

Bourke, C. A. (2003). The effect of shade, shearing and wool type in the protection of Merino sheep from Hypericum perforatum (St John's wort) poisoning. *Australian Veterinary Journal, 81*(8), 494-498.

Briggs, L. R., Towers, N. R., & Molan, P. C. (1994). Development of an enzyme-linked-immunosorbent-assay for analysis of sporidesmin-A and its metabolites in ovine urine and bile. *Journal of Agricultural and Food Chemistry, 42*(12), 2769-2777.

Bruce, S. J., Jonsson, P., Antti, H., Cloarec, O., Trygg, J., Marklund, S. L., & Moritz, T. (2008). Evaluation of a protocol for metabolic profiling studies on human blood plasma by combined ultra-performance liquid chromatography/mass spectrometry: From extraction to data analysis. *Analytical Biochemistry, 372*(2), 237-249.

Bruce, S. J., Tavazzi, I., Parisod, V., Rezzi, S., Kochhar, S., & Guy, P. A. (2009). Investigation of human blood plasma sample preparation for performing metabolomics using ultrahigh performance liquid chromatography/mass spectrometry. *Analytical Chemistry, 81*(9), 3285-3296.

Bylesjo, M., Rantalainen, M., Cloarec, O., Nicholson, J. K., Holmes, E., & Trygg, J. (2006). OPLS discriminant analysis: combining the strengths of PLS-DA and SIMCA classification. *Journal of Chemometrics, 20*(8-10), 341-351.

Campbell, W. M., Dombroski, G. S., Sharma, I., Partridge, A. C., & Collett, M. G. (2010). Photodynamic chlorophyll *a* metabolites, including phytoporphyrin (phylloerythrin), in the blood of photosensitive livestock: Overview and measurement. *New Zealand Veterinary Journal, 58*(3), 146-154.

Cao, M., Fraser, K., & Rasmussen, S. (2013). Computational analyses of spectral trees from electrospray multi-stage mass spectrometry to aid metabolite identification. *Metabolites, 3*(4), 1036-1050.

Castillo, S., Gopalacharyulu, P., Yetukuri, L., & Oresic, M. (2011). Algorithms and tools for the preprocessing of LC-MS metabolomics data. *Chemometrics and Intelligent Laboratory Systems, 108*(1), 23-32.

Chen, C., Gonzalez, F. J., & Idle, J. R. (2007). LC-MS-based metabolomics in drug metabolism. *Drug Metabolism Reviews, 39*(2-3), 581-597.

Chen, T. L., Xie, G. X., Wang, X. Y., Fan, J., Qiu, Y. P., Zheng, X. J., . . . Jia, W. (2011). Serum and Urine Metabolite Profiling Reveals Potential Biomarkers of Human Hepatocellular Carcinoma. *Molecular & Cellular Proteomics, 10*(7).

Chen, X. B., Susmel, P., Stefanon, B., & Orskov, E. R. (1995). *On the use of purine derivatives in spot urine, plasma and milk samples as indicators of microbial protein supply in sheep and cattle*. Santarem, Portugal: Estacao Zootecnica Nacional.

Chvapil, M., & Ryan, J. N. (1973). The pool of free proline in acute and chronic liver injury and its effect on synthesis of collagen and globular proteins. *Agents and Actions, 3*(1), 38-44.

Clare, N. T. (1944). Photosensitivity diseases in New Zealand. III. The photosensitizing agent in facial eczema. *New Zealand Journal of Science and Technology, 25A*, 202-220.

Clare, N. T. (1952). *Photosensitisation Diseases of Domestic Animals*. England: Farnham Royal, Bucks: Commonwealth Agricultural Bureau.

Clare, N. T. (1955). Photosensitisation in animals. *Advances in Veterinary Science, 2*, 182-211.

Clare, N. T., Sandos, J., & Percival, J. C. (1959). Photosensitivity diseases in New Zealand. XVIII. The relationship between the beaker-test and facial eczema toxicity. *New Zealand Journal of Agricultural Research, 2*, 1087-1095.

Clark, R. G., Duganzich, D. M., Mortleman, L., & Fraser, A. J. (1988). The effect of sporidesmin toxicity on ovine serum vitamin-B12 levels. *New Zealand Veterinary Journal, 36*(2), 51-52.

Collett, M. G., & Matthews, Z. M. (2014). Photosensitivity in cattle grazing Brassica crops. *International Journal of Poisonous Plant Research, 3*(1).

Collett, M. G., Sharma, I., Bullock, S. M., Officer, D. L., & Partridge, A. (2008). Spring eczema. *Proceedings of the Society of Dairy Cattle Veterinarians conference*, 71-76.

Collin, R. G., Briggs, L. R., & Towers, N. R. (1995). Development and evaluation of an enzyme-immunoassay for sporidesmin in pasture. *New Zealand Journal of Agricultural Research, 38*(3), 297-302.

Collin, R. G., Crawford, A., Keogh, R., Morris, C., Munday, R., Phua, S., . . . Wesselink, K. (1998a). Recent research in the prevention of facial eczema. *75th Jubilee NZVA Conference. Dairy cattle and industry. 15th Annual Seminar of the Society of Dairy Cattle Veterinarians of the NZVA, Rotorua, New Zealand, 29th June-2nd July, 1998.*, 133-143.

Collin, R. G., Odriozola, E., & Towers, N. R. (1998b). Sporidesmin production by *Pithomyces chartarum* isolates from Australia, Brazil, New Zealand and Uruguay. *Mycological Research, 102*, 163-166.

Collin, R. G., & Towers, N. R. (1995a). Competition of a sporidesmin-producing *Pithomyces* strain with a nontoxigenic *Pithomyces* strain. *New Zealand Veterinary Journal, 43*(4), 149-152.

Collin, R. G., & Towers, N. R. (1995b). First reported isolation from New Zealand pasture of *Pithomyces chartarum* unable to produce sporidesmin. *Mycopathologia, 130*(1), 37-40.

Cooper, E. R., & Walker, D. (1940). Climatic factors relating to outbreaks of facial eczema in New Zealand. *New Zealand Journal of Science and Technology, 22A*, 30-41.

Cordiner, S. J., & Jordan, T. W. (1983). Inhibition by sporidesmin of hepatocyte bile-acid transport. *Biochemical Journal, 212*(1), 197-204.

Craig, A., Cloareo, O., Holmes, E., Nicholson, J. K., & Lindon, J. C. (2006). Scaling and normalization effects in NMR spectroscopic metabonomic data sets. *Analytical Chemistry, 78*(7), 2262-2267.

Cullen, N. G., Beatson, P. R., Lee, R. S. F. D., P.M., & Morris, C. A. (2014). BRIEF COMMUNICATION: Reducing the risk of photosensitisation in dairy cattle undergoing a facial eczema challenge. *Proceedings of the New Zealand Society of Animal Production, 74*, 158-160.

Cullen, N. G., Morris, C. A., & Hickey, S. M. (2006). Genetic parameters for resistance to facial eczema in dairy cattle. *Proceedings of the New Zealand Society of Animal Production, 66*, 310-314.

Cunningham, I. J., Hopkirk, C. E. M., & Filmer, J. F. (1942). Photosensitivity diseases in New Zealand. I. Facial eczema, its clinical, pathological and biochemical characteristics. *New Zealand Journal of Science and Technology, 24A*, 185-198.

Degroot, M. J. M., Vanhelden, M. A. B., Dejong, Y. F., Coumans, W. A., & Vandervusse, G. J. (1995). The influence of lactate, pyruvate and glucose as exogenous substrates on free-radical defense-mechanisms on isolated rat hearts during ischemia and reperfusion. *Molecular and Cellular Biochemistry, 146*(2), 147-155.

Dettmer, K., Aronov, P. A., & Hammock, B. D. (2007). Mass spectrometry-based metabolomics. *Mass Spectrometry Reviews, 26*(1), 51-78.

Di Menna, M. E., & Bailey, J. R. (1973). *Pithomyces chartarum* spore counts in pasture. *New Zealand Journal of Agricultural Research, 16*(3), 343-351.

Di Menna, M. E., Smith, B. L., & Miles, C. O. (2009). A history of facial eczema (pithomycotoxicosis) research. *New Zealand Journal of Agricultural Research, 52*(4), 345-376.

Dillon, P. (2011). *The Irish Dairy Industry: To 2015 and beyond.* Paper presented at the National Dairy Conference, Cork, Ireland.

Dodd, D. C. (1959). The pathology of facial eczema. *Proceedings of the New Zealand Society of Animal Production, 19*, 48-52.

Done, J., Taylor, A., Russell, D. W., & Mortimer, P. H. (1961). Production of sporidesmin and sporidesmolides by *Pithomyces chartarum*. *Journal of General Microbiology, 26*(2), 207-223.

Duffield, T. F., Lissemore, K. D., McBride, B. W., & Leslie, K. E. (2009). Impact of hyperketonemia in early lactation dairy cows on health and production. *Journal of Dairy Science, 92*(2), 571-580.

Duncan, E. J., Dodds, K. G., Henry, H. M., Thompson, M. P., & Phua, S. H. (2007). Cloning, mapping and association studies of the ovine ABCG2 gene with facial eczema disease in sheep. *Animal Genetics, 38*(2), 126-131.

Dunn, W. B., Bailey, N. J. C., & Johnson, H. E. (2005). Measuring the metabolome: current analytical technologies. *Analyst, 130*(5), 606-625.

Dunn, W. B., Broadhurst, D., Begley, P., Zelena, E., Francis-McIntyre, S., Anderson, N., . . . Goodacre, R. (2011a). Procedures for large-scale metabolic profiling of serum and plasma using gas chromatography and liquid chromatography coupled to mass spectrometry. *Nature Protocols, 6*(7), 1060-1083.

Dunn, W. B., Broadhurst, D. I., Atherton, H. J., Goodacre, R., & Griffin, J. L. (2011b). Systems level studies of mammalian metabolomes: the roles of mass spectrometry and nuclear magnetic resonance spectroscopy. *Chemical Society Reviews, 40*(1), 387-426.

Ebbels, T. M. D., Keun, H. C., Beckonert, O. P., Bollard, M. E., Lindon, J. C., Holmes, E., & Nicholson, J. K. (2007). Prediction and classification of drug toxicity using probabilistic modeling of temporal metabolic data: The Consortium on Metabonomic Toxicology screening approach. *Journal of Proteome Research, 6*(11), 4407-4422.

Ellis, D. I., Dunn, W. B., Griffin, J. L., Allwood, J. W., & Goodacre, R. (2007). Metabolic fingerprinting as a diagnostic tool. *Pharmacogenomics, 8*(9), 1243-1266.

Ellis, D. I., & Goodacre, R. (2006). Metabolic fingerprinting in disease diagnosis: biomedical applications of infrared and Raman spectroscopy. *Analyst, 131*(8), 875-885.

Ellis, M. B. (1960). Dematiaceous hyphomycetes. I. *Mycological Papers, 76*, 1-36.

Enjalbert, F., Nicot, M. C., Baourthe, C., & Moncoulon, R. (2001). Ketone bodies in milk and blood of dairy cows: Relationship between concentrations and utilization for detection of subclinical ketosis. *Journal of Dairy Science, 84*(3), 583-589.

Erfle, J. D., Sauer, F. D., & Fisher, L. J. (1974). Interrelationships Between Milk Carnitine and Blood and Milk Components and Tissue Carnitine in Normal and Ketotic Cows. *Journal of Dairy Science, 57*(6), 671-676.

Evans, J. V., McFarlane, D., Reid, C. S. W., & Perrin, D. D. (1957). Photosensitivity diseases in New Zealand IX. The susceptibility of the guinea pig to facial eczema. *New Zealand Journal of Science and Technology, 38A*, 491-496.

Fairclough, R. J., Ronaldson, J. W., Jonas, W. W., Mortimer, P. H., & Erasmuson, A. G. (1984). Failure of immunization against sporidesmin or a structurally related compound to protect ewes against facial eczema. *New Zealand Veterinary Journal, 32*(7), 101-104.

Faulkner, A., & Peaker, M. (1982). Reviews of the progress of dairy science - secretion of citrate into milk. *Journal of Dairy Research, 49*(1), 159-169.

Feng, J. H., Li, X. J., Pei, F. K., Chen, X., Li, S. L., & Nie, Y. X. (2002). H-1 NMR analysis for metabolites in serum and urine from rats administrated chronically with La(NO3)(3). *Analytical Biochemistry, 301*(1), 1-7.

Fickert, P., Zollner, G., Fuchsbichler, A., Stumptner, C., Weiglein, A. H., Lammert, F., . . . Trauner, M. (2002). Ursodeoxycholic acid aggravates bile infarcts in bile duct-ligated and Mdr2 knockout mice via disruption of cholangioles. *Gastroenterology, 123*(4), 1238-1251.

Fischer, H., Moldenhauer, O., & Sus, O. (1931). Justus Liebig's Annals of chemistry on phyllo-erythrin and pseudo-phyllo-erythrin. *Justus Liebigs Annalen Der Chemie, 485*, 1-25.

Fitzgerald, J. M., Collin, R. G., & Towers, N. R. (1998). Biological control of sporidesmin-producing strains of *Pithomyces chartarum* by biocompetitive exclusion. *Letters in Applied Microbiology, 26*(1), 17-21.

Flåøyen, A., & Smith, B. L. (1992). Parenchymal injury and biliary obstruction in relation to photosensitization in sporidesmin-intoxicated lambs. *Veterinary Research Communications, 16*(5), 337-344.

Folch, J., Lees, M., & Stanley, G. H. S. (1957). A simple method for the isolation and purification of total lipids from animal tissues. *Journal of Biological Chemistry, 226*(1), 497-509.

Ford, E. J. H. (1974). Activity of gamma-glutamyl transpeptidase and other enzymes in serum of sheep with liver or kidney damage. *Journal of Comparative Pathology, 84*(2), 231-243.

Ford, E. J. H., & Gopinath, C. (1974). Excretion of phylloerythrin and bilirubin by horse. *Research in Veterinary Science, 16*(2), 186-198.

Ford, E. J. H., & Gopinath, C. (1976). Excretion of phylloerythrin and bilirubin by calves and sheep. *Research in Veterinary Science, 21*(1), 12-18.

Fraser, K., Harrison, S. J., Lane, G. A., Otter, D. E., Hemar, Y., Quek, S. Y., & Rasmussen, S. (2012). Non-targeted analysis of tea by hydrophilic interaction liquid chromatography and high resolution mass spectrometry. *Food Chemistry, 134*(3), 1616-1623.

Fraser, K., Lane, G. A., Otter, D. E., Harrison, S. J., Quek, S. Y., Hemar, Y., & Rasmussen, S. (2014). Non-targeted analysis by LC-MS of major metabolite changes during the oolong tea manufacturing in New Zealand. *Food Chemistry, 151*, 394-403.

Fraser, K., Lane, G. A., Otter, D. E., Hemar, Y., Quek, S. Y., Harrison, S. J., & Rasmussen, S. (2013). Analysis of metabolic markers of tea origin by UHPLC and high resolution mass spectrometry. *Food Research International, 53*(2), 827-835.

Froh, M., Zhong, Z., Walbrun, P., Lehnert, M., Netter, S., Wiest, R., . . . Thurman, R. G. (2008). Dietary glycine blunts liver injury after bile duct ligation in rats. *World Journal of Gastroenterology, 14*(39), 5996-6003.

Galitzer, S. J., & Oehme, F. W. (1978). Photosensitization - literature review. *Veterinary Science Communications, 2*(3), 217-230.

Gallagher, C. H. (1964). Effect of sporidesmin on liver enzyme systems. *Biochemical Pharmacology, 13*(7), 1017-1026.

Garnsworthy, P. C., Masson, L. L., Lock, A. L., & Mottram, T. T. (2006). Variation of milk citrate with stage of lactation and de novo fatty acid synthesis in dairy cows. *Journal of Dairy Science, 89*(5), 1604-1612.

Geishauser, T., Leslie, K., Tenhag, J., & Bashiri, A. (2000). Evaluation of eight cow-side ketone tests in milk for detection of subclinical ketosis in dairy cows. *Journal of Dairy Science, 83*(2), 296-299.

Ghosh, S., Sengupta, A., Sharma, S., & Sonawat, H. M. (2012). Metabolic fingerprints of serum, brain, and liver are distinct for mice with cerebral and noncerebral malaria: A H-1 NMR spectroscopy-based metabonomic study. *Journal of Proteome Research, 11*(10), 4992-5004.

Ghosh, S., Sengupta, A., Sharma, S., & Sonawat, H. M. (2013). Metabolic perturbations of kidney and spleen in murine cerebral malaria: ^{1}H NMR-based metabolomic study. *Plos One, 8*(9), 1-12.

Gilruth, J. A. (1897). *Annual Report of the Department of Agriculture, Wellington, New Zealand*, 58.

Gilruth, J. A. (1908). Report of the New Zealand Department of Agriculture. Appendix VII. Veterinary Division, Wellington, New Zealand. 188-191.

Glenn, B. L., Monlux, A. W., & Panciera, R. J. (1964). A hepatogenous photosensitivity disease of cattle. I. Experimental production and clinical aspects of disease. *Pathologia Veterinaria, 1*(6), 469-484.

Goldsmith, P., Fenton, H., Morris-Stiff, G., Ahmad, N., Fisher, J., & Prasad, K. R. (2010). Metabonomics: A useful tool for the future surgeon. *Journal of Surgical Research, 160*(1), 122-132.

Grace, N. D., Munday, R., Thompson, A. M., Towers, N. R., O'Donnell, K., McDonald, R. M., . . . Ford, A. J. (1997). Evaluation of intraruminal devices for combined facial eczema control and trace element supplementation in sheep. *New Zealand Veterinary Journal, 45*(6), 236-238.

Griffiths, W. J., & Sjovall, J. (2010). Bile acids: analysis in biological fluids and tissues. *Journal of Lipid Research, 51*(1), 23-41.

Groussard, C., Morel, I., Chevanne, M., Monnier, M., Cillard, J., & Delamarche, A. (2000). Free radical scavenging and antioxidant effects of lactate ion: an in vitro study. *Journal of Applied Physiology, 89*(1), 169-175.

Guan, M. M., Xie, L. Y., Diao, C. F., Wang, N., Hu, W. Y., Zheng, Y. Q., . . . Gao, H. C. (2013). Systemic perturbations of key metabolites in diabetic rats during the evolution of diabetes studied by urine metabonomics. *Plos One, 8*(4).

Hagey, L. R., Gavrilkina, M. A., & Hofmann, A. F. (1997). Age-related changes in the biliary bile acid composition of bovids. *Canadian Journal of Zoology-Revue Canadienne De Zoologie, 75*(8), 1193-1201.

Halliwell, B., & Gutteridge, J. M. C. (1999). *Free radicals in biology and medicine* (3 ed.). USA: Oxford Science Publications.

Halouska, S., & Powers, R. (2006). Negative impact of noise on the principal component analysis of NMR data. *Journal of Magnetic Resonance, 178*(1), 88-95.

Hansen, D. E., McCoy, R. D., Hedstrom, O. R., Snyder, S. P., & Ballerstedt, P. B. (1994). Photosensitization associated with exposure to *Pithomyces chartarum* in lambs. *Journal of the American Veterinary Medical Association, 204*(10), 1668-1671.

Harzia, H., Ilves, A., Ots, M., Henno, M., Joudu, I., Kaart, T., . . . Soomets, U. (2013). Alterations in milk metabolome and coagulation ability during the lactation of dairy cows. *Journal of Dairy Science, 96*(10), 6440-6448.

Ho, C. S., Lam, C. W. K., Chan, M. H. M., Cheung, R. C. K., Law, L. K., Lit, L. C. W., . . . Tai, H. L. (2003). Electrospray ionisation mass spectrometry: principles and clinical applications. *The Clinical biochemist. Reviews / Australian Association of Clinical Biochemists, 24*(1), 3-12.

Hoffman, D. L., & Brookes, P. S. (2009). Oxygen Sensitivity of Mitochondrial Reactive Oxygen Species Generation Depends on Metabolic Conditions. *Journal of Biological Chemistry, 284*(24), 16236-16245.

Hohenboken, W. D., Robertson, J. L., Blodgett, D. J., Morris, C. A., & Towers, N. R. (2000). Sporidesmin-induced mortality and histological lesions in mouse lines divergently selected for response to toxins in endophyte-infected fescue. *Journal of Animal Science, 78*(8), 2157-2163.

Holcapek, M., Kolarova, L., & Nobilis, M. (2008). High-performance liquid chromatography-tandem mass spectrometry in the identification and determination of phase I and phase II drug metabolites. *Analytical and Bioanalytical Chemistry, 391*(1), 59-78.

Holmes, E., Nicholls, A. W., Lindon, J. C., Connor, S. C., Connelly, J. C., Haselden, J. N., . . . Nicholson, J. K. (2000). Chemometric models for toxicity classification based on NMR spectra of biofluids. *Chemical Research in Toxicology, 13*(6), 471-478.

Hopkirk, C. S. M. (1936). Facial dermatitis in sheep in New Zealand. A photosensitivity disease of non-pigmented skin. *New Zealand Journal of Agriculture, 52*, 98-103.

Hu, F. Y., Furihata, K., Ito-Ishida, M., Kaminogawa, S., & Tanokura, M. (2004). Nondestructive observation of bovine milk by NMR spectroscopy: Analysis of existing states of compounds and detection of new compounds. *Journal of Agricultural and Food Chemistry, 52*(16), 4969-4974.

Ilcol, Y. O., Ozbek, R., Hamurtekin, E., & Ulus, I. H. (2005). Choline status in newborns, infants, children, breast-feeding women, breast-fed infants and human breast milk. *Journal of Nutritional Biochemistry, 16*(8), 489-499.

Ishihara, K., Katsutani, N., Asai, N., Inomata, A., Uemura, Y., Suganuma, A., . . . Aoki, T. (2009). Identification of urinary biomarkers useful for distinguishing a difference in mechanism of toxicity in rat model of cholestasis. *Basic & Clinical Pharmacology & Toxicology, 105*(3), 156-166.

Jacobsen, N. E. (2007). *NMR spectroscopy explained: simplified theory, applications and examples for organic chemistry and structural biology*. New Jersey: Wiley-Interscience.

Janeway, C. A. J., Travers, P., Walport, M., & Shlomchik, M. J. (2001). The major histocompatibility complex and its functions *Immunobiology: The immune system in health and disease* (5 ed.). New York: Garland Science.

Jiang, C. Y., Yang, K. M., Yang, L., Miao, Z. X., Wang, Y. H., & Zhu, H. B. (2013). A H-1 NMR-based metabonomic investigation of time-related metabolic trajectories of the plasma, urine and liver extracts of hyperlipidemic hamsters. *Plos One, 8*(6).

Johnson, A. E. (1982). Toxicological aspects of photosensitization in livestock. *Journal of the National Cancer Institute, 69*(1), 253-258.

Johnson, W. E., Li, C., & Rabinovic, A. (2007). Adjusting batch effects in microarray expression data using empirical Bayes methods. *Biostatistics, 8*(1), 118-127.

Jordan, T. W., & Pedersen, J. S. (1986). Sporidesmin and gliotoxin induce cell detachment and perturb microfilament structure in cultured liver cells. *Journal of Cell Science, 85*, 33-46.

Katsumi, T., Tomita, K., Leung, P. S. C., Yang, G. X., Gershwin, M. E., & Ueno, Y. (2015). Animal Models of Primary Biliary Cirrhosis. *Clinical Reviews in Allergy & Immunology, 48*(2-3), 142-153.

Kellerman, T. S., Coetzer, J. A. W., Naude, T. W., & Botha, C. J. (2005). *Plant Poisonings and Mycotoxicoses of Livestock in South Africa* (2 ed.): Oxford University Press.

Kim, J. W., Ryu, S. H., Kim, S., Lee, H. W., Lim, M. S., Seong, S. J., . . . Kim, K. B. (2013). Pattern Recognition Analysis for Hepatotoxicity Induced by Acetaminophen Using Plasma and Urinary H-1 NMR-Based Metabolomics in Humans. *Analytical Chemistry, 85*(23), 11326-11334.

Kim, K., Mall, C., Taylor, S. L., Hitchcock, S., Zhang, C., Wettersten, H. I., . . . Weiss, R. H. (2014). Mealtime, Temporal, and Daily Variability of the Human Urinary and Plasma Metabolomes in a Tightly Controlled Environment. *Plos One, 9*(1).

Klein, M. S., Almstetter, M. F., Schlamberger, G., Nurnberger, N., Dettmer, K., Oefner, P. J., . . . Gronwald, W. (2010). Nuclear magnetic resonance and mass spectrometry-based milk metabolomics in dairy cows during early and late lactation. *Journal of Dairy Science, 93*(4), 1539-1550.

Klein, M. S., Buttchereit, N., Miemczyk, S. P., Immervoll, A. K., Louis, C., Wiedemann, S., . . . Gronwald, W. (2012). NMR metabolomic analysis of dairy cows reveals milk glycerophosphocholine to phosphocholine ratio as prognostic biomarker for risk of ketosis. *Journal of Proteome Research, 11*(2), 1373-1381.

Kohler, M., Sandberg, A., Kjellqvist, S., Thomas, A., Karimi, R., Nyren, S., . . . Wheelock, A. M. (2013). Gender differences in the bronchoalveolar lavage cell proteome of patients with chronic obstructive pulmonary disease. *Journal of Allergy and Clinical Immunology, 131*(3), 743-+.

Kotoh, K., Kato, M., Kohjima, M., Tanaka, M., Miyazaki, M., Nakamura, K., . . . Takayanagi, R. (2011). Lactate dehydrogenase production in hepatocytes is increased at an early stage of acute liver failure. *Experimental and Therapeutic Medicine, 2*(2), 195-199.

Koulman, A., Tapper, B. A., Fraser, K., Cao, M. S., Lane, G. A., & Rasmussen, S. (2007). High-throughput direct-infusion ion trap mass spectrometry: a new method for metabolomics. *Rapid Communications in Mass Spectrometry, 21*(3), 421-428.

Kouskoumvekaki, I., & Panagiotou, G. (2011). Navigating the human metabolome for biomarker identification and design of pharmaceutical molecules. *Journal of Biomedicine and Biotechnology, 2011*, 1-19.

Kurt, M., Onal, I. K., Parlak, E., Shorbagi, A., Kekilli, M., Ibis, M., . . . Sasmaz, N. (2010). Do metabolic alterations serve as biochemical markers in the diagnosis of malignant biliary obstruction? An observational study. *European Journal of Gastroenterology & Hepatology, 22*(1), 58-60.

Kutila, T., Pyorala, S., Kaartinen, L., Isomaki, R., Vahtola, K., Myllykoski, L., & Saloniemi, H. (2003). Lactoferrin and citrate concentrations at drying-off and during early mammary involution of dairy cows. *Journal of Veterinary Medicine Series a-Physiology Pathology Clinical Medicine, 50*(7), 350-353.

Larive, C. K., Barding, G. A., & Dinges, M. M. (2015). NMR spectroscopy for metabolomics and metabolic profiling. *Analytical Chemistry, 87*(1), 133-146.

Lavine, B., & Workman, J. (2008). Chemometrics. *Analytical Chemistry, 80*(12), 4519-4531.

Leaver, D. D. (1968). Sporidesmin poisoning in sheep. I. Changes in bile secretion and excretion of sporidesmin in bile. *Research in Veterinary Science, 9*(3), 255-&.

Levy, H. R. (1964). Effects of weaning + milk on mammary fatty acid synthesis. *Biochimica Et Biophysica Acta, 84*(3), 229-&.

Liland, K. H. (2011). Multivariate methods in metabolomics - from pre-processing to dimension reduction and statistical analysis. *Trends in Analytical Chemistry, 30*(6), 827-841.

Lindon, J. C., Keun, H. C., Ebbels, T. M. D., Pearce, J. M. T., Holmes, E., & Nicholson, J. K. (2005). The Consortium for Metabonomic Toxicology (COMET): aims, activities and achievements. *Pharmacogenomics, 6*(7), 691-699.

Lindon, J. C., Nicholson, J. K., & Everett, J. R. (1999). NMR spectroscopy of biofluids. *Annual Reports on Nmr Spectroscopy, Vol 38, 38*, 1-88.

Lindon, J. C., Nicholson, J. K., & Holmes, E. (2007). *The handbook of metabonomics and metabolomics*. Amsterdam: Elsevier.

Lindon, J. C., Nicholson, J. K., Holmes, E., Antti, H., Bollard, M. E., Keun, H., . . . Thomas, C. (2003). Contemporary issues in toxicology - The role of metabonomics in toxicology and its evaluation by the COMET project. *Toxicology and Applied Pharmacology, 187*(3), 137-146.

Linzell, J. L., Mepham, T. B., & Peaker, M. (1976). The secretion of citrate into milk. *Journal of Physiology-London, 260*(3), 739-750.

Liu, M. L., Nicholson, J. K., Parkinson, J. A., & Lindon, J. C. (1997). Measurement of biomolecular diffusion coefficients in blood plasma using two-dimensional H-1-H-1 diffusion-edited total-correlation NMR spectroscopy. *Analytical Chemistry, 69*(8), 1504-1509.

Liu, M. L., Tang, H. R., Nicholson, J. K., & Lindon, J. C. (2002). Use of H-1 NMR-determined diffusion coefficients to characterize lipoprotein fractions in human blood plasma. *Magnetic Resonance in Chemistry, 40*, S83-S88.

Long, L. H., & Halliwell, B. (2009). Artefacts in cell culture: Pyruvate as a scavenger of hydrogen peroxide generated by ascorbate or epigallocatechin gallate in cell culture media. *Biochemical and Biophysical Research Communications, 388*(4), 700-704.

Ludwig, C., & Viant, M. R. (2010). Two-dimensional J-resolved NMR Spectroscopy: Review of a Key Methodology in the Metabolomics Toolbox. *Phytochemical Analysis, 21*(1), 22-32.

Lundstrom, S. L., Yang, J., Kallberg, H. J., Thunberg, S., Gafvelin, G., Haeggstrom, J. Z., . . . Wheelock, C. E. (2012). Allergic Asthmatics Show Divergent Lipid Mediator Profiles from Healthy Controls Both at Baseline and following Birch Pollen Provocation. *Plos One, 7*(3).

MacIntyre, D. A., Jimenez, B., Lewintre, E. J., Martin, C. R., Schafer, H., Ballesteros, C. G., . . . Pineda-Lucena, A. (2010). Serum metabolome analysis by (1)H-NMR reveals differences between chronic lymphocytic leukaemia molecular subgroups. *Leukemia, 24*(4), 788-797.

Madsen, R., Lundstedt, T., & Trygg, J. (2010). Chemometrics in metabolomics- a review in human disease diagnosis. *Analytica Chimica Acta, 659*(1-2), 23-33.

Maher, A. D., Hayes, B., Cocks, B., Marett, L., Wales, W. J., & Rochfort, S. J. (2013). Latent biochemical relationships in the blood-milk metabolic axis of dairy cows revealed by statistical integration of H-1 NMR spectroscopic data. *Journal of Proteome Research, 12*(3), 1428-1435.

Maher, A. D., Zirah, S. F. M., Holmes, E., & Nicholson, J. K. (2007). Experimental and analytical variation in human urine in H-1 NMR spectroscopy-based metabolic phenotyping studies. *Analytical Chemistry, 79*(14), 5204-5211.

Marchlewski, L. (1904). The history of the discovery of the chemical relationship of chlorophyll and blood pigment. *Archiv Fur Die Gesamte Physiologie Des Menschen Und Der Tiere, 102*(1/2), 111-115.

Marieb, E. (2004). *Human Anatomy and Physiology*. New York: Benjamin-Cummings Publishing Company.

McAloon, C. G., Doherty, M. L., O'Neill, H., Badminton, M., & Ryan, E. G. (2015). Bovine congenital erythropoietic protoporphyria in a crossbred limousin heifer in Ireland. *Irish Veterinary Journal, 68*(1), 15.

Mehlman, M. A., Therriau.Dg, & Tobin, R. B. (1971). Carnitine C^{14} metabolism in choline-deficient, alloxandiabetic choline-deficient and insulin-treated rats. *Metabolism-Clinical and Experimental, 20*(1), 100-&.

Middleton, M. C. (1974). Effects of mycotoxin sporidesmin on swelling and respiration of liver-mitochondria. *Biochemical Pharmacology, 23*(4), 801-810.

Miyazaki, K., Nakayama, F., & Koga, A. (1984). Effect of chenodeoxycholic acid and ursodeoxycholic acids on isolated adult human hepatocytes. *Digestive Diseases and Sciences, 29*(12), 1123-1130.

Moan, J., Western, A., & Rimington, C. (1988). Photomodification of porphyrins in biological systems. In G. Moreno (Ed.), *Photosensitisation* (pp. 407-418). Berlin: Springer Verlag.

Moreira, C. N., Souza, S. N., Barini, A. C., Araujo, E. G., & Fioravanti, M. C. S. (2012). Serum gamma-glutamyltransferase activity as an indicator of chronic liver injury in cattle with no clinical signs. *Arquivo Brasileiro De Medicina Veterinaria E Zootecnia, 64*(6), 1403-1410.

Morris, C. A. (2011). Managing increasing facial eczema challenges in dairying. *SFF project report.* Retrieved from http://maxa.maf.govt.nz/sff/about-projects/search/C08-034/

Morris, C. A., Burton, L. J., Towers, N. R., Cullen, N. G., Rendel, J. M., & Johnson, D. L. (1998). Genetics of susceptibility to facial eczema in Friesian and Jersey cattle. *New Zealand Journal of Agricultural Research, 41*(3), 347-357.

Morris, C. A., Cullen, N. G., & Munday, R. (2007). Testing glutathione-S-transferase for an association with facial eczema resistance in cattle. *Proceedings of the New Zealand Society of Animal Production 67th Conference, Wanaka, New Zealand, 20-22 June 2007., 67*, 361-364.

Morris, C. A., Hickey, S. M., DeNicolo, G., & Tempero, H. J. (2002). Lifetime survival of Jersey-sired cows following natural challenge with facial eczema during first lactation. *New Zealand Journal of Agricultural Research, 45*(3), 165-170.

Morris, C. A., Hickey, S. M., & Phua, S. H. (2009). Relationship between blood phylloerythrin concentration and gamma-glutamyltransferase activity in facial eczema-affected cattle and sheep. *Proceedings of the New Zealand Society of Animal Production, 69*, 118 - 122.

Morris, C. A., Phua, S. H., Cullen, N. G., & Towers, N. R. (2013). Review of genetic studies of susceptibility to facial eczema in sheep and dairy cattle. *New Zealand Journal of Agricultural Research, 56*(2), 156-170.

Morris, C. A., Towers, N. R., Hohenboken, W. D., Maqbool, N., Smith, B. L., & Phua, S. H. (2004). Inheritance of resistance to facial eczema: a review of research findings from sheep and cattle in New Zealand. *New Zealand Veterinary Journal, 52*(5), 205-215.

Morris, C. A., Towers, N. R., Smith, B. L., & Southey, B. R. (1991a). Progeny testing bulls for susceptibility to facial eczema. *New Zealand Journal of Agricultural Research, 34*(4), 413-417.

Morris, C. A., Towers, N. R., Tempero, H. J., Cox, N. R., & Henderson, H. V. (1990). Facial eczema in Jersey cattle - heritability and correlation with production. In A. Parry (Ed.), *Proceedings of the New Zealand Society of Animal Production, Vol 50 1990* (pp. 255-259). Hamilton: New Zealand Society of Animal Production Inc.

Morris, C. A., Towers, N. R., Wesselink, C., & Southey, B. R. (1991b). Effects of facial eczema on ewe reproduction and postnatal lamb survival in romney sheep. *New Zealand Journal of Agricultural Research, 34*(4), 407-412.

Morris, C. A., Towers, N. R., Wheeler, M., & Wesselink, C. (1995). Selection for or against facial eczema susceptibility in Romney sheep, as monitored by serum concentrations of a liver enzyme. *New Zealand Journal of Agricultural Research, 38*(2), 211-219.

Mortimer, P. H. (1963). Facial eczema: pathology. *Annual Report, Animal Research in the New Zealand Department of Agriculture*, 27.

Mortimer, P. H. (1971). Sporidesmin poisoning in Jersey cows. *Research in the New Zealand Department of Agriculture: Annual Report of Research Division*, 65-66.

Mortimer, P. H., Di Menna, M. E., & White, E. P. (1978a). Mycotoxicoses in cattle. In T. D. Wyllie & L. G. Moorehouse (Eds.), *Mycotoxic Fungi, Mycotoxins, Mycotoxicoses - An Encyclopedic Handbook. Volume 2. Mycotoxicoses of Domestic and Laboratory Animals, Poultry, and Aquatic Invertebrates and Vertebrates* (pp. 63-72). New York: Marcel Dekker.

Mortimer, P. H., Shorland, F. B., & Taylor, A. (1962). Early hepatic dysfunction preceding biliary obstruction in sheep intoxicated with sporidesmin. *Nature, 194*, 550-551.

Mortimer, P. H., & Smith, B. L. (1983). Fungal toxin induced photosensitisation. In R. F. Keeler & A. T. Tu (Eds.), *In Handbook of Natural Toxins*. New York: Dekker.

Mortimer, P. H., White, E. P., & Di Menna, M. E. (1978b). Mycotoxicoses in sheep. In T. D. Wyllie & L. G. Moorehouse (Eds.), *Mycotoxic Fungi, Mycotoxins, Mycotoxicoses - An Encyclopedic Handbook. Volume 2. Mycotoxicoses of Domestic and Laboratory Animals, Poultry, and Aquatic Invertebrates and Vertebrates* (pp. 195-203). New York: Marcel Dekker.

Morton, J. M., & Campbell, P. H. (1997). Disease signs reported in south-eastern Australian dairy cattle while grazing *Brassica* species. *Australian Veterinary Journal, 75*(2), 109-113.

MPI. (2010). *Dairy*. Retrieved from: http://archive.mpi.govt.nz/agriculture/pastoral/dairy

Munday, R. (1982). Studies on the mechanism of toxicity of the mycotoxin, sporidesmin. 1. Generation of superoxide radical by sporidesmin. *Chemico-Biological Interactions, 41*(3), 361-374.

Munday, R. (1984a). Studies on the mechanism of toxicity of the mycotoxin sporidesmin. 2. Evidence for intracellular generation of superoxide radical from sporidesmin. *Journal of Applied Toxicology, 4*(4), 176-181.

Munday, R. (1984b). Studies on the mechanism of toxicity of the mycotoxin sporidesmin. 3. Inhibition by metals of the generation of superoxide radical by sporidesmin *Journal of Applied Toxicology, 4*(4), 182-186.

Munday, R. (1989). Toxicity of thiols and disulfides - involvement of free-radical species. *Free Radical Biology and Medicine, 7*(6), 659-673.

Munday, R., & Manns, E. (1989). Protection by iron salts against sporidesmin intoxication in sheep. *New Zealand Veterinary Journal, 37*(2), 65-68.

Munday, R., Thompson, A. M., Fowke, E. A., Wesselink, C., Smith, B. L., Towers, N. R., . . . Ford, A. J. (1997). A zinc-containing intraruminal device for facial eczema control in lambs. *New Zealand Veterinary Journal, 45*(3), 93-98.

Munday, R., Thompson, A. M., Smith, B. L., Towers, N. R., O'Donnell, K., McDonald, R. M., & Stirnemann, M. (2001). A zinc-containing intraruminal device for prevention of the

sporidesmin-induced cholangiopathy of facial eczema in calves. *New Zealand Veterinary Journal, 49*(1), 29-33.

Naresh, C. N., Hayen, A., Weening, A., Craig, J. C., & Chadban, S. J. (2013). Day-to-Day Variability in Spot Urine Albumin-Creatinine Ratio. *American Journal of Kidney Diseases, 62*(6), 1095-1101.

New Zealand Dairy Statistics. (2012-2013). Retrieved from: http://www.lic.co.nz/user/file/DAIRY%20STATISTICS%202012-13-WEB.pdf

Nicholson, J. K., Foxall, P. J. D., Spraul, M., Farrant, R. D., & Lindon, J. C. (1995). 750-MHz H-1 and H-1-C-13 NMR-spectroscopy of human blood-plasma. *Analytical Chemistry, 67*(5), 793-811.

Nie, H. G., Liu, R. R., Yang, Y. Y., Bai, Y., Guan, Y. F., Qian, D. Q., . . . Liu, H. W. (2010). Lipid profiling of rat peritoneal surface layers by online normal- and reversed-phase 2D LC QToF-MS. *Journal of Lipid Research, 51*(9), 2833-2844.

Nishijima, T., Nishina, M., & Fujiwara, K. (1997). Measurement of lactate levels in serum and bile using proton nuclear magnetic resonance in patients with hepatobiliary diseases: Its utility in detection of malignancies. *Japanese Journal of Clinical Oncology, 27*(1), 13-17.

Northfield, T. C., Ahmed, H., Jazwari, R., & Zentler-Munro, P. (Eds.). (2000). *Bile acids in hepatobiliary disease* (1 ed.). Netherlands: Springer.

Odunsi, K., Wollman, R. M., Ambrosone, C. B., Hutson, A., McCann, S. E., Tammela, J., . . . Alderfer, J. L. (2005). Detection of epithelial ovarian cancer using H-1-NMR-based metabonomics. *International Journal of Cancer, 113*(5), 782-788.

Oshima, M., & Fuse, H. (1981). Citric acid concentration in sub-clinical mastitic milk. *Journal of Dairy Research, 48*(3), 387-392.

Ozmen, O., Sahinduran, S., Haligur, M., & Albay, M. K. (2008). Clinicopathological studies on facial eczema outbreak in sheep in southwest Turkey. *Tropical Animal Health and Production, 40*(7), 545-551.

Pardee, A. B., & Potter, V. R. (1949). Malonate inhibition of oxidations in the krebs tricarboxylic acid cycle. *Journal of Biological Chemistry, 178*(1), 241-250.

Pence, M. E., & Liggett, A. D. (2002). Congenital erythropoietic protoporphyria in a Limousin calf. *Journal of the American Veterinary Medical Association, 221*(2), 277-279.

Percival, J. C. (1959). Photosensitivity diseases in New Zealand. XVII. The association of *Sporidesmium bakeri* with facial eczema. *New Zealand Journal of Agricultural Research, 2*, 1041-1056.

Perrin, D. D. (1957). Photosensitivity disease in New Zealand. X. The guinea pig as an experimental animal in the investigation of facial eczema. *New Zealand Journal of Science and Technology, 38A*, 669-679.

Perrin, D. D. (1958a). Determination of phylloerythrin in blood. *Biochemical Journal, 68*, 314-318.

Perrin, D. D. (1958b). Form in which phylloerythrin occurs in bile and blood. *Biochemical Journal, 68*, 318-319.

Perrin, D. D., White, E. P., & Clare, N. T. (1953). Some recent advances in facial eczema research. *Proc. 13th. Ann. Conf. N.Z. Soc. anim. Prod., 13*, 121-125 pp.

Pinotti, L. (2012). *Vitamin-Like Supplementation in Dairy Ruminants: The Case of Choline*.

Pinto, C., Santos, V. M., Dinis, J., Peleteiro, M. C., Fitzgerald, J. M., Hawkes, A. D., & Smith, B. L. (2005). Pithomycotoxicosis (facial eczema) in ruminants in the Azores, Portugal. *Veterinary Record, 157*(25), 805-809.

Psychogios, N., Hau, D. D., Peng, J., Guo, A. C., Mandal, R., Bouatra, S., . . . Wishart, D. S. (2011). The human serum metabolome. *Plos One, 6*(2), 1-23.

Qiu, Y., & Ree, D. (2014). Gas Chromatography in Metabolomics Study. In X. Guo (Ed.), *Advances in gas chromatography*: InTech.

Quinlan, C. L., Orr, A. L., Perevoshchikova, I. V., Treberg, J. R., Ackrell, B. A., & Brand, M. D. (2012). Mitochondrial Complex II Can Generate Reactive Oxygen Species at High Rates in Both the Forward and Reverse Reactions. *Journal of Biological Chemistry, 287*(32), 27255-27264.

Radostits, O. M., Gay, C. C., Blood, D. C., & Hinchcliff, K. W. (2000). *Veterinary Medicine: A Textbook of the Diseases of Cattle, Sheep, Pigs, Goats, and Horses* (9th ed.): Saunders Ltd.

Ramadan, Z., Jacobs, D., Grigorov, M., & Kochhar, S. (2006). Metabolic profiling using principal component analysis, discriminant partial least squares, and genetic algorithms. *Talanta, 68*, 1683-1691.

Richardson, O. C., Scott, M. L. J., Tanner, S. F., Waterton, J. C., & Buckley, D. L. (2012). Overcoming the low relaxivity of gadofosveset at high field with spin locking. *Magnetic Resonance in Medicine, 68*(4), 1234-1238.

Robertson, D. G., Watkins, P. B., & Reily, M. D. (2011). Metabolomics in toxicology: preclinical and clinical applications. *Toxicological Sciences, 120*, S146-S170.

Russell, D. W. (1960). Sporidesmolide-I, a metabolic product of *Sporidesmium bakeri* Syd. *Biochimica Et Biophysica Acta, 45*(2), 411-412.

Russell, D. W. (1962). Depsipeptides of *Pithomyces chartarum* - structure of sporidesmolide I. *Journal of the Chemical Society*(0), 753-761.

Saitoh, W., Yamauchi, S., Watanabe, K., Takasaki, W., & Mori, K. (2014). Metabolomic analysis of arginine metabolism in acute hepatic injury in rats. *Journal of Toxicological Sciences, 39*(1), 41-50.

Schade, D. S. (1982). The role of catecholamines in metabolic acidosis. *Ciba Found Symp, 87*.

Scheie, E., & Flåøyen, A. (2003). Fluorescence spectra and measurement of phylloerythrin (phytoporphyrin) in plasma from clinically healthy sheep, goats, cattle and horses. *New Zealand Veterinary Journal, 51*(4), 191-193.

Scheie, E., Flåøyen, A., Moan, J., & Berg, K. (2002). Phylloerythrin: Mechanisms for cellular uptake and location, photosensitisation and spectroscopic evaluation. *New Zealand Veterinary Journal, 50*(3), 104-110.

Scheie, E., Ryste, E. V., & Flaoyen, A. (2003a). Measurement of phylloerythrin (phytoporphyrin) in plasma or serum and skin from sheep photosensitised after ingestion of Narthecium ossifragum. *New Zealand Veterinary Journal, 51*(3), 99-103.

Scheie, E., Smith, B. L., Cox, N., & Flaoyen, A. (2003b). Spectrofluorometric analysis of phylloerythrin (phytoporphyrin) in plasma and tissues from sheep suffering from facial eczema. *New Zealand Veterinary Journal, 51*(3), 104-110.

Schilling, C., Zuccollo, J., & Nixon, C. (2010). *Dairy's role in sustaining New Zealand - the sector's contribution to economy*. Retrieved from

Schmidl, M. V. F. (1986). *Laboratory Testing in Veterinary Medicine, Diagnosis and Clinical Monitoring*. Mannheim: Boehringer Mannheim.

Schnackenberg, L. K., Dragan, Y. P., Reily, M. D., Robertson, D. G., & Beger, R. D. (2007). Evaluation of NMR spectral data of urine in conjunction with measured clinical chemistry and

histopathology parameters to assess the effects of liver and kidney toxicants. *Metabolomics, 3*(2), 87-100.

Seawright, A. A., & Watt, D. A. (1972). Congenital Porphyria in a Bovine Carcase. *Australian Veterinary Journal, 48*(1), 35-35.

Shennan, D. B., & Peaker, M. (2000). Transport of milk constituents by the mammary gland. *Physiological Reviews, 80*(3), 925-951.

Siuzdak, G. (1996). *Mass Spectrometry for Biotechnology*. San Diego, California, USA: Academic Press.

Siviero, I., Ferrante, S. M. R., Meio, I. B., Madi, K., & Chagas, V. L. (2008). Hepatobiliary effects of cholic and lithocholic acids: experimental study in hamsters. *Pediatric Surgery International, 24*(3), 325-331.

Skotnicka, E., Muszczynski, Z., Dudzinska, W., & Suska, M. (2007). A review of the renal system and diurnal variations of renal activity in livestock. *Irish Veterinary Journal, 60*(3), 161-168.

Smeaton, D. C. (2003a). The "faecal" method for spore counting to assess facial eczema risk. In D. C. Smeaton (Ed.), *Profitable Beef Production - A Guide to Beef Production in New Zealand* (pp. 220). New Zealand: New Zealand Beef Council.

Smeaton, D. C. (2003b). The "wash" method for facial eczema spore counting on pasture. In D. C. Smeaton (Ed.), *Profitable Beef Production - A Guide to Beef Production in New Zealand* (pp. 217-219). New Zealand: New Zealand Beef Council.

Smith, B. L. (2000). Effects of low dose rates of sporidesmin given orally to sheep. *New Zealand Veterinary Journal, 48*(6), 176-181.

Smith, B. L., Asher, G. W., Thompson, K. G., & Hoggard, G. K. (1997). Hepatogenous photosensitisation in fallow deer (*Dama dama*) in New Zealand. *New Zealand Veterinary Journal, 45*(3), 88-92.

Smith, B. L., Briggs, L. R., Embling, P. P., Hawkes, A. D., & Towers, N. R. (1999). Urinary excretion of immunoreactive sporidesmin metabolites in sheep in relation to factors influencing susceptibility to sporidesmin intoxication. *New Zealand Veterinary Journal, 47*(1), 13-19.

Smith, B. L., Coe, B. D., & Embling, P. P. (1978). Protective effect of zinc-sulfate in a natural facial eczema outbreak in dairy cows. *New Zealand Veterinary Journal, 26*(12), 314-315.

Smith, B. L., & Embling, P. P. (1991). Facial eczema in goats - the toxicity of sporidesmin in goats and its pathology. *New Zealand Veterinary Journal, 39*(1), 18-22.

Smith, B. L., & O'Hara, P. J. (1978). Bovine photosensitization in New Zealand. *New Zealand Veterinary Journal, 26*(1-2), 2-5.

Smith, B. L., & Towers, N. R. (2002). Mycotoxicoses of grazing animals in New Zealand. *New Zealand Veterinary Journal, 50*(3), 28-34.

Smith, B. L., Towers, N. R., Jordan, R. B., & Mills, R. A. (1983). Zinc in the drinking water of dairy cattle for facial eczema control. *Dairy Farming Annual, 35*, 62-74.

Smith, B. L., Towers, N. R., Munday, R., Morris, C. A., & Collin, R. G. (1998). *Control of the mycotoxic hepatogenous photosensitization, facial eczema, in New Zealand*.

Spivey, J. R., Bronk, S. F., & Gores, G. J. (1993). Glycochenodeoxycholate-induced lethal hepatocellular injury in rat hepatocytes - role of ATP depletion and cytosolic-free calcium. *Journal of Clinical Investigation, 92*(1), 17-24.

Srivastava, S., Roy, R., Kumar, S., Gupta, H. O., Singh, D., Kushwaha, J. K., . . . Sonkar, A. A. (2013). Cholesterol and its esters as serum biomarkers in malignant obstructive jaundice: a single step H-1 NMR metabolomic approach. *Metabolomics, 9*(6), 1181-1191.

Starnes, H. F., Conti, P. S., Warren, R. S., Jeevanandam, M., & Brennan, M. F. (1987). Altered peripheral amino-acid uptake in obstructive-jaundice. *Journal of Surgical Research, 42*(4), 383-393.

Steffert, I. J. (1970). *Facial eczema: the extent of damage in dairy cows*.

Sundekilde, U., Larsen, L., & Bertram, H. (2013a). NMR-based milk metabolomics. *Metabolites, 3*(2), 204-222.

Sundekilde, U. K., Frederiksen, P. D., Clausen, M. R., Larsen, L. B., & Bertram, H. C. (2011). Relationship between the metabolite profile and technological properties of bovine milk from two dairy breeds elucidated by NMR-based metabolomics. *Journal of Agricultural and Food Chemistry, 59*(13), 7360-7367.

Sundekilde, U. K., Poulsen, N. A., Larsen, L. B., & Bertram, H. C. (2013b). Nuclear magnetic resonance metabonomics reveals strong association between milk metabolites and somatic cell count in bovine milk. *Journal of Dairy Science, 96*(1), 290-299.

Synge, R. L. M., & White, E. P. (1959). Sporidesmin - a substance from *Sporidesmium-bakeri* causing lesions characteristic of facial eczema. *Chemistry & Industry*, 1546-1547.

Szymanska, E., Saccenti, E., Smilde, A. K., & Westerhuis, J. A. (2012). Double-check: validation of diagnostic statistics for PLS-DA models in metabolomics studies. *Metabolomics, 8*(1), S3-S16.

Tang, H. R., Wang, Y. L., Nicholson, J. K., & Lindon, J. C. (2004). Use of relaxation-edited one-dimensional and two dimensional nuclear magnetic resonance spectroscopy to improve detection of small metabolites in blood plasma. *Analytical Biochemistry, 325*(2), 260-272.

Tapp, H. S., & Kemsley, E. K. (2009). Notes on the practical utility of OPLS. *TrAC Trends in Analytical Chemistry, 28*(11), 1322-1327.

Teahan, O., Gamble, S., Holmes, E., Waxman, J., Nicholson, J. K., Bevan, C., & Keun, H. C. (2006). Impact of analytical bias in metabonomic studies of human blood serum and plasma. *Analytical Chemistry, 78*(13), 4307-4318.

Team, R. D. C. (2012). *R: A language and environment for statistical computing*. R Foundation for Statistical Computing, Vienna, Austria.

Tennant, B. C. (1998). Lessons from the porphyrias of animals. *Clinics in Dermatology, 16*(2), 307-315.

Towers, N. R. (1970). Tissue distribution and excretion of radioactivity in rats dosed with sporidesmin-S-35. *New Zealand Journal of Agricultural Research, 13*(2), 428-436.

Towers, N. R. (1978). The incidence of subclinical facial eczema in selected Waikato dairy herds. *New Zealand Veterinary Journal, 26*(6), 142-145.

Towers, N. R. (1986). Facial eczema - problems and successes in control. *Proceedings of the New Zealand Grassland Association, 47*, 121-127.

Towers, N. R., & Smith, B. L. (1978). Protective effect of zinc sulfate in experimental sporidesmin intoxication of lactating dairy cows. *New Zealand Veterinary Journal, 26*(8), 199-202.

Towers, N. R., & Stratton, G. C. (1978). Serum gamma-glutamyl transferase as a measure of sporidesmin-induced liver damage in sheep. *New Zealand Veterinary Journal, 26*(4), 109-112.

Trivedi, D. K., & Iles, R. K. (2012). The application of SIMCA P+ in shotgun metabolomics analysis of ZIC HILIC-MS spectra of human urine - experience with Shimadzu IT-TOF and profiling data extraction software. *Journal of Chromatographic Separation Techniques, 3*(6), 1-5.

Trottier, J., Bialek, A., Caron, P., Straka, R. J., Heathcote, J., Milkiewicz, P., & Barbier, O. (2012). Metabolomic profiling of 17 bile acids in serum from patients with primary biliary cirrhosis and primary sclerosing cholangitis: A pilot study. *Digestive and Liver Disease, 44*(4), 303-310.

van den Berg, R. A., Hoefsloot, H. C. J., Westerhuis, J. A., Smilde, A. K., & van der Werf, M. J. (2006). Centering, scaling, and transformations: improving the biological information content of metabolomics data. *Bmc Genomics, 7*.

Wakil, S. J. (1961). Mechanism of fatty acid synthesis. *Journal of Lipid Research, 2*(1), 1-24.

Want, E. J., Coen, M., Masson, P., Keun, H. C., Pearce, J. T. M., Reily, M. D., . . . Nicholson, J. K. (2010). Ultra performance liquid chromatography-mass spectrometry profiling of bile acid metabolites in biofluids: application to experimental toxicology studies. *Analytical Chemistry, 82*(12), 5282-5289.

Want, E. J., Masson, P., Michopoulos, F., Wilson, I. D., Theodoridis, G., Plumb, R. S., . . . Nicholson, J. K. (2013). Global metabolic profiling of animal and human tissues via UPLC-MS. *Nature Protocols, 8*(1), 17-32.

Waters, N. J., Holmes, E., Williams, A., Waterfield, C. J., Farrant, R. D., & Nicholson, J. K. (2001). NMR and pattern recognition studies on the time-related metabolic effects of alpha-naphthylisothiocyanate on liver, urine, and plasma in the rat: An integrative metabonomic approach. *Chemical Research in Toxicology, 14*(10), 1401-1412.

Watson, J. T., & Sparkman, O. D. (2007). *Introduction to mass spectrometry: Instrumentation, applications and strategies for data interpretation* (4 ed.). West Sussex, England: John Wiley & Sons, Ltd.

Westerhuis, J. A., Hoefsloot, H. C. J., Smit, S., Vis, D. J., Smilde, A. K., van Velzen, E. J. J., . . . van Dorsten, F. A. (2008). Assessment of PLSDA cross validation. *Metabolomics, 4*(1), 81-89.

Wheelock, A. M., & Wheelock, C. E. (2013). Trials and tribulations of 'omics data analysis: assessing quality of SIMCA-based multivariate models using examples from pulmonary medicine. *Molecular Biosystems, 9*(11), 2589-2596.

White, E. P. (1958). Photosensitivty diseases in New Zealand. XIII. Substances isolated from concentrates of facial eczema grass. *New Zealand Journal of Agricultural Research, 1*, 859-865.

White, E. P., Mortimer, P. H., & di Menna, M. E. (1977). Chemistry of the sporidesmins. In T. D. Wyllie & L. G. Moorehouse (Eds.), *Mycotoxic Fungi, Mycotoxins, Mycotoxicoses - an Encyclopedic Handbook. Volume 1. Mycotoxic Fungi and Chemistry of Mycotoxins* (pp. 427-447). New York: Marcel Dekker.

Wiklund, S., Johansson, E., Sjostrom, L., Mellerowicz, E. J., Edlund, U., Shockcor, J. P., . . . Trygg, J. (2008). Visualization of GC/TOF-MS-based metabolomics data for identification of biochemically interesting compounds using OPLS class models. *Analytical Chemistry, 80*(1), 115-122.

Wishart, D. S., Jewison, T., Guo, A. C., Wilson, M., Knox, C., Liu, Y., . . . Scalbert, A. (2013). HMDB 3.0 - The Human Metabolome Database in 2013. *Nucleic Acids Research, 41*(D1), 801 - 807.

Wood, S. N. (2006). *Generalized Additive Models: An introduction with R*: Chapman and Hall/CRC.

Wood, S. N. (2011). Fast stable restricted maximum likelihood and marginal likelihood estimation of semiparametric generalized linear models. *Journal of the Royal Statistical Society (B), 73*(1), 3-36.

Woodcock, J. C., Henderson, W., & Miles, C. O. (2001). Metal complexes of the mycotoxins sporidesmin A and gliotoxin, investigated by electrospray ionisation mass spectrometry. *Journal of Inorganic Biochemistry, 85*(2-3), 187-199.

Woolbright, B. L., Dorko, K., Antoine, D. J., Clarke, J. I., Gholami, P., Li, F., . . . Jaeschke, H. (2015). Bile acid-induced necrosis in primary human hepatocytes and in patients with obstructive cholestasis. *Toxicology and Applied Pharmacology, 283*(3), 168-177.

Woolbright, B. L., Li, F., Xie, Y. C., Farhood, A., Fickert, P., Trauner, M., & Jaeschke, H. (2014). Lithocholic acid feeding results in direct hepato-toxicity independent of neutrophil function in mice. *Toxicology Letters, 228*(1), 56-66.

Worley, B., & Powers, R. (2013). Multivariate analysis in metabolomics. *Current Metabolomics, 1*, 92-107.

Wu, H. F., Zhang, X. Y., Li, X. J., Li, Z. F., Wu, Y. J., & Pei, F. K. (2005). Comparison of metabolic profiles from serum from hepatotoxin-treated rats by nuclear-magnetic-resonance-spectroscopy-based metabonomic analysis. *Analytical Biochemistry, 340*(1), 99-105.

Wyllie, T. D., & Moorehouse, L. G. (1978). *Mycotoxic fungi, mycotoxins, mycotoxicoses - an encyclopedic handbook. Volume 2. Mycotoxicoses of domestic and laboratory animals, poultry, and aquatic invertebrates and vertebrates*. New York: Marcel Dekker.

Xia, J., Bjorndahl, T. C., Tang, P., & Wishart, D. S. (2008). MetaboMiner - Semi-automated identification of metabolites from 2D NMR spectra of complex biofluids. *Bmc Bioinformatics, 9*(507).

Xiao, J. F., Zhou, B., & Ressom, H. W. (2012). Metabolite identification and quantitation in LC-MS/MS-based metabolomics. *Trac-Trends in Analytical Chemistry, 32*, 1-14.

Zeisel, S. H. (2006). Choline: Critical role during fetal development and dietary requirements in adults *Annual Review of Nutrition* (Vol. 26, pp. 229-250). Palo Alto: Annual Reviews.

Zhang, A., Sun, H., Wang, P., Han, Y., & Wang, X. (2012a). Modern analytical techniques in metabolomics analysis. *Analyst, 137*(2), 293-300.

Zhang, G., Sadhukhan, S., Tochtrop, G. P., & Brunengraber, H. (2011). Metabolomics, pathway regulation, and pathway discovery. *The Journal of Biological Chemistry, 286*(27), 23631-23635.

Zhang, J., Wei, S., Liu, L., Gowda, G. A. N., Bonney, P., Stewart, J., . . . Raftery, D. (2012b). NMR-based metabolomics study of canine bladder cancer. *Biochimica Et Biophysica Acta-Molecular Basis of Disease, 1822*(11), 1807-1814.

Zhang, S. C., Gowda, G. A. N., Ye, T., & Raftery, D. (2010). Advances in NMR-based biofluid analysis and metabolite profiling. *Analyst, 135*(7), 1490-1498.

Zhang, Y. C., Hong, J. Y., Rockwell, C. E., Copple, B. L., Jaeschke, H., & Klaassen, C. D. (2012c). Effect of bile duct ligation on bile acid composition in mouse serum and liver. *Liver International, 32*(1), 58-69.

Zheng, P., Gao, H. C., Li, Q., Shao, W. H., Zhang, M. L., Cheng, K., . . . Xie, P. (2012). Plasma metabonomics as a novel diagnostic approach for major depressive disorder. *Journal of Proteome Research, 11*(3), 1741-1748.

Zuber, V., & Strimmer, K. (2009). Gene ranking and biomarker discovery under correlation. *Bioinformatics, 25*(20), 2700-2707.

Appendices

Appendix 1

Liver histology grading

Cow#	Liver lobe	Peribiliary concentric fibrosis and/or oedema	Ductular hyperplasia	Arteriolar hyperplasia	Portal fibroplasia	Portal inflammation	Parenchymal necrosis	Total Score
22	V	0	0	0	0	0	0	0
	C	1	0	0	0	0	0	1
64	V	1	0	0	0	1	0	2
	C	1	0	0	0	1	0	2
152	V	1	0	0	0	0	0	1
	C	0	0	0	0	0	0	0
195	V	1	0	0	0	0	0	1
	C	1	0	0	0	0	0	1
222	V	0	1	1	1	1	0	4
	C	1	1	1	1	1	0	5
239	V	3	2	1	2	1	3	12
	C	3	2	1	2	1	3	12
	Q	3	1	0	1	3	3	11
244*	V	1	0	0	0	0	0	1
	C	1	0	0	0	0	1	2
	R	3	2	2	2	3	2	14
282	V	1	3	3	2	1	0	10
	C	1	3	3	2	1	0	10
298	V	2	2	2	3	2	0	11
	C	2	2	2	3	2	0	11
312	V	2	3	2	3	2	0	12
	C	0	0	0	0	1	0	1
317	V	1	3	3	2	1	0	10
	C	1	3	3	2	1	0	10
374	V	1	0	0	0	0	0	1
	C	1	0	0	0	0	0	1
384	V	0	0	0	0	0	0	0
	C	0	0	0	0	0	0	0
393	V	2	2	2	3	1	0	10
	C	3	3	2	3	2	0	13
395	V	1	0	0	0	0	0	1
	C	2	2	2	3	2	0	11
420	V	1	0	0	0	0	0	1
	C	1	0	0	0	0	0	1
424	V	1	0	0	0	0	0	1
	C	1	0	0	0	0	0	1
	R	2	2	2	3	1	0	10
440	V	2	2	2	3	2	0	11
	C	2	2	2	3	2	0	11
448	V	1	0	0	0	1	0	2
	V	1	0	0	0	1	0	2
450	V	2	2	2	2	2	0	10
	C	2	3	3	3	2	0	13

(V=ventral lobe, C=caudate lobe, Q=quadrate lobe, R=right lobe, 0 = normal, 1 = mild, 2 = moderate, 3 = severe (*One portal vein scar))

Appendix 2

The buckets contributing to the differentiation of serum samples that were processed in different years after the sporidesmin trial, by p-JRES ^{1}H NMR spectroscopy. The samples processed in 2011 were all Monday samples from the trial, while those processed in 2013 were the Wednesday and Friday samples, as well as some quality control Monday samples.

A clear separation was seen between the two years, which did not allow the combination of the datasets for statistical analysis. Only buckets with a VIPcv value > 1 and p(corr)[1] > 0.4 are listed.

^{1}H shift (ppm)	Direction of change†
1.18	↑
1.38	↓
3.26	↑
3.46	↑
3.5	↑
3.54	↑
3.66	↑
3.82	↑
3.86	↑
4.18	↓
5.42	↓

†The direction of change is relative to 2011 i.e. a down regulation (↓) represents a decrease in the level of this metabolite in the 2013 samples in relation to the 2011 level of this metabolite

Appendix 3

Scores and S-plots showing differentiation between the clinical group and all others (*Figure A2.1*), and the days which the clinical cows showed the first clinical signs in comparison to all other days.

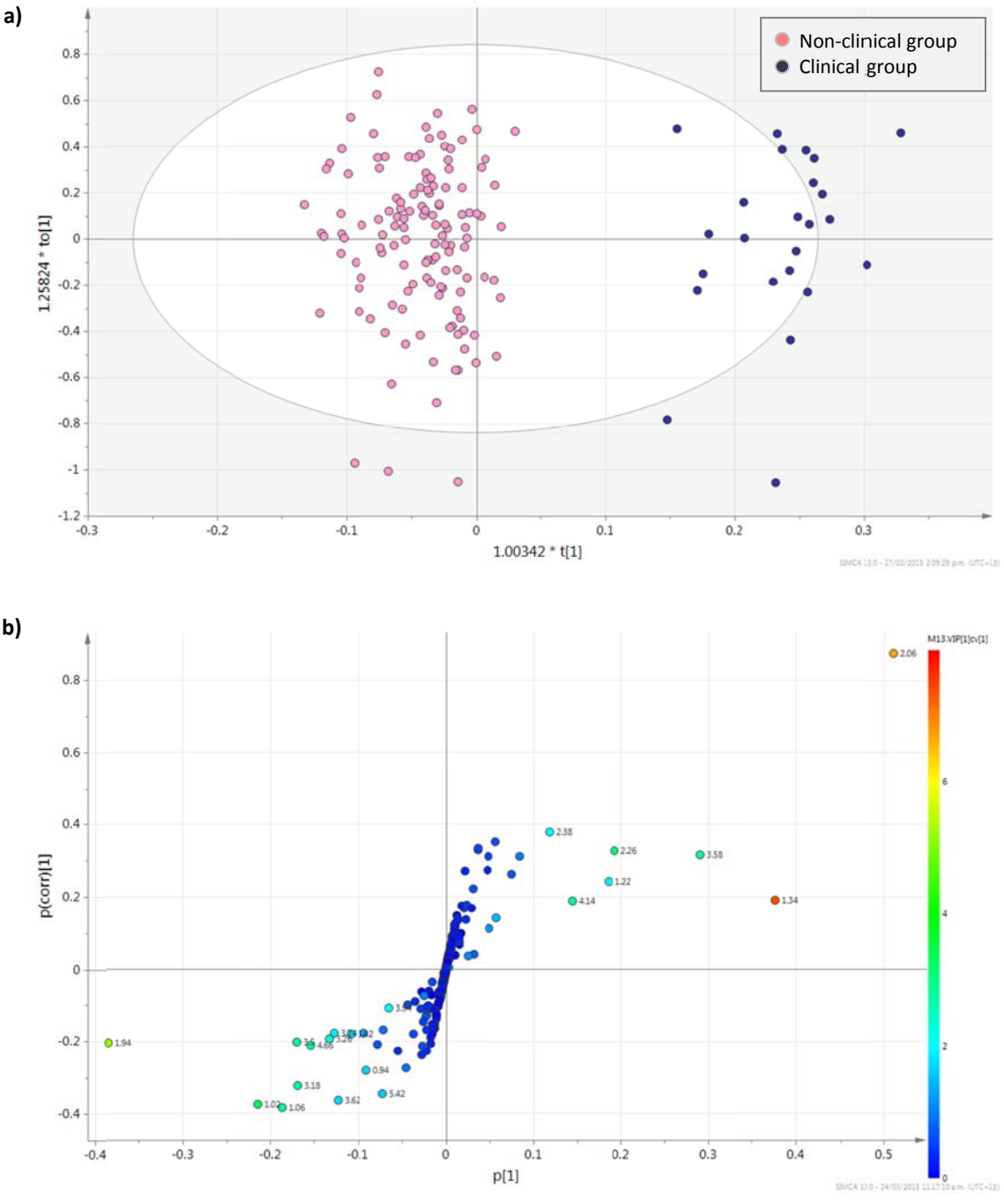

Figure A2.1 *OPLS-DA of p-JRES serum samples, defined by the clinical class, therefore comparing all clinical cow samples after dosing to all other groups and all control days; a) scores plot showing the clinical cow samples orientating to the right, away from all other samples, b) S-plot representing the main buckets causing separation between the classes (VIPcv > 1)*

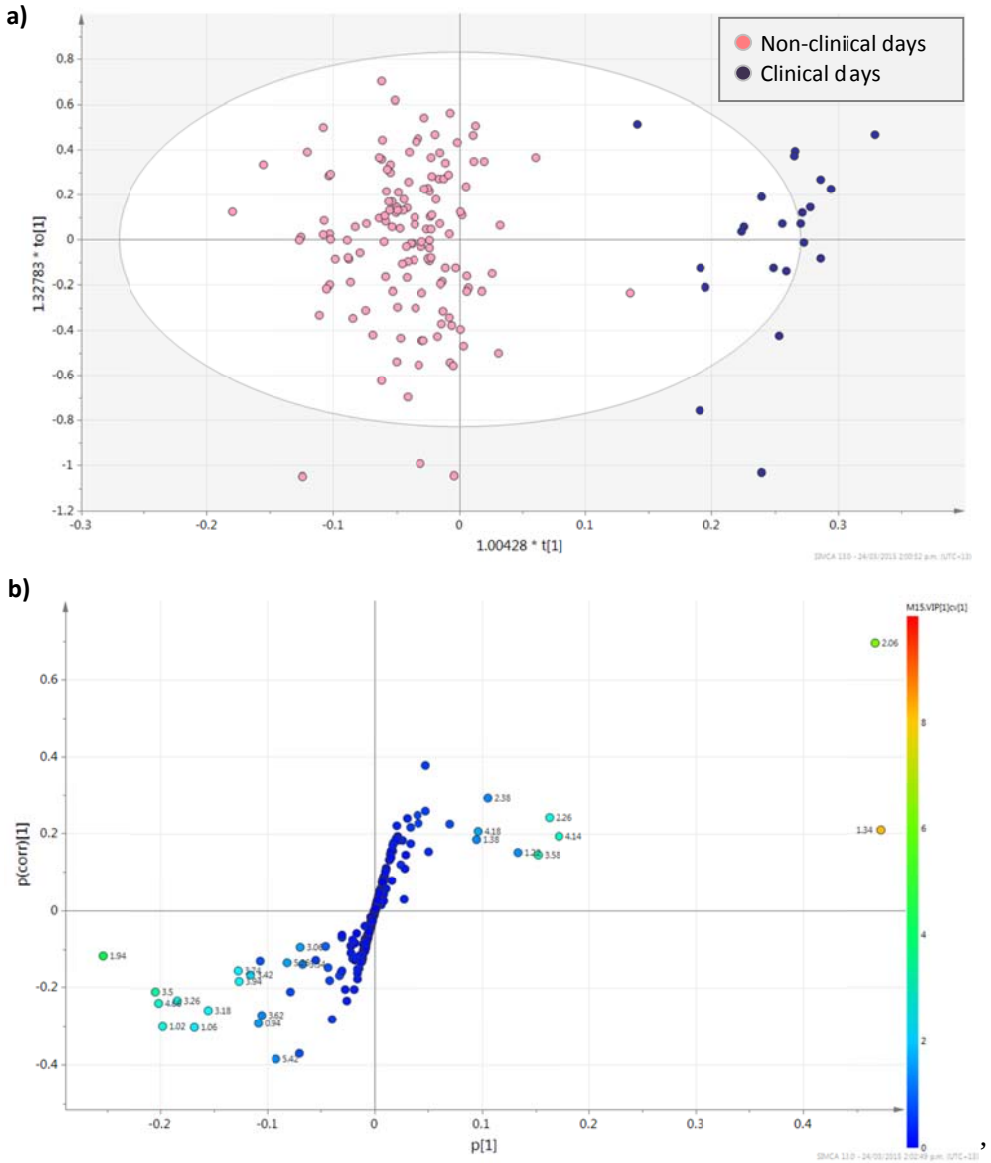

Figure A2.2 OPLS-DA of all p-JRES serum samples, defined by clinical days, therefore comparing samples from clinical cows taken after they were identified as showing clinically photosensitive signs, and comparing these to all other samples a) scores plot showing a clear separation between the classes, b) the S-plot identified two main buckets to be contributing to the separation (2.06 and 1.34 ppm) with a p(corr)[1] > 0.4

Appendix 4

The buckets contributing to the differentiation of serum samples that were processed in different years after the sporidesmin trial, by diffusion-edited ^{1}H NMR spectroscopy (0.08 ppm). A clear separation was seen between the two years, which did not allow the combination of the datasets for statistical analysis. Only buckets with a VIPcv value > 1 and p(corr)[1] > 0.4 are listed

^{1}H shift (ppm)	**Direction of change†**
0.92	↓
1.00	↓
2.04	↓
2.60	↑
3.40	↑
3.72	↓
4.44	↑
4.52	↑
6.84	↑
6.92	↑
7.64	↑
7.96	↑
8.20	↑

†The direction of change is relative to 2011 i.e. a down regulation (↓) represents a decrease in the level of this metabolite in the 2013 samples in relation to the 2011 level of this metabolite.

Appendix 5

The combined ranking statistics for the *p*-JRES ^{1}H NMR serum time series analysis; showing the top 40 buckets, in the order of combined ranking, lowest to highest

F	P	mz	col	sda_rank	P_rank	comb_rank	sda
2.480399	0.003	6.89999962	78	4	2	1	27.7891
3.168432	0.0067	0.85999978	212	2	6	2	43.87922
4.694831	0.0103	2.0599997	182	1	8	3	72.94529
2.991964	0.003	3.29999971	151	8	3	4	21.65271
2.264999	0.0119	1.17999971	204	5	9	5	25.78411
2.297156	0.025	2.01999974	183	3	13	6	31.23357
2.085413	0.0243	0.93999976	210	7	12	7	25.14319
1.735939	0.0219	5.69999981	108	9	11	8	19.01932
1.909529	0.0042	9.89999962	3	17	4	9	12.28702
1.883461	0.0419	5.21999979	120	13	19	10	13.49166
1.762263	0.0361	5.37999964	116	18	18	11	12.24753
1.769085	0.0342	6.37999964	91	19	17	12	12.05718
1.617067	0.0734	8.46000004	39	24	25	13	10.77292
1.473769	0.0954	2.49999976	171	26	28	14	10.67868
1.478609	0.1267	4.25999975	127	16	35	15	12.31416
1.785692	0.0916	3.61999965	143	29	27	16	9.763296
1.774481	0.0255	2.81999969	163	37	15	17	8.869994
1.3993	0.1156	7.29999971	68	30	31	18	9.55009
1.565519	0.0735	6.0199995	100	35	26	19	9.040557
1.475612	0.18	1.01999974	208	11	45	20	15.0152
2.025214	0.0049	8.41999912	40	51	5	21	7.463793
1.310374	0.172	9.53999996	12	31	42	22	9.486383
1.545129	0.0537	8.53999996	37	49	22	23	7.588839
1.411975	0.2175	5.4199996	115	6	54	24	25.39488
1.728797	0.0255	7.17999983	71	53	14	25	7.296378
1.655513	0.1425	2.73999977	165	45	38	26	7.941444
1.344685	0.2343	1.0599997	207	15	57	27	12.35789
1.267195	0.1933	8.65999985	34	33	49	28	9.394233
1.691487	0.0493	9.13999939	22	56	21	29	7.114149
1.352509	0.1276	7.0199995	75	48	36	30	7.604798
1.245699	0.2009	5.53999949	112	38	50	31	8.646198
2.121203	0.0332	2.93999958	160	62	16	32	6.497541
1.893256	0.0083	7.45999956	64	66	7	33	6.29859
1.19364	0.252	6.21999979	95	23	63	34	10.80335
1.22033	0.2599	3.37999964	149	14	66	35	12.36535
1.341718	0.2051	2.69999981	166	43	52	36	8.125642
1.31753	0.1664	0.21999976	228	60	41	37	6.680533
1.416808	0.1084	7.49999952	63	71	29	38	5.89141
1.217572	0.3012	3.21999979	153	12	78	39	14.6184

Appendix 6

The combined ranking statistics for NOESY ^{1}H NMR urine time series analysis; showing the top 40 buckets, in the order of combined ranking, lowest to highest

F	P	mz	col	sda_rank	P_rank	comb_rank	sda
2.697822	0.0119	7.25999975	69	7	1	1	41.4984
2.134528	0.0536	7.05999947	74	3	9	2	50.62697
2.756004	0.0163	2.33999968	175	11	2	3	31.92123
1.96752	0.0466	3.4199996	148	10	7	4	33.65307
1.907024	0.0872	0.93999976	210	2	15	5	63.19392
1.66805	0.0839	6.93999958	77	12	13	6	30.67043
1.678992	0.1081	2.0599997	182	1	20	7	88.77811
2.51989	0.029	7.21999979	70	20	4	8	25.18215
2.107464	0.0517	1.89999974	186	24	8	9	22.27058
1.554364	0.1005	2.85999966	162	19	17	10	25.6053
1.864971	0.109	0.69999975	216	18	21	11	25.90957
1.638314	0.1239	2.09999967	181	15	25	12	28.68436
3.172561	0.017	3.25999975	152	35	3	13	16.20725
1.424616	0.1504	1.41999972	198	21	29	14	23.88523
1.637584	0.0844	1.85999978	187	41	14	15	14.04148
1.296757	0.1851	4.0199995	133	26	37	16	21.05926
2.098658	0.066	0.97999972	209	50	10	17	11.74712
1.233728	0.2663	4.13999987	130	5	54	18	48.11811
1.414635	0.1735	6.61999941	85	43	35	19	13.20888
1.301626	0.2393	6.21999979	95	31	47	20	17.25987
2.645053	0.0391	2.73999977	165	58	5	21	10.22603
1.172118	0.2923	2.65999961	167	16	59	22	26.64161
1.227059	0.2299	6.53999949	87	45	44	23	12.50847
1.313635	0.2109	1.25999975	202	53	41	24	11.61348
1.197045	0.2996	4.17999983	129	33	61	25	17.02817
1.432943	0.151	3.21999979	153	63	30	26	10.05998
1.155381	0.3154	6.69999981	83	27	68	27	20.13917
1.688183	0.1221	7.33999968	67	70	24	28	9.589395
1.220097	0.2894	7.0199995	75	46	58	29	12.34099
1.527481	0.1275	2.57999969	169	71	26	30	9.242012
1.372722	0.1821	1.17999971	204	68	36	31	9.907313
1.203363	0.2487	6.81999969	80	59	50	32	10.20179
1.12497	0.345	2.13999963	180	22	75	33	23.41996
1.223388	0.2533	2.29999971	176	64	51	34	10.05668
1.362751	0.1933	5.33999968	117	73	39	35	8.877814
1.355897	0.1663	6.65999985	84	78	34	36	8.25097
1.046733	0.3996	7.69999981	58	6	87	37	42.288
1.251908	0.2332	9.73999977	7	76	45	38	8.447595
1.02371	0.4153	3.09999967	156	9	89	39	38.85288

Appendix 7

The combined ranking statistics for NOESY ^{1}HNMR milk time series analysis; showing the top 40 buckets, in the order of combined ranking, lowest to highest

F	P	ppm	col	sda_rank	P_rank	comb_rank	sda
1.677404	0.0412	2.4400003	87	4	4	1	29.77827
1.909014	0.0698	8.11999989	24	1	8	2	46.2194
1.898576	0.0291	8.60000038	18	17	2	3	6.989107
2.230416	9.00E-04	6.11999989	49	20	1	4	6.247561
1.512319	0.1002	4.36000013	63	7	19	5	13.0892
1.676422	0.0803	8.27999973	22	19	10	6	6.564437
1.425732	0.1331	4.28000021	64	15	27	7	8.403989
1.522699	0.1621	3.08000016	79	3	31	8	37.35353
1.461326	0.0898	2.92000008	81	32	15	9	3.865347
1.402516	0.126	2.84000015	82	26	25	10	4.281074
1.600665	0.0808	7.72000027	29	36	11	11	3.389486
1.409957	0.1485	8.44000053	20	25	30	12	4.558042
1.260195	0.2202	7.16000032	36	18	36	13	6.821942
1.379999	0.1862	3.16000009	78	23	35	14	5.87359
1.599916	0.1056	8.03999996	25	40	20	15	3.271591
1.238072	0.2946	6.20000029	48	2	46	16	38.55524
1.242069	0.2253	9	13	28	37	17	4.0379
1.511037	0.0983	6.68000031	42	48	18	18	2.994612
1.246764	0.2287	4.20000029	65	35	38	19	3.415132
1.128668	0.3299	1.80000019	95	14	50	20	8.4731
1.540469	0.1205	6.5999999	43	47	24	21	3.004936
1.163396	0.293	3.56000018	73	31	45	22	3.9644
1.450489	0.1191	6.92000008	39	53	23	23	2.584543
1.227759	0.2295	4.51999998	61	42	40	24	3.213477
1.425179	0.114	7	38	56	22	25	2.457421
1.081379	0.3817	3.00000024	80	8	62	26	12.3162
1.072769	0.3822	3.48000026	74	6	63	27	13.78116
1.593425	0.0751	8.52000046	19	64	9	28	2.202037
1.078709	0.3645	5.32000017	59	29	58	29	4.030736
1.203056	0.2452	2.60000014	85	52	41	30	2.592581
1.371059	0.1464	5.48000002	57	60	29	31	2.296575
1.585397	0.087	7.96000004	26	66	14	32	2.10462
1.135669	0.3314	1.72000027	96	46	51	33	3.040352
1.121438	0.3409	9.96000004	1	45	53	34	3.047999
1.406369	0.1311	0.44000024	112	65	26	35	2.187059
1.04553	0.406	3.24000025	77	30	64	36	4.027271
1.143976	0.3062	9.80000019	3	51	49	37	2.682474
1.718289	0.0618	8.35999966	21	71	7	38	2.025307
1.036535	0.4217	1.40000021	100	34	65	39	3.546078

Appendix 8

Hotellings T^2 exclusions for C18 (-) UPLC/ESI-MS identified in the initial PCA analysis.

Sample	Trial Day	Group	Sample T^2 crit	Method T^2 crit (99 %)
440	4	Clinical	28.426	11.5110 Range [1 - 3]
244	4	Non-responder	14.900	
152	14	Control	14.502	
64	44	Subclinical	15.817	
22	39	Control	15.717	
440*	23	Clinical	19.595	17.2112 Range [1 - 6]
420	-12	Subclinical	24.770	
395	-5	Subclinical	20.496	
384	37	Control	22.929	
374	25	Non-responder	19.345	
298	16	Clinical	21.011	
244	14	Non-responder	27.878	
195	-3	Subclinical	19.440	
152	39	Control	19.080	
22	11	Control	17.540	
152	25	Control	12.207	11.5169 Range [1-3]
384	18	Control	11.727	
395	28	Subclinical	12.075	

* Repeat sample

Appendix 9

PCA Hotelling T^2 line plot of C18 (+) UPLC/ESI-MS, using no scaling, before any exclusions were made.

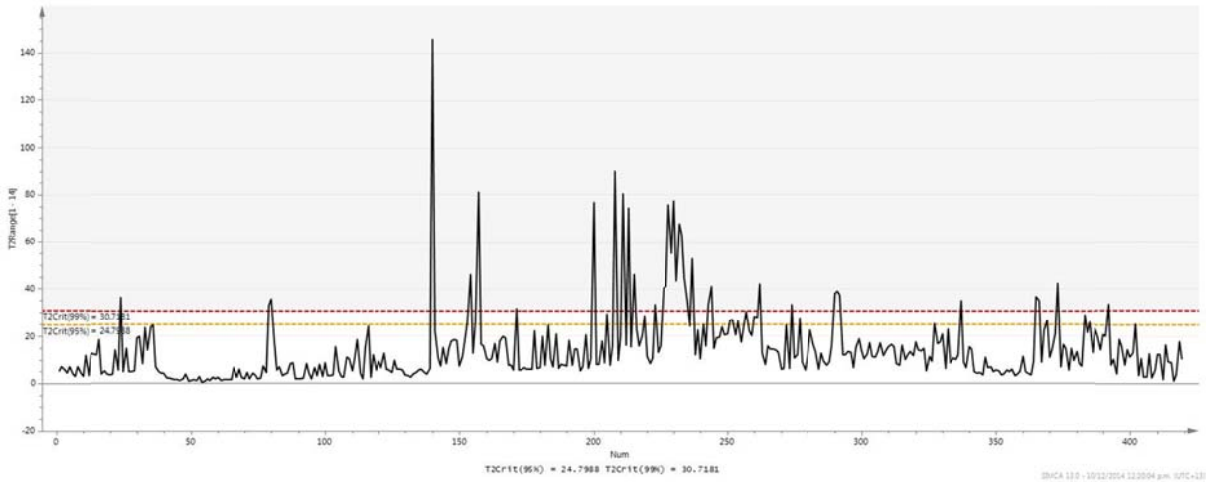

Hotellings T^2 exclusions for C18 (+) LC/ESI-MS identified in the initial PCA analysis.

Sample	Trial Day	Group	Sample T^2 crit	Method T^2 crit (99 %)
440	0	Clinical	36.018	
152	7	Control	33.527	
424	7	Subclinical	35.252	
152	35	Control	152.950	
424	-5	Subclinical	80.326	
222	37	Subclinical	29.272	
195	-5	Non-responder	31.968	
424	16	Subclinical	68.897	
244	16	Non-responder	79.861	
244*	-7	Non-responder	75.029	
420	-5	Subclinical	69.675	
22	16	Control	45.406	
64	-10	Subclinical	68.726	
395	30	Subclinical	69.360	
298	4	Clinical	73.259	28.9267 Range [1 – 13]
64	7	Subclinical	64.486	
195	-10	Non-responder	48.786	
384	44	Control	38.095	
317	-10	Clinical	44.981	
395	4	Subclinical	36.500	
64*	4	Subclinical	43.226	
312	-3	Subclinical	36.360	
222	25	Subclinical	37.111	
64*	30	Subclinical	35.534	
317	-3	Clinical	33.083	
312	39	Subclinical	36.890	
312	11	Subclinical	32.273	
195	25	Non-responder	39.009	
424	18	Subclinical	31.804	

* Repeat sample